



**Exploiting Thermally-Reversible
Chemistry for Controlling the
Crosslinking of Polymer Networks**

Michael E. Budd

**Thesis submitted to the University of Reading for the Degree of
Doctor of Philosophy**

Department of Chemistry

2016

Declaration

I confirm that this thesis is my own work and the use of all material from other sources has been properly and fully acknowledged.

Michael E. Budd

Acknowledgements

I would like to thank my supervisor Wayne Hayes for giving me the chance to undertake this project and all the guidance he has given me over the years. I would like to acknowledge BAE Systems for the funding of this project and special thanks are extended to Rebecca Stevens and Richard Arthur for all their advice.

Further thanks are conveyed to the technical staff of University of Reading, particularly Martin Reeves, Nicholas Michael and Radoslaw Kowalczyk for all of their invaluable assistance. The input of Dr Peter Harris from the Centre for Advanced Microscopy at the University of Reading is also acknowledged

Finally I would also like to thank the past and present members of the Wayne Hayes research group for making the past three years enjoyable. Particular thanks are extended to Dr Daniel Smith, Clare Higgins and Ben Baker.

Thesis Abstract

High explosives are highly sensitive to accidental detonation by impact, fire, shrapnel and small arms fire. This sensitivity can be reduced by storing the energetic material within a rubbery polymer matrix and are known as plastic bonded explosives (PBX). The current procedure used to manufacture PBX involves mixing the energetic material with a hydroxy-functionalised aliphatic polymer. Upon the addition of an isocyanate crosslinker an immediate polymerisation occurs and thus the rapidly curing mixture must be used to fill the missile or shells, referred to as 'stores'. This process can lead to poor distribution of the crosslinker resulting in the formation of an inhomogeneously crosslinked matrix and the formation of voids. One solution to this problem involves containing the crosslinker within polyurethane microcapsules that are uniformly dispersed in the explosive-polymer mixture. Upon the application of a stimulus the crosslinker can be released from the microcapsules and the formation of a uniformly crosslinked PBX achieved. Herein is reported the design and synthesis of polyurethane microcapsules that release isocyanate crosslinkers when desired using a thermal stimulus. This has been achieved by exploiting the thermally-reversible nature of oxime-urethane and Diels-Alder adducts that have been incorporated into the shell wall of the microcapsules. An alternative approach to controlling the polymerisation of PBX materials has also been achieved using thermally-reversible blocked isocyanates that regenerate the isocyanate crosslinker when exposed to heat.

Synopsis

Chapter 1 describes the current procedures used to bind high explosives within polyurethane rubber matrices. The problems and limitations of this procedure are outlined and a potential solution utilising microencapsulation technology is proposed. The first section of this chapter reviews the literature surrounding the applications, synthesis and controlled release of microencapsulated active liquid agents. The second section of this chapter investigates potential thermally-labile bonds that could be incorporated into the shell wall of microcapsules in order to generate microencapsulated crosslinkers that are released upon exposure to the application of heat.

Chapter 2 describes how thermally-labile oxime-urethane bonds can be incorporated into the shell wall of microcapsules by first synthesising an isocyanate-terminated shell wall precursor. A library of shell wall precursors that possess varying degrees of steric hindrance around the thermally-labile bond have been generated. Methods for observing the dissociation of the shell wall precursor have been investigated including variable temperature infra-red spectroscopy (VTIR), differential scanning calorimetry (DSC) and thermogravimetric analysis. VTIR spectroscopic methods were demonstrated to provide the most reliable data and results revealed that increasing the steric hindrance around the oxime-urethane reduced the temperature at which dissociation occurred.

Chapter 3 reports the synthesis of microcapsules using an interfacial polymerisation technique employing the shell wall precursors described in **Chapter 2** in order to incorporate a thermally-labile oxime-urethane within the shell walls. The release of the core contents from these microcapsules using an application of a heat stimulus was investigated and the capability of these microcapsules to cure hydroxy-functionalised aliphatic polymers was demonstrated. Many reaction parameters are associated with the interfacial polymerisation approach to microcapsule synthesis and the second section of this chapter describes how modification of these parameters can be used to control the physical properties of microcapsules - microcapsule diameter, shell wall thickness and core loading. In addition, the microencapsulation of a dye, β -carotene, is described and how UV-visible spectroscopy can be used to quantify the release of the core contents from microcapsules.

Chapter 4 reports the design and synthesis of microcapsules that contain a thermally-reversible Diels-Alder adduct within the shell wall. This chapter first describes the design and synthesis of an isocyanate-terminated shell wall precursor that contains the Diels-Alder adduct and is capable of further chain extension to form microcapsules. The second part of this chapter describes the synthesis and characterisation of microcapsules synthesised using an interfacial polymerisation technique employing the generated shell wall precursor. The potential of these microcapsules to release their core contents upon exposure to a heat stimulus is reported. In addition, a method to increase the mechanical strength of the microcapsules is described.

Chapter 5 describes how thermally-labile blocked isocyanates can be employed to generate active isocyanate crosslinkers when desired using an application of heat. A range of blocking groups - amines, amides, oximes, aromatic heterocycles and phenols were used to block isophorone diisocyanate. The potential of these molecules to regenerate the active isocyanate moiety and thus cure hydroxy-functionalised polymers at elevated temperatures is reported. Of these blocking groups, oximes were demonstrated to possess the most ideal solubility and curing characteristics. The second section of this chapter focuses how the dissociation temperature of oxime-blocked isocyanates - designated herein as oxime-urethanes - can be controlled by modification of the steric and electronic properties of the oxime. The final section reports the potential of these oxime-urethanes to cure hydroxy-functionalised polymers and how the curing reaction can be monitored.

List of Abbreviations, Formulae and Symbols

ATR	Attenuated total reflectance
CaH ₂	Calcium hydride
CDCl ₃	Deuterated chloroform
CHCl ₃	Chloroform
CO ₂	Carbon dioxide
Đ	Dispersity
Da	Dalton
DBTDL	Dibutyltin dilaurate
DCPD	Dicyclopentadiene
DMAP	4-Dimethylaminopyridine
DMSO	Dimethylsulfoxide
DSC	Differential scanning calorimetry
ESEM	Environmental scanning electron microscopy
ESI	Electrospray ionisation
Et ₂ O	Diethyl ether
Et ₃ N	Triethylamine
EtOAc	Ethyl acetate
EtOH	Ethanol
FTIR	Fourier transform infrared
GPC	Gel permeation chromatography
H ₂ O	Water
HCl	Hydrochloric acid
HDI	Hexamethylene diisocyanate
HF	Hydrogen fluoride
HTPB	Hydroxy-terminated polybutadiene

IPDI	Isophorone diisocyanate
<i>i</i> Pr	<i>iso</i> -Propyl
kHz	Kilohertz
<i>m</i>	<i>meta</i>
m.p.	Melting point
MDI	Methylene diisocyanate
Me	Methyl
MeOH	Methanol
MgSO ₄	Magnesium sulfate
MHz	Megahertz
μm	Micrometres
M _n	Number average molecular mass
M _p	Initial mass of polymer
M _{r_s}	Molecular mass of solvent
MS	Mass spectrometry
M _s	Mass of solvent
M _w	Weight average molecular mass
NaCl	Sodium chloride
NaHCO ₃	Sodium hydrogen carbonate
NaOH	Sodium hydroxide
NCO	Isocyanate
NH ₄ Cl	Ammonium chloride
NMR	Nuclear magnetic resonance
<i>o</i>	<i>ortho</i>
<i>p</i>	<i>para</i>
PBX	Plastic bonded explosive

PCM	Phase change material
Ph	Phenyl
PNIPAM	Poly(<i>N</i> -isopropylacrylamide)
PTFE	Polytetrafluoroethylene
Q ₁₅	Moles of toluene absorbed by 1g of polymer after 15 minutes
RDX	Research department explosive
rpm	Revolutions per minute
SEM	Scanning electron microscopy
TBAF	Tetrabutylammonium fluoride
TBDMSCI	^t Butyldimethylsilyl chloride
^t Bu	<i>tert</i> -Butyl
TDI	Toluene diisocyanate
T _g	Glass transition temperature
TGA	Thermogravimetric analysis
THF	Tetrahydrofuran
TMS	Tetramethyl silane
TMXDI	Tetramethylxylylene diisocyanate
TNT	Trinitrotoluene
UCA	Ultrasound contrast agent
UV	Ultraviolet
VTIR	Variable temperature infrared
W	Watt
XDI	Xylylene diisocyanate

Table of Contents

Chapter 1 Introduction	1
Abstract.....	1
1.1. High Explosives.....	1
1.2. Design of Explosive Shells.....	2
1.3. Rowanex 1100 1A.....	4
1.4. The Microencapsulation Approach to the Controlled Delivery of Crosslinkers.....	5
1.4.1. Microcapsules.....	5
1.5. Microcapsule Applications.....	6
1.5.1. Microencapsulation of Fragrances.....	6
1.5.2. Microencapsulation of Agrochemicals.....	6
1.5.3. Microencapsulation of Food Additives.....	7
1.5.4. Microencapsulation of Pharmaceuticals.....	7
1.5.5. Microencapsulation of Phase Change Materials.....	7
1.5.6. Functional Textiles.....	8
1.5.7. Healable Materials.....	8
1.6. Microcapsule Synthesis.....	9
1.6.1. Dispersion Polymerisation Approach to Microcapsule Synthesis.....	10
1.6.2. Interfacial Polymerisation Approach to Microcapsule Synthesis.....	11
1.6.3. Multi-Walled Microcapsules.....	13
1.7. Microcapsule Properties.....	14
1.7.1. Microcapsule Diameter and Size Distribution.....	14
1.7.2. Shell Wall Thickness.....	15
1.7.3. The Microcapsule Core.....	15
1.7.4. Physical Strength of Microcapsules.....	16

1.8. Microcapsule Release Triggers	16
1.8.1. Release of Microcapsules with External Pressure	16
1.8.2. Release of Microcapsules Using Ultrasound	16
1.8.3. Release of Microcapsules Using a Chemical Trigger	18
1.8.4. Release of Microcapsules by Irradiation with Light	18
1.8.5. Release of Microcapsules by Exposure to Heat	18
1.9. Thermally Labile Linkers	19
1.10. Blocked Isocyanates	20
1.10.1. The Effect of Isocyanate Structure on Dissociation Temperature	21
1.10.2. Aromatic Heterocycles Blocking Groups	22
1.10.3. Isocyanates Blocked With Bulky Secondary Amines	23
1.10.4. Phenolic and Alcohol Blocking Groups	25
1.10.5. Oxime Blocking Groups	26
1.10.6. Amide Blocking Groups	28
1.10.7. The Effect of Catalysts on Dissociation Temperature	28
1.10.8. Measuring the Dissociation Temperature	28
1.11. Project Aims	29
1.12. References	30
Chapter 2	
Design of Thermally-Degradable Polymeric Shell Wall Precursors by Exploiting the Thermally Reversible Oxime-Urethane Bond	39
Abstract	39
2.1. Introduction	39
2.2. Results and Discussion	40
2.2.1. Protection of the Hydroxy-Functionalised Ketones	42
2.2.2. Conversion of Protected Ketones to Oximes	43
2.2.3. Synthesis of Thermally-Labile Oxime-Urethane	45

2.2.4. Deprotection to Reveal Reactive Phenolic Functionality	47
2.2.5. Synthesis of Isocyanate-Terminated Shell Wall Precursors	49
2.2.6. The Dissociation of Thermally Labile Linkers	51
2.2.6.1. Variable Temperature Infra-red Spectroscopy	52
2.2.6.2. Differential Scanning Calorimetry	54
2.2.6.3. Thermogravimetric Analysis	55
2.3. Conclusion	57
2.4. Experimental	57
2.5. References	73

Chapter 3

Synthesis of Thermally-Releasable Microcapsules for the Controlled Delivery of Isocyanate Crosslinkers	75
Abstract	75
3.1. Introduction	75
3.2. Results and Discussion	77
3.2.1. Optical Microscopic Analysis	79
3.2.2. Analysis Using Scanning Electron Microscopy	81
3.2.3. FTIR Spectroscopic Analysis of Microencapsulated Core	83
3.2.4. ¹ H NMR Spectroscopic Analysis of the Microencapsulated Core	84
3.2.5. Thermogravimetric Analysis of the Microencapsulated Core	85
3.2.6. Release of Microencapsulated Core Using a Heat Stimulus	86
3.2.7. Delayed Cure of HTPB Using Microencapsulated Crosslinkers	88
3.2.8. Control of the Microcapsule Properties	90
3.2.8.1. The Effect of the Rate of Agitation	91
3.2.8.2. The Effect of the Surfactant Concentration	93
3.2.8.3. The Effect of the Hydrophobic Solvent	94
3.2.8.4. The Effect of the Concentration of the Shell Wall Precursor	95

3.2.8.5. The Effect of the Reaction Time.....	96
3.2.8.6. Maximising the IPDI Content of Microcapsules.....	97
3.2.8.7. The Effect of the Chain Extender Concentration.....	98
3.2.9. Microencapsulation of a Dye.....	99
3.3. Conclusion.....	101
3.4. Experimental.....	102
3.5. References.....	108
Chapter 4	
Exploiting Reversible Diels-Alder Adducts for the Design of	
Thermally-Releasable Microcapsules	110
Abstract.....	110
4.1. Introduction.....	110
4.2. Results and Discussion.....	111
4.2.1. Protection of Maleic Anhydride with Furan.....	112
4.2.2. Conversion of Protected Maleic Anhydride to Maleimide.....	113
4.2.3. Deprotection to form Hydroxy-Functionalised Maleimide.....	114
4.2.4. Diels-Alder Reaction of Maleimide and Furfuryl Alcohol.....	115
4.2.4. Synthesis of the Shell Wall Precursor.....	115
4.2.4. Dissociation of the Diels-Alder Adduct.....	117
4.2.5. Synthesis of Microcapsules.....	118
4.2.6. Optical Microscopic Analysis of Microcapsules.....	119
4.2.7. Analysis of Microcapsules using Scanning Electron Microscopy.....	119
4.2.8. Analysis of Microencapsulated Core using FTIR Spectroscopy.....	120
4.2.9. ¹ H NMR Spectroscopic Analysis of the Microencapsulated Core.....	121

4.2.10. Release of Microencapsulated Core Using a Heat Stimulus	122
4.2.11. Increasing the Mechanical Strength of Microcapsules	123
4.3. Conclusion	124
4.4. Experimental	125
4.5. References	128
Chapter 5	
Delayed Quick-Cure of Hydroxy-Terminated Polybutadiene using Thermally-Reversible Blocked Isocyanates	130
Abstract	130
5.1. Introduction	130
5.2. Results and Discussion	132
5.2.1. Amine Blocking Groups	132
5.2.2. Amide Blocking Groups	133
5.2.3. Oxime Blocking Groups	134
5.2.4. Aromatic Heterocycle Blocking Groups	136
5.2.5. Phenol Blocking Groups	136
5.2.6. Dissociation of Blocked-IPDI	137
5.2.7. Cure of HTPB using Blocked-IPDI	139
5.2.8. Effect of Steric Hindrance on the Dissociation of Oxime-Urethanes	140
5.2.9. Electron Effects on the Dissociation of Oxime-Urethanes	141
5.2.10. Curing Studies of HTPB Using Oxime-Urethanes	143
5.2.11. Monitoring the Curing of HTPB	145
5.2.12. Synthesis of Blocked Isocyanate Prepolymer	147
5.3. Conclusion	148
5.4. Experimental	149
5.5. References	165

Chapter 6 Conclusions	167
Chapter 7 Future Perspectives	170
Chapter 8 Appendix	174

Chapter 1

Introduction

Abstract

Modern high explosives consist of an energetic material bound within a rigid polymer matrix and are thus known as plastic or polymer bonded explosives (PBX). The current method for the manufacture of such materials involves addition of a diisocyanate crosslinker to multi-component formulation featuring the explosive and a hydroxy-functionalised elastomeric polymer in order to generate a stable polymer network post cure. This chapter first describes this process and highlights the drawbacks resulting from the immediate polymerisation reaction between the isocyanate and polymer that ensues. The use of microencapsulation technologies to deliver the crosslinker in PBX systems is postulated as a potential solution in order to yield a more desirable end product. The second part of this chapter reviews state-of-the-art microencapsulation technologies describing how microcapsules can be designed with specific properties in order to achieve the release of the diisocyanate crosslinker when desired using an external application of heat.

1.1. High Explosives

An explosive is defined as a substance that upon ignition undergoes rapid chemical reactions, releasing large quantities of heat and causing a massive increase to the surrounding pressure.¹ Explosives first appeared in Europe as early as 13th century, known as black powder, the crude mixture comprised charcoal, potassium nitrate and sulfur. In 1846, Italian chemist Ascanio Sobrero successfully nitrated glycerol to form the highly sensitive explosive nitroglycerine. The subsequent dangers associated with the poor stability of nitroglycerine prevented its extensive use in military applications and led to the development of more stable high explosives such as trinitrotoluene (TNT) which saw large-scale employment in the First World War. Further research in the field has seen modern munitions replacing TNT with the more powerful high explosive cyclotrimethylenetrinitramine *Research Department Explosive* (RDX, Type 1) (Figure 1.1).¹ The development of high explosives evolved conjointly with their methods of deployment. Two decades after the synthesis of nitroglycerine, Alfred Nobel observed the explosive could be desensitized by dispersing it in clay. Nobel patented his invention as 'dynamite' in 1867. The concept of desensitization by

dispersing in a matrix has not changed since this time. Since the Second World War high explosives have been desensitised using polymer matrices, commonly referred to as 'Plastic or Polymer Bonded Explosives' (PBX).²

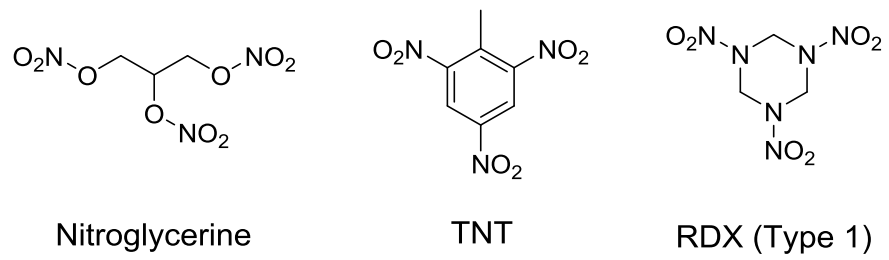


Figure 1.1. The structures of high explosives - nitroglycerine, trinitrotoluene (TNT) and Research Department Explosive (RDX).

1.2. Design of Explosive Shells

The earliest bombs consisted of a black powder packed into cases of canvas, wood or iron, detonated by a slow burning fuse. By the early 20th century high explosives were contained in steel case projectiles, referred to as 'stores'. The bulk explosive payload is relatively insensitive, requiring a fuse to detonate the explosive (Figure 1.2).

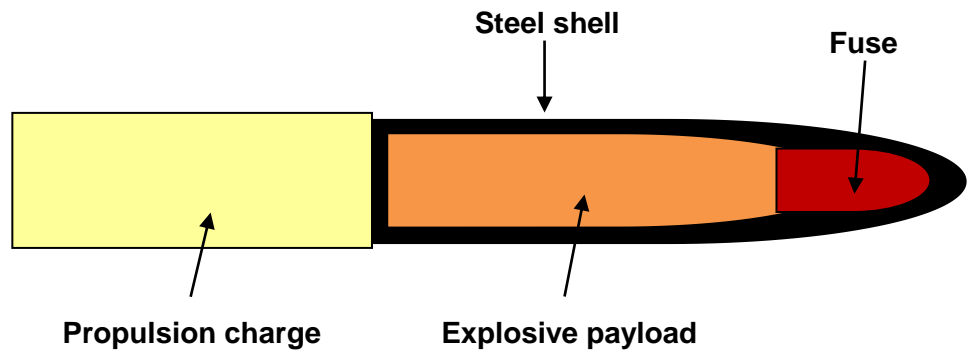
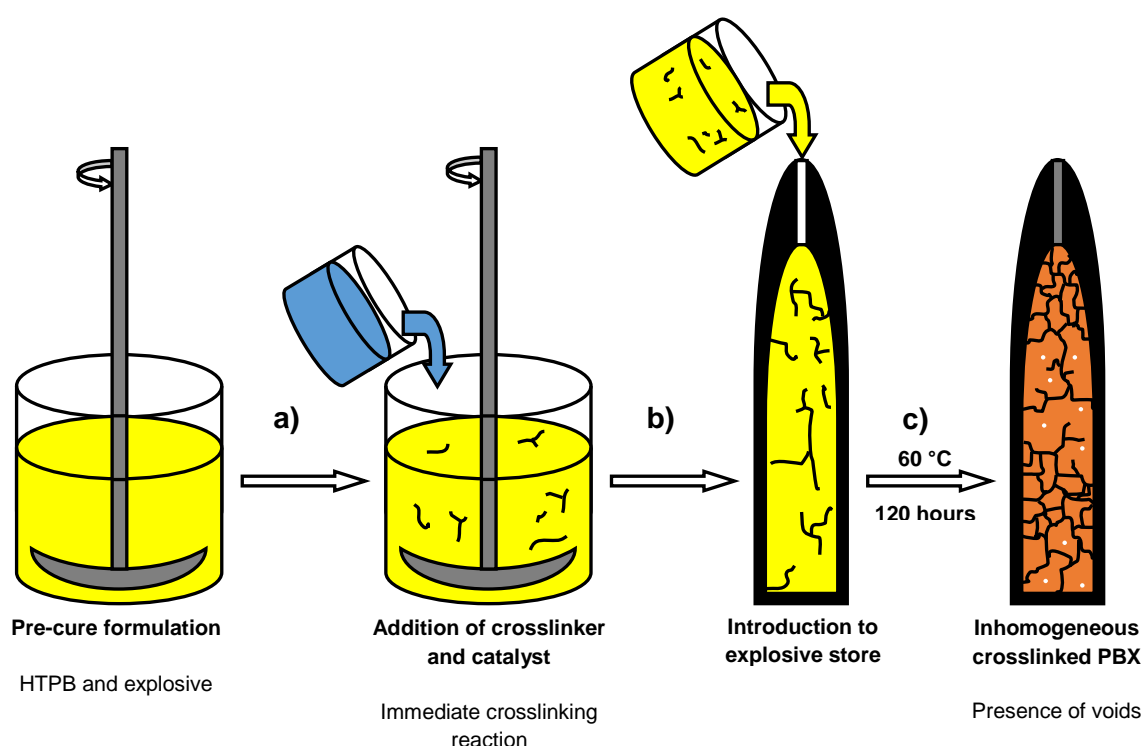


Figure 1.2. Simple design of an explosive shell, highlighting the propulsion charge, explosive payload, shell and fuse.

In the early years of the 20th century, explosives were introduced to the store by a melt-cast process. The explosive formulation was melted and poured into the store. However, during the cooling and resolidification process adverse conditions could lead to cracking and formation of voids. Upon firing, these voids experience an increase in G-force to an excess of 13,000 G, a change that causes an extreme adiabatic compression process, sufficiently increasing the temperature above the explosives ignition point, thus posing a potentially fatal hazard to the gun operative. In addition, high explosives are susceptible to small arms fire, shrapnel and external fire.

This sensitiveness to impact can be avoided by incorporating PBX within the stores, effectively desensitising the explosive material. The current process used to incorporate PBX within explosive stores involves mixing the explosive with a hydroxyl-functionalised aliphatic polymer to form a pre-cure, the form in which the mixture is stored in. Curing is initiated by addition of a crosslinker plus a catalyst and the resultant mixture is then warmed to 55 - 70 °C. Upon the addition of the crosslinker, an instantaneous crosslinking reaction occurs and thus filling of the stores must commence immediately before extensive crosslinking can occur. The filled stores are cured in an oven at 60 °C for a period of 120 hours to ensure exhaustive crosslinking occurs (Scheme 1.1).



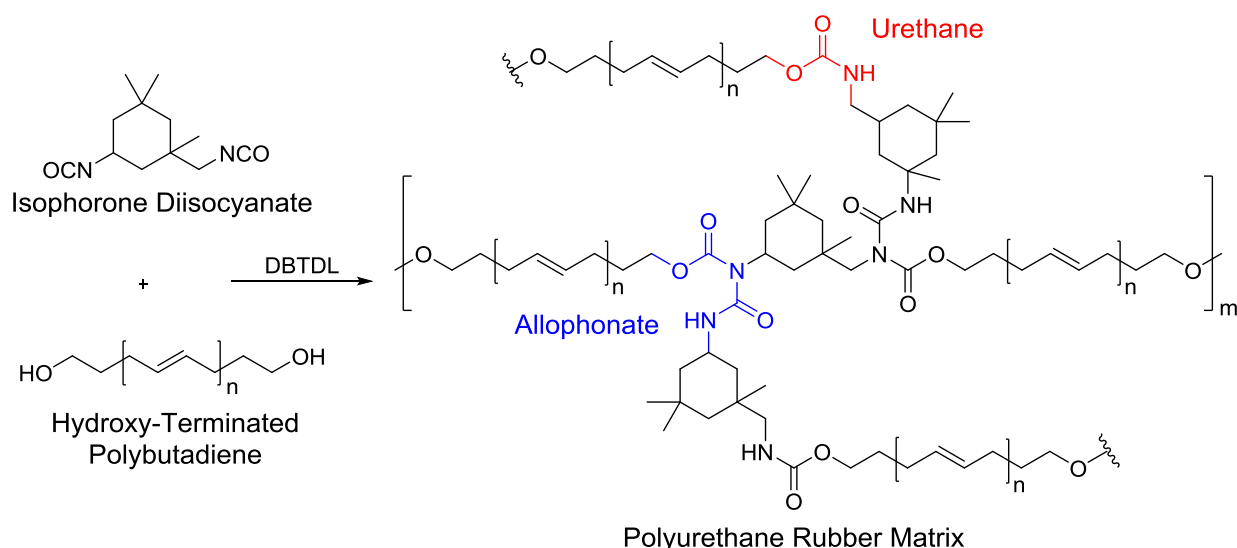
Scheme 1.1. Scheme illustrating the current method involved in casting PBX in stores, highlighting **a)** the addition of a crosslinker and catalyst, **b)** introduction to the explosive store and **c)** the formation of an inhomogeneous crosslinked PBX.

However, the manufacturing process can prove to be unreliable. The dispersion of the crosslinker in the mixture is not always even, leading to regions of low crosslinking density and the presence of voids. In addition, as a result of the ongoing crosslinking reaction, consecutively filled stores possess an increasingly inhomogeneous crosslinked PBX. The process also imposes restrictions on the catalyst concentration. In order to reduce the rate of crosslinking reaction the catalyst is in very low

concentration levels (0.01 wt %), which in turn, contributes to poor crosslinking density and a product of variable quality.

1.3. Rowanex 1100 1A

One PBX formulation developed for use in explosive stores is Rowanex 1100 1A. It is comprised primarily of RDX and is bound in a rubbery polyurethane matrix prepared from hydroxy-terminated polybutadiene (HTPB) plus a crosslinker, isophorone diisocyanate (IPDI). The crosslinking reaction is catalysed by dibutyltin dilaurate (DBTDL) (Scheme 1.2). The hydroxyl moiety of HTPB reacts with the electrophilic carbon of the isocyanate units of IPDI to form urethane linkages. Furthermore, within the polymerisation matrix, reaction of isocyanate and the urethane nitrogen leads to the formation of allophanate crosslinks.



Scheme 1.2. Scheme representing the crosslinking of HTPB with IPDI when catalysed with DBTDL.

The components of Rowanex 1100 are listed in Table 1.1. It consists of RDX, HTPB pre-polymer, a plasticiser, an antioxidant to inhibit oxidation of material, a surfactant, IPDI crosslinker, DBTDL catalyst and an antifoaming agent.

Table 1.1. Rowanex 1100 1A explosive formulation.

Constituent	Composition (wt %)
RDX	> 80
HTPB R45HT	< 20
Plasticiser	
Antioxidant	
Surfactant	
IPDI	
DBTDL	
Antifoaming Agent	

1.4. The Microencapsulation Approach to Controlled Delivery of Crosslinkers

Within the context of this investigation, it is proposed that microencapsulation technology will allow the uniform delivery of the crosslinker IPDI, thus achieving a homogeneously crosslinked rubber matrix. In addition, microencapsulation of the crosslinker may have several other benefits - control of the crosslinking reaction until desired can be achieved; thus filling of the stores does not need to occur immediately, the catalyst concentration can be increased; further contributing to the formation of a more uniform matrix and prevention of the exposure of toxic isocyanates to the process engineers.

1.4.1. Microcapsules

Microencapsulation involves the envelopment of a core substance within a protective shell which is typically composed of either - gel, surfactant, electrolyte³ or polymer.⁴ Polymer microcapsules can be classified into three types - mononuclear,⁵ polynuclear⁶ and matrix.^{7,8}

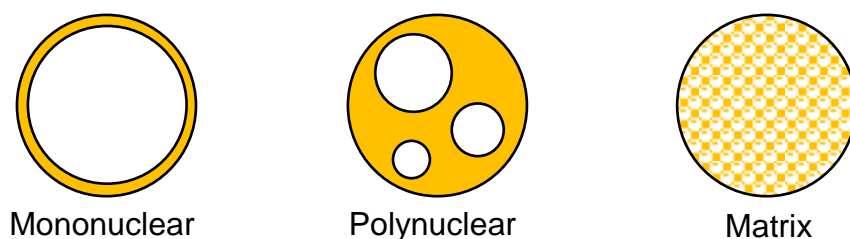


Figure 1.3. Design of mononuclear, polynuclear and matrix microcapsules.

Mononuclear microcapsules consist of a solid shell that surrounds a central core and polynuclear microcapsules are comprised of many cores within the solid shell. In contrast, matrix-type microcapsules do not possess a core - rather, the active substance is bound within the polymer matrix (Figure 1.3).⁵ Mononuclear microcapsules are typically spherical, between 1 - 1000 μm in diameter and deliver the highest payload of encapsulated core.⁹

1.5. Microcapsule Applications

The intrinsic microcapsule core encompasses the active agent which may be solid, liquid or gas depending on its ultimate application.⁹ A range of liquid active agents have been enclosed in microcapsules, including - fragrances,^{10 11} pesticides and agrochemicals,¹² food additives¹³ pharmaceuticals and industrial chemicals,¹⁴ The following section reviews the literature surrounding the uses of microencapsulated liquid agents.

1.5.1. Microencapsulation of Fragrances

Fragrances and perfumes are used extensively in textiles, cosmetics, deodorants and scented household items. However, the high volatility of fragrant molecules restricts the active lifetime of the scent.¹⁵ Microencapsulation technologies prolong the lifetime of fragrances by allowing a sustained release of the active agent,^{16,17} retaining up to 90% of the fragrance after a period of 100 days.¹⁸ Release mechanisms of microencapsulated fragrances have been developed¹⁹ by exploiting the degradation of encapsulated α -ketoesters. Exposure of such moieties to UV-light generates gaseous CO_2 , causing an increase in the internal pressure of the microcapsules sufficient to rupture the microcapsules and releasing the fragrance. Further to this, microcapsules that release fragrances upon exposure to acidic environments such as sweat have been reported.^{20,21}

1.5.2. Microencapsulation of Agrochemicals

Pesticides and other agrochemicals exhibit high volatility and toxicity, reducing their activity and posing a health exposure risk. Microencapsulation offers a method of gradually releasing the active agent, thus prolonging the activity of these expensive chemicals and preventing exposure.^{22,23,24} In conjunction with the microencapsulation of conventional chemical pesticides, the encapsulation of insect pheromones have been investigated.²⁵ The release of the pheromone around crops disrupts the insects

mating process, resulting in the reduction of the insect population and in turn increasing the crop yield.²⁶

1.5.3. Microencapsulation of Food Additives

Recently, there has been a growing interest in microencapsulation of active agents used specifically in the food industry.²⁷ Many food additives exhibit poor stability towards oxidation, high reactivity to other components present in food and indeed certain additives are irritant in high concentrations preventing their extensive use in food products.^{28,29} Microencapsulation offers a route to overcome these problems and many food additives have now been stored in microcapsules, including - vitamins, fatty acids, minerals and antioxidants.²⁷

1.5.4. Microencapsulation of Pharmaceuticals

Microencapsulation is being employed increasingly in drug delivery vehicles. Many drugs are susceptible to chemical and enzymatic degradation - insulin for example is degraded by the acidic conditions of the stomach and as such must be administered intravenously. Microencapsulated insulin prevents drug degradation and can be released from the microcapsules in the circulatory system.³⁰ Many anticancer drugs exhibit high toxicity, attacking cancerous and healthy tissue indiscriminately. Employing microcapsules as drug carriers allows release of the drug to the targeted site, preventing exposure to healthy cells whilst simultaneously achieving an increased payload.^{31,32} Microencapsulated drug delivery was further developed³³ by incorporating magnetic nanoparticles into the microcapsules, allowing the drugs to be directed to the targeted site with the application of a magnetic field.

1.5.5. Microencapsulation of Phase Change Materials

Certain substances undergo phase changes at a near constant temperature and are capable of releasing and storing large amounts of energy during the change. These are known as phase change materials (PCMs) and are employed in systems required to absorb or release large quantities of heat.³⁴ Typically, PCMs need to be bound within polymer matrices in order to prevent loss during melting and improve conductivity. Unfortunately, PCMs leak from such composites significantly limiting their lifetime capability.³⁵ Storing PCMs within polymer microcapsules avoids leakage whilst still providing good conductivity.³⁶

1.5.6. Functional Textiles

Microcapsules containing a host of active liquid agents have been bound to the fibres of textiles to fabricate a wide range of functional materials.³⁷ Microcapsules containing a number of fragrances have been used to prolong the freshness of clothing and linen.³⁸ Microencapsulated insect repellents bound to linen have been produced³⁹ to combat malaria and other insect borne diseases. A method of prolonged drug delivery using textiles that incorporate microencapsulated pharmaceuticals has been demonstrated.⁴⁰ Clothing and blankets for use in extreme weather conditions that have potential to absorb or release heat by exploiting microencapsulated PCMs have been developed.⁴¹ In addition, functional fabrics have been employed for protection of military personnel against chemical weapons. Microcapsules bound to the fabric fibres contain decontamination agents that chemical warfare agents diffuse into and undergo irreversible degradation reactions.⁴²

1.5.7. Healable Materials

Microencapsulation technology has been employed to deliver crosslinkers in self-healing composites.⁴³ Polymer materials are used extensively in electronics, the automotive industry, coatings and extreme environments such as aircraft fuselages.^{44,45} The harsh conditions of chemical attack, radiation, abrasion and impact experienced by these materials leads to the formation of micro-cracks.⁴⁶ The ability to heal such defects reduces polymer degradation and maintenance down-time. Microcapsules containing healing agents have been synthesised and incorporated into polymer composites and matrices.⁴³ Upon the formation of cracks, the microcapsules are ruptured, releasing the healing agent and drawing it to the damaged area via capillary action, subsequently repairing the damage.⁴⁷ An epoxy matrix containing Grubb's catalyst and urea-formaldehyde capsules containing dicyclopentadiene (DCPD) has demonstrated successfully this healing strategy (Scheme 1.3).⁴⁸ The drawback of this technology is that the healed area is composed of a different polymer to the epoxy matrix with only 75 % of the original toughness. This performance differential renders the heterogeneous composite vulnerable to further microcrack formation. This approach was developed further by Yang *et al.* to encapsulate IPDI⁴⁹ and hexamethylene diisocyanate (HDI)⁵⁰ in polyurethane microcapsules using an interfacial polymerisation technique.⁴⁹ Once embedded in an epoxy matrix the healing technology functions in an analogous fashion to the DCPD systems.⁵⁰ An additional

limitation is that once a region has been healed, further damage events in the area cannot be healed again.^{51,52}

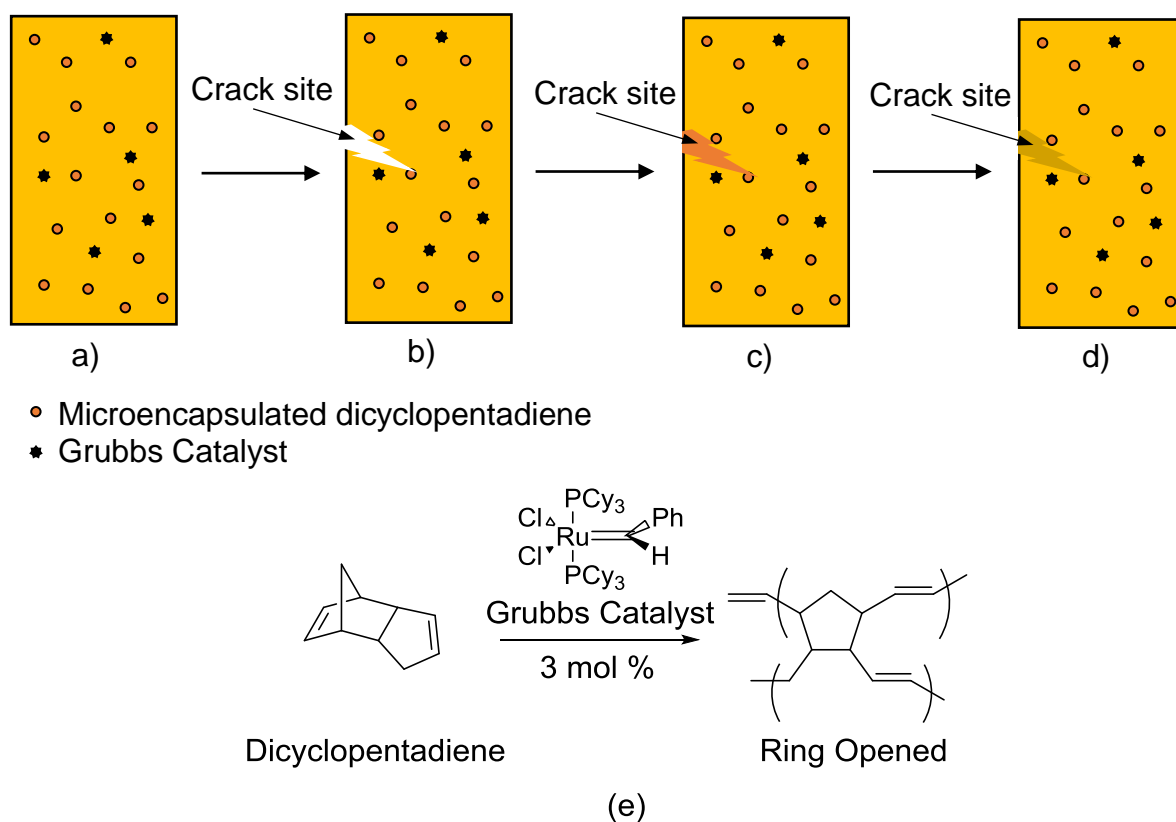


Figure 1.4. Microcapsule release in a self-healing composite. **a)** pristine material, **b)** crack-formation, **c)** crack-propagation and rupture of the macrocapsules, **d)** crack-healing via metathesis polymerisation and **e)** ring opening metathesis polymerisation of DCPD.

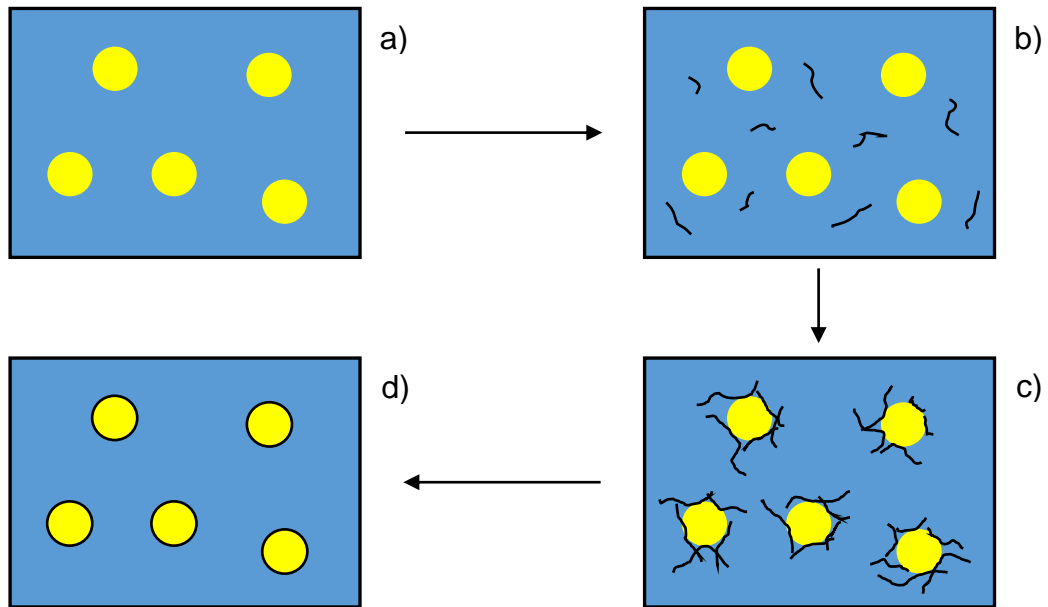
One solution to this issue was to incorporate refillable microtubules that span the composite matrix which enabled repeated delivery of the healing agent to the same damaged zone.⁵³ Indeed the self-healing ability of this composite material was demonstrated over several break-heal cycles.

1.6. Microcapsule Synthesis

Microcapsule synthesis can be achieved using a variety of techniques. These are conveniently categorised into chemical and physical approaches. Physical methods include - suspension crosslinking,⁵⁴ solvent evaporation,⁵⁵ coacervation,⁵⁶ spray drying,⁵⁷ layer-by-layer deposition,⁵⁸ supercritical fluid expansion⁵⁹ and the spinning disk approach.⁶⁰ Chemical methods include suspension polymerisation,⁶¹ emulsion polymerisation,⁶² interfacial polymerisation⁶³ and dispersion polymerisation.⁶⁴ Of these techniques, interfacial polymerisation and dispersion polymerisation most commonly are used to encapsulate liquid active agents.⁹

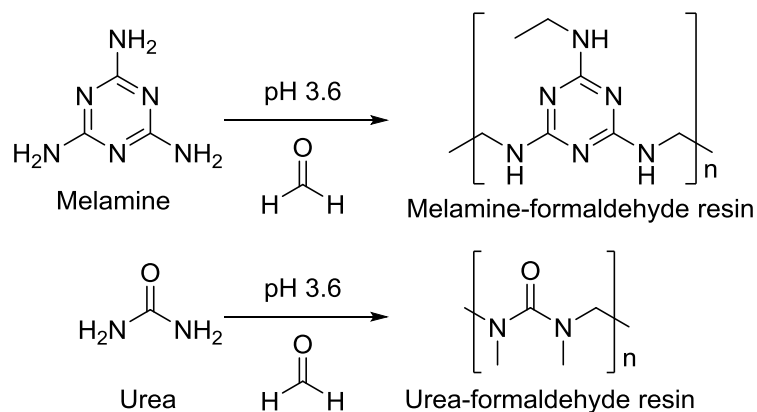
1.6.1. Dispersion Polymerisation Approach to Microcapsule Synthesis

Microencapsulation using this technique involves dissolving the core material in a water-immiscible organic solvent followed by emulsion in the polymerisation medium (Scheme 1.4).⁶⁵



Scheme 1.3. Synthesis of microcapsules using dispersion polymerisation technique. **a)** core dispersed in polymerisation medium, **b)** oligomers begin to form, **c)** polymers collapse on surface of oil droplet and **d)** formation of the microcapsule shell.

Following initiation, a polymerisation ensues and oligomers begin to form. Eventually polymers collapse onto the surface of the emulsion droplet and after several hours of reaction, the oil droplet is enveloped in a polymeric shell enclosing the active agent.⁶⁶ Most dispersion polymerisation encapsulations involve the reaction of formaldehyde with either melamine⁶⁷ or urea⁶⁸ at a controlled pH (3.5) to form an amino resin shell (Scheme 1.5).



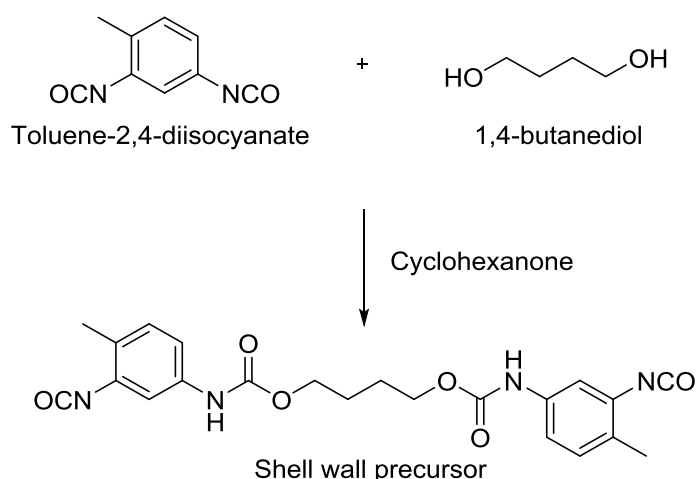
Scheme 1.4. Synthesis of melamine-formaldehyde and urea-formaldehyde resins.

This approach to microencapsulation has been used to encapsulate pesticides and active agents able to provide self-healing ability in polymer materials.^{69, 70} The technique allows control of microcapsule properties by careful modification of the reaction procedure parameters, including - pH, monomer concentration, surfactant concentration and the agitation rate.⁷¹

1.6.2. Interfacial Polymerisation Approach to Microcapsule Synthesis

Interfacial polymerisation offers a simple and reliable approach to the synthesis of microcapsules. Microencapsulation typically employs oil-in-water emulsions.⁷² However, water-in-oil⁷³ and oil-in-oil⁷⁴ emulsions have also been developed. The microcapsule shell is formed by a condensation polymerisation reaction at the liquid-liquid interface and usually employs polyisocyanates in the oil phase polymerised with polyols and polyamines to give polyurethane⁷⁵ and polyurea⁷⁶ shells, respectively. Polyamide microcapsules can also be synthesised by corresponding reaction of polyacylchlorides and polyamines.⁷⁷

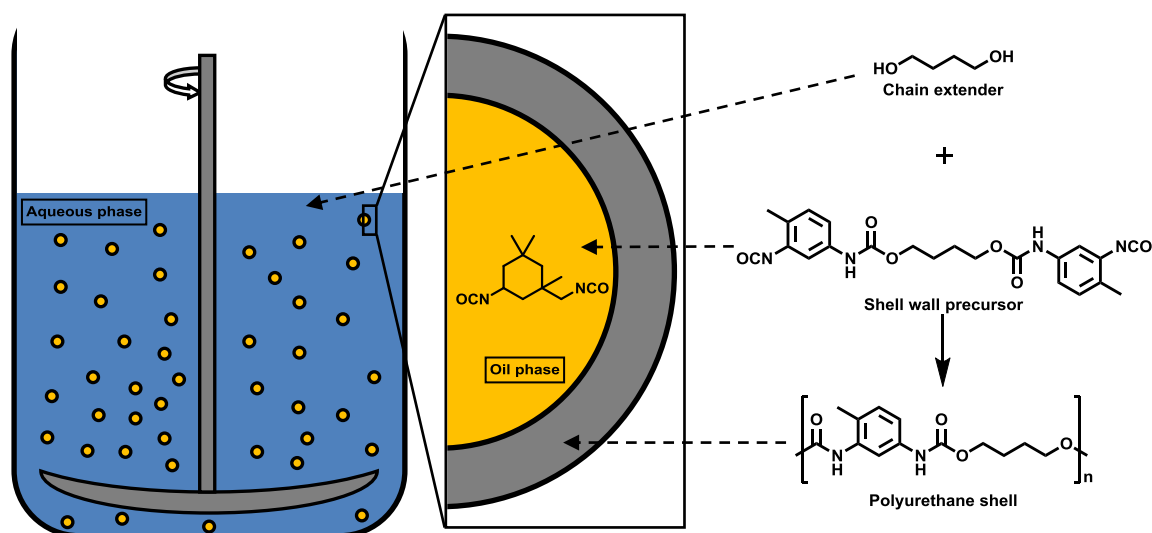
Yang *et al.*⁴⁹ microencapsulated IPDI successfully in polyurethane microcapsules. This was achieved by reaction of toluene-2,4-diisocyanate (TDI) with 1,4-butanediol to yield an isocyanate-terminated shell wall precursor capable of further chain extension (Scheme 1.6) to form a microcapsule shell.



Scheme 1.5. Reaction of toluene-2,4-diisocyanate with 1,4-butanediol to yield a shell wall precursor.

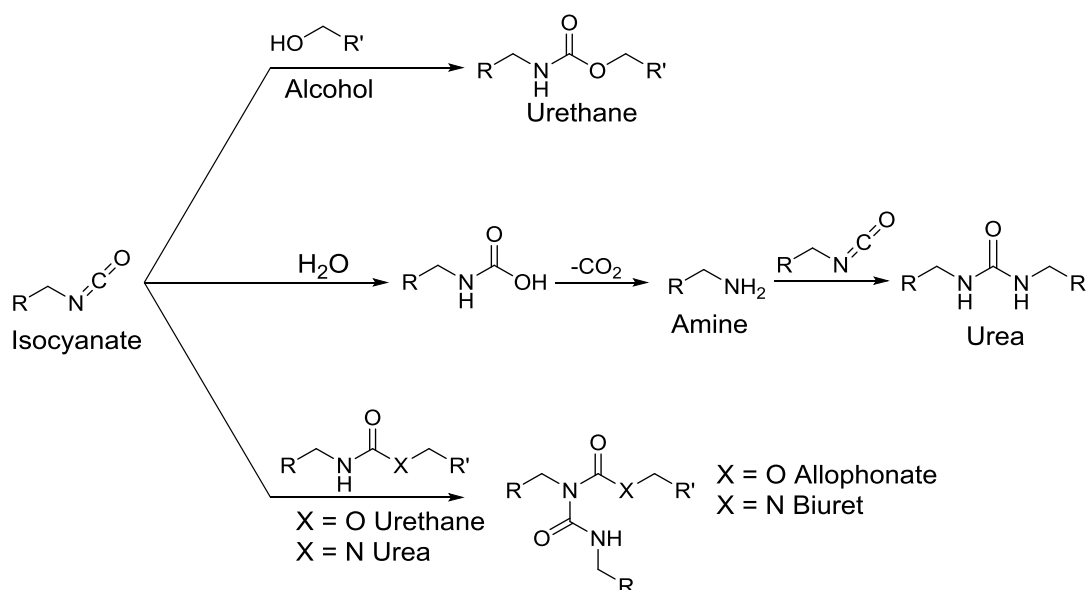
Microcapsules were formed following emulsification of a hydrophobic solution of the shell wall precursor and IPDI in water with the aid of a surfactant and mechanical agitation. Upon the addition of 1,4-butanediol, chain-extension occurred at the oil-

water interface forming a polyurethane shell that enveloped the active IPDI core (Scheme 1.7). The reaction of IPDI was avoided as a result of the high reactivity of TDI outcompeting the relatively less reactive IPDI crosslinker.^{78,79}



Scheme 1.6. Synthesis of microcapsules using interfacial polymerisation showing the emulsified oil droplets containing the shell wall precursor reacting at the oil-water interface to form microcapsules.

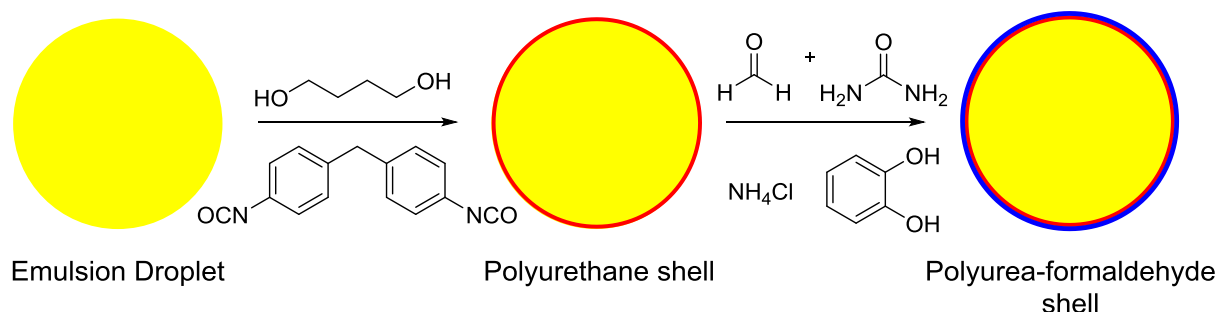
In this approach to polyurethane microcapsules, a reaction occurs predominately between the alcohol and isocyanate moieties of the polymerisation agents, although reaction with water is also expected. Subsequent decarboxylation to form an amine allows polymerisation with further isocyanate to form a urea. In addition, crosslinking occurs between the urethane and urea nitrogen with residual unreacted isocyanate present to form allophanate and biuret crosslinks (Scheme 1.8).^{80,81}



Scheme 1.7. Reactions involved in the synthesis of polyurethane microcapsules.

1.6.3. Multi-Walled Microcapsules

Microcapsules are prone to damage and leakage which ultimately reduces their shelf-lives. In order to increase their strength and durability, microcapsules with multiple layered shells have been developed. Caruso *et al.* have developed⁸² a synthesis that encompasses sequential interfacial and dispersion polymerisations to yield microcapsules that possess an internal polyurethane shell and an external polyurea-formaldehyde shell (Scheme 1.9). These microcapsules demonstrated an increased mechanical strength and an improved stability at high temperatures (180 °C). Multi-walled polyurethane-urea microcapsules have also been synthesised by Yang *et al.*, using a similar approach and these materials also exhibit an increase in thermal stability.⁸³



Scheme 1.8. Synthesis of multi-walled polyurethane-urea microcapsules, highlighting the formation of an initial polyurethane shell and a polyurea-formaldehyde shell.

1.7. Microcapsule Properties

The interfacial polymerisation approach allows control of the microcapsules properties - diameter and size distribution, shell wall thickness, payload of core in microcapsules and physical strength (Figure 1.4).⁴⁹ These properties can be controlled by careful modification of the synthetic parameters - rate of agitation,⁸⁴ concentration of shell wall precursor, concentration of chain extender, selection of the solvent, concentration of active encapsulant, surfactant concentration,⁸⁵ reaction temperature⁸⁶ and reaction time.⁸⁷

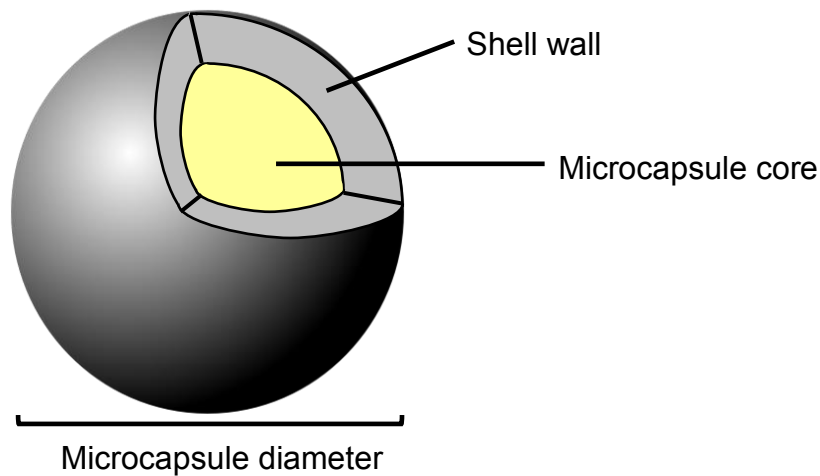


Figure 1.5. Design of a mononuclear microcapsule showing the microcapsule diameter, shell wall and microencapsulated core.

1.7.1. Microcapsule Diameter and Size Distribution

Microcapsule diameter can be controlled by rate of agitation⁸⁸ and concentration of the surfactant.⁸⁵ Interfacial polymerisation employs mechanical agitation of the emulsion to ensure the formation of uniformly sized oil droplets. Increasing the speed of agitation imparts a greater degree of shear force experienced by the emulsion leading to smaller oil droplets and in turn the formation of smaller microcapsules. Increasing agitation rate also narrows the size distribution,^{49,50,88} granting a way of designing microcapsules with diameters within a desired range.

Surfactants are employed in interfacial polymerisation in order to achieve a stable emulsion.⁸⁹ These amphiphilic materials work by reducing the surface tension at the oil-water interface and increasing the concentration of surfactant reduces the surface tension of the emulsion, thus forming smaller oil droplets, leading to the formation of smaller microcapsules and a uniform size distribution.^{85,90} Cellulose-based surfactants

such as gum arabic are often utilised,⁸⁹ although polymeric surfactants such as polyvinyl alcohol are also used.⁹¹

Selection of the hydrophobic solvent is also important. Organic solvents possess different surface tensions⁹² and thus employing different solvents will lead to the formation of different sized oil droplets.

1.7.2. Shell Wall Thickness

The physical strength of microcapsules is largely dependent on the thickness of the shell wall⁹³ and control of this property is important in order to design microcapsules that possess suitable strength. Microcapsule shell wall thickness can be controlled by reaction temperature, reaction time, use of catalysts and concentration of shell wall precursor.

It has been reported⁸⁶ that at higher temperatures the rate of the isocyanate-alcohol reaction during microcapsule synthesis is increased. By increasing the inclusion of IPDI in shell wall synthesis, thicker shell walls are formed and therefore increase the mechanical strength of the microcapsules.⁵⁰

Control of the microcapsule shell wall thickness can also be achieved by changing the reaction time.⁷⁰ It is thought that as the initial polymer shell forms, the chain extender will then diffuse across the membrane allowing further reaction to continue. A longer reaction time will, therefore, lead to an increase in shell wall thickness.^{87,50}

Urethane formation can be catalysed using a range of reagents. Typically tertiary amines⁹⁴ and organo-tin(VI)⁹⁵ complexes are employed in the synthesis of polyurethane microcapsules. Addition of catalysts to the oil phase may provide a way to controlling the shell wall thickness by increasing the contribution of aliphatic isocyanate to shell wall synthesis, allowing the formation of a thicker shell wall.

1.7.3. The Microcapsule Core

The microcapsule core typically consists of the active agent and a solvent. Ideally, the delivery of the maximum amount of active agent is desired and this payload can be controlled by changing the ratio of active agent and solvent used in microcapsule synthesis.⁴³ However, Yang *et al.*, have observed⁴⁹ agglomeration when the loading of microcapsules exceeded 70 % in IPDI filled microcapsules. Therefore, a careful

balance must be found between achieving a maximum payload whilst avoiding undesired agglomeration.

1.7.4. Physical Strength of Microcapsules

The physical strength of microcapsules is largely affected by the shell wall thickness and microcapsule diameter. Smaller microcapsules with thicker shell walls have been shown to possess a greater degree of physical strength when compared to larger microcapsules.⁹³ However, the nature and chemical composition of the shell wall polymer is also important. A degree of elasticity in microcapsule shell is desired, preventing damage during synthesis and also leading to the formation of stronger, more spherical microcapsules.^{96,97,98} The use of trifunctional isocyanate-terminated shell wall precursors leads to smaller more uniform microcapsules⁹⁹ and in turn increasing their physical strength.

1.8. Microcapsule Release Triggers

The release of the core content from microcapsules allows a desired controlled delivery of active agents. This objective has led to the development of a range of triggering mechanisms that cause the release of the microencapsulated core upon exposure to a specific stimulus including - external pressure, ultrasound, chemical (typically pH), light and heat.^{72,100}

1.8.1. Release of Microcapsules with External Pressure

Perhaps the most simplistic triggering mechanism is the release of the encapsulated core upon exposure to an external pressure. The force is sufficient to bring about a breach to the structural integrity of the microcapsule.⁹³ This trigger is used in self-healing composites where the material experiences a break thus causing the release of microcapsule core into the fracture site.⁴³

1.8.2. Release of Microcapsules Using Ultrasound

Ultrasonic radiation is a way of inducing pressure on the microcapsule surface without mechanical influence. There are two strategies of ultrasound which could be used to release microcapsules - acoustic cavitation and therapeutic ultrasound. Acoustic cavitation uses ultrasound at frequencies of 20 - 40 kHz, the sound waves bring about the formation and rapid collapse of microbubbles resulting in a short-lived high energy, high pressure environment (Figure 1.5).¹⁰¹

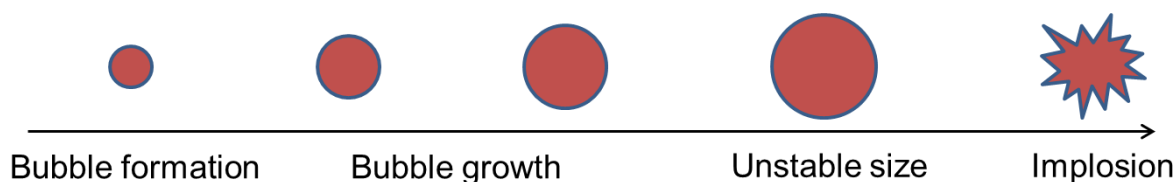


Figure 1.6. The formation and rapid growth of air-filled microbubbles followed by implosion, observed in ultrasonic cavitation phenomena.

Ultrasonic degradation of chain growth polymers has been well-reported.^{102,103} These studies involved irradiation of polymer solutions with a frequency of high powered ultrasound (24 kHz, 100 W)¹⁰⁴ to degrade polymers to a limiting molecular weight (Figure 1.6).

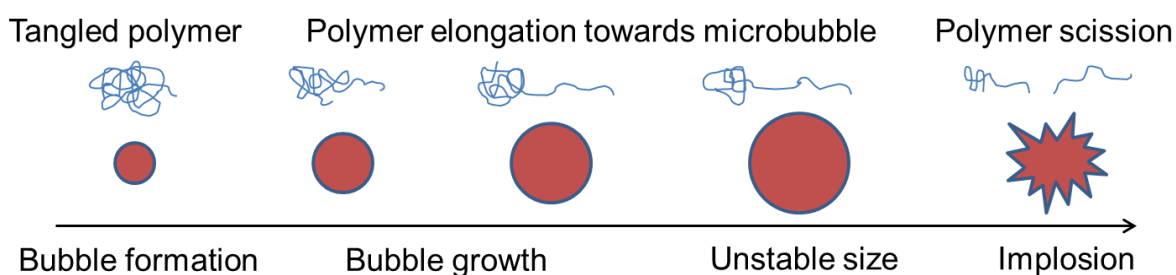
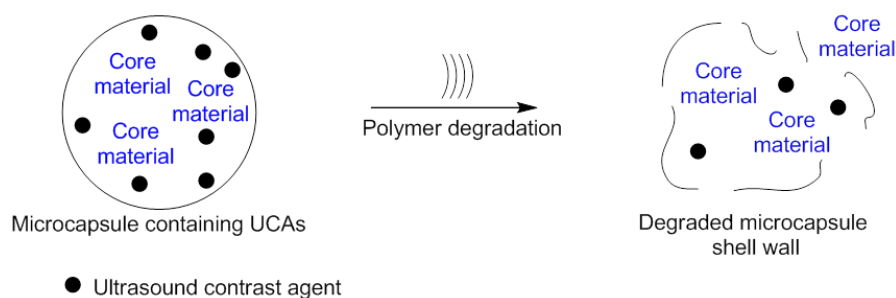


Figure 1.7. The effect of ultrasonic cavitation on linear polymers in solution.

Previous studies¹⁰⁵ conducted at The University of Reading demonstrated the release of IPDI and pyrene filled microcapsules. A suspension of microcapsules in CDCl_3 was irradiated with a frequency of ultrasound (44 kHz) for 1 hour. The release of pyrene from the microcapsules was recorded using fluorescence spectrophotometry to reveal almost complete release of pyrene from the polyurethane microcapsules.

High frequency, low powered therapeutic ultrasound (1 - 2.5 MHz, 0.035 - 0.5 W)¹⁰⁶ has been used to release polylactide microbubble ultrasound contrast agents (UCAs). Upon application of ultrasound, the UCAs resonate and bring about the degradation of the microcapsule shell wall (Scheme 1.10).^{107,108}



Scheme 1.9. The ultrasonic release of polymer-shelled microcapsules containing ultrasound contrast agents.

1.8.3. Release of Microcapsules using a Chemical Trigger

The need for drug delivery mechanisms has increased in recent years and as a result, many anti-cancer drugs have been encapsulated. The pH in cancerous tissue is lower than that of healthy tissue and release mechanisms have been developed to exploit this change,¹⁰⁹ often employing the acid catalysed covalent bond cleavage of acetal, orthoester, imine, hydrazone or ester linkages (Figure 1.7) in the polymer of the microcapsule shell wall.¹¹⁰ Upon the change in pH, the labile bond is cleaved causing the depolymerisation of the polymer shell of the microcapsule, releasing the core contents.

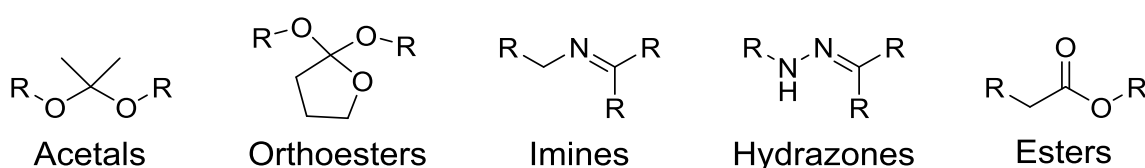


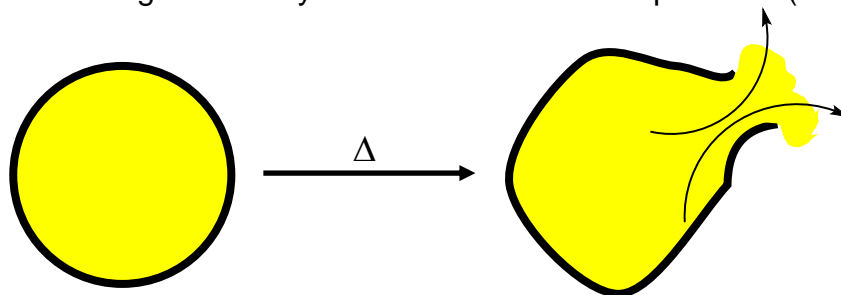
Figure 1.8. Structures of acetals, orthoesters, imines, hydrazones and esters.

1.8.4. Release of Microcapsules by Irradiation with Light

The release of active agents from microcapsules has been achieved by using light to switch polyelectrolyte microcapsules causing changes to the shell wall that lead to the formation of pores, allowing the core to be released.¹¹¹ Another route is to incorporate self-immolative polymers into the microcapsule shell that degrades upon exposure to different wavelengths of light causing rupture of the microcapsule and release of the core.¹¹²

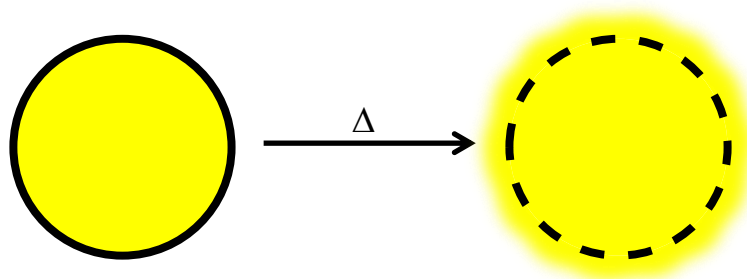
1.8.5. Release of Microcapsules by Exposure to Heat

Release of microcapsules by exposure to heat can be achieved by heating the material above the boiling point of the core solvent causing rupture of the microcapsule shell brought about by the increase in internal pressure (Scheme 1.11).⁷²



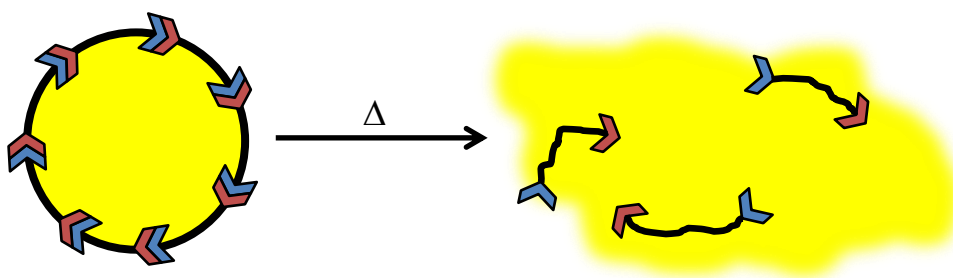
Scheme 1.10. The rupture of microcapsules achieved by heating above the boiling point of the encapsulated core.

Another method involves incorporating poly(*N*-isopropylacrylamide) (PNIPAM) into the pores of microcapsules. When exposed to heat PNIPAM shrinks, effectively opening the pores and allowing the release of the microcapsule core (Scheme 1.12).¹¹³



Scheme 1.11. Release of core from microcapsules by incorporating PNIPAM within the shell of the microcapsule. PNIPAM shrinks upon exposure to heat revealing pores in the microcapsule shell wall.

One approach that has not been widely documented in the literature is the incorporation of a thermally-labile linker within the polymer backbone of the microcapsule shell wall. Eggers *et al.* reported¹¹⁴ the synthesis of microcapsules prepared using a complex coacervation technique that incorporated thermally-labile maleimide-furan Diels-Alder adduct within the microcapsule shell wall. Release of the microcapsule core was achieved at 90 °C (Scheme 1.13). However, to date polyurethane microcapsules have not been prepared using an interfacial polymerisation approach that incorporate thermally-reversible bonds within the polymeric backbone of the microcapsule shell wall.

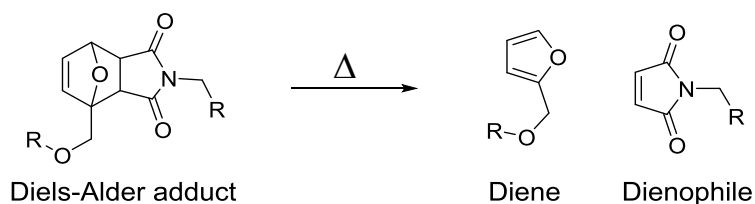


Scheme 1.12. Release of core from microcapsules achieved by depolymerisation of the microcapsule shell wall.

1.9. Thermally Labile Linkers

The field of thermally-cleavable covalent bonds has been, to date, dominated by the use of the retro-Diels-Alder reaction. The Diels-Alder adduct constructed from an

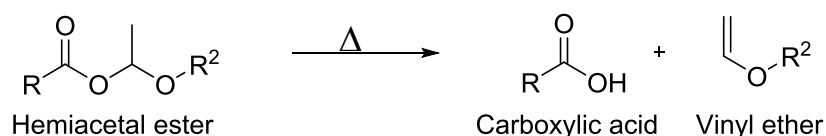
aromatic diene is stable at ambient temperature - however, elevated temperatures favour the reverse reaction, regenerating the diene and dienophile (Scheme 1.14).



Scheme 1.13. The retro Diels-Alder reaction of a maleimide-furan adduct, regenerating the furanyl diene and maleimide dienophile.

As such, the retro Diels-Alder reaction is employed extensively in thermally-healable materials. Generally, the reverse reaction requires in excess of 100 °C although recent developments have yielded adducts that cleave as low as 25 °C.¹¹⁵ Maleimide-furan Diels-Alder adducts have increasingly been applied in release and degradable polymer systems.^{116,117}

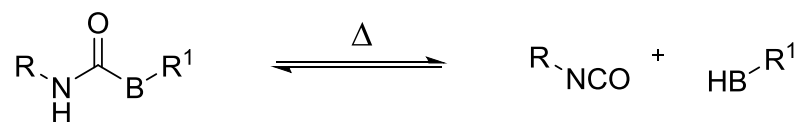
Another thermally labile bond is the hemiacetal ester.¹¹⁸ Upon exposure to heat at 80 °C, the hemiacetal is transformed into a carboxylic acid with the elimination of vinyl ether. The hemiacetal ester linker has been employed in degradable and recyclable epoxy resin composites (Scheme 1.15).¹¹⁹



Scheme 1.14. Dissociation of hemiacetal esters to form carboxylic acid and vinyl ether.

1.10. Blocked Isocyanates

Isocyanates react rapidly with H₂O and as a result, coating formulations containing free isocyanate exhibit poor stability and can polymerise readily even under mild conditions.¹²⁰ This has led to the development¹²¹ of blocking groups that protect the isocyanate moiety. The blocking reaction is reversible, generating free isocyanate when desired by the application of heat (Scheme 1.16). Extensive ranges of blocking groups have been patented and been the subject of several reviews.^{121,122,123} In the majority, studies of blocked isocyanates have been concerned primarily with the regeneration of active isocyanate, although these degradable systems have also featured in degradable polymer systems.¹²⁴



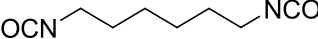
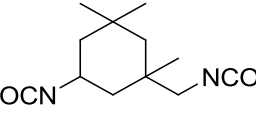
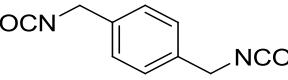
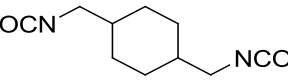
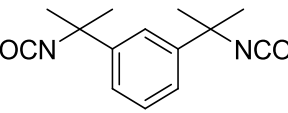
Scheme 1.15. Dissociation of a blocked isocyanate, generating the isocyanate moiety and the blocking group (B).

Blocking groups include - aromatic heterocycles, amines, phenols, oximes and amides.¹²² The following section serves to review the literature of these blocking groups, the temperature at which the reverse reaction can occur and their use as thermally-labile linkers in polymeric systems.

1.10.1. The Effect of Isocyanate Structure on Dissociation Temperature

It has been shown¹²⁵ that the structure of the isocyanate can have an effect on the dissociation temperature of the blocked isocyanate. Aromatic isocyanates typically dissociate at lower temperatures as a result of the increased electron withdrawing effect of the aromatic ring. Steric hindrance surrounding the isocyanate moiety also contributes to a lower dissociation temperature. Marumatsu *et al.* investigated¹²⁵ the dissociation temperature of a range of methyl ethyl ketoxime blocked isocyanates using thermogravimetric analysis (TGA). It was found that xylylene diisocyanate (XDI) had a lower dissociation temperature than the corresponding aliphatic H₆XDI. In addition, sterically hindered tetramethylxylylene diisocyanate (TMXDI) possessed an even lower dissociation temperature (Table 1.2).

Table 1.2. Dissociation temperatures of methyl ethyl ketoxime blocked HDI, IPDI, XDI, H₆XDI and TMXDI, highlighting the importance of electronic and steric affects.

Isocyanate	Structure	Dissociation Temperature (°C)
Hexamethylene diisocyanate (HDI)		132
Isophorone diisocyanate (IPDI)		121
Xylylene diisocyanate (XDI)		140
H ₆ -xylylene diisocyanate (H ₆ XDI)		147
Tetramethylxylylene diisocyanate (TMXDI)		100

1.10.2. Aromatic Heterocycles Blocking Groups

Aromatic heterocycles that possess an acidic hydrogen are often used to block isocyanate functionalities. Imidazole has been patented extensively as a blocking agent for isocyanates.^{126,127} Such blocked isocyanates are typically used to crosslink hydroxyl-functionalised pre-polymers used in coatings and adhesives.¹²⁸ Mühlebach reported¹²⁹ the synthesis of pyrazole-blocked isocyanates. TGA studies of IPDI blocked with 3,5-dimethylpyrazole revealed regeneration of the isocyanate at 150 °C with complete dissociation by 230 °C. Pyrazole blocked isocyanates have been used to cure amine terminated prepolymers and this was achieved within minutes at 100-120 °C. HDI isocyanurate trimer blocked with 3,5-dimethylpyrazole possessed dissociation temperatures between 115-135 °C have been used to cure polyurethane coatings.¹³⁰ Increasing the substitution on the pyrazole has proven to decrease the dissociation temperature. 1,2,4-Triazole-blocked isocyanates have been used to cure urethane films between 110-160 °C (Figure 1.8).^{131,132}

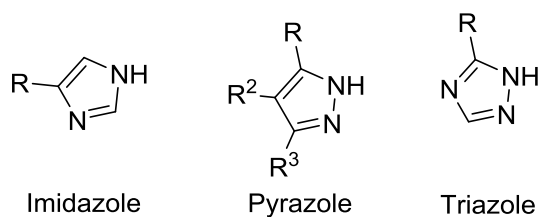
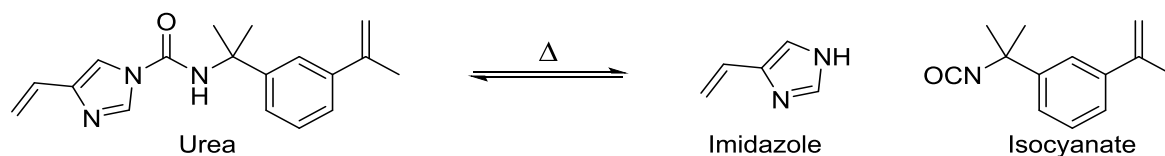


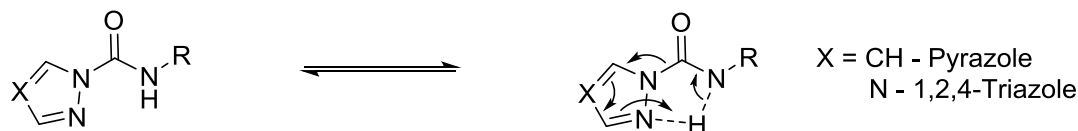
Figure 1.9. Generic structures of imidazole, pyrazole and triazole.

Heterocycle-blocked isocyanates have also been used in vinyl polymers,¹³³ incorporating thermally reversible urea crosslinks formed by a reaction of 4-vinylimidazole and 3-isopropenyl- α,α -dimethyl-benzyl isocyanate (Scheme 1.17).



Scheme 1.16. Dissociation of a urea crosslink to form 4-vinylimidazole and 3-isopropenyl- α,α -dimethyl-benzyl isocyanate.

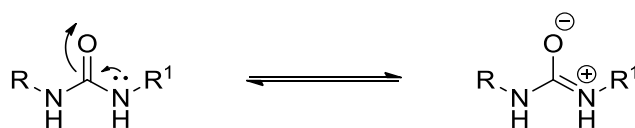
The dissociation mechanism for such aromatic heterocycles operates by forming a five membered complex that leads to deprotonation of the urea followed by subsequent dissociation (Scheme 1.18).¹³⁴



Scheme 1.17. The five-membered complex that aids in the deprotonation of the urea proton, leading to its dissociation.

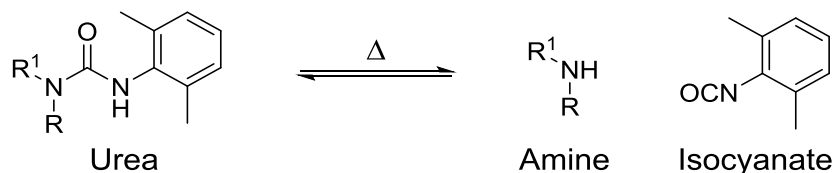
1.10.3. Isocyanates Blocked With Bulky Secondary Amines

Ureas are stabilised by conjugation between the lone pair of the nitrogen and the π -electrons of the carbonyl (Scheme 1.19). Introducing bulky groups onto the urea nitrogen hinders this stabilising effect, reducing the strength of the urea bond thus leading to its dissociation under mild conditions.¹³⁵



Scheme 1.18. Conjugation of the urea bond that increases its stability.

Stowell *et al.* investigated¹³⁶ the effect of bulky groups on ureas on the dissociation temperature to generate amine and isocyanate (Scheme 1.20). ¹H NMR spectroscopic analysis revealed the percentage of dissociation of these ureas between 40 and 140 °C. Increasing the steric hindrance on the blocking amine significantly reduced the dissociation temperature (Figure 1.9).



Scheme 1.19. General dissociation of a sterically hindered urea to yield a secondary amine and isocyanate.

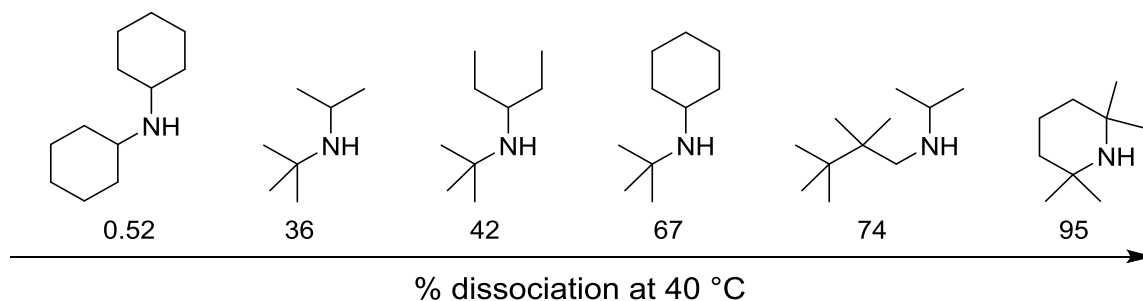
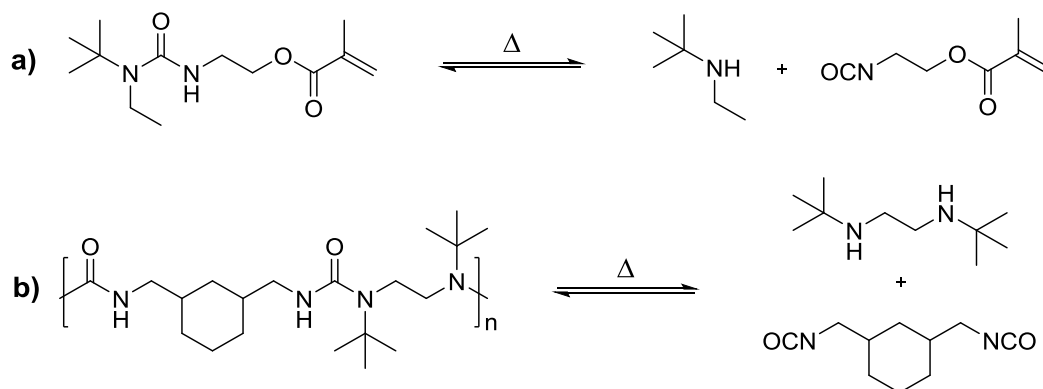


Figure 1.10. The effect of steric hindrance on the dissociation of ureas.

The self-healing potential of these 'dynamic' ureas was investigated.¹³⁷ The dissociation of 1-(*Tert*-butyl)-1-ethylurea reached equilibria after 20 hours at 37 °C. When inserted into a polyurea, experiments using gel permeation chromatography (GPC) revealed depolymerisation was achieved after 12 hours at the same temperature.

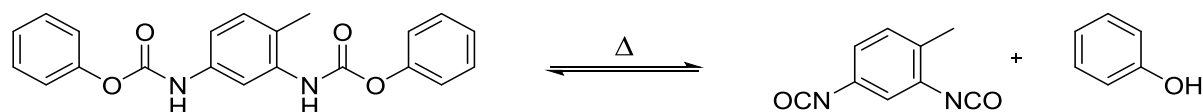
Sankar *et al.* reported¹⁵¹ a series of aromatic secondary amines used to block TDI. The blocked isocyanates were used to cure HTPB upon the application of heat. Variable temperature IR (VTIR) spectroscopy was used to identify the appearance of the characteristic isocyanate absorbance which subsequently diminished as curing of HTPB was achieved. The dissociation temperature was reduced by the presence of electron withdrawing groups at the *para*-position and increased by increasing electron density onto the aromatic ring. Dissociation temperatures can also be controlled (125-150 °C) by modifying the substituents on the aromatic ring.



Scheme 1.20. a) Dissociation reaction of 1-(*tert*-butyl)-1-ethylurea to yield corresponding isocyanate and amine. b) Dissociation of a polyurea bearing thermally reversible ureas.

1.10.4. Phenolic and Alcohol Blocking Groups

Urethanes formed from alkyl-alcohols dissociate at high temperatures (typically ~250 °C) and are thus not commonly used to block isocyanates,¹³⁸ although, dissociation of isopropyl alcohol blocked IPDI has been reported¹³⁹ to occur from 180 °C. Conversely, the urethane linkage between aromatic isocyanates and phenols is unstable at high temperatures (Scheme 1.22).



Scheme 1.21. Dissociation of TDI blocked with phenol to generate free diisocyanate.

Kothandaraman and Nasar reported¹⁴⁰ the synthesis and dissociation of a series of phenol-blocked toluene diisocyanates measured using variable temperature FTIR spectroscopy. Generally, the presence of electron donating groups reduced the dissociation temperature in contrast to that observed in aromatic amines (Figure 1.10).

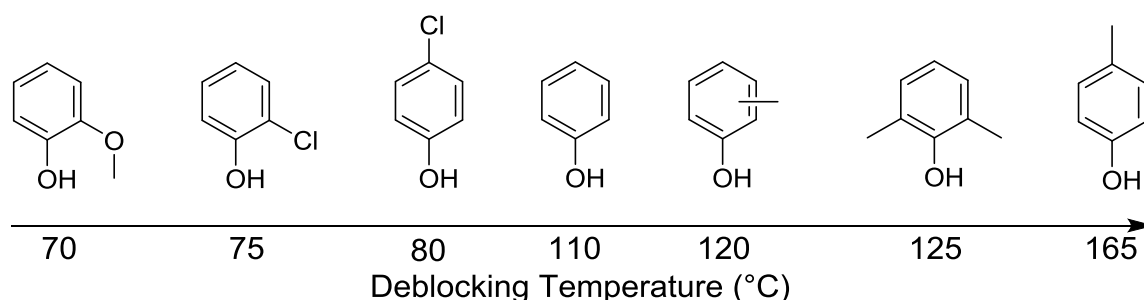


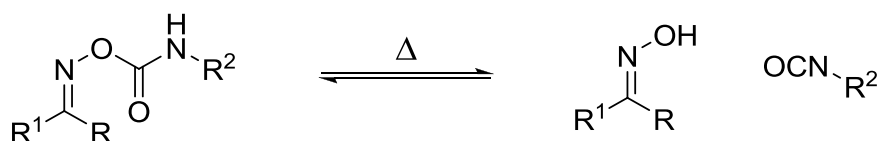
Figure 1.11. Dissociation temperatures of isocyanates blocked with substituted phenols, observed using FTIR spectroscopy.¹⁴⁰

IPDI and HDI have been blocked with bisphenol A and 4-hydroxybenzoic acid ethyl ester.¹³⁹ FTIR spectroscopy revealed the generation of free HDI at 118 and 162 °C when blocked with bisphenol A and 4-hydroxybenzoic acid ethyl ester, respectively.

The corresponding blocked IPDI required much higher temperatures, 177 and 183 °C respectively, and maximum dissociation was not achieved until ~ 230 °C.

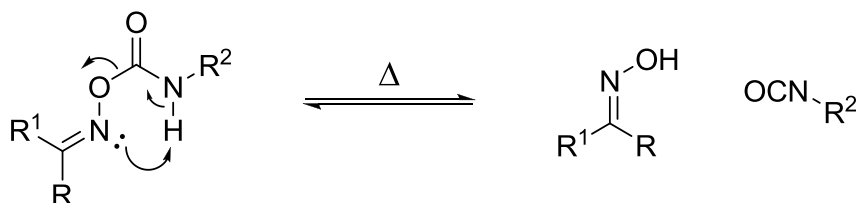
1.10.5. Oxime Blocking Groups

Oximes are used widely as thermally-labile blocking agents as a result of their low dissociation temperature and high reactivity with isocyanates, avoiding the use of catalysts in their preparation (Scheme 1.23).¹²² They are often found in industrial applications including automotive coatings.⁸¹



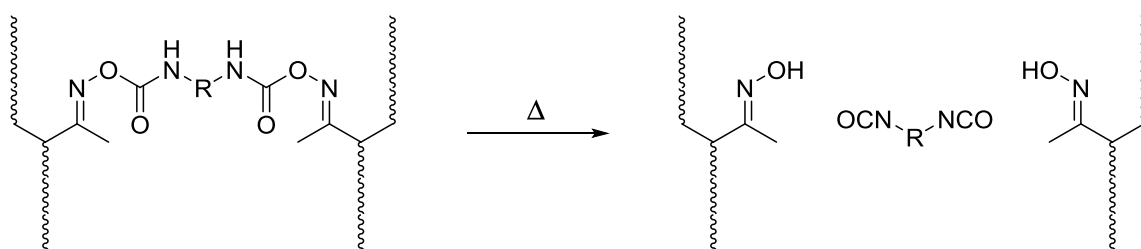
Scheme 1.22. General dissociation reaction of an oxime-urethane to form the corresponding isocyanate and oxime.

The dissociation mechanism is believed¹⁴¹ to occur in a similar manner observed in pyrazole blocked isocyanates, in which a five-membered transition state leads to deprotonation of the urethane nitrogen (Scheme 1.24).



Scheme 1.23. Dissociation mechanism of isocyanates blocked with oximes at elevated temperatures.

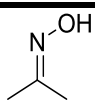
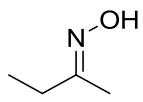
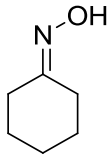
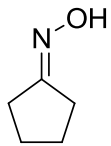
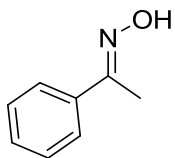
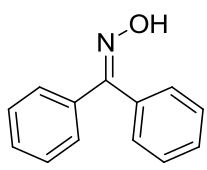
Thermally-reversible oxime-urethanes have been employed as crosslinks in thermally-degradable polymers used as templates in the manufacture of microchips.¹²⁴ Templates are usually crosslinked polymers that can be difficult to remove without the use of harsh conditions. Employing thermally labile crosslinks allows easy removal of the template as a result of this heat-triggered depolymerisation (Scheme 1.25).



Scheme 1.24. Dissociation of oxime-urethane crosslinks used in polymers applied as templates in the manufacture of microchips.

The effect of steric hindrance on the rate of dissociation has been investigated¹⁴² and it was found that more sterically hindered oximes dissociate faster. This observation was supported¹⁴³ by a further study investigating the curing of epoxy pre-polymers with a range of oxime blocked isocyanate-terminated pre-polymers, derived from TDI. The curing time was measured at 60, 100, 120 and 140 °C (Table 1.3).

Table 1.3. Curing times of epoxy using isocyanates blocked with oximes at 60, 100, 120 and 140 °C.

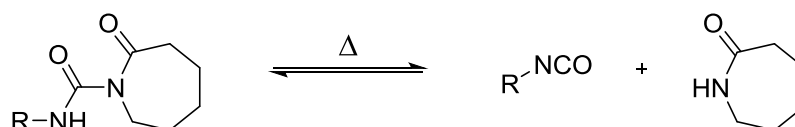
Oxime	Cure time at:			
	60 °C	100 °C	120 °C	140 °C
	1 day	15 minutes	10 minutes	5 minutes
	10 hours	15 minutes	10 minutes	5 minutes
	1 day	30 minutes	20 minutes	15 minutes
	Immediate	Immediate	Immediate	Immediate
	2 days	1 hour	45 minutes	15 minutes
	5 days	2 hours	1 hour	30 minutes

To date, the electronic effects on the dissociation of isocyanates blocked with aromatic oximes have not been widely explored. Kothandaraman *et al.* reported¹⁴⁴ that the dissociation of TDI blocked with analogues of benzophenone oxime was reduced by the presence of electron-donating methoxy moieties and in turn increased by the presence of electron-withdrawing chlorine. Further to this, the effect appeared to be

dependent on its position on the aromatic ring - *meta*-methyl substituted benzophenone oximes leading to a reduction in dissociation temperature and *ortho* and *para*-methyl substituted benzophenone oximes increasing the dissociation temperature.

1.10.6. Amide Blocking Groups

Amides react readily with isocyanates¹⁴⁵ and ϵ -caprolactam is a commonly encountered blocking agent found in powder coating formulations,¹⁴⁶ typically dissociating around 130 °C (Scheme 1.26).



Scheme 1.25. Dissociation reaction of urea blocked with ϵ -caprolactam.

Muramatsu *et al.* found¹²⁵ that ϵ -caprolactam possessed a relatively high dissociation temperature when compared to other amides. HDI was blocked with ϵ -caprolactam, methyl acetamide, succinimide and acetamide. The dissociation temperature decreased in that order – 157, 130, 110 and 100 °C, respectively.

Subramani *et al.* have developed^{147, 148} a range of water-borne polyurethane dispersions that utilise MDI and TDI blocked with a mixture of ϵ -caprolactam, methyl ethyl ketoxime and 3,5-dimethylpyrazole. The formulation recipe of the dispersions was modified to achieve a range of curing temperatures from 74 to 200 °C.

1.10.7. The Effect of Catalysts on Dissociation Temperature

Since DBDTL is present in Rowanex 1100 1A formulation, it is necessary to consider the effect a catalyst has on the dissociation temperature. Blocked isocyanates are often used in formulations containing catalysts. It has been found that the presence of a catalyst does not affect the dissociation temperature, instead increasing the rate of the curing of the formulations and allowing side reactions such as allophanate formation to occur.^{149,150}

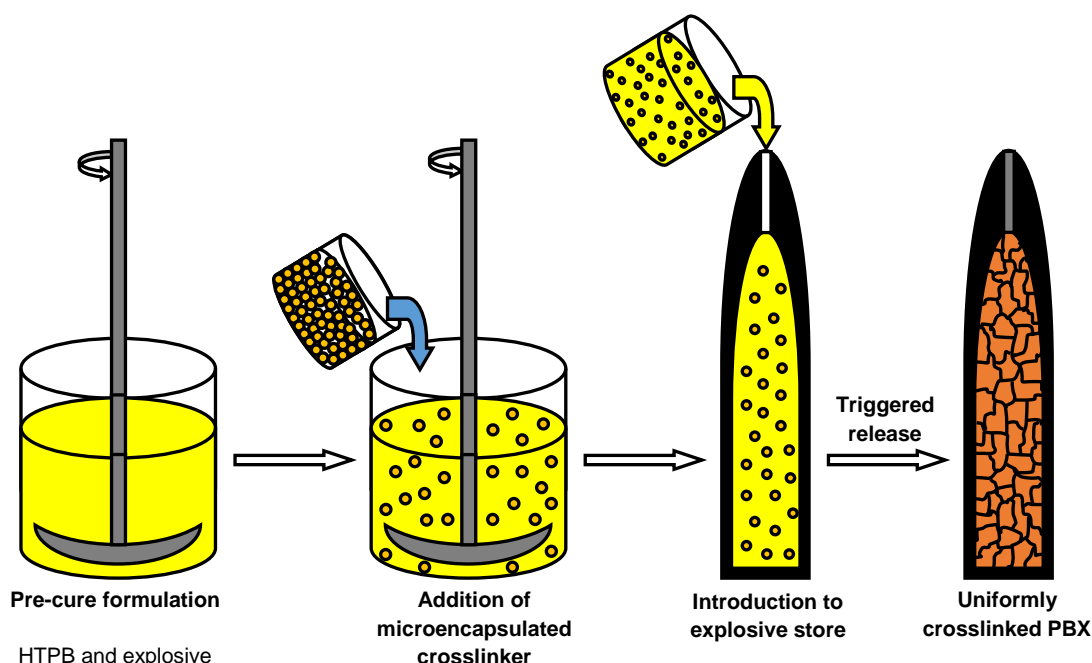
1.10.8. Measuring the Dissociation Temperature

There are a number of techniques used to measure the dissociation temperature. VTIR spectroscopy is commonly used.¹⁵¹ The blocked isocyanate is heated until the absorbance characteristic of the isocyanate stretching vibration is observed.

Thermogravimetric analysis (TGA) has also been used to study the loss of volatile blocking groups.¹⁵² Differential scanning calorimetry (DSC) measures thermal change in the blocked isocyanate as the dissociation occurs. Another method used to measure the dissociation temperature involves assessment of the volume of CO₂ evolved from a reaction of the generated isocyanate and water.¹⁵³ The blocked diisocyanate is heated in saturated solution barium hydroxide. Upon dissociation a reaction ensues between isocyanate and water. The subsequent decarboxylation leads to a further reaction between CO₂ and barium hydroxide to yield insoluble barium bicarbonate. However, each technique can accord a different dissociation temperature for the same blocked isocyanate.^{153,154}

1.11. Project Aims

Microencapsulation offers a route to deliver crosslinkers when desired, providing control over the polymerisation process used to bond explosives. This modified process shown in Scheme 1.27 prevents undesired crosslinking prior to filling of stores. A uniform delivery of crosslinker will also prevent the formation of voids and lead to the formation of a homogeneously crosslinked PBX material. The use of microencapsulated crosslinkers may allow for the increase in catalyst concentration, thus reducing cure times and contributing to an improved quality of curing.



Scheme 1.26. Modified process for the manufacture of PBX highlighting addition of microencapsulated crosslinker, introduction to explosive store and formation of a uniformly crosslinked rubber matrix following a release mechanism.

The introduction of a new explosive formulation into a store requires a process of material and article qualification in order to prove safe function of the system. This is a long and expensive process. Thus, a new explosive formulation must not be generated and existing formulations such as Rowanex 1100 1A cannot be significantly modified. The microcapsules must be composed primarily of polyurethane to match the PBX material and the ageing characteristics of the stores must not be affected. In addition, high costs are associated with changes to the current mixing and filling process, therefore this should not be significantly altered.

A previous study¹⁰⁵ at the University of Reading led to the development of the synthesis of microcapsules containing IPDI. The use of ultrasound to effect the release of the microcapsule core was demonstrated, however, the extreme local environment created by ultrasonic cavitation could cause detonation of the explosive. Triggered release of microcapsules using light is not viable since light is unable to penetrate deeply into the opaque Rowanex 1100 1A formulation. Thus, a release mechanism using exposure to a heat stimulus is the most ideal triggering mechanism.

The aim of this project can be described by five sub-targets. Firstly, a polymeric linker that degrades upon the application of a stimulus of heat was developed. This was achieved by exploiting the thermally reversible nature of the oxime-urethane bond. Secondly, the incorporation of these linkers into the polymer shell of microcapsules has been described and the control of microcapsule properties developed. Thirdly, the triggering of thermally-releasable microcapsules has been demonstrated and the curing of HTPB was achieved. Microcapsules have also been synthesised that incorporate a thermally-reversible Diels-Alder adduct within the shell wall. Finally, the use of blocked isocyanates to directly cure HTPB has been investigated.

1.12. References

- ¹ J. P. Agrawal and R. Hodgson, *Organic Chemistry of Explosives*, Wiley, Chichester, 2007.
- ² S. Fordham, *High Explosives and Propellants*, Pergamon Press Ltd., Oxford, 1980.
- ³ C. S. Peyratout and L. Dähne, *Angew. Chem.*, 2004, **43**, 3762-3783.
- ⁴ H. N. Yow and A. F. Routh, *Soft Matter*, 2006, **2**, 940-949.
- ⁵ R. Dubey, T.C. Shami and K.U. Bhasker Rao, *Defence Sci. J.*, 2009, **59**, 82-95.

- ⁶ R. Atkin, P. Davies, J. Hardy and B. Vincent, *Macromolecules*, 2004, **37**, 7979-7985.
- ⁷ E. Taqieddin and M. Amiji, *Biomaterials*, 2004, **25**, 1937-1945.
- ⁸ V. Araujo, A. Gamboa, N. Caro, L. Abugoch, M. Gotteland, F. Valenzuela, H. A. Merchant, A. W. Basit and C. Tapia, *J. Pharm. Sci.*, 2013, **102**, 2748-2759.
- ⁹ S. K. Ghosh, *Functional Coatings by Polymer Microencapsulation*, Wiley, Chichester, 2006.
- ¹⁰ S. N. Rodrigues, I. Fernandes, I. M. Martins, V. G. Mata, F. Barreiro and A. E. Rodrigues, *Ind. Eng. Chem. Res.*, 2008, **47**, 4142-4147.
- ¹¹ B. Peña, C. Panisello, G. Aresté, R. Garcia-Valls and T. Gumí, *Chem. Eng. J.*, 2012, **179**, 394-403.
- ¹² A. Ahmadi, *Asian J. Chem.*, 2007, **19**, 187-194.
- ¹³ S. S. Kuang, J.C. Oliveira and A.M. Crean, *Crit. Rev. Food Sci.*, 2010, **50**, 951-968.
- ¹⁴ Á. Alcázar, A. de Lucas, M. Carmona, J. F. Rodríguez, *React. Funct. Polym.*, 2011, **71**, 891-898.
- ¹⁵ R. Teixeira and C. S. Nogueira, *J. Text. I.*, 2010, **103**, 269-282.
- ¹⁶ K. Hong and S. Park, *Matter. Chem. Phys.*, 1999, **58**, 128-131.
- ¹⁷ S. Park, Y. Shin and J. Lee, *J. Colloid Interf. Sci.*, 2001, **241**, 502-508.
- ¹⁸ Y. Li, Y. Huang, H. Fan and Q. Xia, *J. Appl. Polym. Sci.*, 2014, **131**, 40053.
- ¹⁹ N. Paret, A. Trachsel, D. L. Berthier and A. Herrmann, *Angew. Chem. Int. Edit.*, 2015, **54**, 2275-2279.
- ²⁰ M. J. Patterson, S. D. R. Galloway and M. A. Nimmo, *Exp. Physiol.*, 2000, **85**, 869-875.
- ²¹ I. Hofmeister, K. Landfester and A. Taden, *Macromolecules*, 2014, **47**, 5768-5773.
- ²² F. T. Lee, P. Nicholson, J. Szamosi and W. T. Sommer, *Official Gazette of the United States Patent and Trademark Office Patents*, 2002, **1261**.
- ²³ L. Zhu, Z. H. Wang, S. T. Zhang and X. Y. Long, *J. Pestic. Sci.*, 2010, **35**, 339-343.
- ²⁴ J. S. Yang, H. B. Ren and X. J. Xie, *Biomacromolecules*, 2011, **12**, 2982-2987.
- ²⁵ A. L. Ilichev, L. L. Stelinski, D. G. Williams and L. J. Gut, *J. Encon. Entomol.*, 2006, **99**, 2048-2054.
- ²⁶ C. Zengliang, F. Yuling and Z. Zhongning, *Chinese Sci. Bull.*, 2007, **57**, 1365-1371.

- ²⁷ P. M. M. Schrooyen, R. van der Meer and C. G. De Kruif, *P. Nutr. Soc.*, 2001, **60**, 475-479.
- ²⁸ Y. Wang, Z. X. Lu, H. Wu and F. X. Lv, *Int. J. Food Microbiol.*, 2009, **136**, 71-74.
- ²⁹ H. Wu, N. Xue, C. L. Hou, J. T. Feng and X Zhang, *Food Chem.*, 2015, **175**, 344-349.
- ³⁰ P. C. Naha, V. Kanchan, P. K. Manna and A. K. Panda, *J. Microencapsul.*, 2008, **25**, 248-256.
- ³¹ L. J. de Cock, S. de Koker, B. G. de Geest, J. Grooten, C. Vervaet, J. P. Remon, G. B. Sukhurokov and M. N. Antipina. *Angew. Chem. Int. Ed.*, 2010, **49**, 6954-6973.
- ³² B. G. de Geest, S. de Koker, G. B. Sukhurokov, O. Kreft, W. J. Parak, A. G. Skirach, J. Demeester, S. C. De Smedt and W. E. Hennink, *Soft Matter*, 2009, **5**, 282-291.
- ³³ J. Wei, X. J. Ju, X. Y. Zou, R. Xie, W. Wang, Y. M. Liu and L. Y. Chu, *Adv. Funct. Mater.*, 2014, **24**, 3312-3323.
- ³⁴ M. M. Farid, A. M. Khudair, S. A. K. Razack and S. Al-Hallaj, *Energ. Convers. Manage.*, 2004, **45**, 1597-1615.
- ³⁵ Y. P. Zhang, K. P. Lin, R. Yang, H. F. Di and Y. Jiang, *Energ. Buildings*, 2006, **38**, 1262-1269.
- ³⁶ A. Jamekhorsid, S. M. Sadrameli and M. Farid, *Renew. Sust. Energ. Rev.*, 2014, **31**, 531-542.
- ³⁷ C. S. N. R. Teixeira, I. M. D. Martins, V. L. G. Mata, M. F. F. Barriero and A. E. Rodrigues, *J. Text. I.*, 2012, **103**, 269-282.
- ³⁸ J. Hu, M. Chen, Z. Xiao and J. Zhang, *J. Appl. Polym. Sci.*, 2015, **132**, 41678.
- ³⁹ G. Nelson, *Int. J. Pharm.*, 2002, **242**, 55-62.
- ⁴⁰ M. I. Re and B. Biscans, *Powder Technol.*, 1999, **101**, 120-133.
- ⁴¹ L. Sanchez-Silva, J. F. Rodriguez, A. Romero and P. Sanchez, *J. Appl. Polym. Sci.*, 2012, **124**, 4809-4818.
- ⁴² D. R. Cowsar, US Patent, *Novel fabric containing microcapsules of chemical decontaminants encapsulated within semipermeable polymers*, 1980, 4,201,822.
- ⁴³ S. R. White, N. R. Sottos, P. H. Geubelle, J. S. Moore, M. R. Kessler, S. R. Sriram, E. N. Brown and S. Viswanathan, *Nature*, 2001, **409**, 794-797.

- 44 S. Burattini, B. W. Greenland, D. Chappell, H.M. Colquhoun and W. Hayes, *Chem. Soc. Rev.*, 2010, **39**, 1973-1985.
- 45 B. J. Blaiszik, S. L. B. Kramer, S. C. Olugebefola, J. S. Moore, N. R. Sottos and S. R. White, *Annu. Rev. Mater. Res.*, 2010, **40**, 179-211.
- 46 T. Osswald and G. Menges, *Materials Science of Polymers for Engineers*, Hanser Publishers, Munich, 2003.
- 47 L. M. Meng, Y. C. Yuan, M. Z. Rong and M. Q. Zhang, *J. Mater. Chem.*, 2010, **20**, 6030-6038.
- 48 E. N. Brown, M. R. Kessler, J. S. Moore, N. R. Sottos and S. R. White, *J. Microencapsul.*, 2003, **20**, 719-730.
- 49 J. L. Yang, M. R. Kessler, J. S. Moore, S. R. White and N. R. Sottos, *Macromolecules*, 2008, **41**, 9650-9655.
- 50 M. Huang and J. Yang, *J. Mater. Chem.*, 2011, **21**, 11123-11130.
- 51 S. H. Cho, H. M. Andersson, S. R. White, N. R. Sottos and P. V. Braun, *Adv. Mater.*, 2006, **18**, 997-1000.
- 52 M. W. Keller, S. R. White and N. R. Sottos, *Adv. Funct. Mater.*, 2007, **17**, 2399-2404.
- 53 K. S. Toohey, N. R. Sottos, J. A. Lewis, J. S. Moore and S. R. White, *Nat. Mater.*, 2007, **6**, 581-586.
- 54 R. Arshady, *Polym. Eng. Sci.*, 1989, **29**, 1746-1758.
- 55 P. B. O'Donnell and J. W. McGinty, *Adv. Drug Deliver. Rev.*, 1997, **28**, 25-42.
- 56 T. M. Chang, *Science*, 1964, **146**, 524-525.
- 57 A. Gharsallaoui, G. Roudaut, O. Chambin, A. Voilley and R. Saurel, *Food Res. Int.*, 2007, **40**, 1107-1121.
- 58 A. P. R. Johnston, C. Cortez, A. S. Angelatos and F. Caruso, *Curr. Opin. Colloid In.*, 2006, **11**, 203-209.
- 59 N. Elvassore and A. Bertucco, *Ind. Eng. Chem. Res.*, 2001, **40**, 795-800.
- 60 Y. Senuma, C. Lowe, Y. Zweifel, J. G. Hilborn and I. Marison, *Biotechnol. Bioeng.*, 2000, **67**, 616-622.
- 61 G. T. Vladisavljevic and R. A. Williams, *Adv. Colloid Interfac.*, 2005, **113**, 1-20.
- 62 M. V. Sefton and W. T. K. Stevenson, *Adv. Polym. Sci.*, 1993, **107**, 143-197.
- 63 P. Rambourg, J. Lévy and M. C. Lévy, *J. Pharm. Sci.*, 1982, 753-758.

- ⁶⁴ K. Dietrich, H. Herma, R. Nastke, E. Bonatz and W. Teige, *Acta Polym.*, 1989, **40**, 243-251.
- ⁶⁵ R. Arshady and M. H. George, *Polym. Eng. Sci.*, 1993, **33**, 865-876.
- ⁶⁶ L. Yuan, G. Liang, J. Q. Xie, L. Li and J. Guo, *Polymer*, 2006, **47**, 5338-5349.
- ⁶⁷ K. Dietrich, E. Bonatz, H. Geistlinger, H. Herma, R. Nastke, H. J. Purz, M. Schlawne and W. Teige, *Acta Polym.*, 1989, **40**, 325-331.
- ⁶⁸ S. Cosco, V. Ambrogi, P. Musto and C. Carfagna, *J. Appl. Polym. Sci.*, 2007, **105**, 1400-1411.
- ⁶⁹ B. Alic, U. Sebenik and M. Kranjc, *J. Appl. Polym. Sci.*, 2011, **119**, 3687-3695.
- ⁷⁰ L. Groenendaal, F. Jonas, D. Freitag, H. Pielartzik and J. R. Reynolds, *Adv. Mater.*, 2000, **7**, 3317-3319.
- ⁷¹ C. Fan, J. Tang and X. Zhou, *J. Appl. Polym. Sci.*, 2013, **129**, 2848-2856.
- ⁷² A. P. Esser-Kahn, S. A. Odom, N. R. Sottos, S. R. White and J. S. Moore, *Macromolecules*, 2011, **44**, 5539-5553.
- ⁷³ F. Salaün, G. Bedek, E. Devaux, D. Dupont and L. Gengembre, *J. Membrane Sci.*, 2011, **370**, 3-33.
- ⁷⁴ M. Kobašlija and D. T. McQuade, *Macromolecules*, 2006, **39**, 6371-6375.
- ⁷⁵ J. F. Su, L. X. Wang and L. Ren, *Colloid. Surface. A*, 2007, **299**, 268-275.
- ⁷⁶ T. Takahashi, Y. Taguchi and M. Tanaka, *J. Appl. Polym. Sci.*, 2007, **106**, 3786-3791.
- ⁷⁷ W. Chen, X. Liu and D. W. Lee, *J. Mater. Sci.*, 2012, **47**, 2040-2044.
- ⁷⁸ M. Sato, *J. Org. Chem*, 1962, **27**, 819-825.
- ⁷⁹ J. Li, A. P. Hitchcock, H. D. H. Stöver and I. Shirley, *Macromolecules*, 2009, **42**, 2428-2432.
- ⁸⁰ A. Lapprand, F. Boisson, F. Delolme, F. Me´chin and J. P. Pascault, *Polym. Degrad. Stabil.*, 2005, **90**, 363-373.
- ⁸¹ S. Lee and D. Randall, *The Polyurethanes Book*, Wiley, Chichester, 2002.
- ⁸² M. M. Caruso, B. J. Blaisik, H. Jin, S. R. Schelkopf, D. S. Stradley, N. R. Sottos, S. R. White and J. S. Moore, *ACS Appl. Mater. Interface.*, 2010, **2**, 1195-1199.
- ⁸³ Y. Yang, Z. Wei, C. Wang and Z. Tong, *ACS Appl. Mater. Interface.*, 2013, **5**, 2495-2502.
- ⁸⁴ P. M. Armenante and Y. T. Huang, *Ind. Eng. Chem. Res.*, 1992, **31**, 1398-1406.

- ⁸⁵ L. M. Dong, J. Z. Shoa, L. Q. Cao, Y. Z. Wu and K. H. Zhang, *P. Int. Conf. Adv. Text. Mater. Manuf. Technol.*, 2008, 160-165.
- ⁸⁶ Y. Frère, L. Danicher and P. Gramain, *Eur. Polym. J.*, 1998, **34**, 193-199.
- ⁸⁷ K. Dietrich, E. Bonatz, R. Nastke, H. Herma, M. Walter and W. Teige, *Acta Polym*, 1990, **41**, 91-95.
- ⁸⁸ P. Ni, M. Zhang and N. Yan, *J. Membrane. Sci.*, 1995, **105**, 51-55.
- ⁸⁹ R. Heinrich, H. Frensch and K. Albrecht, US Patent, *Pressure-resistant polyurethane-polyurea particles for the encapsulation of active ingredients and process for their manufacture*, 1980, 4 230 809.
- ⁹⁰ F. Saluan, E. Devaux, S. Bourbigot and P. Rumeau, *C. Eng. J.*, 2009, **155**, 457-465.
- ⁹¹ S. Alexandridou, C. Kiparissides, F. Mange and A. Foissy, *J. Microencapsul.*, 2001, **18**, 767-781.
- ⁹² J. J. Jasper, *J. Phys. Chem. Ref. Data*, 1972, **1**, 841-1009.
- ⁹³ T. Ohtsubo, S. Tsuda, and K. Tsuji, *Polymer*, 1991, **32**, 2395-2399.
- ⁹⁴ D. E. Work, R. L. Hart and D. R. Virgallito, US Patent, *Method for microencapsulating water-soluble or water-dispersible or water-sensitive materials in an organic continuous phase*, 1999, 5 911 923.
- ⁹⁵ S. Fiori and A. Mariani, *Macromolecules*, 2003, **36**, 2674-2679.
- ⁹⁶ B. S. Kim, H. Y. Jeong and B. K. Kim, *Colloid. Surface. A.*, 2005, **268**, 60-67.
- ⁹⁷ K. Hong and S. Park, *React. Funct. Polym.*, 1999, **42**, 193-200.
- ⁹⁸ H. Zhang and X. Wang, *Sol. Energ. Mater. Sol. C.*, 2009, **93**, 1366-1376.
- ⁹⁹ E. Campos, R. Cordeiro, A. C. Campos, C. Matos and M. H. Gil, *Colloid. Surface. B.*, 2011, **88**, 477-482.
- ¹⁰⁰ H. C. Wang, Y. Zhang, C. M. Possanza, S. C. Zimmerman, J. Cheng, J. S. Moore, K. Harris and J. S. Katz, *ACS Appl. Mater. Interface.*, 2015, **7**, 6369-6382.
- ¹⁰¹ M. W. A. Kuijpers, P. D. Iedema, M. F. Kemmere and J. T. F. Keurentjes, *Polymer*, 2004, **45**, 6461-6467.
- ¹⁰² J. Chakraborty, J. Sarkar, R. Kumar and G. Madras, *Polym. Degrad. Stabil.* 2004, **85**, 555-558.
- ¹⁰³ S. P. Vijayalakshmi and G. Madras, *Polym. Degrad. Stabil.*, 2005, **90**, 116-122.
- ¹⁰⁴ M. T. Taghizadeh and T. Asadpour, *Ultrason. Sonochem.*, 2009, **19**, 280-286.

- ¹⁰⁵ M. E. Budd, MSc Thesis, University of Reading, 2013.
- ¹⁰⁶ S. Thirumalai, M. Mobed-Miremedi and M. Sridar-Keralapura, *33rd Annual International Conference of the IEEE EMBS*, Boston, Massachusetts USA, August 2011.
- ¹⁰⁷ M. R. Böhmer, C. H. T. Chlon, B. I. Raju, C. T. Chin, T. Shevchenko and A. L. Klibanov, *J. Control. Release*, 2010, **148**, 18-24.
- ¹⁰⁸ D. M. El-Sherif, J. D. Lathia, N. T. Le and M. A. Wheatley, *J. Biomed. Mater. Res. A*, 2004, **68**, 71-78.
- ¹⁰⁹ Y. Qui and K. Park, *Adv. Drug Delivery Rev.*, 2001, **53**, 321-339.
- ¹¹⁰ S. Binauld and M. H. Stenzel, *Chem. Commun.*, 2013, **49**, 2082-2102.
- ¹¹¹ M. Bedard, B. de Geest, A. Skirtach, H. Mohwald and G. Sukhorukov, *Adv. Colloid Interf. Sci.*, 2010, **158**, 2-14.
- ¹¹² N. Fomina, C. McFearin, M. Sermsakdi, O. Edigin and A. Almutairi, *J. Am. Chem. Soc.*, 2010, **132**, 9540-9542.
- ¹¹³ L. Chu, S. Park, T. Yamaguchi and S. Nakao, *Langmuir*, 2002, **18**, 1856-1864.
- ¹¹⁴ K. Eggers, D. Szopinski and G. A. Luinstra, *Macromol. Symp.*, 2014, **346**, 32-35.
- ¹¹⁵ P. J. Boul, P. Reutenauer and J. M. Lehn, *Org. Lett.*, 2005, **7**, 15-18.
- ¹¹⁶ S. Yamashita, H. Fukushima, Y. Niidome, T. Mori, Y. Katayama and T. Niidome, *Langmuir*, 2011, **27**, 14621-14626.
- ¹¹⁷ K. C. Koehler, K. S. Anseth and C. N. Bowman, *Biomacromolecules*, 2013, **14**, 538-547.
- ¹¹⁸ Y. Nakane, M. Ishidoya and T. Endo, *J. Polym. Sci. Pol. Chem.*, 1999, **37**, 609-614.
- ¹¹⁹ H. Otsuka, H. Fujiwara and T. Endo, *J. Polym. Sci. Pol. Chem.*, 1999, **37**, 4478-4482.
- ¹²⁰ A. Blencowe, A. Clarke, M. G. B. Drew, W. Hayes, A. Slark and P. Woodward, *React. Funct. Polym.*, 2006, **66**, 1284-1295.
- ¹²¹ Z. W. Wicks, *Prog. Org. Coat.*, 1981, **9**, 3-28.
- ¹²² D. A. Wicks and Z. W. Wicks, *Prog. Org. Coat.*, 1999, **36**, 148-172.
- ¹²³ E. Delebecq, J. P. Pascault, B. Boutevin and F. Ganachaud, *Chem. Rev.*, 2013, **113**, 80-118.

- ¹²⁴ W. H. Heath, F. Palmieri, J. R. Adams, B. K. Long, J. Chute, T. W. Holcombe, S. Zieren, M. J. Truitt, J. L. White and C. G. Wilson, *Macromolecules*, 2008, **41** 719-726.
- ¹²⁵ I. Muramatsu, Y. Tanimoto, M. Kase and N. Okoshi, *Prog. Org. Coat.*, 1993, **22**, 279-286.
- ¹²⁶ F. W. C. Lee and K. S. B. Dublin, US Patent, *Single package epoxy resin system*, 1985, 4 533 715,
- ¹²⁷ Beitchman and P. J. Zaluzka, US Patent, *Isocyanate blocked imidazoles and imidazolines for epoxy powder coating*, 1982, 4 335 228.
- ¹²⁸ A. Wenning and F. Schmitt, Canadian Patent, *Pulverulent compounds, a process for their preparation and use*, 1998, 2 210 043.
- ¹²⁹ A. Mühlebach, *J. Polym. Sci. Pol. Chem.*, 1994, **32**, 753-765.
- ¹³⁰ M. T. Keck, R. J. Lewarchik and J. C. Allman, US Patent, *Non-blistering thick film coating compositions and method for providing non-blistering thick film coatings on metal surfaces*, 1997, 5 688 598.
- ¹³¹ E. Charriere and J. M. Bernard, US Patent, *Mixed masked (poly)isocyanates*, 2005, 6 965 007.
- ¹³² P. Ardaud, F. J. Williams, J. M. Bernard and B. Vogin, US Patent, *Composition which is useful for obtaining a matt or satin coating, use of this composition and coating thus obtained*, 2003, 6 627 725.
- ¹³³ J. Y. Chang, S. K. Do and M. J. Han, *Polymer*, 2001, **42**, 7589-7594.
- ¹³⁴ A. S. Nasar, S. Subramani and G. Radhakrishnan, *Polym. Int.* 1999, **48**, 614-620.
- ¹³⁵ M. Hutchby, C. E. Houlden, J. G. Ford, S. N. G. Tyler, M. R. Gagne, G. C. Lloyd-Jones and K. I. Booker-Milburn, *Angew. Chem. Int. Ed.*, 2009, **48**, 8721-8724.
- ¹³⁶ J. C. Stowell and S. J. Padegimas, *J. Org. Chem.*, 1974, **39**, 2448-2449.
- ¹³⁷ H. Ying, Y. Zhang and J. Cheng, *Nat. Commun.*, 2014, **5**, 3218-3226.
- ¹³⁸ Z. R. Wicks, *Prog. Org. Coat.*, 1975, **3**, 73-99.
- ¹³⁹ M. Gedan-Smolka, L. Häußler and D. Fischer, *Thermochim. Acta*, 2000, **351**, 95-105.
- ¹⁴⁰ A. S. Nasar, V. Shrinivas, T. Shanmugam and A. Raghavan, *J. Polym. Sci. Pol. Chem.*, 2004, **42**, 4047-4055.
- ¹⁴¹ A. W. Levine and J. Fech, *J. Org. Chem.*, 1972, **37**, 1500-1503.

- ¹⁴² J. S. Witzeman, *Prog. Org. Coat.*, 1996, **27**, 269-276.
- ¹⁴³ G. B. Guise, G. N. Freeland and G. C. Smith, *J. Appl. Polym. Sci.*, 1979, **23** 353-365.
- ¹⁴⁴ H. Kothandaraman and R. Thangavel, *J. Polym. Sci. Pol. Chem.*, 1993, **31**, 2653-2657.
- ¹⁴⁵ P. F. Wiley, *J. Am. Chem. Soc.*, 1949, **71**, 1310-1311.
- ¹⁴⁶ R. Gras and E. Wolf, German Patent, *Blocked isocyanate and isocyanurate - containing compounds*, 1978, 2 712 931.
- ¹⁴⁷ S. Subramani, Y. J. Park, Y. S. Lee and J. H. Kim, *Prog. Org. Coat.*, 2003, **48**, 71-79.
- ¹⁴⁸ S. Subramani, I. W. Cheong and J. H. Kim, *Prog. Org. Coat.*, 2004, **51**, 329-338.
- ¹⁴⁹ G. M. Carlson, C. M. Neag, C. Kuo and T. Provder, *Polym. Sci. Technol.*, 1987, **36**, 197.
- ¹⁵⁰ W. J. Blank, Z. A. He and M. E. Picci, *prep. PMSE Div. ACS Mtg.*, 1998.
- ¹⁵¹ G. Sankar and A. S. Nasar, *J. Polym. Sci. Pol. Chem.* 2007, **45**, 1557-1570.
- ¹⁵² A. S. Nasar, S. Subramani and G. Radhakrishnan, *J. Polym. Sci. Pol. Chem.*, 1999, **37**, 1815-1821.
- ¹⁵³ S. Mohanty and N. Krishnamurti, *Eur. Polym. J.*, 1998, **34**, 77-83.
- ¹⁵⁴ H. Kothandaraman and A. S. Nasar, *Polymer*, 1993, **34**, 610-615.

Chapter 2

Design of Thermally-Degradable Polymeric Shell Wall Precursors by Exploiting the Thermally Reversible Oxime-Urethane Bond

The following chapter has, in part, been published by the author as a patent application in collaboration with BAE Systems plc. - *M. E. Budd, W. C. Hayes, R. Stephens, Great British/European Patent Application, 'Cast Explosive Composition', 2015, GB1511876.2/EP15275168.1.*

Abstract

The release of contents from microcapsules using a thermal stimulus has, to date, been limited to either heating above the boiling point of the encapsulated core to bring about rupture of the shell or by inducing phase changes of the microcapsule shell to reveal a porous structure. An alternative approach is to incorporate thermally-labile linkers within the microcapsule polymer shell that dissociate upon the application of heat, resulting in the release of the microencapsulated core. Oxime-urethanes are labile when exposed to even moderate temperatures and have been employed as degradable crosslinking units in polymers. The temperature at which the oxime-urethane bond breaks has been shown to be affected by the steric hindrance around the thermally-labile bond, thus allowing control of the temperature at which dissociation occurs. This chapter describes the synthesis of isocyanate-terminated shell wall precursors containing thermally-labile oxime-urethane linkages. Furthermore, control of the dissociation temperature is demonstrated by modifying the steric hindrance around the thermally-labile bond.

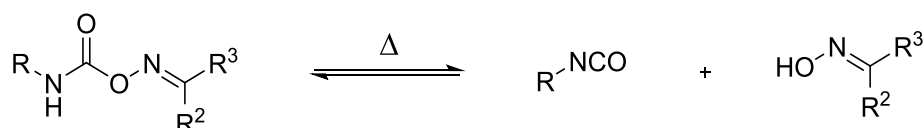
2.1. Introduction

Release mechanisms for microcapsules operate by responding to external stimuli that initiate either chemical or physical changes in the microcapsule shell wall that ultimately result in fracture or degradation and thus the desired release of their encapsulated active agents.¹ Microcapsules that respond to a range of stimuli have been developed depending on their target application - pressure,² chemical (*i.e.* change in pH or solvent),^{3,4} light,⁵ ultrasound⁶ and exposure to elevated temperature.⁷ The contraction of poly(*N*-isopropylacrylamide) (PNIPAM) when exposed to heat has been exploited for the thermal release of microcapsules.⁷ Upon the application of a

thermal stimulus PNIPAM shrinks to cause shell wall rupture or exposure of pores within the microcapsule shell wall.^{8, 9} However, to date, the disassembly of polyurethane microcapsule shell walls by the application of a heat stimulus has not been reported.

Thermally reversible covalent bonds such as Diels-Alder adducts¹⁰ and hindered urea bonds¹¹ have been incorporated within the bulk matrix of crosslinked polymers in order to generate self-healing and healable materials.

Oxime-urethane systems are reversible at elevated temperatures, regenerating the oxime and isocyanate (Scheme 2.1). These systems are commonly referred to as 'blocked isocyanates' in the adhesives industry and are used frequently to generate isocyanate crosslinkers in one pot adhesive formulations upon thermal stimulation.¹²⁻¹⁹



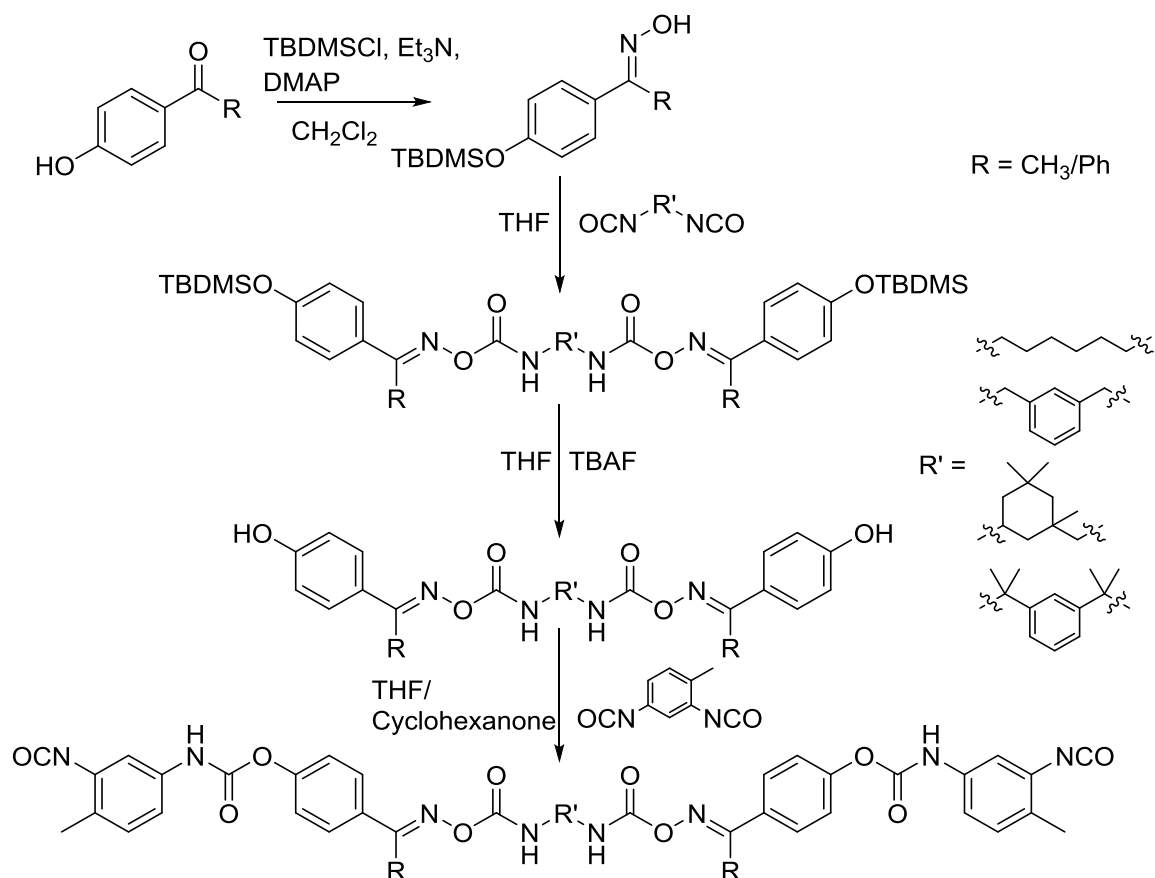
Scheme 2.1. Thermally reversible oxime-urethane bond regenerating isocyanate and oxime. Oxime-urethanes systems have also been employed²⁰ as thermally degradable crosslinks in polymers used for the application of thermally-strippable templates employed in the manufacture of microchips.

2.2. Results and Discussion

The synthesis of microcapsules that incorporate stimuli-responsive groups within the microcapsule shell wall can be achieved using an interfacial polymerisation technique. The interfacial polymerisation approach to the synthesis of microcapsules requires the generation of an appropriate isocyanate-terminated shell wall precursor. Previous studies²¹ carried out at the University of Reading identified that toluene-2,4-diisocyanate (TDI) terminated shell wall precursors possessed the ideal reactive properties to synthesise microcapsules. Thus a synthetic route was designed to yield an isocyanate-terminated shell wall precursor that contained a thermally-labile oxime-urethane bond and was capable of further chain extension to form microcapsules.

The synthesis of shell wall precursors was achieved by initial protection of a hydroxy-functionalised ketone (**2.1a-b**) followed by the conversion to the corresponding oxime (**2.2a-b**). The reaction of the generated oxime with a diisocyanate afforded a thermally labile oxime-urethane (**2.3a-h**). Deprotection to reveal the hydroxyl functionality

(**2.4a-h**) then allowed reaction with toluene-2,4-diisocyanate (TDI) to afford an isocyanate-terminated shell wall precursor (**2.5a-h**) (Scheme 2.3).



Scheme 2.2. Synthesis of a thermally-labile oxime-urethane by initial conversion of a ketone to the corresponding oxime followed by reaction with an isocyanate. Subsequent deprotection to reveal the alcohol moiety allowed reaction with TDI to yield the desired shell wall precursor.

The mixing temperatures of Rowanex 1100 is typically between 55-70 °C, so ideally, the release of the core contents from microcapsules will use an application temperature above 70 °C, in order to prevent undesired polymerisation during the mixing phase. For safety concerns and in order to avoid additional processing costs the release temperature should not exceed 120 °C, well below the ignition temperature of RDX (~220 °C), therefore, it was important to design shell wall precursors that dissociate within this temperature range. The steric hindrance around the oxime-urethane has a significant effect on the temperature at which these functional groups dissociate.^{17,18,19} Thus, a library of shell wall precursors that possessed different degrees of steric hindrance proximal to the thermally-labile bond were synthesised. This was achieved by employing two different oximes, generated from 4'-hydroxyacetophenone and 4-hydroxybenzophenone (Figure 2.1).

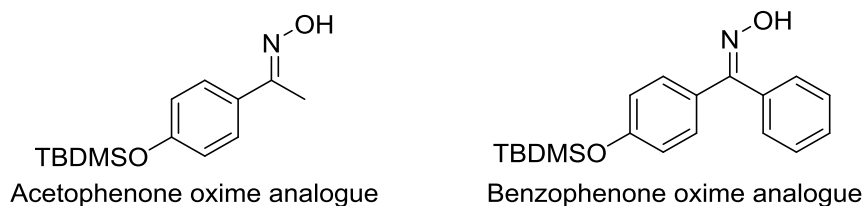


Figure 2.1. Structures of protected analogues of 4'-hydroxyacetophenone oxime and 4-hydroxybenzophenone oxime

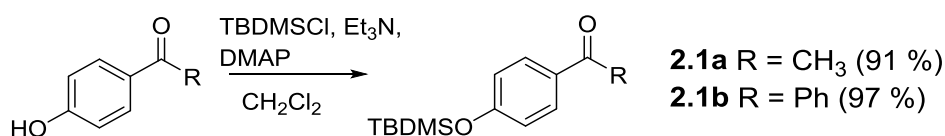
Steric hindrance was further imparted on the oxime-urethane by reaction of each oxime with a combination of four different diisocyanates - hexamethylene diisocyanate (HDI), *m*-xylylene diisocyanate (XDI), isophorone diisocyanate (IPDI) and *m*-tetramethylene diisocyanate (TMXDI) (Table 2.1).

Table 2.1. Structures of hexamethylene diisocyanate (HDI), *m*-xylylene diisocyanate (XDI), isophorone diisocyanate (IPDI) and *m*-tetramethylxylylene diisocyanate (TMXDI).

Diisocyanate	Structure
Hexamethylene diisocyanate (HDI)	
<i>m</i> -Xylylene diisocyanate (XDI)	
Isophorone diisocyanate (IPDI)	
<i>m</i> -Tetramethylxylylene diisocyanate (TMXDI)	

2.2.1. Protection of the Hydroxy-Functionalised Ketones

Phenolic hydroxyls react readily with isocyanates and thus it was necessary to protect the hydroxyl moiety of the ketones in order to prevent undesired reactions. Protection of both ketones was afforded by reaction with *tert*-butyldimethylsilyl chloride (TBDMSCl) and trimethylamine in the presence of a catalytic quantity of 4-dimethylaminopyridine (DMAP) yielding the desired products **2.1a/b** as white coloured crystals following purification by column chromatography (Scheme 2.3).



Scheme 2.3. Synthesis of silyl-protected oximes from 4'-hydroxyacetophenone (**2.1a**) and 4-hydroxybenzophenone (**2.1b**) using TBDMSCl, Et₃N and DMAP.

^1H NMR spectroscopic analysis of **2.1a** revealed the presence of resonances at 0.26 and 1.01 ppm corresponding to the newly formed silyl protecting group (Figure 2.2). The protection of the alcohol moiety was also confirmed using FTIR spectroscopy, which revealed the absence of an absorption at $\sim 3300\text{ cm}^{-1}$ characteristic of the OH stretching vibration.

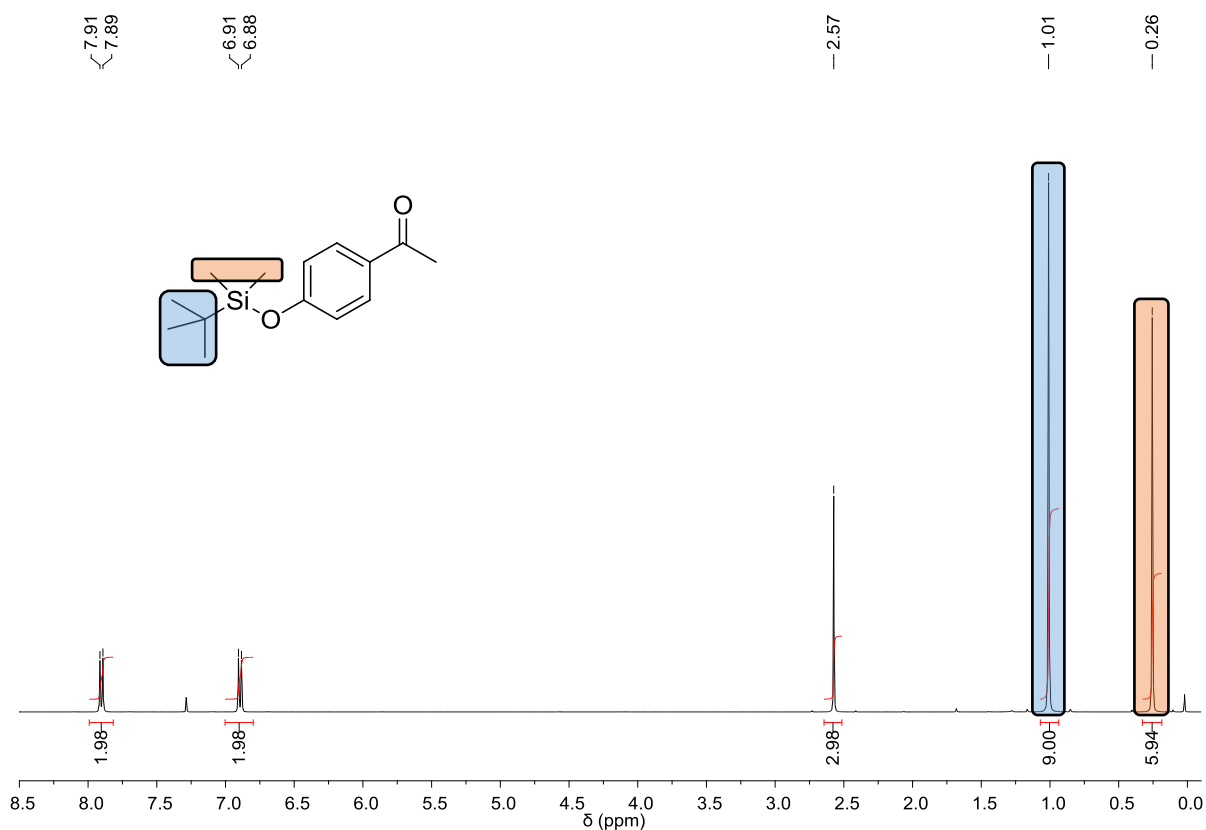
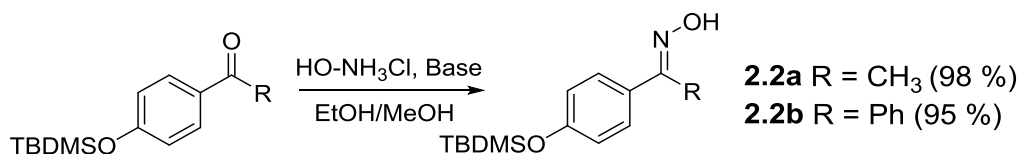


Figure 2.2. ^1H NMR spectrum of **2.1a** synthesised using TBDMSCl and triethylamine in the presence of a catalytic quantity of DMAP, highlighting the formed silyl-protecting group.

2.2.2. Conversion of Protected Ketones to Oximes

Conversion of **2.1a** to an oxime **2.2a** required the reaction of the ketone with hydroxylamine hydrochloride under reflux in the presence of a molar quantity of triethylamine. Workup by washing with H_2O afforded the desired oxime without the need for further purification (Scheme 2.4).



Scheme 2.4. Conversion of protected ketones to oximes using hydroxylamine hydrochloride in the presence of a base.

Ketones impart an electron withdrawing effect on a benzene ring - upon the conversion to an oxime this electron withdrawing effect is reduced. This affect can be observed using ^1H NMR spectroscopic analysis, where a change in the chemical shift of the resonance corresponding to protons at the *ortho*-position of the aromatic ring move upfield from 7.90 to 7.51 ppm. Further analysis using ^{13}C NMR spectroscopy revealed the disappearance of a ketone resonance characteristic of a carbonyl carbon at 196.9 ppm and the appearance of a carbon corresponding to C=N-OH functionality at 156.8 ppm (Figure 2.3).

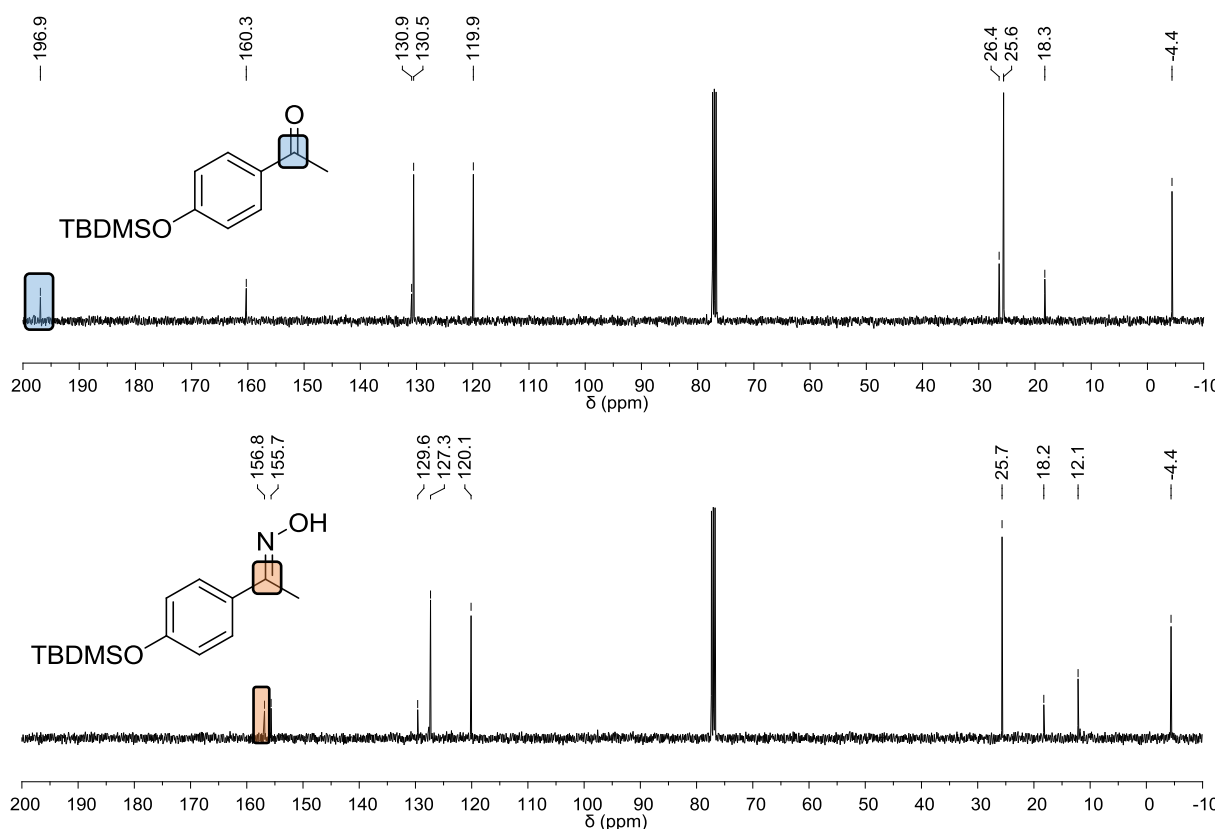


Figure 2.3. ^{13}C NMR spectra of **2.1a** (above) and **2.2a** (below) highlighting the change in the resonances upon conversion from a ketone to an oxime.

The increased steric hindrance on the protected benzophenone **2.1b** prevented conversion to the oxime using sterically encumbered bases such as triethylamine. Thus, reaction could only be achieved by employing smaller bases such as pyridine in order to yield the oxime **2.2b**. ^1H NMR spectroscopic analysis of **2.2b** revealed the presence of two resonances at 6.77 and 6.90 ppm that corresponded to the aromatic protons at the *meta*-position, suggesting the oxime was obtained as a mixture of *E* and *Z* isomers. A further pair of resonances at 8.78 and 8.93 were evident that correspond to the oxime proton (Figure 2.4).

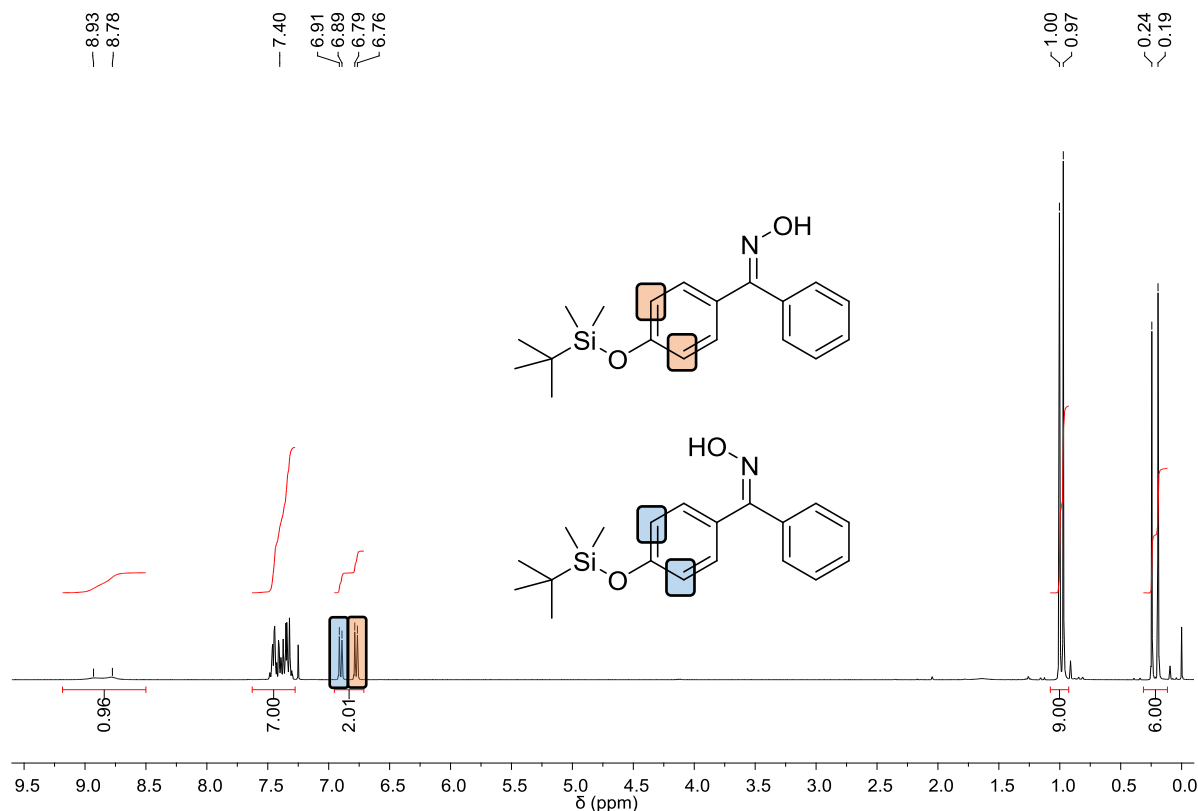
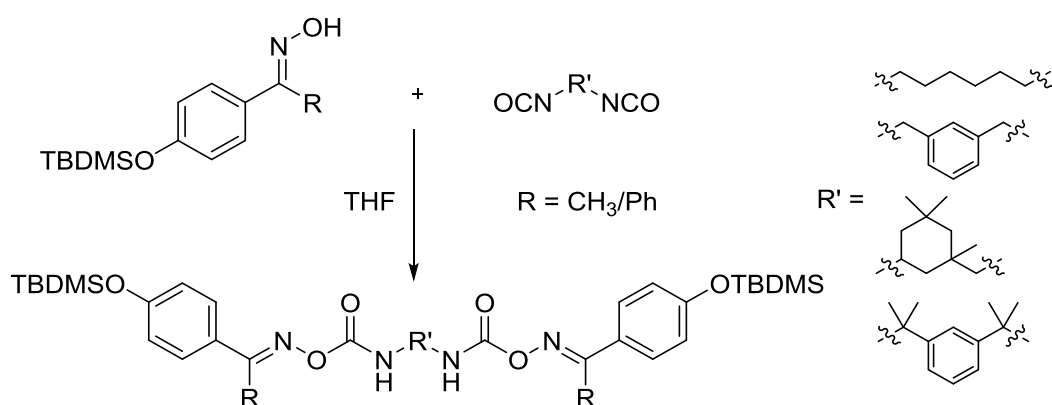


Figure 2.4. ^1H NMR spectrum of silyl-protected benzophenone oxime **2.2b**, highlighting the formation of a mixture of *E* and *Z* isomers.

2.2.3. Synthesis of Thermally-Labile Oxime-Urethane

Oxime-urethanes were obtained by the reaction of an excess oxime and diisocyanate in tetrahydrofuran (THF) under reflux for a period of 18-24 hours under an atmosphere of argon (Scheme 2.5).



Scheme 2.5. Reaction of an oxime and diisocyanate to yield an oxime urethane that can dissociate upon the application of heat.

Following purification by column chromatography oxime-urethanes, **2.3a-h**, were yielded as white crystalline powders. Table 2.2 lists the library of oxime-urethanes synthesised by combination of the two oximes and four diisocyanates.

Table 2.2. List of different oxime-urethanes synthesised from different oximes and diisocyanates.

	Oxime	Diisocyanate	Yield (%)
2.3a	Acetophenone	HDI	88
2.3b	Benzophenone	HDI	85
2.3c	Acetophenone	XDI	54
2.3d	Benzophenone	XDI	95
2.3e	Acetophenone	IPDI	quant.
2.3f	Benzophenone	IPDI	95
2.3g	Acetophenone	TMXDI	33
2.3h	Benzophenone	TMXDI	75

The oxime urethanes were characterised by a range of spectroscopic techniques including ^1H NMR spectroscopy. The presence of a resonance corresponding to the urethane NH at 6.49 ppm was observed. In addition, FTIR spectroscopic analysis revealed the presence of an absorbance at $\sim 1721\text{ cm}^{-1}$ corresponding to the carbonyl functionality of the formed oxime-urethane (Figure 2.5).

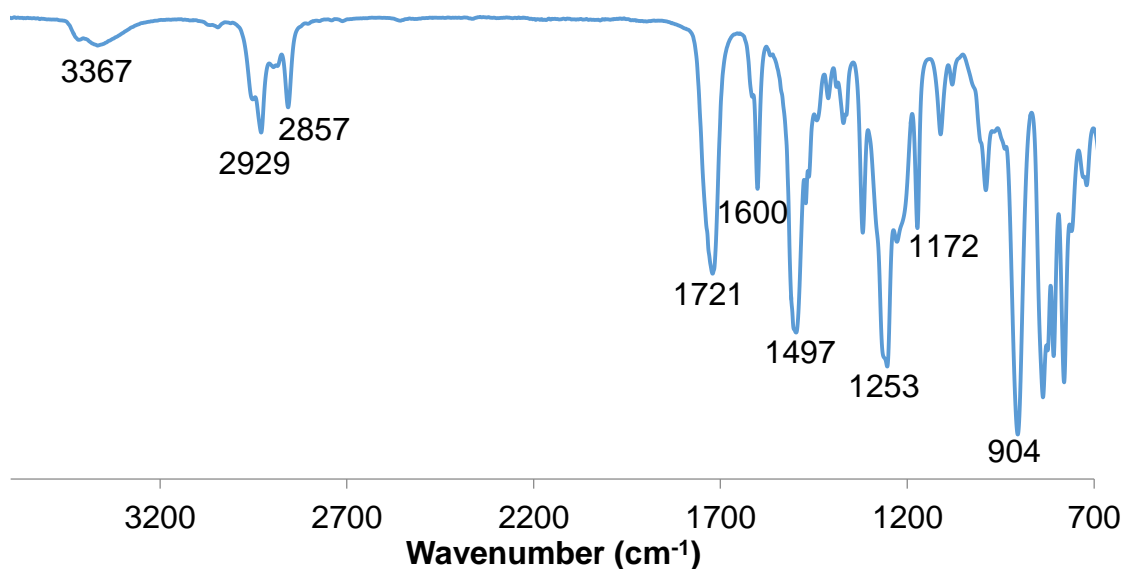


Figure 2.5. FTIR spectrum of oxime urethane **2.3a** synthesised by reaction of hexamethylene diisocyanate and protected acetophenone oxime, highlighting absorbances at 3367, 2929, 2857, 1721, 1600, 1497, 1293, 1172 and 904 cm^{-1} .

With the exception of **2.3g** and **2.3h**, all of the oxime-urethanes were obtained in high yields without the need for catalysts. As a result of the high steric hindrance of TMXDI, long reaction times were required in order to afford the desired oxime-urethane. The use of a catalytic quantity of dibutyltin dilaurate (DBTDL) reduced this reaction time to 48 hours. However, the presence of the catalyst led to the formation of a side product that was isolated using column chromatography. ^1H NMR spectroscopic analysis of the isolated compound revealed that an undesired reaction had occurred which led to the cleavage of the silyl-ether protecting group. Integration of resonances at 0.21 and 0.98 ppm corresponding to the protecting group were exactly half of the desired di-protected oxime-urethane, **2.3h** (Figure 2.6).

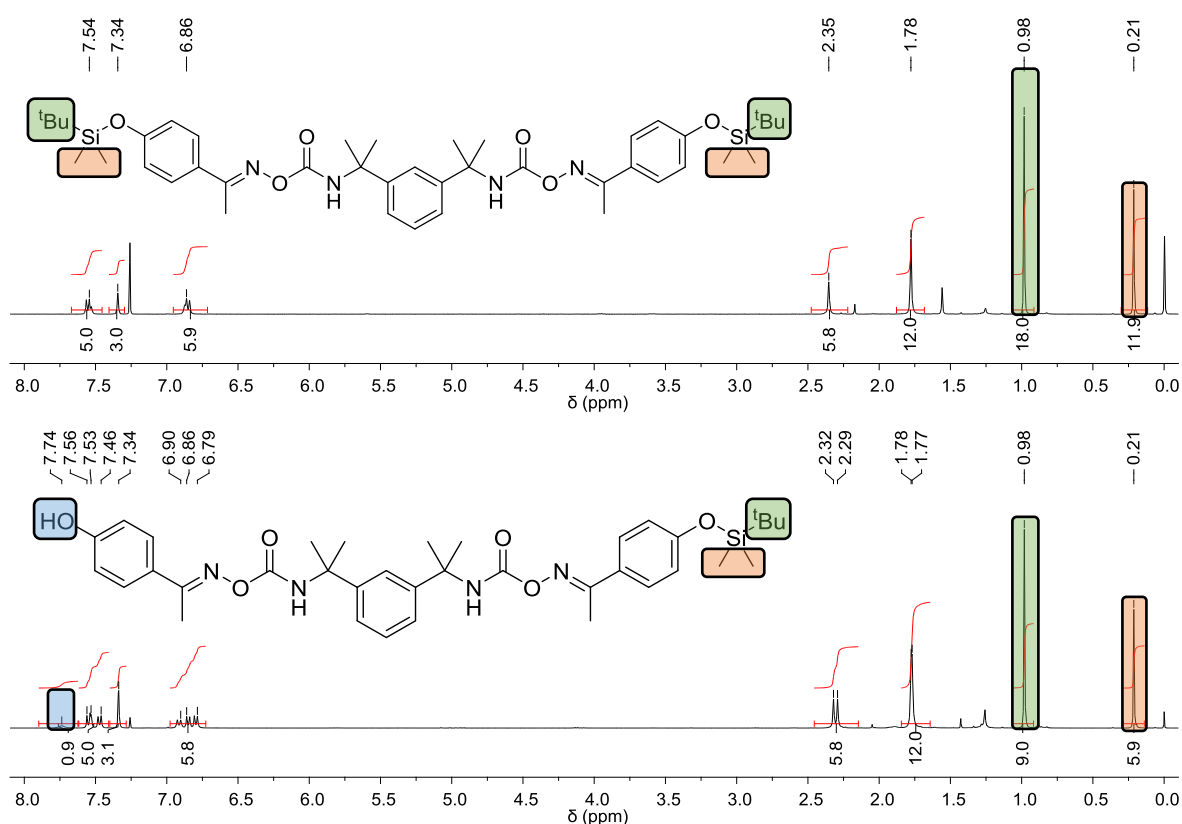
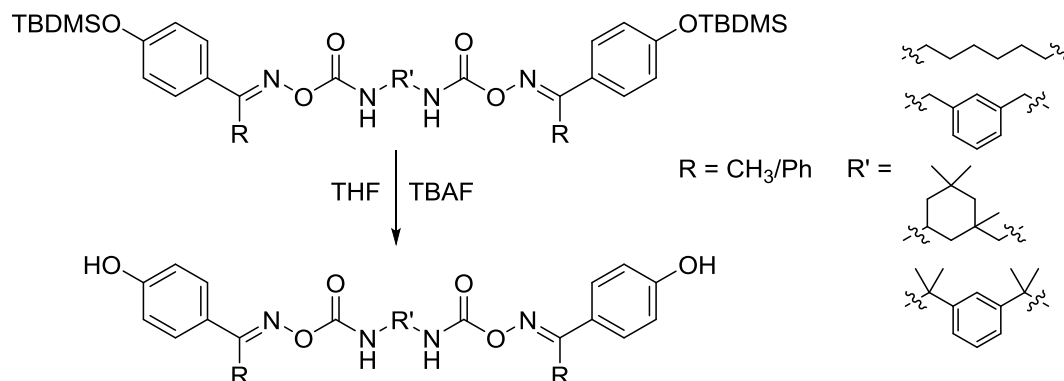


Figure 2.6. ^1H NMR spectra of di-protected oxime urethane (**2.3h**) (above) and mono-protected oxime urethane side product (below).

2.2.4. Deprotection to Reveal Reactive Phenolic Functionality

In order to synthesize an isocyanate-terminated shell wall precursor, first, it was necessary to remove the silyl protecting group to reveal the hydroxyl functionality. Deprotection can be achieved by reaction with HF-pyridine,¹⁹ however, it was found that deprotection could also be achieved using tetrabutylammonium fluoride (TBAF), avoiding high hazards to health associated with HF-pyridine. The deprotected oxime-

urethanes, **2.4a-h**, were obtained as white powders following workup by washing with CHCl_3 (Scheme 2.6).



Scheme 2.6. Deprotection of silyl-ethers using TBAF to reveal the hydroxyl functionality

The deprotected oxime-urethane was analysed with a range of techniques including ^1H NMR spectroscopy. Successful deprotection was confirmed as the proton resonances at 0.22 and 0.99 ppm that correspond to the silyl protecting group were not evident. In addition, FTIR spectroscopic analysis revealed a broad absorption at 3278 cm^{-1} , characteristic of the hydroxyl functionality (Figure 2.7).

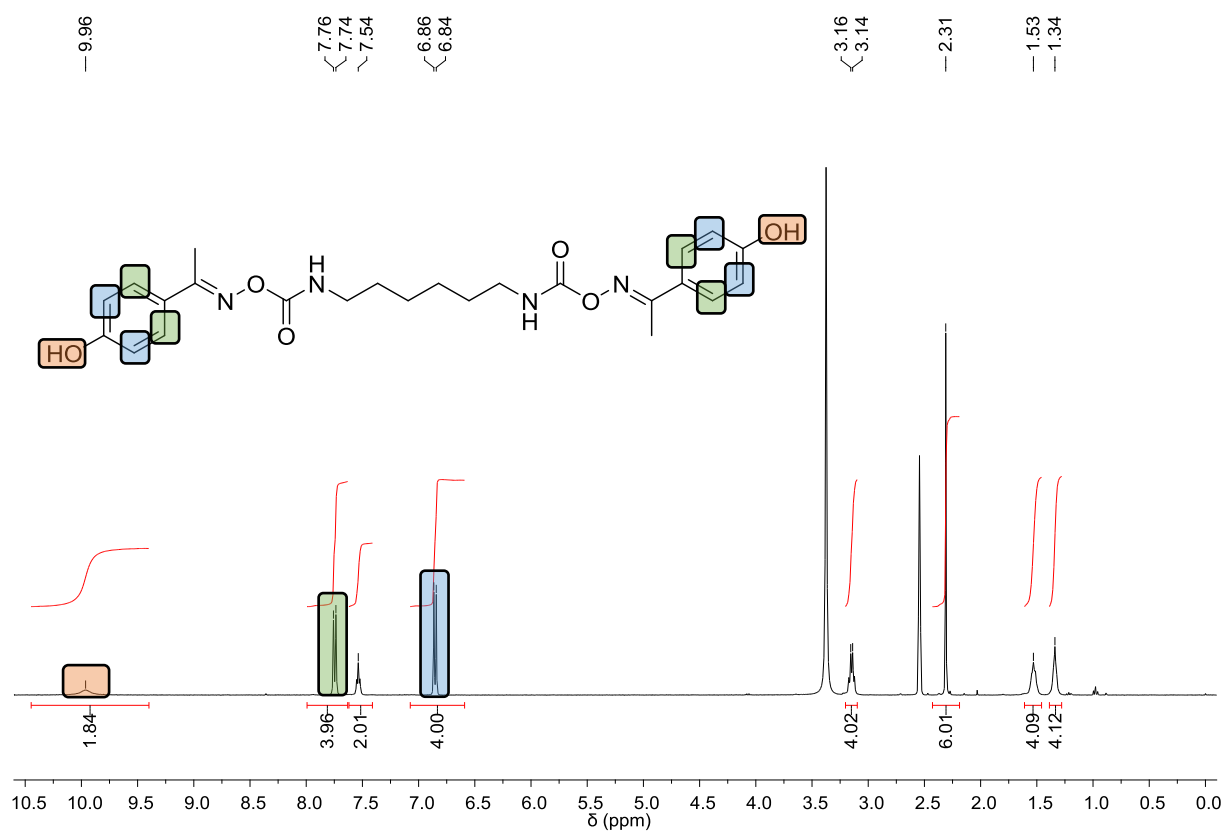
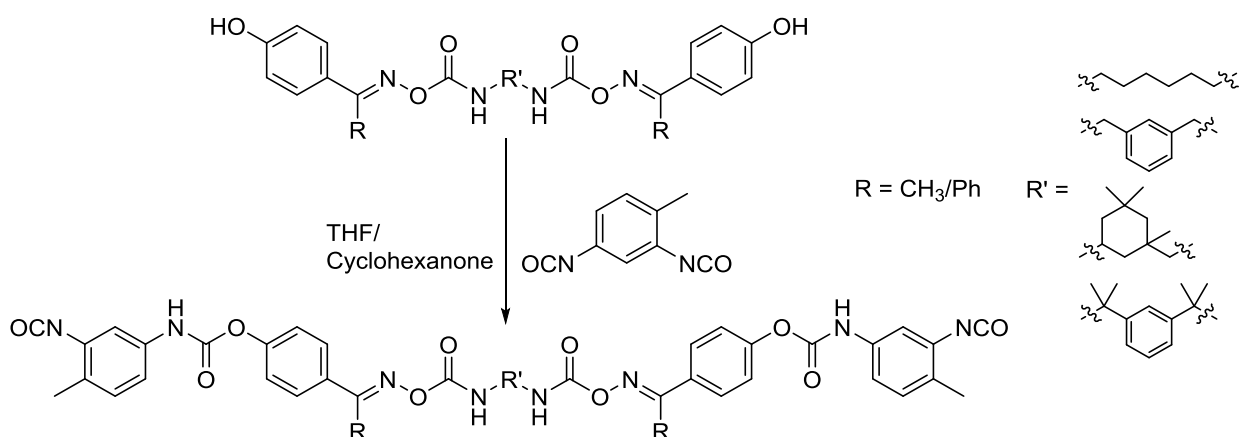


Figure 2.7. ^1H NMR spectrum of deprotected oxime-urethane synthesised from HDI and acetophenone oxime, highlighting the absence of resonances corresponding to the cleaved silyl protecting group.

2.2.5. Synthesis of Isocyanate-Terminated Shell Wall Precursors

The hydroxy end group moieties of the deprotected oxime-urethanes were then reacted with an excess of TDI to give isocyanate-terminated shell wall precursors bearing a thermally-degradable oxime-urethane **2.5a-h** (Scheme 2.7). All shell wall precursors exhibited good solubility in common organic solvents with the exception of precursors synthesised from XDI which proved to be unsuitable candidates for the synthesis of microcapsules.



Scheme 2.7. Synthesis of an isocyanate-terminated shell wall precursors **2.5a-h**, achieved by the reaction of the hydroxyl functionality of the deprotected oxime-urethane and an excess of toluene-2,4-diisocyanate (TDI).

As a result of the sensitivity of the isocyanate functional group to moisture, spectroscopic analysis was only performed on the crude material. The isocyanate functionality of the shell wall precursor is central to microcapsule synthesis and the stretching vibration of this moiety can be easily observed using FTIR spectroscopy. The IR spectrum revealed a strong absorption band at 2264 cm^{-1} corresponding to the isocyanate moiety. Further absorptions at 3287 , 1704 , 1596 , 1502 , 1196 and 900 cm^{-1} were also observed, correlating of N-H, urethane C=O, C=N, C-N, C-O and N-O functionalities (Figure 2.8).

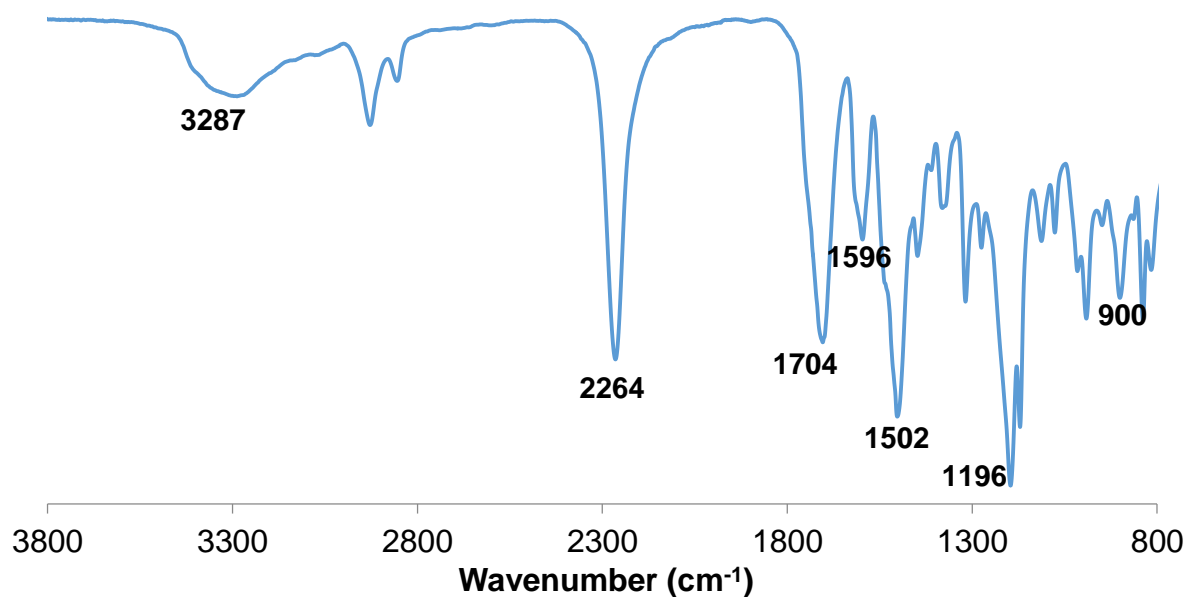


Figure 2.8. FTIR spectrum of isocyanate terminated shell wall precursor bearing a thermally-degradable linker (2.5). Highlighting key absorptions at 3287, 2264, 1704, 1596, 1502, 1196 and 900 cm⁻¹ corresponding to N-H, NCO, urethane C=O, C=N, C-N, C-O and N-O functionalities.

Terminating the deprotected oxime-urethanes with diisocyanate can lead to the formation of oligomers via a polymerisation reaction of the hydroxyl compound and TDI. Ideally, the formation of oligomers is undesired since increasing the molecular weight can result in poor solubility, hindering the formation of the microcapsule shell wall. Thus, it was important to measure the molecular weight of the shell wall precursor. Mass spectrometry was unable to accurately measure the molecular weight of the shell wall precursors. Thus molecular weight determination was achieved by end group analysis using titration analysis.

End group analysis involved reacting the isocyanate functional groups of the shell wall precursor with a known excess quantity of ⁿdibutylamine to form a urea. The resultant urea/amine mixture was titrated with HCl, using bromophenol blue to indicate the end point by a blue to yellow colour change. Comparison of this titre against that of blank ⁿdibutylamine solution allowed the calculation of the isocyanate composition of the shell wall precursor using Equation 1.1.

$$\text{NCO \%} = \left[\frac{(V_{\text{Blank}} - V_{\text{Sample}}) \times N \times 0.0420}{\text{Sample Mass}} \right] \times 100 \quad \text{Equation 1.1}$$

Where: V_{Blank} = blank titre, V_{Sample} = sample titre and N = normality of HCl.

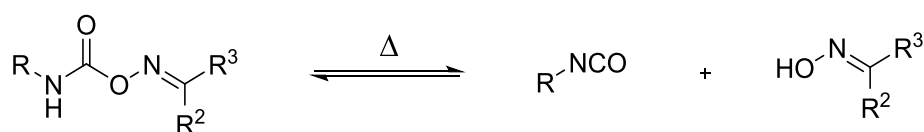
The degree of polymerisation can thus be determined by comparison of the observed isocyanate composition against the predicted value for the desired shell-wall precursors. The synthesised shell wall precursors all possess isocyanate compositions close to the predicted values suggesting the synthesis of the desired shell wall precursors has been achieved (Table 2.3).

Table 2.3. List of the isocyanate compositions and the predicted values of the isocyanate-terminated shell wall precursors **2.5a-h**.

	Oxime	Isocyanate	Predicted NCO %	Observed NCO %
2.5a	Acetophenone	HDI	10	11
2.5b	Benzophenone	HDI	9	9
2.5e	Acetophenone	IPDI	10	11
2.5f	Benzophenone	IPDI	8	8
2.5g	Acetophenone	TMXDI	9	10
2.5h	Benzophenone	TMXDI	8	9

2.2.6. The Dissociation of Thermally Labile Linkers

In order to design microcapsules that release their core contents at specific temperatures, it was important to observe the thermal dissociation of the oxime-urethane linkers. A range of analytical techniques have been used to observe this dissociation including - variable temperature infra-red spectroscopy (VTIR),²² thermogravimetric analysis (TGA)²³ and differential scanning calorimetry (DSC).²⁴



Scheme 2.8. Schematic representing the reversible reaction of oxime-urethanes when exposed to heat.

The dissociation of oxime-urethanes regenerates isocyanate and oxime moieties (Scheme 2.8). Isocyanates possess a characteristic stretching vibration observed as an absorption at $\sim 2250 \text{ cm}^{-1}$ in the IR spectrum. Thus VTIR can be employed as an effective analytical tool for the dissociation reaction. Analysis of the protected oxime **2.3a-h** was carried out to avoid any possible interference that could occur resulting from reactions of deprotected oxime-urethanes **2.4a-h**, or isocyanate-terminated shell wall precursors **2.5a-h**.

2.2.6.1. Variable Temperature Infra-red Spectroscopy

The oxime-urethanes **2.3a-h** were dissolved in dried tetraethylene glycol dimethyl ether in a concentration of 3.0 M. This solution was injected into a variable temperature IR spectroscopy cell utilising NaCl windows separated by a 0.050 mm PTFE spacer. The cell was placed in a variable temperature cell holder and an IR spectrum recorded at 10 °C increments with a FTIR spectrometer and the appearance of an absorption corresponding to the isocyanate functionality formed upon dissociation was observed.

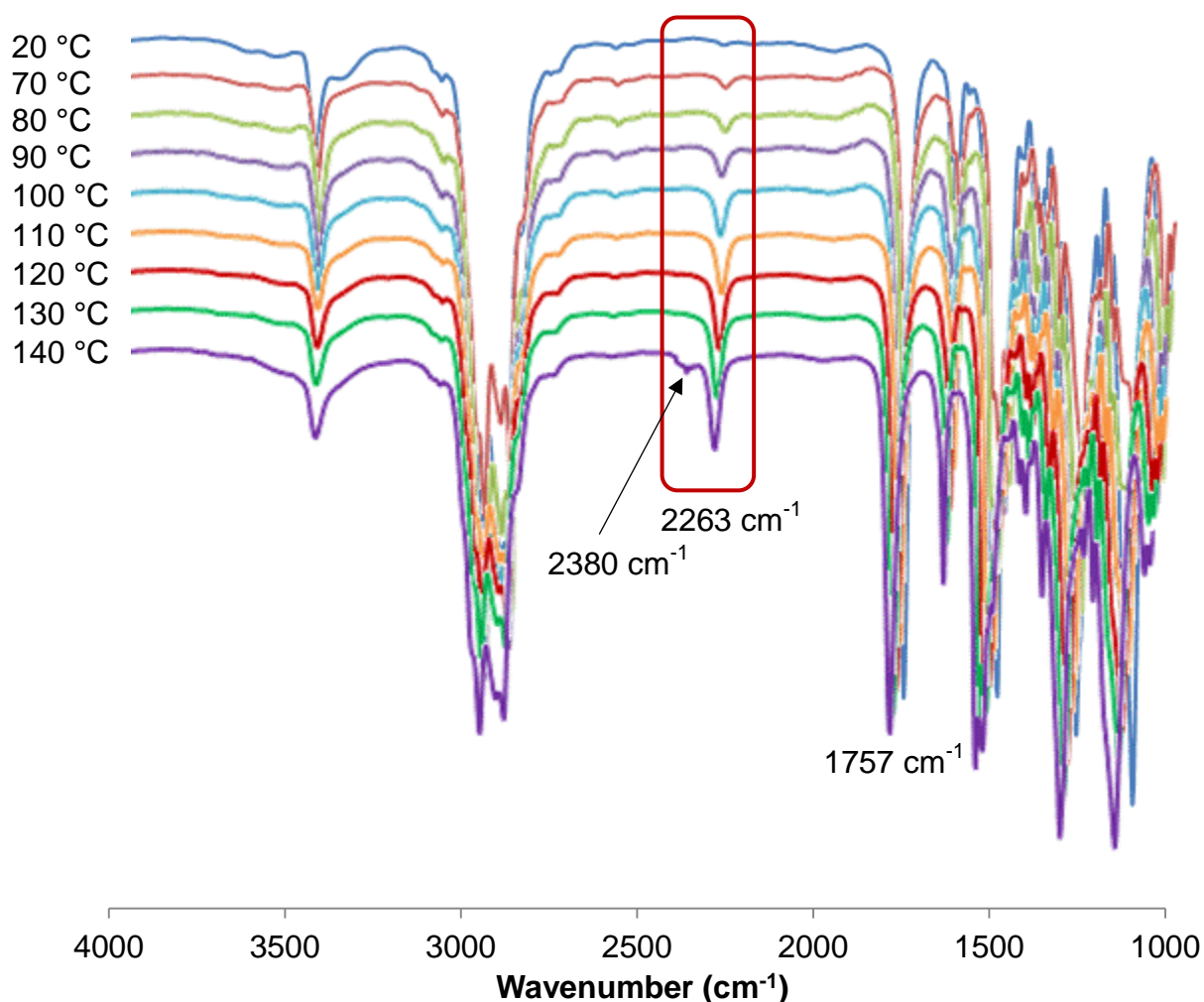


Figure 2.9. Variable-temperature IR spectra of oxime-urethane at 10 °C increments between 20 and 70 °C, highlighting the appearance of an absorbance corresponding to the isocyanate moiety.

Figure 2.9 displays the VTIR experiment of **2.3h**. At 20 °C, an absorbance corresponding to the C=O functionality of the oxime-urethane at 1757 cm⁻¹ was observed. Upon increasing the temperature to 70 °C, an absorbance characteristic of

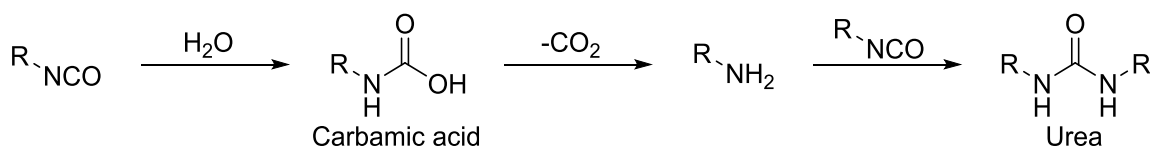
the isocyanate moiety appeared at 2263 cm^{-1} . Literature studies quote this value as the dissociation temperature.²² Further increasing the temperature led to an increase in the intensity of this absorption indicating the dissociation occurred over a broad temperature range.

The onset dissociation of the oxime-urethane linkers are listed in Table 2.4 and the results demonstrate how modifying the steric hindrance around the oxime-urethane can have a significant effect on the dissociation temperature. Employing sterically encumbered isocyanates leads to a significant reduction of the dissociation temperature and could allow the tailor of microcapsules designed to release their core contents at a specific temperature. Further control of the dissociation has been achieved by using a more sterically encumbered oxime, reducing the dissociation temperature by an additional 5-20 °C. These results are in agreement with degradation data reported in literature studies.²²

Table 2.4. List of dissociation temperatures of different oxime-urethanes **2.3a-h** using VTIR spectroscopy.

	Oxime	Diisocyanate	Dissociation Temperature (°C)
2.3a	Acetophenone	HDI	120
2.3b	Benzophenone	HDI	100
2.3c	Acetophenone	XDI	110
2.3d	Benzophenone	XDI	90
2.3e	Acetophenone	IPDI	100
2.3f	Benzophenone	IPDI	90
2.3g	Acetophenone	TMXDI	70
2.3h	Benzophenone	TMXDI	65

When the temperature reaches 140 °C a further absorption appears at 2383 cm^{-1} typical of an absorption corresponding to carbon dioxide. Although great care was taken to remove water from the system - the solvent was dried prior to the experiment, NaCl windows were desiccated over phosphorous pentoxide and the experiment was performed inside a sealed cell - the observed carbon dioxide may have formed by decarboxylation of carbamic acid, resulting from the reaction of generated isocyanate and water. The resultant amine then has the capability to react with further isocyanate to form a urea (Scheme 2.9).



Scheme 2.9. Reaction of isocyanate and water followed by decarboxylation to generate an amine. Further reaction with isocyanates yielding a urea.

To support this observation, pure TMXDI was heated in the same conditions and a similar result was observed. At room temperature an absorption typical of the isocyanate vibration was observed at 2271 cm^{-1} and upon further heating to $140 \text{ }^\circ\text{C}$, an absorption appeared at 2380 cm^{-1} . Further absorptions at 3420 and 1734 cm^{-1} correspond to N-H and C=O vibrations, respectively, suggest the formation of a urea (Figure 2.10). This may prevent the observation of dissociation above $140 \text{ }^\circ\text{C}$ and thus poses a limitation on VTIR spectroscopy as a tool to analyse the dissociation of blocked isocyanates.

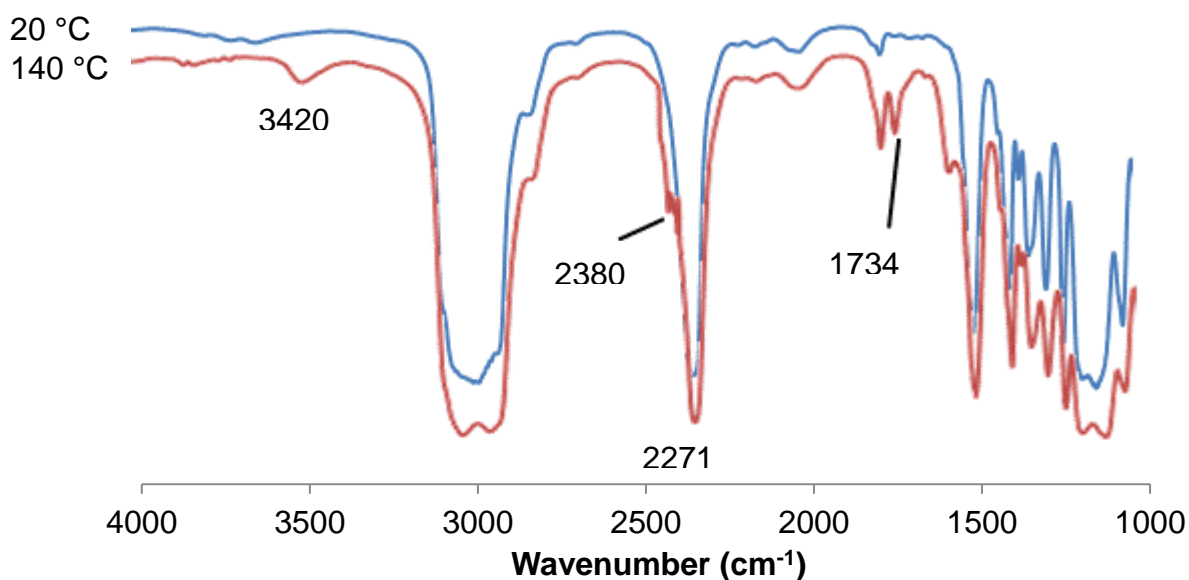


Figure 2.10. FTIR spectra of TMXDI at $20 \text{ }^\circ\text{C}$ and $140 \text{ }^\circ\text{C}$, observing the appearance of an absorbance at 2380 cm^{-1} corresponding to evolved carbon dioxide.

2.2.6.2. Differential Scanning Calorimetry

Differential scanning calorimetry (DSC) has also been used to observe the dissociation of blocked isocyanates in literature studies.^{24,25} Heat is absorbed as dissociation occurs and appears as an endothermic thermal transition. The oxime-urethanes, **2.3a-h**, were heated at a rate of $10 \text{ }^\circ\text{C}/\text{minute}$ under an atmosphere of nitrogen.

Figure 2.11 shows the DSC trace of **2.3h**. An initial endothermic transition is observed at $50 \text{ }^\circ\text{C}$ corresponding to a melting point. No further thermal changes are observed

until a broad endotherm at 141 °C that may correspond to the dissociation of the oxime-urethane. Literature studies typically quote the dissociation temperature at this point.²⁴ Although VTIR studies observe the onset of dissociation of **2.3h** at 70 °C, a thermal transition was not observed using DSC at this temperature. It has been reported²⁶ in literature studies that different techniques used to measure the dissociation of blocked isocyanates afford different results.²⁷

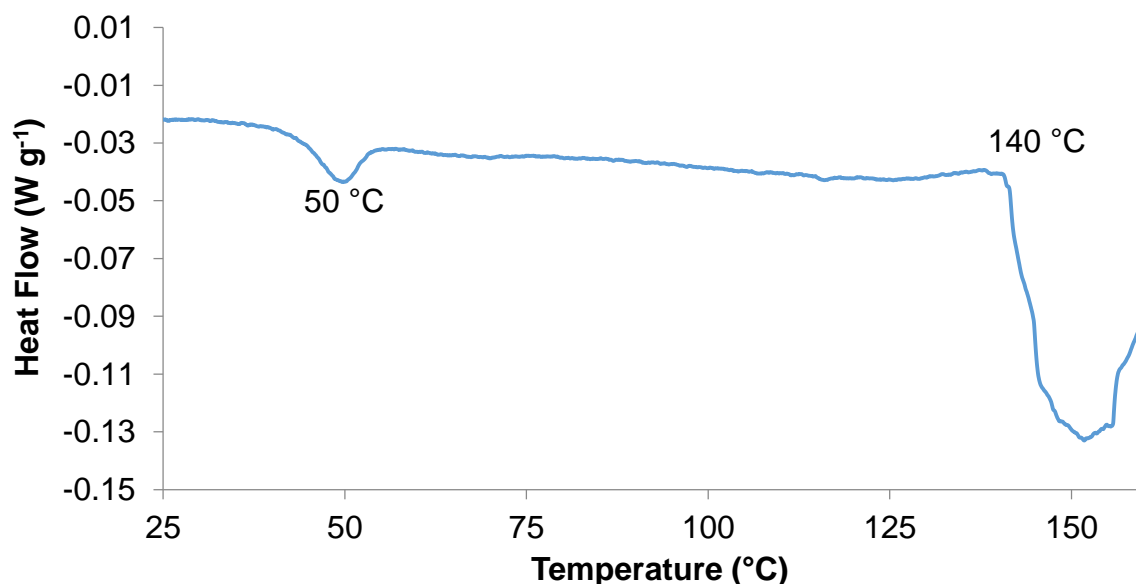


Figure 2.11. DSC trace of oxime-urethane synthesised from TMXDI and protected acetophenone oxime.

Although a dissociation temperature was obtained for **2.3h**, generally DSC proved to be an ineffective technique to analyse the dissociation of these oxime-urethanes. The dissociation of oxime-urethanes has been reported²⁴ to be a slow process and occurs over a large temperature range. As a result, the endothermic transitions observed are often very broad, thus assigning a temperature of dissociation is difficult and unreliable.

2.2.6.3. Thermogravimetric Analysis

Thermogravimetric analysis can also allow observation of the dissociation of blocked isocyanates²³ if the temperature reaches or exceeds the boiling point of the reaction products. Figure 2.12 shows the TGA trace of **2.3h**. The sample was heated at a rate of 10 °C/minute under an atmosphere of nitrogen and the dissociation temperature is typically quoted at the temperature at which 5 wt% of the sample is lost.²⁴ TGA was also performed on the individual oximes **2.2a** and **2.2b** revealing degradation temperatures at 160 °C and 177 °C, respectively. Although VTIR spectroscopic studies

suggest dissociation arises at 70 °C, no weight change was observed until 177 °C leading to almost complete weight loss by 270 °C. It was clear that weight loss of **2.2h** at 177 °C was caused by the degradation of the released oxime and therefore TGA was demonstrated to be an impractical technique for measuring the dissociation of these oxime-urethanes. TGA of the oxime-urethanes revealed weight loss at either 160 °C or 175 °C resulting from the degradation of the generated oximes (Table 2.5).

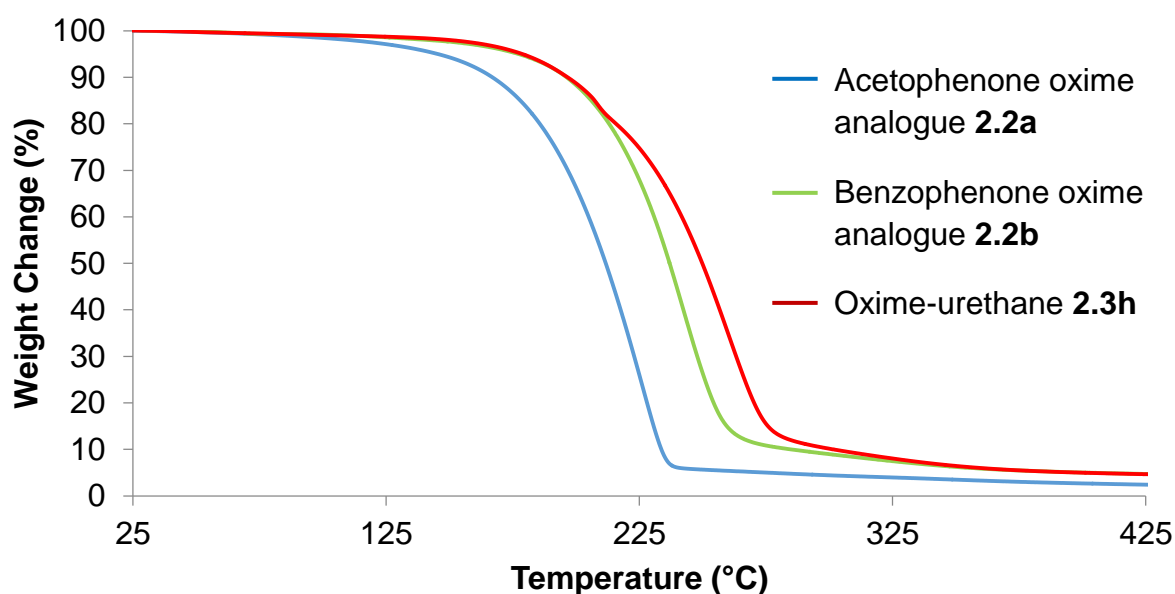


Figure 2.12. TGA trace of oxime-urethane synthesised from TMXDI and protected benzophenone oxime

Table 2.5. List of degradation temperatures of different oxime-urethanes using TGA

	Oxime	Diisocyanate	Degradation Temperature (°C)
2.3a	Acetophenone	HDI	158
2.3b	Benzophenone	HDI	170
2.3c	Acetophenone	XDI	161
2.3d	Benzophenone	XDI	176
2.3e	Acetophenone	IPDI	168
2.3f	Benzophenone	IPDI	174
2.3g	Acetophenone	TMXDI	164
2.3h	Benzophenone	TMXDI	177

2.3. Conclusion

This chapter has described the design and synthesis of isocyanate-terminated shell wall precursors that possess a thermally-labile oxime-urethane bond and are capable of further chain extension to form microcapsules. The synthetic route employed involved the initial synthesis of protected hydroxy-functionalised acetophenone and benzophenone oximes from the corresponding ketones. Reaction of the oximes with a range of diisocyanates - HDI, XDI, IPDI and TMXDI, yielded a library of oxime-urethanes possessing varying degrees of steric hindrance. Subsequent deprotection of these molecules to reveal the phenolic moiety allowed reaction with an excess of toluene-2,4-diisocyanate to afford the isocyanate-terminated shell wall precursors. VTIR spectroscopic analysis was employed to observe the dissociation of the oxime-urethane bond, revealing the temperature of dissociation is dependent on the degree of steric hindrance around the bond. DSC was demonstrated to be an ineffective tool for observing the dissociation and thus could not be used to corroborate the results obtained using VTIR spectroscopic analysis. TGA was demonstrated to be unsuitable tool for the measurement of the dissociation of oxime-urethanes detecting only the degradation of the dissociated oximes. The successful incorporation of thermally-labile oxime-urethanes into polyurethane microcapsules is described in **Chapter 3**.

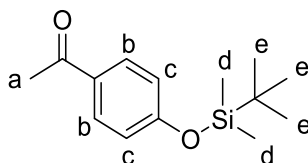
2.4. Experimental

Chemicals. All chemicals and reagents were purchased from Sigma Aldrich with the exception of xylylene diisocyanate (XDI) which was purchased from Tokyo Chemicals Industry and dibutyltin dilaurate (DBTDL) which was provided by BAE Systems plc. Tetrahydrofuran (THF) was distilled from sodium and benzophenone, dichloromethane was distilled from CaH_2 and tetraethylene glycol dimethylether was vacuum distilled from CaH_2 (100 °C, 0.1 mmHg). All other chemicals were used as supplied without further purification.

Equipment. ^1H and ^{13}C NMR spectra were obtained using a Bruker Nanobay 400 MHz spectrometer operating at 400 MHz and 100 MHz, respectively, referenced to the residual ^1H solvent signal either from the deuterated chloroform (CDCl_3) used (7.26 ppm), tetramethylsilane (TMS), deuterated dimethylsulfoxide (DMSO-d_6) used (2.50 ppm) or deuterated acetone (acetone-d_6) used (2.05 ppm). FTIR spectra were obtained using a Perkin Elmer Spectrum 100, using a PE Universal ATR sampling

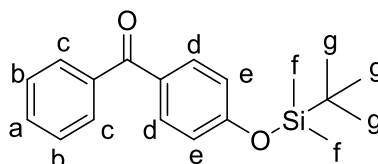
accessory. Mass spectrometry was conducted using a ThermoFisher Scientific Orbitrap XL LCMS operating an electrospray ioniser (ESI). VTIR spectroscopy was carried out using a Perkin Elmer Spectrum 100 utilising a Specac variable temperature cell holder employing a static liquid sample cell. Differential scanning calorimetry (DSC) was carried out using a TA Instruments Q2000 calorimeter. Thermogravimetric analysis employed a TA instruments Q50 thermogravimetric analyser.

Silyl-protection of 4'-hydroxyacetophenone **2.1a**²⁰



4'-Hydroxyacetophenone (1.00 g, 7.3 mmol), *tert*-butyldimethylsilylchloride (TBDMSCl) (1.22 g, 8.1 mmol), 4-dimethylaminopyridine (DMAP) (0.027 g, 0.2 mmol) and triethylamine (0.82 g, 8.1 mmol) were dissolved in dry dichloromethane (20 mL) and stirred at room temperature for 18 hours under an atmosphere of argon. The solution was washed sequentially with NH₄Cl (saturated), H₂O, dried over MgSO₄, filtered, concentrated *in vacuo* and then purified by column chromatography (R_f = 0.25, 5 % EtOAc/hexane) to yield a white crystalline solid **2.1a** (1.67 g, 91 %) (m.p. 38-39 °C). ¹H NMR (400 MHz, CDCl₃) δ_H (ppm): 0.26 (6H, s, H_d), 1.01 (9H, s, H_e), 2.57 (3H, s, H_a), 6.90 (2H, app. d *J* = 9.0 Hz, H_c), 7.90 (2H, app. d *J* = 9.0 Hz, H_b); ¹³C NMR (100 MHz, CDCl₃) δ_C (ppm): -4.2, 18.4, 25.8, 26.5, 120.1, 130.7, 131.0, 160.4, 197.1; FTIR (ATR) ν (cm⁻¹): 2928 (C-H), 2895 (C-H), 2857 (C-H), 1674 (C=O), 1253 (Si-O) 1175 (C-O); ESIMS calculated mass (C₁₄H₂₂O₂Si+H)⁺ 251.1462 found 251.1461.

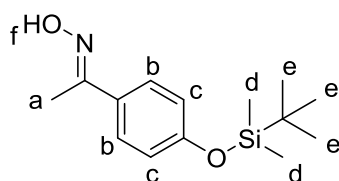
Silyl-protection of 4-hydroxybenzophenone **2.1b**



4-Hydroxybenzophenone (3.59 g, 18.1 mmol), TBDMSCl (3.00 g, 20.0 mmol), DMAP (0.073 g, 0.6 mmol) and triethylamine (2.02 g, 20.0 mmol) were dissolved in dry dichloromethane (40 mL) and stirred at room temperature for 18 hours under an atmosphere of argon. The solution washed sequentially with NH₄Cl (saturated), H₂O, dried over MgSO₄ followed by filtration and the solution was concentrated *in vacuo* and

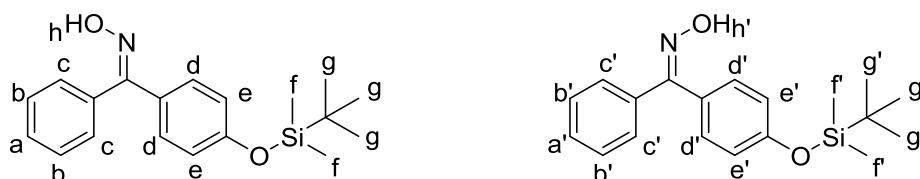
then purified by column chromatography ($R_f = 0.25$, 5 % EtOAc/hexane) to leave a colourless oil **2.1b** (5.50 g, 97 %). ^1H NMR (400 MHz, CDCl_3) δ_{H} (ppm): 0.25 (6H, s, H_f), 1.00 (9H, s, H_g), 6.90 (2H, app. d $J = 9.0$ Hz, H_e), 7.47 (2H, app. t $J = 7.0$ Hz, H_b), 7.56 (1H, app. t $J = 7.5$ Hz, H_a), 7.76 (2H, br. m, H_d) 7.78 (2H, br. m, H_c); ^{13}C NMR (100 MHz, CDCl_3) δ_{C} (ppm): -4.3, 18.3, 25.6, 119.7, 128.2, 129.7, 130.7, 131.9, 132.5, 138.2, 159.9, 195.5; FTIR (ATR) ν (cm^{-1}): 2954 (C-H), 2929 (C-H), 2867 (C-H), 1654 (C=O stretch), 1263 (Si-O stretch) 1165 (C-O stretch); ESIMS calculated mass ($\text{C}_{19}\text{H}_{23}\text{O}_2\text{Si}+\text{H}$) $^+$ 313.1618 found 313.1620.

Conversion of **2.1a** to the corresponding oxime **2.2a**²⁰



Protected 4'-hydroxyacetophenone **2.1a** (1.55 g, 6.2 mmol), hydroxylamine hydrochloride (0.47 g, 6.8 mmol) and triethylamine (0.75 g, 7.4 mmol) were dissolved in EtOH (20 mL) and maintained under reflux for 18 hours. EtOH was removed *in vacuo* and the resultant solid dissolved in EtOAc, washed with H_2O and dried over MgSO_4 followed by filtration and the solvent removed *in vacuo* to give a white solid **2.2a** (1.60 g, 98 %) (m.p. 67-71 °C). ^1H NMR (400 MHz, CDCl_3) δ_{H} (ppm): 0.21 (6H, s, H_d), 0.98 (9H, s, H_e), 2.27 (3H, s, H_a), 6.84 (2H, app. d $J = 9.0$ Hz, H_c), 7.51 (2H, app. d $J = 9.0$ Hz, H_b), 8.82 (1H, br. s, H_f); ^{13}C NMR (100 MHz, CDCl_3) δ_{C} (ppm): -4.2, 12.3, 18.4, 25.8, 120.3, 127.5, 129.8, 155.8, 157.0; FTIR (ATR) ν (cm^{-1}): 3239 (O-H), 2954 (C-H), 2929 (C-H), 2858 (C-H), 1601 (C=N), 1259 (Si-O), 1172 (C-O), 911 (N-O); ESIMS calculated mass ($\text{C}_{14}\text{H}_{23}\text{O}_2\text{NSi}+\text{H}$) $^+$ 266.1571 found 266.1659.

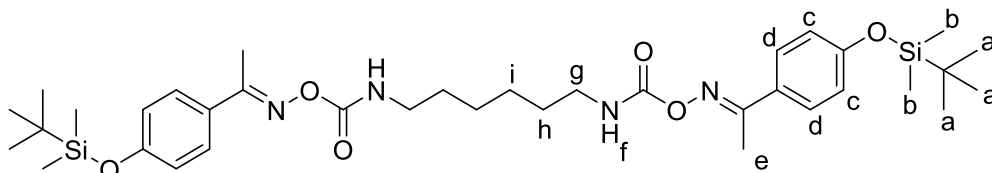
Conversion of **2.1b** to the corresponding oxime **2.2b**



Protected 4'-hydroxyacetophenone **2.1b** (1.01 g, 3.2 mmol), hydroxylamine hydrochloride (0.245 g, 3.5 mmol) and pyridine (0.278 g, 3.5 mmol) were dissolved in

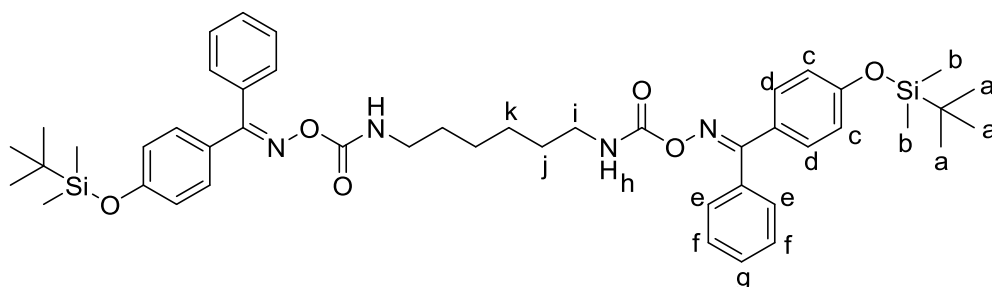
EtOH (40 mL) and maintained under reflux for 24 hours. EtOH was removed *in vacuo* and the resultant solid dissolved in EtOAc and washed sequentially with NH₄Cl (saturated), H₂O and dried over MgSO₄ followed by filtration and the solvent removed *in vacuo* to give a white solid **2.2b** as a mixture of *E/Z* isomers (1:1) (0.998 g, 95 %) (m.p. 65-67 °C). *E*-isomer: ¹H NMR (400 MHz, CDCl₃) δ_H (ppm): 0.19 (6H, s, H_f), 0.97 (9H, s, H_g), 6.78 (2H, app. d *J* = 9.0 Hz, H_e), 7.34 (2H, br. m, H_b), 7.37 (1H, br. m, H_a), 7.39 (2H, br. m, H_d), 7.41 (2H, br. m, H_c); 8.78 (1H, br. s, H_h); ¹³C NMR (100 MHz, CDCl₃) δ_C (ppm): -4.4, 14.2, 18.2, 60.5, 116.9, 125.1, 128.2, 129.3, 131.2, 136.8, 157.1, 171.2; *Z*-isomer: ¹H NMR (400 MHz, CDCl₃) δ_H (ppm): 0.24 (6H, s, H_f), 1.00 (9H, s, H_g), 6.90 (2H, app. d *J* = 9.0 Hz, H_e), 7.35 (2H, br. m, H_b), 7.37 (1H, br. m, H_a), 7.41 (2H, br. m, H_c), 7.44 (2H, br. m, H_d); 8.92 (1H, br. s, H_h); ¹³C NMR (100 MHz, CDCl₃) δ_C (ppm): -4.3, 21.1, 25.6, 60.5, 119.9, 128.3, 129.0, 129.1, 132.9, 156.4, 157.7, 171.2; FTIR (ATR) ν (cm⁻¹): 3251 (O-H), 2954 (C-H), 2928 (C-H), 2857 (C-H), 1601 (C=N), 1252 (Si-O), 1160 (C-O), 908 (N-O); ESIMS calculated mass (C₁₉H₂₅O₂NSi+H)⁺ 328.1727 found 328.1729.

Synthesis of oxime-urethane **2.3a**²⁰



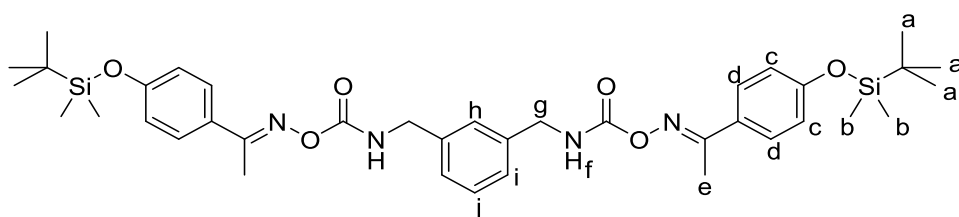
Protected 4'-hydroxyacetophenone oxime **2.2a** (1.36 g, 5.1 mmol) and hexamethylene diisocyanate (HDI) (0.391 g, 2.3 mmol) were dissolved in dry tetrahydrofuran (THF) (20 mL) and maintained under reflux for 18 hours in an argon atmosphere. The solvent was removed *in vacuo* and the crude product purified by column chromatography (*R*_f = 0.2, 30 % EtOAc/hexane) to give a white solid **2.3a** (1.40 g, 88 %) (m.p. 95-98 °C). ¹H NMR (400 MHz, CDCl₃) δ_H (ppm): 0.22 (12H, s, H_b), 0.99 (18H, s, H_a), 1.41 (4H, br. m, H_i), 1.61 (4H, br. m, H_h), 2.39 (6H, s, H_e), 3.33 (4H, q *J* = 6.5 Hz, H_g), 6.49 (2H, br. m, H_f), 6.87 (4H, app. d *J* = 9.0 Hz, H_c), 7.57 (4H, app. d *J* = 9.0 Hz, H_d); ¹³C NMR (100 MHz, CDCl₃) δ_C (ppm): -4.4, 14.3, 18.3, 25.6, 26.4, 29.8, 41.0, 120.3, 127.7, 128.2, 155.8, 158.1, 159.6; FTIR (ATR) ν (cm⁻¹): 3367 (N-H), 2929 (C-H), 2857 (C-H), 1721 (C=O), 1600 (C=N), 1497 (C-N), 1253 (Si-O), 1172 (C-O), 904 (N-O); ESIMS calculated mass (C₃₆H₅₈O₆N₄Si₂+H)⁺ 699.3968 found 699.3967.

Synthesis of oxime-urethane **2.3b**



Protected 4-hydroxybenzophenone oxime **2.2b** (0.906 g, 2.8 mmol) and HDI (0.233 g, 1.38 mmol) were dissolved in dry THF (40 mL) and maintained under reflux for 18 hours. The solvent was removed *in vacuo* to leave a yellow oil which was purified by column chromatography (R_f 0.26, 30 % EtOAc/hexane) to yield a white solid **2.3b** (0.960 g, 85 %) (m.p. 61-65°C). ^1H NMR (400 MHz, CDCl_3) δ_{H} (ppm): 0.21-0.24 (12H, s, H_b), 0.98-1.00 (18H, s, H_a), 1.41 (4H, br. m, H_k), 1.62 (4H, br. m, H_j), 3.32 (4H, q $J = 6.5$ Hz, H_i), 6.40 (1H, br. m, H_h), 6.50 (1H, br. m, H_i), 6.82 (2H, app d $J = 9.0$ Hz, H_c), 6.82 (2H, app d $J = 9.0$ Hz, H_d), 7.32-7.50 (14H, m, H_{defg}); ^{13}C NMR (100 MHz, CDCl_3) δ_{C} (ppm): -4.4, 18.2, 25.6, 26.4, 29.8, 41.1, 119.6, 120.0, 124.5, 127.9, 128.2, 128.4, 129.1, 129.6, 130.3, 130.5, 131.8, 132.3, 135.8, 155.5, 155.6, 157.3, 158.3, 161.1, 161.2; FTIR (ATR) ν (cm^{-1}): 3350 (N-H), 2929 (C-H), 2857 (C-H), 1722 (C=O), 1602 (C=N), 1505 (C-N), 1254 (Si-O), 1164 (C-O), 908 (N-O); ESIMS calculated mass ($\text{C}_{46}\text{H}_{62}\text{O}_6\text{N}_4\text{Si}_2+\text{H}$) $^+$ 823.4281 found 823.4298.

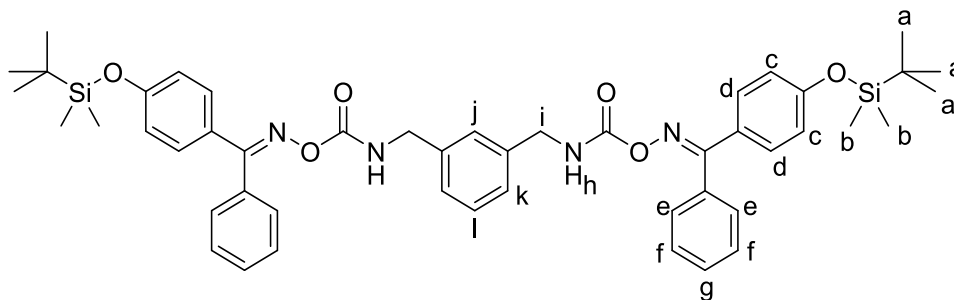
Synthesis of oxime-urethane **2.3c**



Protected 4'-hydroxyacetophenone oxime **2.2a** (0.195 g, 0.8 mmol) and xylylene diisocyanate (XDI) (0.050 g, 0.3 mmol) were dissolved in THF (10 mL) and maintained under reflux for 24 hours. The solvent was removed *in vacuo* to leave a pale yellow oil which was purified by column chromatography (R_f 0.30, 30 % EtOAc/hexane) to give a white solid **2.3c** (0.104 g, 54 %) (m.p. 48-51 °C). ^1H NMR (400 MHz, CDCl_3) δ_{H} (ppm): 0.21 (12H, s, H_b), 0.98 (18H, s, H_a), 2.39 (6H, s, H_e), 4.53 (4H, s, H_g), 6.84 (2H, br. m, H_f), 6.85 (4H, app. d $J = 9.0$ Hz, H_c), 7.30 (3H, br. m, H_{hi}), 7.32 (1H, m, H_j), 7.55 (4H,

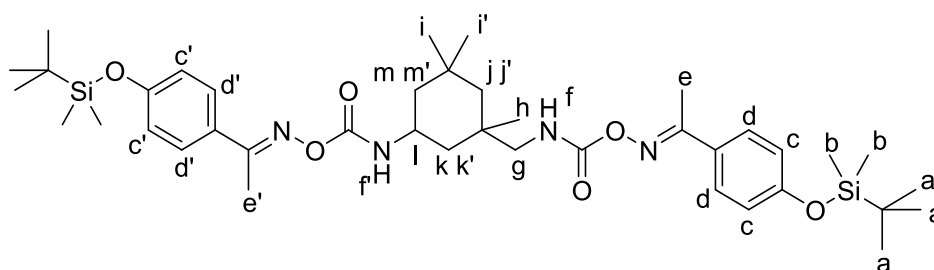
app. d $J = 9.0$ Hz, H_d); ^{13}C NMR (100 MHz, CDCl_3) δ_{C} (ppm): -4.4, 14.4, 18.2, 25.6, 44.9, 120.3, 126.8, 126.8, 127.6, 128.3, 129.2, 138.7, 155.9, 158.1, 160.0; FTIR (ATR) ν (cm^{-1}): 3399 (N-H), 2929 (C-H), 2857 (C-H), 1743 (C=O), 1600 (C=N), 1486 (C-N), 1253 (Si-O), 1171 (C-O), 906 (N-O); ESIMS calculated mass ($\text{C}_{38}\text{H}_{54}\text{O}_6\text{N}_4\text{Si}_2+\text{H}$)⁺ 719.3655 found 719.3658.

Synthesis of oxime-urethane **2.3d**



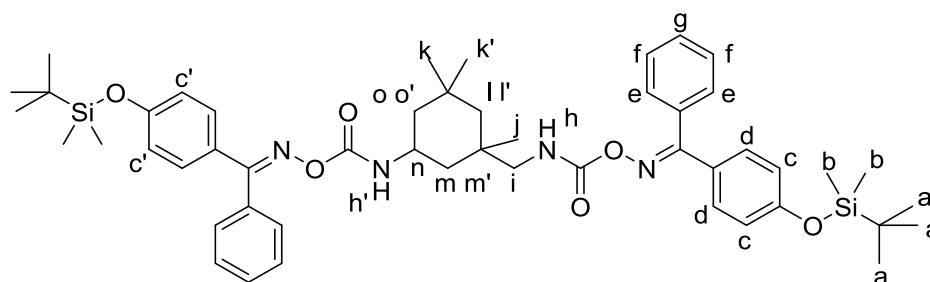
Protected 4-hydroxybenzophenone oxime **2.2b** (1.65 g, 5.1 mmol) and XDI (0.317 g, 1.68 mmol) were dissolved in dry THF (40 mL) and maintained under reflux for 18 hours. The solvent was removed *in vacuo* to leave a yellow oil which was purified by column chromatography (R_f 0.14, 20 % EtOAc/hexane) to yield a white solid **2.3d** (1.35 g, 95 %) (m.p. 53-56 °C). ^1H NMR (400 MHz, CDCl_3) δ_{H} (ppm): 0.20-0.24 (12H, s, H_b), 0.97-1.00 (18H, s, H_a), 4.53 (4H, s, H_i), 6.73 (1H, br. m, H_h), 6.80 (2H, app. d $J = 8.5$ Hz, H_c), 6.84 (1H, br. m, $H_{h'}$), 6.87 (2H, app. d $J = 8.5$ Hz, $H_{c'}$) 7.29-7.48 (18H, br. m, H_{defgijkl}); ^{13}C NMR (100 MHz, CDCl_3) δ_{C} (ppm): -4.4, 18.2, 25.6, 45.0, 119.6, 120.0, 124.5, 126.9, 127.0, 127.7, 128.3, 128.4, 129.2, 129.9, 130.4, 130.6, 131.8, 132.2, 135.6, 138.7; FTIR (ATR) ν (cm^{-1}): 3412 (N-H), 2929 (C-H), 2857 (C-H), 1727 (C=O), 1602 (C=N), 1504 (C-N), 1254 (Si-O), 1164 (C-O), 907 (N-O); ESIMS calculated mass ($\text{C}_{48}\text{H}_{58}\text{O}_6\text{N}_4\text{Si}_2+\text{Na}$)⁺ 865.3787 found 865.3761.

Synthesis of oxime-urethane **2.3e**



Protected 4'-hydroxyacetophenone oxime **2.2a** (4.44 g, 16.7 mmol) and isophorone diisocyanate (IPDI) (1.86 g, 8.4 mmol) were dissolved in THF (40 mL) and maintained under reflux for 24 hours. The solvent was removed *in vacuo* to leave a pale yellow solid **2.2e** (6.64 g, quant.) (m.p. 63-83 °C). ^1H NMR (400 MHz, CDCl_3) δ_{H} (ppm): 0.22 (12H, s, H_b), 0.99 (18H, s, H_a), 1.02 (3H, s, H_i), 1.06 (1H, m, H_m), 1.09 (1H, m, H_j), 1.12 (3H, m, H_h), 1.15 (1H, m, H_k), 1.17 (3H, s, $\text{H}_{i'}$), 1.28 (1H, m, $\text{H}_{j'}$), 1.85 (1H, m, $\text{H}_{m'}$), 1.88 (1H, m, $\text{H}_{k'}$), 2.38 (3H, m, H_e), 2.40 (3H, m, $\text{H}_{e'}$), 3.12 (1H, br. m, H_l), 4.00 (2H, br. m, H_g), 6.26 (1H, br. m, H_f), 6.62 (1H, br. m, $\text{H}_{f'}$), 6.87 (2H, app. d $J = 6.0$ Hz, H_c), 6.89 (2H, app. d $J = 6.0$ Hz, $\text{H}_{c'}$), 7.56 (2H, app. d $J = 6.0$ Hz, H_d); 7.57 (2H, app. d $J = 6.0$ Hz, $\text{H}_{d'}$); ^{13}C NMR (100 MHz, CDCl_3) δ_{C} (ppm): -4.4, 14.4, 18.3, 23.3, 32.0, 35.1, 36.6, 41.7, 44.9, 46.2, 47.3, 55.0, 120.3, 127.7, 128.2, 156.2, 158.7, 159.7; FTIR (ATR) ν (cm^{-1}): 3408 (N-H), 2929 (C-H), 2857 (C-H), 1722 (C=O), 1601 (C=N), 1504 (C-N), 1266 (Si-O), 1172 (C-O), 906 (N-O); ESIMS calculated mass ($\text{C}_{40}\text{H}_{64}\text{O}_6\text{N}_4\text{Si}_2+\text{Na}$) $^+$ 775.4236 found 775.4257.

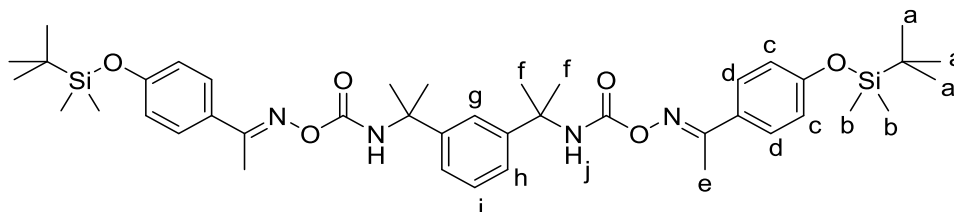
Synthesis of oxime-urethane **2.3f**



Protected 4-hydroxybenzophenone oxime **2.2b** (3.60 g, 11.0 mmol) and IPDI (1.22 g, 5.5 mmol) were dissolved in dry THF (40 mL) and maintained under reflux for 24 hours. The solvent was removed *in vacuo* to leave a yellow oil which was purified by column chromatography (R_f 0.18, 20 % EtOAc/hexane) to yield a white solid **2.3f** (8.01 g, 95 %) (m.p. 57-58 °C). ^1H NMR (400 MHz, CDCl_3) δ_{H} (ppm): 0.21-0.24 (12H, s, H_b), 0.98-

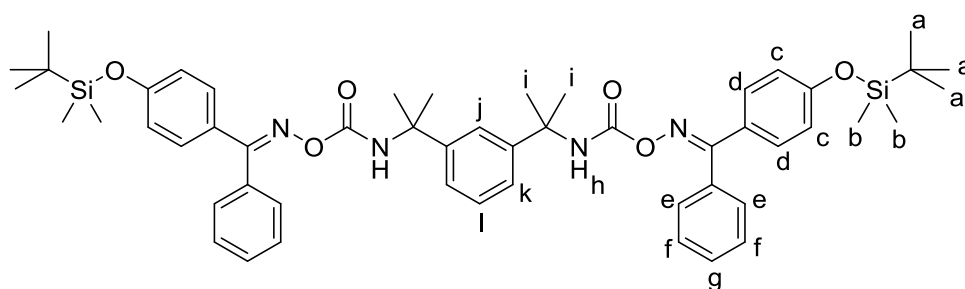
1.00 (18H, s, H_a), 1.00 (3H, s, H_k), 1.06 (1H, m, H_o), 1.09 (1H, m, H_l), 1.12 (3H, m, H_{k'}), 1.12 (3H, m, H_j), 1.17 (1H, m, H_m), 1.31 (1H, m, H_r), 1.85 (1H, m, H_{o'}), 1.85 (1H, m, H_{m'}), 3.11 (2H, br. m, H_i), 4.00 (1H, br. m, H_n), 6.51 (1H, br. m, H_h), 6.63 (1H, br. m, H_{h'}), 6.82 (2H, br. m, H_c), 6.88 (2H, br. m, H_{c'}), 7.31-7.57 (14H, m, H_{defg}); ¹³C NMR (100 MHz, CDCl₃) δ_C (ppm): -4.4, 18.2, 32.0, 35.1, 36.6, 41.7, 45.0, 46.3, 47.2, 54.9, 119.6, 120.0, 127.7, 128.3, 128.5, 129.2, 130.3, 131.8, 156.0, 158.3, 161.2; FTIR (ATR) ν (cm⁻¹): 3412 (N-H), 2929 (C-H), 2857 (C-H), 1732 (C=O), 1602 (C=N), 1505 (C-N), 1265 (Si-O), 1163 (C-O), 907 (N-O); ESIMS calculated mass (C₅₀H₆₈O₆N₄Si₂+Na)⁺ 899.4548 found 899.4570.

Synthesis of oxime-urethane **2.3g**



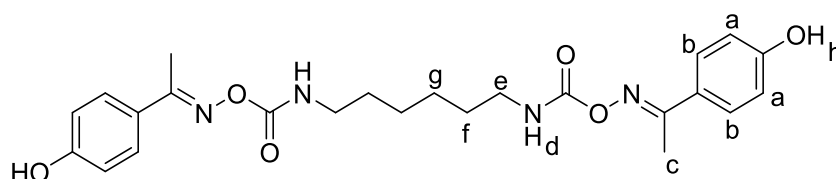
Protected 4'-hydroxyacetophenone oxime **2.2a** (5.0 g, 18.9 mmol), dibutyltin dilaurate (DBTDL) (0.505 g, 0.8 mmol) and tetramethylxylylene diisocyanate (TMXDI) (1.54 g, 6.3 mmol) were dissolved in THF (40 mL) and maintained under reflux for 24 hours. The solvent was removed *in vacuo* to leave a pale yellow oil which was purified by column chromatography (R_f 0.19, 20 % EtOAc/hexane) to give a white solid **2.3g** (1.6 g, 33 %) (m.p. 43-44 °C). ¹H NMR (400 MHz, CDCl₃) δ_H (ppm): 0.22 (12H, s, H_b), 0.99 (18H, s, H_a), 1.78 (12H, s, H_f), 2.36 (6H, s, H_e), 6.85 (4H, app. d *J* = 9.0 Hz, H_c), 6.88 (2H, br. m, H_j), 7.35 (3H, br. m, H_{gh}), 7.54 (1H, br. m, H_i), 7.56 (4H, app. d *J* = 9.0 Hz, H_d); ¹³C NMR (100 MHz, CDCl₃) δ_C (ppm): -4.4, 14.2, 18.3, 25.6, 29.2, 56.0, 120.3, 121.2, 123.3, 127.7, 128.1, 128.7, 147.0, 153.5, 158.0, 159.1; FTIR (ATR) ν (cm⁻¹): 3357 (N-H), 2928 (C-H), 2857 (C-H), 1722 (C=O), 1601 (C=N), 1496 (C-N), 1254 (Si-O), 1172 (C-O), 905 (N-O); ESIMS calculated mass (C₄₂H₆₂O₆N₄Si₂+H)⁺ 775.4281 found 775.4286.

Synthesis of oxime-urethane **2.3h**



Protected 4-hydroxybenzophenone oxime **2.2b** (3.60 g, 11.0 mmol), DBTDL (0.253 g, 0.4 mmol) and TMXDI (0.896 g, 3.7 mmol) were dissolved in dry THF (40 mL) and maintained under reflux for 72 hours. The solvent was removed *in vacuo* to leave a yellow oil which was purified by column chromatography ($R_f = 0.17$, 10 % EtOAc/hexane) to yield a white solid **2.3h** (2.50 g, 75 %) (m.p. 51-57 °C). ^1H NMR (400 MHz, CDCl_3) δ_{H} (ppm): 0.20-0.24 (12H, s, H_b), 0.97-1.00 (18H, s, H_a), 1.78 (12H, s, H_i), 6.74 (1H, br. m, H_h), 6.80 (2H, app. d $J = 9.0$ Hz, H_c), 6.85 (1H, br. m, H_l), 6.87 (2H, app. d $J = 9.0$ Hz, H_c'), 7.32-7.55 (18H, br. m, $\text{H}_{\text{defgijkl}}$); ^{13}C NMR (100 MHz, CDCl_3) δ_{C} (ppm): -4.4, 18.2, 25.6, 29.1, 56.1, 119.6, 120.0, 121.3, 123.4, 127.9, 128.2, 128.4, 128.7, 129.1, 130.2, 131.8, 135.7, 147.0, 153.4, 158.3, 160.8; FTIR (ATR) ν (cm^{-1}): 3398 (N-H), 2928 (C-H), 2856 (C-H), 1748 (C=O), 1602 (C=N), 1506 (C-N), 1254 (Si-O), 1163 (C-O), 907 (N-O); ESIMS calculated mass ($\text{C}_{52}\text{H}_{66}\text{O}_6\text{N}_4\text{Si}_2+\text{Na}$)⁺ 921.4413 found 921.4390.

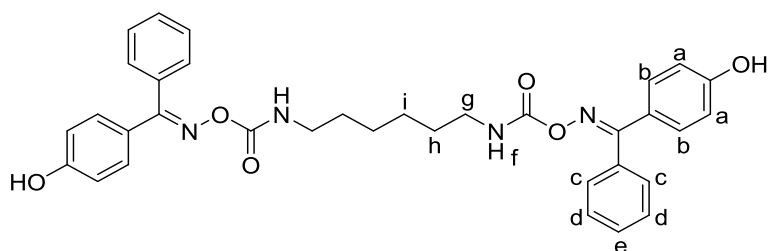
Deprotection of silyl-ethers to form **2.4a**



Oxime-urethane **2.3a** (2.93 g, 4.2 mmol) was dissolved in THF (20 mL) and tetrabutylammonium fluoride (TBAF) (1.0 M) (4.2 mL, 4.2 mmol) was added and stirred at room temperature for 1 hour. The reaction was quenched with NH_4Cl (20 mL) (saturated) and the product extracted with EtOAc (50 mL). The organic extract was washed with H_2O (3 x 50 mL), dried over MgSO_4 followed by filtration and the solvent removed *in vacuo* to give a pale yellow solid which was purified by washing sequentially with Et_2O (3 x 50 mL) and CHCl_3 (2 x 50 mL) leaving a white solid that degraded before melting **2.4a** (1.78 g, 90 %). ^1H NMR (400 MHz, $\text{DMSO}-d_6$) δ_{H} (ppm):

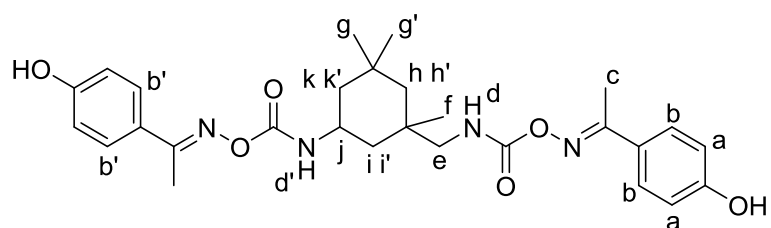
1.34 (4H, br. m, H_g), 1.53 (4H, br. m, H_f), 2.31 (6H, s, H_c), 3.15 (4H, q $J = 6.5$ Hz, H_e), 6.85 (4H, app. d $J = 9.0$ Hz, H_a), 7.54 (2H, br. m, H_d), 7.75 (4H, app. d $J = 9.0$ Hz, H_b), 9.96 (2H, s, H_h); ¹³C NMR (100 MHz, DMSO-*d*₆) δ_C (ppm): 13.21, 26.0, 29.3, 40.4, 115.2, 125.1, 128.5, 154.9, 158.7, 159.5; FTIR (ATR) ν (cm⁻¹): 3407 (O-H) 3278 (N-H), 2929 (C-H), 2856 (C-H), 1714 (C=O), 1600 (C=N), 1505 (C-N), 1278 (C-O), 904 (N-O); ESIMS calculated mass (C₂₄H₃₀O₆N₄+Na)⁺ 493.2058 found 493.2053.

Deprotection of silyl-ethers to form **2.4b**



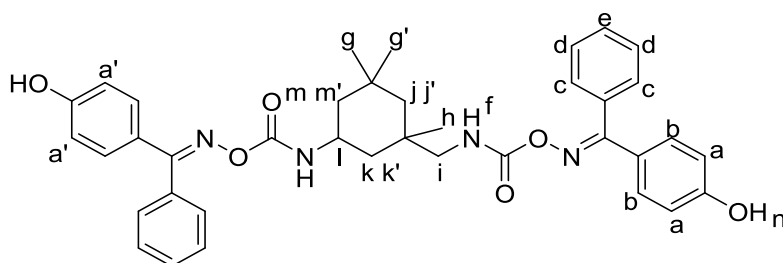
Oxime-urethane **2.3b** (1.23 g, 1.5 mmol) was dissolved in THF (20 mL) and TBAF (1.0 M) (1.5 ml, 1.5 mmol) was added and stirred at room temperature for 1 hour. The reaction was quenched with NH₄Cl (20 mL) (saturated) and the product extracted with EtOAc (50 mL). The organic extract was washed with H₂O (3 x 50 mL), dried over MgSO₄ followed by filtration and the solvent removed *in vacuo* to give a pale yellow solid which was purified by washing sequentially with Et₂O (3 x 50 mL) and CHCl₃ (2 x 50 mL) leaving a white solid **2.4b** (0.86 g, 96 %) (m.p. 105-108 °C). ¹H NMR (400 MHz, DMSO-*d*₆) δ_H (ppm): 1.32 (4H, br. m, H_i), 1.51 (4H, br. m, H_h), 3.13 (4H, br. m, H_g), 6.84 (2H, app. d $J = 9.0$ Hz, H_a), 6.91 (2H, app. d $J = 9.0$ Hz, H_{a'}), 7.59 (2H, br. m, H_f), 7.22-7.58 (14H, br. m, H_{bcd_e}), 9.96 (2H, s, H_j); ¹³C NMR (100 MHz, DMSO-*d*₆) δ_C (ppm): 25.9, 29.2, 40.4, 115.0, 115.3, 122.2, 125.0, 128.3, 128.7, 129.2, 130.0, 130.4, 131.0, 132.6, 135.3, 154.8, 158.7, 159.9, 160.6; FTIR (ATR) ν (cm⁻¹): 3407 (O-H), 3264 (N-H) 2929 (C-H), 2857 (C-H), 1712 (C=O), 1600 (C=N), 1514 (C-N), 1278 (C-O), 904 (N-O); ESIMS calculated mass (C₃₄H₃₄O₆N₄+Na)⁺ 617.2371 found 617.2370.

Deprotection of silyl-ethers to form 2.4e



Oxime-urethane **2.3e** (3.46 g, 4.6 mmol) was dissolved in THF (20 mL) and TBAF (1.0 M) (4.6 ml, 4.6 mmol) was added and stirred at room temperature for 1 hour. The reaction was quenched with NH₄Cl (20 mL) (saturated) and the product extracted with EtOAc (50 mL). The organic extract was washed with H₂O (3 x 50 mL), dried over MgSO₄ followed by filtration and the solvent removed *in vacuo* to give a pale yellow solid which was purified by washing sequentially with Et₂O (3 x 50 mL) and CHCl₃ (2 x 50 mL) leaving a white solid **2.4e** (2.31 g, 96 %) (m.p. 104-110 °C). ¹H NMR (400 MHz, DMSO-*d*₆) δ_H (ppm): 0.97 (3H, s, H_g), 1.08 (1H, m, H_h), 1.08 (3H, m, H_f), 1.11 (3H, m, H_{g'}), 1.15 (1H, m, H_k), 1.16 (1H, m, H_i), 1.23 (1H, m, H_{h'}), 1.47 (1H, m, H_{k'}), 1.57 (1H, m, H_{j'}), 2.94 (6H, s, H_c), 3.18 (1H, m, H_j), 3.81 (2H, m, H_e), 6.86 (4H, m, H_a), 7.25 (1H, m, H_d), 7.46 (1H, m, H_{d'}), 7.71 (2H, app. d *J* = 8.5 Hz, H_b), 7.73 (2H, app. d *J* = 8.5 Hz, H_{b'}), 9.96 (2H, br. s, H_l); ¹³C NMR (100 MHz, DMSO-*d*₆) δ_C (ppm): 23.2, 31.5, 35.0, 36.5, 40.8, 44.3, 44.4, 45.0, 46.5, 54.1, 115.2, 128.4, 128.5, 154.1, 155.5, 159.0, 159.5; FTIR (ATR) ν (cm⁻¹): 3412 (O-H), 3283 (N-H), 2965 (C-H), 2943 (C-H), 1710 (C=O), 1610 (C=N), 1500 (C-N), 1227 (C-O), 912 (N-O); ESIMS calculated mass (C₂₈H₃₆O₆N₄+Na)⁺ 547.2527 found 547.2524.

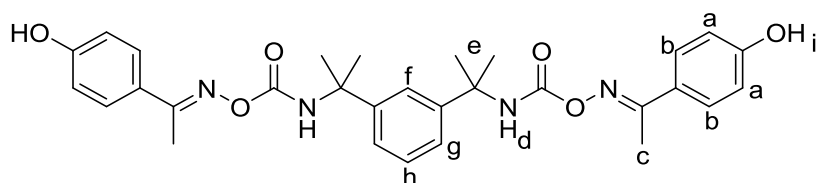
Deprotection of silyl-ethers to form 2.4f



Oxime-urethane **2.3f** (2.50 g, 2.9 mmol) was dissolved in THF (20 mL) and TBAF (1.0 M) (2.9 ml, 2.9 mmol) was added and stirred at room temperature for 1 hour. The reaction was quenched with NH₄Cl (20 mL) (saturated) and the product extracted with EtOAc (50 mL). The organic extract was washed with H₂O (3 x 50 mL), dried over MgSO₄ followed by filtration and the solvent removed *in vacuo* to give a pale yellow

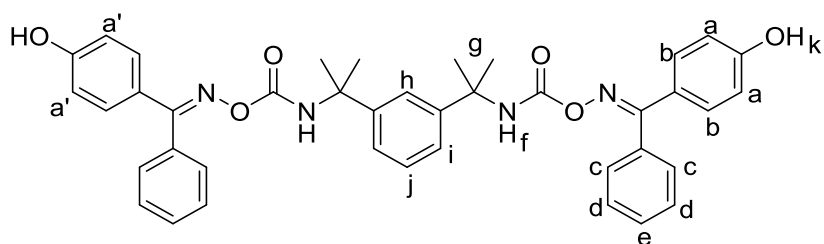
solid which was purified by washing sequentially with Et₂O (3 x 50 mL) and CHCl₃ (2 x 50 mL) leaving a white solid **2.4f** (1.34 g, 72 %) (m.p. 114-120°C). ¹H NMR (400 MHz, DMSO-*d*₆) δ_H (ppm): 0.92 (3H, s, H_g), 1.01 (1H, s, H_j), 1.02 (3H, s, H_h), 1.08 (1H, m, H_m), 1.15 (1H, m, H_k), 1.16 (3H, m, H_{g'}), 1.21 (1H, m, H_{j'}), 1.48 (1H, m, H_{m'}), 1.52 (1H, m, H_{k'}), 2.91 (2H, m, H_i), 3.77 (1H, m, H_l), 6.81 (2H, br. m, H_a), 6.88 (2H, app. d *J* = 8.5 Hz, H_{a'}), 7.21-7.53 (14H, m, H_{bcdde}), 7.48 (2H, m, H_f), 10.05 (2H, br. s, H_n); ¹³C NMR (100 MHz, DMSO-*d*₆) δ_C (ppm): 23.3, 27.5, 31.6, 34.5, 35.1, 40.9, 44.5, 45.1, 46.9, 54.3, 115.6, 128.3, 128.7, 130.0, 130.4, 131.2, 132.3, 155.5, 158.7, 160.1; FTIR (ATR) ν (cm⁻¹): 3412 (O-H), 3295 (N-H), 2963 (C-H), 2946 (C-H), 1715 (C=O), 1612 (C=N), 1500 (C-N), 1226 (C-O), 911 (N-O); ESIMS calculated mass (C₃₈H₄₀O₆N₄+Na)⁺ 671.2840 found 671.2839.

Deprotection of silyl-ethers to form **2.4g**



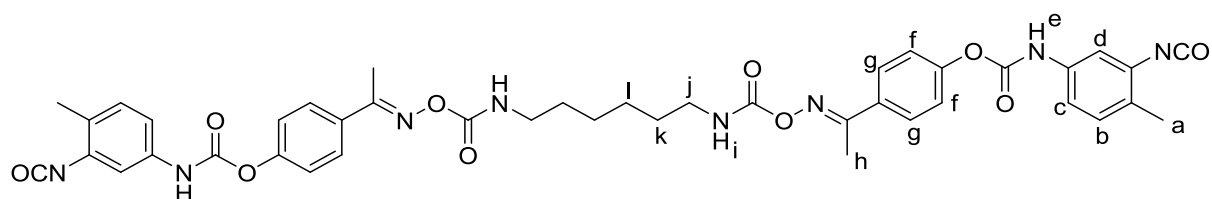
Oxime-urethane **2.3g** (0.781 g, 1.0 mmol) was dissolved in THF (20 mL) and TBAF (1.0 M) (1.0 ml, 1.0 mmol) was added and stirred at room temperature for 1 hour. The reaction was quenched with NH₄Cl (20 mL) (saturated) and the product extracted with EtOAc (50 mL). The organic extract was washed with H₂O (3 x 50 mL), dried over MgSO₄ followed by filtration and the solvent removed *in vacuo* to give a pale yellow solid which was purified by washing sequentially with Et₂O (3 x 50 mL) and CHCl₃ (2 x 50 mL) leaving a white solid **2.4g** (0.490 g, 90 %) (m.p. 92-100 °C). ¹H NMR (400 MHz, DMSO-*d*₆) δ_H (ppm): 1.63 (12H, s, H_e), 2.29 (6H, s, H_c), 6.81 (4H, app. d *J* = 9.0 Hz, H_a), 7.27 (3H, m, H_fg), 7.46 (1H, m, H_h), 7.55 (2H, br. m, H_d), 7.62 (4H, app. d *J* = 8.0 Hz, H_b), 9.93 (2H, s, H_i); ¹³C NMR (100 MHz, DMSO-*d*₆) δ_C (ppm): 13.2, 43.9, 79.1, 115.2, 125.0, 125.7, 125.8, 128.2, 128.6, 139.6, 155.2, 159.0, 159.6; FTIR (ATR) ν (cm⁻¹): 3378 (O-H), 3230 (N-H), 2993 (C-H), 2953 (C-H), 1706 (C=O), 1605 (C=N), 1499 (C-N), 1238 (C-O), 911 (N-O); ESIMS calculated mass (C₃₀H₃₄O₆N₄+Na)⁺ 569.2371 found 569.2367.

Deprotection of silyl-ethers to form **2.4h**



Oxime-urethane **2.3h** (1.00 g, 1.1 mmol) was dissolved in THF (20 mL) and TBAF (1.0 M) (1.1 ml, 1.1 mmol) was added and stirred at room temperature for 1 hour. The reaction was quenched with NH_4Cl (20 mL) (saturated) and the product extracted with EtOAc (50 mL). The organic extract was washed with H_2O (3 x 50 mL), dried over MgSO_4 followed by filtration and the solvent removed *in vacuo* to give a pale yellow solid which was purified by washing sequentially with Et_2O (3 x 50 mL) and CHCl_3 (2 x 50 mL) leaving a white solid **2.4h** (0.666 g, 86 %) (m.p. 102-105 °C). ^1H NMR (400 MHz, $\text{DMSO}-d_6$) δ_{H} (ppm): 1.65 (12H, s, H_g), 6.83 (2H, br. m, H_a), 6.91 (2H, br. m, H_a), 7.19-7.63 (18H, br. m, $\text{H}_{bcdehij}$), 7.55 (2H, br. m, H_f), 9.83 (2H, s, H_k); ^{13}C NMR (100 MHz, $\text{DMSO}-d_6$) δ_{C} (ppm): 55.2, 115.0, 115.4, 122.3, 127.4, 128.2, 128.4, 128.6, 129.9, 130.8, 131.2, 147.1, 154.9, 155.1, 159.9, 161.1; FTIR (ATR) ν (cm^{-1}): 3410 (O-H), 3256 (N-H), 2984 (C-H), 2955 (C-H), 1716 (C=O), 1608 (C=N), 1491 (C-N), 1231 (C-O), 943 (N-O); ESIMS calculated mass ($\text{C}_{40}\text{H}_{38}\text{O}_6\text{N}_4+\text{Na}$) $^+$ 693.2684 found 693.2687.

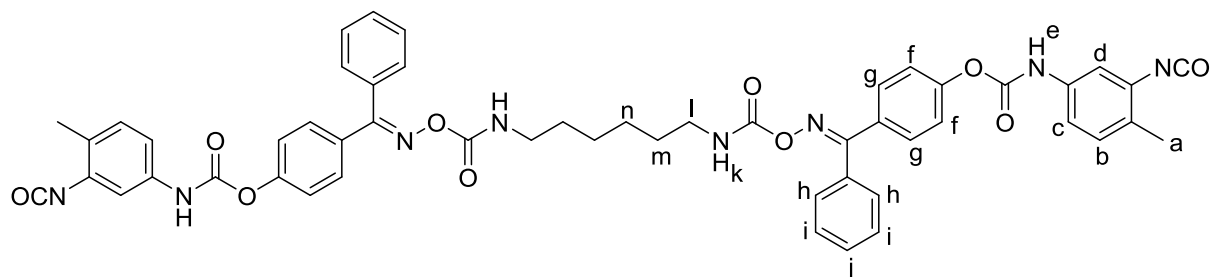
Synthesis of shell wall precursor **2.5a**



Deprotected oxime-urethane **2.4a** (0.620 g, 1.3 mmol) and toluene-2,4-diisocyanate (TDI) (0.643 g, 3.7 mmol) were dissolved in cyclohexanone (30 mL) and stirred 80 °C under an atmosphere of argon for 18 hours. The solvent was removed by vacuum distillation and excess TDI was removed by washing with cyclohexane (3 x 50 mL) at 80 °C leaving a pale yellow solid that decomposed before melting **2.5a** (0.981 g, 92 %). ^1H NMR (400 MHz, $\text{DMSO}-d_6$) δ_{H} (ppm): 1.41 (4H, br. m, H_i), 1.60 (4H, br. m, H_k), 2.28 (6H, s, H_h), 2.40 (6H, s, H_a), 3.27 (4H, br. m, H_j), 6.75 (4H, app. d $J = 9.0$ Hz, H_f), 7.29

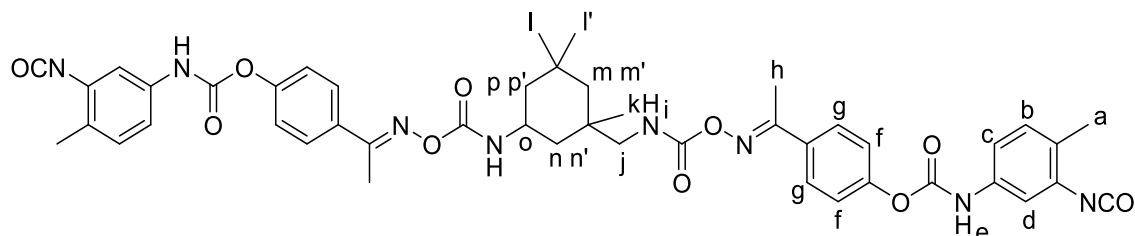
(2H, m, H_b), 7.39 (2H, br. m, H_i), 7.55 (4H, app. d $J = 9.0$ Hz, H_g), 7.70 (2H, m, H_d), 7.86 (2H, m, H_c), 8.75 (2H, s, H_e); ¹³C NMR (100 MHz, DMSO-*d*₆) δ_C (ppm): 13.1, 16.7, 25.7, 29.8, 40.7, 115.3, 115.9, 116.2, 117.0, 122.1, 128.2, 128.6, 133.4, 155.5, 155.6, 155.7, 159.1, 159.3; FTIR (ATR) ν (cm⁻¹): 3287 (N-H), 2928 (C-H), 2854 (C-H), 2264 (NCO), 1704 (C=O), 1596 (C=N), 1502 (C-N), 1196 (C-O), 900 (N-O).

Synthesis of shell wall precursor 2.5b



Deprotected oxime-urethane **2.4b** (0.250 g, 0.42 mmol) and TDI (0.205 g, 1.2 mmol) were dissolved in THF (30 L) and maintained under reflux for 24 hours. The solvent was removed *in vacuo* and excess TDI was removed by washing with cyclohexane (3 x 60 mL) at 80 °C to leave a yellow solid **2.5b** (0.447 g, 100 %) (m.p. 98-102 °C). ¹H NMR (400 MHz, Acetone-*d*₆) δ_H (ppm): 1.41 (4H, m, H_n), 1.61 (4H, m, H_m), 2.27 (6H, s, H_a), 3.28 (4H, m, H_i), 7.10-7.63 (24H, m, H_{bcdgfhij}), 7.10-7.63 (2H, m, H_k), 8.49 (2H, s, H_e); ¹³C NMR (100 MHz, Acetone-*d*₆) δ_C (ppm): 17.6, 27.0, 31.9, 41.7, 115.8, 117.1, 122.6, 122.7, 127.0, 129.3, 129.4, 129.5, 129.8, 130.6, 131.1, 131.8, 132.4, 133.1, 133.5, 139.9, 153.4; FTIR (ATR) ν (cm⁻¹): 3284 (N-H), 2928 (C-H), 2860 (C-H), 2262 (NCO), 1721 (C=O), 1593 (C=N), 1501 (C-N), 1194 (C-O), 957(N-O).

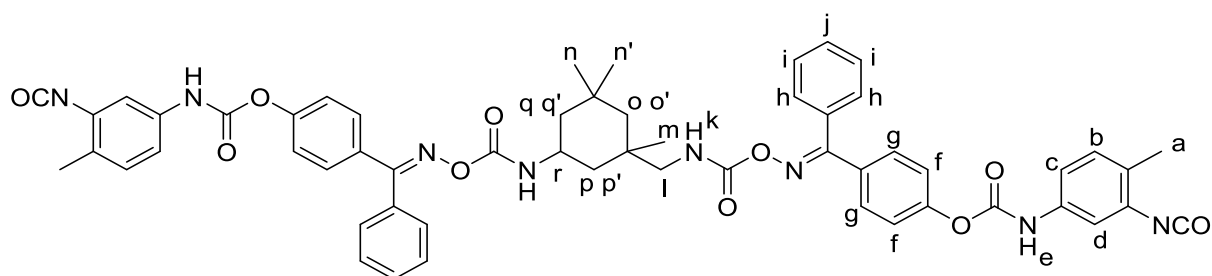
Synthesis of shell wall precursor 2.5e



Deprotected oxime-urethane **2.4e** (0.679 g, 1.3 mmol) and TDI (0.631 g, 3.6 mmol) were dissolved in THF (30 mL) and maintained under reflux for 24 hours. The solvent was removed *in vacuo* and excess TDI was removed by washing with cyclohexane (3 x 60 mL) at 80 °C to leave a yellow solid **2.5e** (1.10 g, 98 %) (m.p. 117-121 °C).

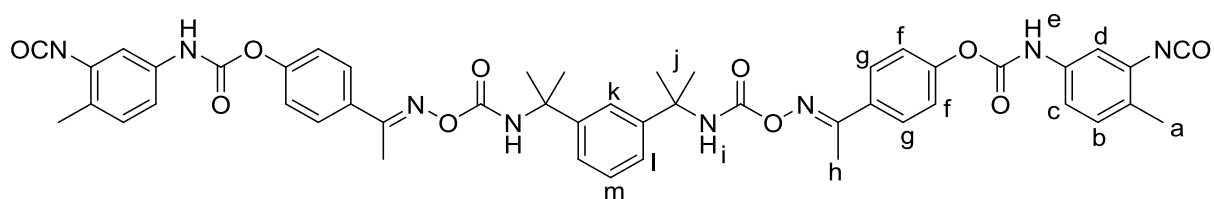
^1H NMR (400 MHz, Acetone- d_6) δ_{H} (ppm): 0.97 (3H, s, H_l), 1.11 (3H, m, H_k), 1.15 (3H, m, H_l), 1.21 (1H, m, H_m), 1.22 (1H, m, H_n), 1.25 (1H, m, H_p), 1.28 (1H, m, H_m), 1.74 (1H, m, H_p), 1.76 (1H, m, H_n), 2.29-2.37 (6H, s, H_a), 2.40 (6H, s, H_h), 3.09 (1H, m, H_o), 4.00 (2H, m, H_j), 6.88-7.37 (10H, br. m, H_{bcdf}), 7.50 (2H, m, H_i), 7.86 (4H, m, H_g), 8.32 (2H, s, H_e); ^{13}C NMR (100 MHz, Acetone- d_6) δ_{C} (ppm): 14.0, 17.6, 27.5, 32.5, 35.5, 37.6, 42.1, 45.9, 47.8, 55.4, 115.9, 117.1, 122.8, 123.2, 128.9, 131.5, 131.8, 132.4, 133.2, 138.5, 152.2, 155.0, 156.3, 159.6; FTIR (ATR) ν (cm^{-1}): 3290 (N-H), 2981 (C-H), 2923 (C-H), 2262 (NCO), 1722 (C=O), 1592 (C=N), 1503 (C-N), 1195 (C-O), 913 (N-O).

Synthesis of shell wall precursor **2.5f**



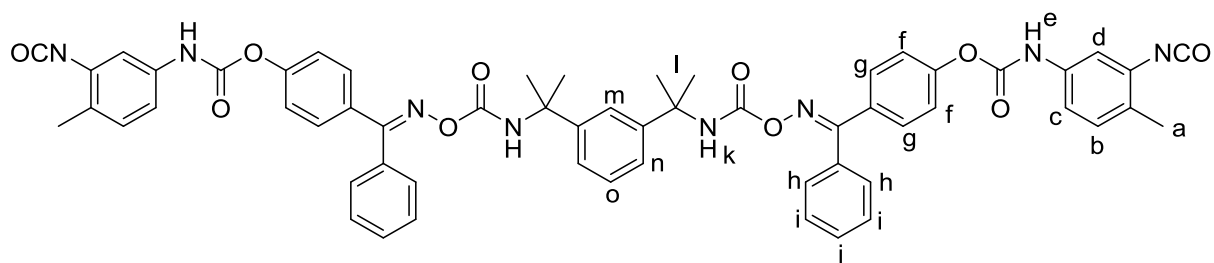
Deprotected oxime-urethane **2.4f** (0.205 g, 0.3 mmol) and toluene-2,4-diisocyanate (0.154 g, 0.9 mmol) were dissolved in THF (30 mL) and maintained under reflux for 48 hours. The solvent was removed *in vacuo* and the resultant solid washed with cyclohexane (3 x 60 mL) at 80 °C to leave a pale yellow solid **2.5f** (0.313 g, 98 %) (m.p. 135-139 °C). ^1H NMR (400 MHz, Acetone- d_6) δ_{H} (ppm): 0.96 (3H, s, H_n), 1.08 (3H, m, H_m), 1.12 (3H, m, H_n), 1.18 (1H, m, H_o), 1.24 (1H, m, H_p), 1.24 (1H, m, H_q), 1.25 (1H, m, H_o), 1.73 (1H, m, H_p), 1.75 (1H, m, H_q), 2.05-2.15 (6H, s, H_a), 3.06 (1H, m, H_r), 3.97 (2H, m, H_i), 6.96-7.37 (24H, m, $\text{H}_{bcdfghij}$), 6.96-7.37 (2H, m, H_k), 8.32 (2H, s, H_e); ^{13}C NMR (100 MHz, Acetone- d_6) δ_{C} (ppm): 13.9, 17.6, 17.7, 20.4, 23.6, 24.4, 26.2, 27.9, 28.1, 31.0, 115.8, 117.1, 122.7, 127.0, 129.2, 129.4, 129.7, 129.8, 130.5, 131.5, 131.8, 133.1, 139.9, 153.3; FTIR (ATR) ν (cm^{-1}): 3298 (N-H), 2925 (C-H), 2266 (NCO), 1723 (C=O), 1595 (C=N), 1504 (C-N), 1197 (C-O), 961 (N-O).

Synthesis of shell wall precursor **2.5g**



Deprotected oxime-urethane **2.4g** (0.603 g, 1.1 mmol) and TDI (0.538 g, 3.1 mmol) were dissolved in THF (30 mL) and heated to 50 °C for a period of 24 hours. The solvent was removed *in vacuo* and excess TDI was removed by washing with cyclohexane (3 x 60 mL) at 80 °C to leave a yellow solid **2.5g** (0.822 g, 84 %) (m.p. 86-91 °C). ^1H NMR (400 MHz, Acetone- d_6) δ_{H} (ppm): 1.78 (12H, s, H_j), 2.27-3.31 (6H, s, H_a), 2.89 (6H, s, H_h), 7.13-7.54 (14H, br. m, H_{bcdf}), 7.71 (2H, s, H_j), 7.94 (4H, app. d $J = 9.0$ Hz, H_g), 8.35 (2H, s, H_e); ^{13}C NMR (100 MHz, Acetone- d_6) δ_{C} (ppm): 14.2, 17.7, 30.6, 61.9, 115.9, 116.8, 117.1, 118.0, 121.5, 124.2, 125.7, 127.1, 128.8, 129.5, 131.5, 131.7, 133.2, 133.5, 138.3, 147.3, 153.7, 160.9; FTIR (ATR) ν (cm^{-1}): 3357 (N-H), 2979 (C-H), 2924 (C-H), 2255 (NCO), 1723 (C=O), 1593 (C=N), 1505 (C-N), 1193 (C-O), 901(N-O).

Synthesis of shell wall precursor **2.5h**



Deprotected oxime-urethane **2.4h** (0.560 g, 0.8 mmol) and TDI (0.349 g, 2.0 mmol) were dissolved in THF (30 mL) and heated to 60 °C for a period of 24 hours. The solvent was removed *in vacuo* and excess TDI was removed by washing with cyclohexane (3 x 60 mL) at 80 °C to leave a yellow solid **2.5h** (0.875 g, 100 %) (m.p. 93-96 °C). ^1H NMR (400 MHz, Acetone- d_6) δ_{H} (ppm): 1.44 (12H, s, H_l), 2.26-2.31 (6H, s, H_a), 7.12-7.66 (28H, m, $\text{H}_{\text{bcdfghijmno}}$), 7.12-7.66 (2H, m, H_k), 8.19 (2H, s, H_e); ^{13}C NMR (100 MHz, Acetone- d_6) δ_{C} (ppm): 17.7, 27.5, 116.0, 116.7, 117.2, 118.0, 122.2, 122.6, 122.8, 123.2, 127.2, 129.3, 129.4, 129.7, 129.8, 130.8, 131.4, 131.7, 133.2, 133.3,

139.7, 152.7, 152.8, 153.9, 162.5; FTIR (ATR) ν (cm^{-1}): 3289 (N-H), 2979 (C-H), 2922 (C-H), 2261 (NCO), 1724 (C=O), 1590 (C=N), 1501 (C-N), 1165 (C-O), 996 (N-O).

2.5. References

- ¹ S. H. Cho, H. M. Andersson, S. R. White, N. R. Sottos and P. V. Braun, *Adv. Mater.*, 2006, **18**, 997-1000.
- ² T. Ohtsubo, S. Tsuda and K. Tsuji, *Polymer*, 1991, **32**, 2395-2399.
- ³ A. P. Esser-Khan, N. R. Sottos, S. R. White and J. S. Moore, *J. Am. Chem. Soc.*, 2010, **132**, 10266-10268.
- ⁴ A. N. Zelikin, J. F. Quinn and F. Caruso, *Biomacromolecules*, 2006, **7**, 27-30.
- ⁵ N. Fomina, C. McFearin, M. Sermsakdi, O. Edigin and A. Almutairi, *J. Am. Chem. Soc.*, 2010, **132**, 9540-9542.
- ⁶ M. R. Böhmer, C. H. T. Chlon, B. I. Raju, C. T. Chin, T. Shevchenko and A. L. Klibanov, *J. Control. Release*, 2010, **148**, 18-24.
- ⁷ L. Chu, S. Park, T. Yamaguchi and S. Nakao, *Langmuir*, 2002, **18**, 1856-1864.
- ⁸ W. Yang, R. Xie, X. Pang, X. Ju and L. Chu, *J. Membr. Sci.*, 2008, **321**, 324-330.
- ⁹ Z. Lu, M. D. Prouty, Z. Guo, V. O. Golub, C. S. S. R. Kumar and Y. M. Lvov *Langmuir*, 2005, **21**, 2042-2050.
- ¹⁰ T. A. Plaisted and S. Nermat-Nasser, *Acta Materiala*, 2007, **55**, 5684-5696.
- ¹¹ H. Ying, Y. Zhang and J. Cheng, *Nat. Commun.*, 2014, **5**, 3218-3226.
- ¹² A. Blencowe, A. Clarke, M. G. B. Drew, W. Hayes, A. Slark, P. Woodward, *React. Funct. Polym.*, 2006, **66**, 1284-1295.
- ¹³ Z. W. Wicks, *Prog. Org. Coat.*, 1981, **9**, 3-28.
- ¹⁴ D. A. Wicks and Z. W. Wicks, *Prog. Org. Coat.*, 1999, **36**, 148-172.
- ¹⁵ E. Delebecq, J. P. Pascault, B. Boutevin and F. Ganachaud, *Chem. Rev.*, 2013, **113**, 80-118.
- ¹⁶ S. Lee and D. Randall, *The Polyurethanes Book*, Wiley, Chichester, 2002.
- ¹⁷ I. Muramatsu, Y. Tanimoto, M. Kase and N. Okoshi, *Prog. Org. Coat.*, 1993, **22**, 279-286.
- ¹⁸ J. S. Witzeman, *Prog. Org. Coat.*, 1996, **27**, 269-276.
- ¹⁹ G. B. Guise, G. N. Freeland and G. C. Smith, *J. Appl. Polym. Sci.*, 1979, **23** 353-365.

- ²⁰ W. H. Heath, F. Palmieri, J. R. Adams, B. K. Long, J. Chute, T. W. Holcombe, S. Zieren, M. J. Truitt, J. L. White and C. G. Wilson, *Macromolecules*, 2008, **41** 719-726.
- ²¹ M. E. Budd, MSc Thesis, *Microencapsulation Approach for Use in Delayed Quick-Cure Munitions*, University of Reading, 2013.
- ²² G. Sankar and A. S. Nasar, *J. Polym. Sci. Polym. Chem.* 2007, **45**, 1557-1570.
- ²³ A. S. Nasar, S. Subramani and G. Radhakrishnan, *J. Polym. Sci. Polym. Chem.*, 1999, **37**, 1815-1821.
- ²⁴ T. Shen, M. Lu and L. Liang, *Macromol. Res.*, 2012, **20**, 827-834.
- ²⁵ J. M. Lee, S. Subramani, Y. S. Lee and J. H. Kim, *Macromol. Res.*, 2005, **13**, 427-434.
- ²⁶ H. Kothandaraman and A. S. Nasar, *Polymer*, 1993, **34**, 610-615.
- ²⁷ S. Mohanty and N. Krishnamurti, *Eur. Polym. J.*, 1998, **34**, 77-83.

Chapter 3

Synthesis of Thermally-Releasable Microcapsules for the Controlled Delivery of Isocyanate Crosslinkers

The following chapter has, in part, been published by the author as a patent application in collaboration with BAE Systems plc. - *M. E. Budd, W. C. Hayes, R. Stephens, Great British/European Patent Application, 'Cast Explosive Composition', 2015, GB1511876.2/EP15275168.1.*

Abstract

The current procedure used to bind explosives within polyurethane matrices involves the addition of a diisocyanate crosslinker to a mixture of the explosive and hydroxy-terminated polybutadiene (HTPB). The ensuing polymerisation reaction can prevent the uniform distribution of the crosslinker and can lead to several detrimental processes that generate an unusable product that must be wasted. By containing IPDI within polyurethane microcapsules, the uniform delivery of the crosslinker may be achieved. Following an application of a heat stimulus, IPDI can be released from the microcapsules thus achieving the uniform cure of HTPB. The following chapter describes the synthesis of microcapsules that release their core contents upon the application of heat using an interfacial polymerisation technique employing the shell wall precursors described in **Chapter 2**. The capability of these IPDI filled microcapsules to achieve the controlled cure of HTPB has been demonstrated. This chapter also investigates how the physical properties of microcapsules can be controlled in order to tailor microcapsules towards their specific application in the use of quick cure munitions.

3.1. Introduction

Modern explosives consist of the energetic material bound within a rubbery polymer matrix and are known as plastic or polymer bonded explosives (PBX). The current method employed to produce PBX matrices involves the addition of a diisocyanate crosslinker along with a catalyst to a mixture of the explosive in a hydroxy-functionalised polymer. One such PBX formulation, Rowanex 1100 1A utilises isophorone diisocyanate (IPDI) and hydroxy-terminated polybutadiene (HTPB) in a polymerisation catalysed by dibutyltin dilaurate (DBTDL). Upon the addition of IPDI an immediate polymerisation reaction occurs and thus the rapidly curing material must be

deployed without delay. This can lead to several problems - the cured PBX can be inhomogeneous with regions of poor crosslinking density, the quality of the matrix varies with consecutively filled stores, the formation of voids that can cause accidental detonation of the explosive upon firing and ultimately can lead to wasting of material associated with high disposal costs. It is hoped that these problems can be resolved by uniformly delivering the IPDI crosslinker in polyurethane microcapsules. This modified process must meet specific criteria - the generation of new explosive formulations requires requalification, a long and expensive process; thus existing explosive formulations must not be significantly altered, microcapsule shells must be composed primarily of polyurethane in order to match the PBX material and the lifetimes of the stores must not be changed.

Microcapsules that respond to a range of stimuli have been developed including - pressure,¹ chemical (*i.e.* change in pH or solvent),² light,³ ultrasound⁴ and exposure to elevated temperature.⁵ Explosive formulations such as Rowanex 1100 1A are opaque and thus light is unable to penetrate deeply. The extreme local environment created by ultrasonic cavitation may be sufficient to cause detonation of the explosive. Therefore, release of microcapsules using an external application of heat is the most favoured mechanism.

Many physical techniques have been developed for the synthesis of microcapsules including - suspension crosslinking,⁶ solvent evaporation,⁷ coacervation,⁸ spray drying,⁹ layer-by-layer deposition,¹⁰ supercritical fluid expansion¹¹ and the spinning disk approach.¹² Chemical methods include suspension polymerisation,¹³ emulsion polymerisation,¹⁴ interfacial polymerisation¹⁵ and dispersion polymerisation.¹⁶ Of these techniques, interfacial polymerisation and dispersion polymerisation most commonly are used to encapsulate liquid active agents.¹⁴ Previous studies conducted¹⁷ at the University of Reading demonstrated how IPDI crosslinkers can be contained in polyurethane microcapsules synthesised using an interfacial polymerisation technique.

This chapter first describes how the isocyanate-terminated shell wall precursors containing thermally-labile oxime-urethanes described in **Chapter 2** were used to synthesise microcapsules. The potential of the afforded microcapsules to release their core contents upon the application of a heat stimulus has been investigated. The second part of this chapter describes how the physical properties of microcapsules can be controlled in order to tailor microcapsules with specific properties.

3.2. Results and Discussion

The microencapsulation of IPDI in polyurethane microcapsules **3.1a-h** using an interfacial polymerisation approach first requires the synthesis of an appropriate isocyanate-terminated shell wall precursor and this has been described in **Chapter 2** (Table 3.1).

Table 3.1. Structures of shell wall precursors synthesised in **Chapter 2**.

Shell wall precursor	Structure
2.5a	
2.5b	
2.5e	
2.5f	
2.5g	
2.5h	

The synthetic procedure used to generate microcapsules initially involves the dissolution of the shell wall precursor and IPDI in a hydrophobic solvent that possesses a boiling point $>150\text{ }^{\circ}\text{C}$ - this is to prevent evaporation of the core during microcapsule synthesis - suitable candidates are chlorobenzene, 1,2-dichlorobenzene, 1,2,4-trichlorobenzene, phenylacetate and ethyl phenylacetate. All shell wall

precursors **2.5a-h** exhibited good solubility in either 1,2-dichlorobenzene and ethyl phenylacetate. However, upon the addition of IPDI precipitation of **2.5a** occurred, thus microencapsulation of IPDI could not be achieved using this shell wall precursor. A similar problem was encountered for **2.3f**, although solubilisation was achieved by the addition of anisaldehyde (5 wt. %) (Table 3.2).

Table 3.2. Solubilisation data of shell wall precursors **2.5a-h** in preparation for microcapsule synthesis.

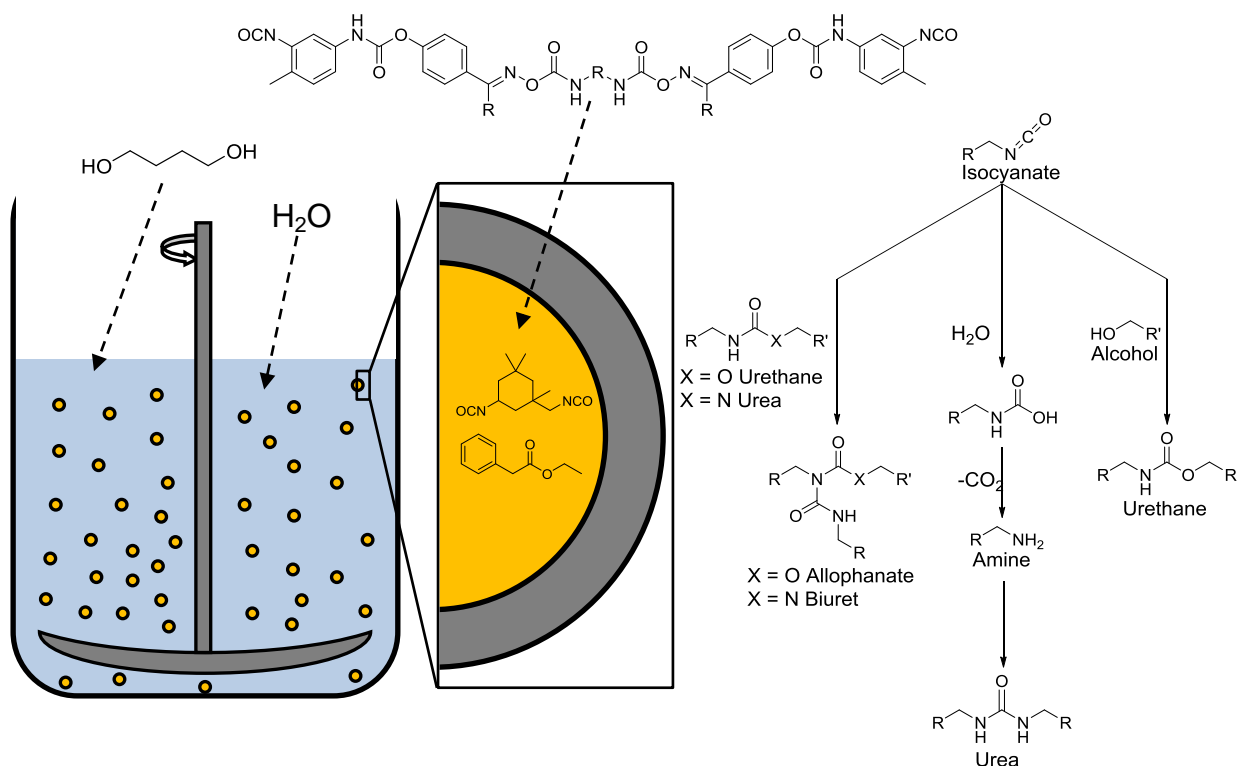
Shell wall precursor	Microcapsules	Soluble in 1,2-dichlorobenzene/ethyl phenylacetate	Soluble in Solvent and IPDI
2.5a	3.1a	Yes	No
2.5b	3.1b	Yes	Yes
2.5e	3.1e	Yes	Yes
2.5f	3.1f	Yes *	Yes
2.5g	3.1g	Yes	Yes
2.5h	3.1h	Yes	Yes

* 5 wt. % anisaldehyde added

Following dissolution of the shell wall precursor and IPDI in a solvent, the organic phase was emulsified in water with aid of a surfactant, gum arabic (15 wt. %), and mechanical agitation provided by an overhead stirrer driving a three-bladed marine-type impeller at a rate of 1000 rpm. Subsequent addition of 1,4-butanediol as a chain extender allowed polymerisation to occur at the oil-water interface of the emulsion oil micro-droplets. The interfacial polymerisation reaction occurs primarily with the relatively more reactive aromatic isocyanate-terminated shell wall precursors, leaving the majority of the IPDI to be encapsulated.¹⁸

In addition to the alcohol isocyanate polymerisation reaction, a variety of reactions can occur at the oil-water interface.¹⁹ Water is able to react with the isocyanates to form a carbamic acid, subsequent decarboxylation results in the formation of an amine that can react with further isocyanate to form a urea. Allophonate and biuret crosslinks are also generated from the reactions of isocyanate and urethane and urea, respectively (Scheme 3.1). The microcapsules were obtained by filtration followed by washing with H₂O and were then allowed to dry for a period of 48 hours prior to analysis.

The yielded microcapsules were analysed using a range of analytical techniques including - optical microscopy, scanning electron microscopy (SEM), ^1H NMR spectroscopy, infra-red spectroscopy and thermogravimetric analysis (TGA).



Scheme 3.1. Interfacial polymerisation technique employed for the synthesis of microcapsules.

3.2.1. Optical Microscopic Analysis

Optical microscopy allows visual confirmation of the successful microencapsulation of a liquid core and can also allow the measurement of the microcapsule diameters and size distribution.²⁰ Microcapsules synthesised using shell wall precursor **2.5a** yielded mechanically robust microcapsules that possessed good quality spherical shapes. Upon crushing the microcapsules between two microscope slides the release of a liquid core was observed. Microencapsulation using **2.5b** led to the formation of puckered-shaped microcapsules that ruptured with little force. It has been reported²¹ that such shapes can be caused by mechanically-weak microcapsule shells and could be a result of the sterically encumbered nature of the shell wall precursor, preventing the formation of a strong polymer shell. Microencapsulation using **2.5e** afforded spherical microcapsules - however, they exhibited poor mechanical strength, rupturing easily. This result suggests the highly encumbered IPDI-based shell wall precursor prevented the formation of a strong microcapsule shell. Analysis of microcapsules

synthesised using **2.5f** revealed that upon crushing between two microscope slides no liquid core was released. The reaction of isocyanates and aldehydes at high temperatures $\sim 200\text{ }^{\circ}\text{C}$ has been reported²² and the presence of anisaldehyde may have led to the formation of solid particles rather than the desired mononuclear microcapsules. Microcapsules yielded using **2.5g** afforded robust spherical microcapsules, suggesting that the high steric hindrance of the TMXDI-based shell wall precursor did not prevent the formation of strong microcapsules. Synthesis of microcapsules using **2.5h** generated microcapsules that ruptured during filtration. Careful handling allowed capture of microscopic images - however no further analysis could be obtained (Figure 3.1). A correlation between the steric hindrance of the shell wall precursor and the afforded microcapsules was observed. As a result of high steric hindrance, benzophenone oxime-based shell wall precursors **2.5b,f,h** prevented the formation of robust microcapsules. Further to this, the sterically encumbered IPDI-based shell wall precursors **2.5e-f** also led to microcapsules with poor mechanical strength. In comparison, HDI and TMXDI based precursors generated microcapsules that exhibited high mechanical strength.

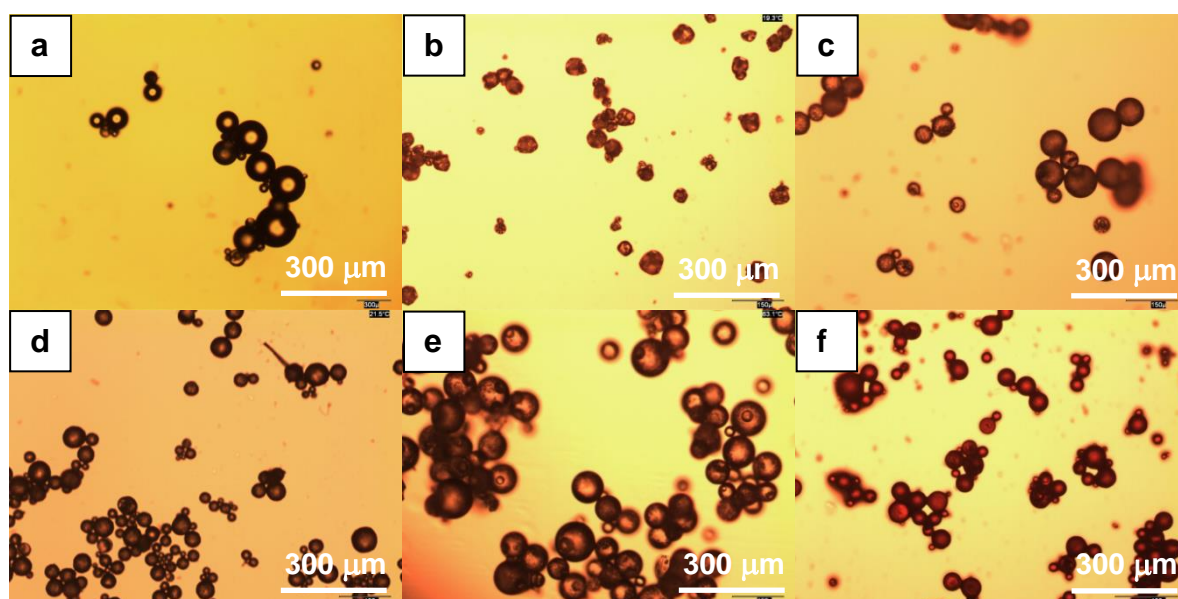


Figure 3.1. Optical microscopic images of microcapsules before crushing between microscope slides a) 3.1a, b) 3.1b, c) 3.1e, d) 3.1f, e) 3.1g and f) 3.1h.

The diameter of microcapsules **3.1a-h** was measured using optical microscopy which revealed that the microcapsules all possessed a similar average diameter (33-68 μm). The uniformity of the microcapsule diameter was also measured and it was revealed that all the microcapsules with the exception of **3.1a** were afforded within a narrow size

range (Table 3.3). The hydrophobic solvent 1,2-dichlorobenzene was employed in the synthesis of **3.1a** whereas microcapsules **3.1b-3.1h** were afforded using ethyl phenylacetate and may have contributed to this result.

Table 3.3. Average microcapsule diameter and size distribution of microcapsules **3.1a-3.1h**.

Shell wall precursor	Microcapsules	Average Diameter (μm)	Size Range (μm)
2.5a	3.1a	59	17-302
2.5b	3.1b	45	9-83
2.5e	3.1e	42	15-99
2.5f	3.1f	33	8-75
2.5g	3.1g	68	22-117
2.5h	3.1h	35	5-84

3.2.2. Analysis Using Scanning Electron Microscopy

Scanning electron microscopy (SEM) allows the high resolution microscopic analysis of microcapsules,²³ allowing images to be obtained of the exterior and interior morphologies of the microcapsule shell wall. The obtained microcapsules were prepared for SEM analysis by first sputtering with a layer of gold and imaged using a scanning electron microscope in a high vacuum (0.45 torr). Analysis revealed that mononuclear microcapsules **3.1a** were generated that possessed a smooth exterior surface morphology. Images obtained of **3.1b** revealed non-spherical microcapsules that had a rough surface morphology - literature studies have reported²¹ that microcapsules that contain stimuli-responsive linkages within the shell wall of the microcapsule possess such surface morphologies. In addition, the exterior shells of **3.1e** were revealed to be slightly puckered. This may result from the formation of a structurally weak microcapsule shell wall and supports the poor mechanical strength observed of **3.1b** and **3.1e**. Microscopic images of the exterior shell of **3.1f** discovered a rough surface morphology and further analysis of a crushed microcapsule revealed the absence of an internal cavity, supporting optical microscopic observations that solid particles had been generated and not the desired mononuclear microcapsules. SEM analysis of **3.1g** observed spherical microcapsules that possessed smooth exterior shell walls (Figure 3.2).

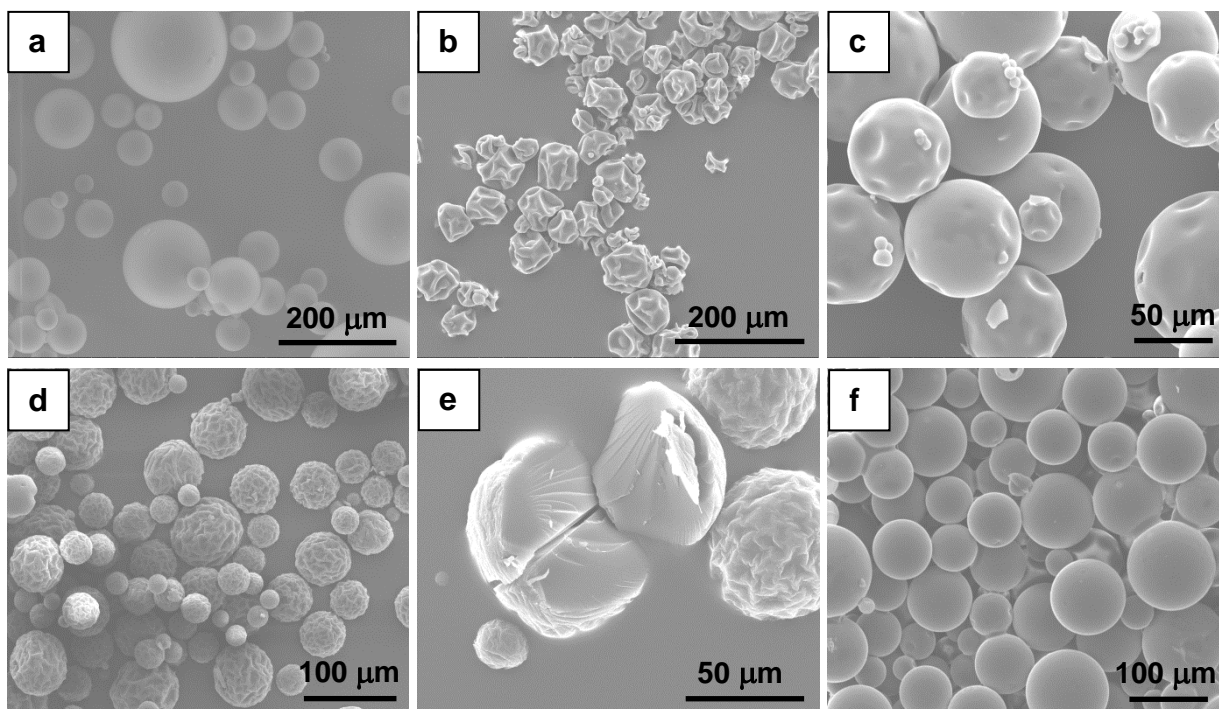


Figure 3.2. Scanning electron microscopic images of microcapsules **a) 3.1a, b) 3.1b, c) 3.1e, d) 3.1f, e) 3.1g** (crushed) and **f) 3.1h**.

SEM analysis of cross-sections of microcapsules can allow the measurement of the microcapsule shell wall thickness.²⁴ Samples of microcapsules were embedded in an epoxy resin and allowed to cure for a period of 48 hours. Cross-sections were prepared using an ultramicrotome employing a glass knife and analysed using an environmental scanning electron microscope operating in a thin aqueous atmosphere (0.68 torr). Figure 3.3 shows an image of a microcapsule cross-section highlighting the microcapsule shell wall and lists the average shell wall thickness observed of microcapsules **3.1a-3.1g**.

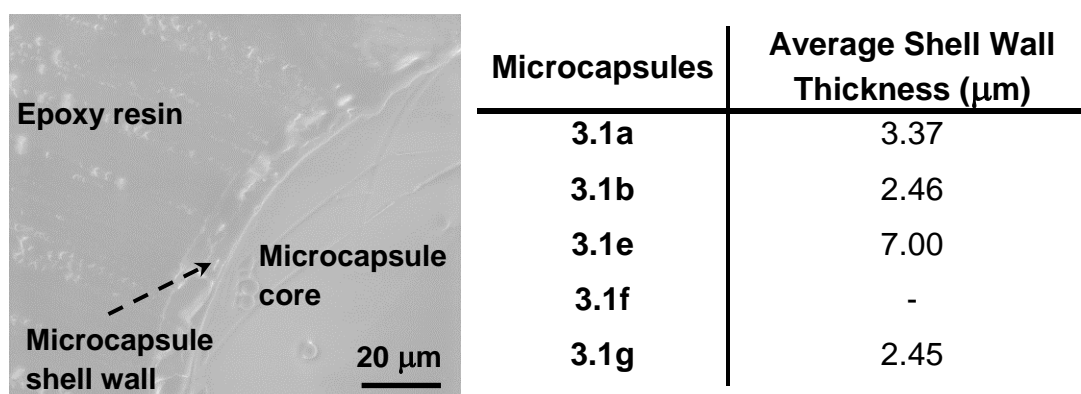


Figure 3.3. SEM image of a microcapsule **3.1g** cross-section and list of the average shell wall thicknesses of microcapsules **3.1a-3.1h**.

The average shell wall thickness of **3.1a**, **3.1b** and **3.1g** were within 2-4 μm , which is concurrent with literature results for microcapsules of this size.¹⁸ However, the average shell wall thickness of microcapsules **3.1e** were much larger than expected, the sterically encumbered nature of the shell wall precursor **2.5e** may have led to the formation of a polymeric shell with a low density and may have in turn contributed to the poor structural strength of the microcapsules.

3.2.3. FTIR Spectroscopic Analysis of Microencapsulated Core

In order to achieve the delivery of isocyanate crosslinkers, the encapsulation of active isocyanate was desired. Thus, it was important to confirm the microencapsulation of the active isocyanate crosslinker. Isocyanates possess a characteristic stretching vibration that appears as an absorption in an IR spectrum at $\sim 2250\text{ cm}^{-1}$. A sample of microcapsules was crushed and the released core analysed using FTIR spectroscopy.¹⁸

A broad absorption at 2258 cm^{-1} was observed, corresponding to the isocyanate moiety of IPDI, confirming the envelopment of the active isocyanate crosslinker within polyurethane microcapsules. A further notable absorption at 1736 cm^{-1} was observed that is likely to correspond to the urethane carbonyl functional group of the polyurethane microcapsule shell wall (Figure 3.4).

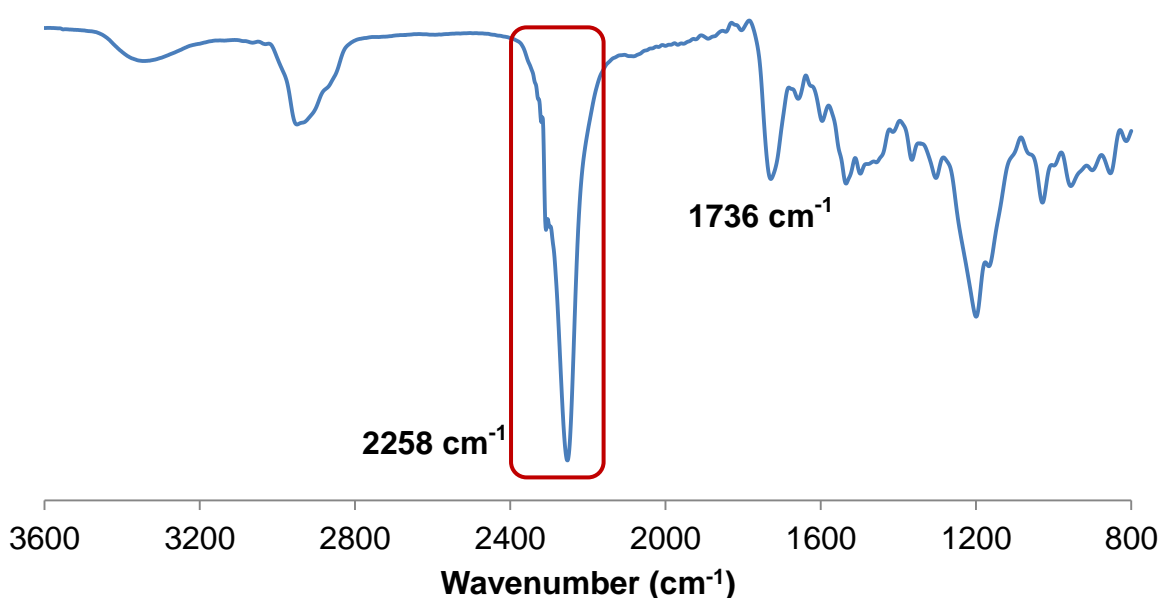


Figure 3.4. FTIR spectrum of released core of microcapsules **3.1g**, highlighting an absorbance at 2258 cm^{-1} corresponding to the isocyanate moiety of encapsulated IPDI.

3.2.4. ^1H NMR Spectroscopic Analysis of the Microencapsulated Core

^1H NMR spectroscopy is a powerful analytical tool employed in the characterisation of organic molecules. Analysis of the microcapsules with this technique provides examination of the composition of the microencapsulated core.²⁵ A sample of microcapsules was crushed and the released core dissolved in CHCl_3 and followed by filtration to remove the solid microcapsule shell wall. The obtained ^1H NMR spectrum of the microcapsule core was compared to individual spectra of IPDI and ethyl phenylacetate revealing a clear overlap between the separate isocyanate and solvent components and the microcapsule core, corroborating the observation of the microencapsulation of IPDI using FTIR spectroscopic analysis (Figure 3.5).

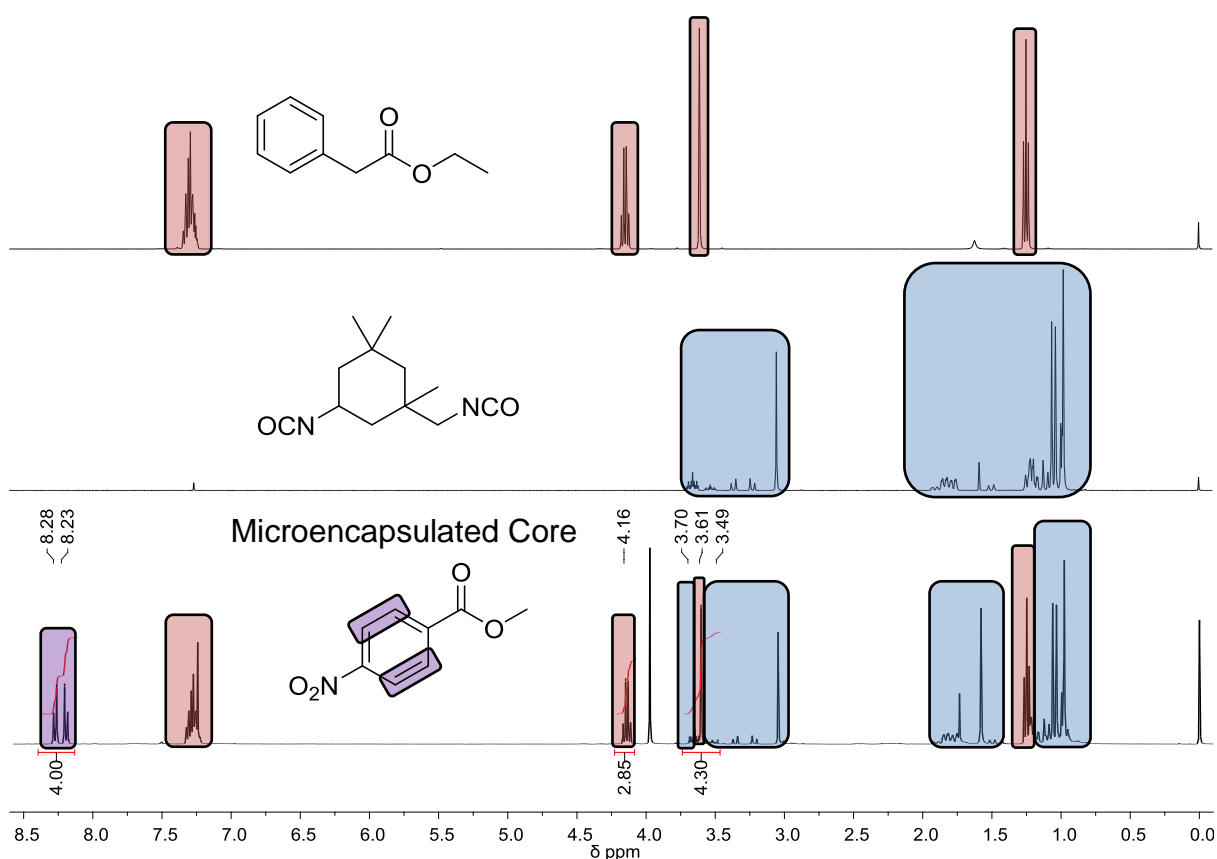


Figure 3.5. ^1H NMR spectra of separate components of released core of microcapsules **3.1g** - ethyl phenylacetate and IPDI. ^1H NMR spectra of microencapsulated core with an internal standard - methyl 4-nitrobenzoate

^1H NMR spectroscopy can also be used to quantify the microencapsulated core by the addition of a known quantity of an internal standard. Methyl 4-nitrobenzoate was employed because its spectroscopic resonances did not overlap with the encapsulated components. Comparing the integration of the resonances corresponding to the internal standard at 8.23-8.28 ppm with those of ethyl phenyl acetate at 4.16 ppm and

IPDI 3.49-3.70 ppm allowed calculation of the composition of the microencapsulated core. Microcapsules **3.1a**, **3.1e** and **3.1g** all possessed core compositions within the range 49-66 wt. % which is concurrent with literature studies.¹⁸ Microcapsules **3.1b**, however, possessed a relatively low core composition suggesting the core had leaked from the microcapsules and leading to the formation of puckered microcapsules observed using SEM. As expected, a low core composition was observed in microcapsules **3.1f** (Table 3.4).

Table 3.4. List of the core compositions of microcapsules **3.1a-3.1g**, measured using ¹H NMR spectroscopic analysis.

Microcapsules	Solvent Composition (wt. % of microcapsule)	IPDI Composition (wt. % of microcapsule)
3.1a	49	-
3.1b	14	18
3.1e	22	36
3.1f	6	7
3.1g	27	39

3.2.5. Thermogravimetric Analysis of the Microencapsulated Core

Thermogravimetric analysis (TGA) can be used to measure the weight loss of a sample upon heating. Thus, literature studies have employed²⁶ TGA to quantify the volatile components of the microencapsulated core. A sample of microcapsules was crushed prior to analysis and heated at a rate of 10 °C minute⁻¹ under an atmosphere of argon (Figure 3.6).

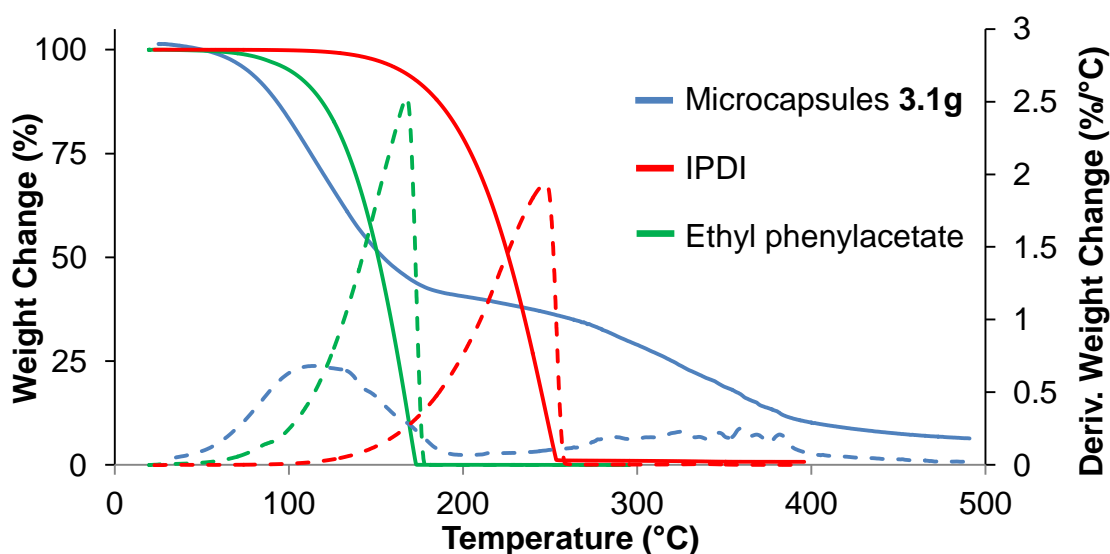


Figure 3.6. TGA curves and derivatives of crushed microcapsules **3.1g**, IPDI and ethyl phenylacetate.

Weight loss was observed almost immediately until just below 200 °C, corresponding to the loss of 58 wt. % of the sample. A further weight change between 200-250 °C of 5 wt. % is observed. TGA of the separate components suggests that these weight changes are associated with the sequential loss of ethyl phenylacetate followed by IPDI - however, the observed weight compositions do not correlate with the data derived from ¹H NMR spectroscopic analysis. It is possible that ethyl phenylacetate and IPDI evolve jointly from the crushed microcapsules and thus a combined weight loss of 64 wt. % between 20-250 °C corroborates the core composition results observed using ¹H NMR spectroscopic analysis (Table 3.5). Further weight loss above 250 °C likely corresponds to the degradation of the polyurethane microcapsule shell wall.

Table 3.5. List of the core compositions of microcapsules **3.1a-3.1g**.

Microcapsules	Core Composition Using TGA (wt. %)	Core Composition Using ¹ H NMR (wt. %)
3.1a	44	49
3.1b	26	32
3.1e	41	58
3.1f	11	13
3.1g	64	66

3.2.6. Release of Microencapsulated Core Using a Heat Stimulus

Microcapsules **3.1a-3.1g** have been synthesised using a shell wall precursor that possesses a thermally-labile oxime-urethane bond and thus incorporating the labile bond within the polymer of the microcapsule shell (Figure 3.7). The potential of these microcapsules to release the encapsulated IPDI crosslinker upon the exposure to a heat stimulus was investigated. Microcapsules **3.1a-3.1g** were heated to 200 °C at a rate of 1 °C/minute using a hot stage mounted to an optical microscope utilising a digital camera. In conjunction with optical microscopy, microcapsules were analysed using SEM after heating (Figure 3.7).

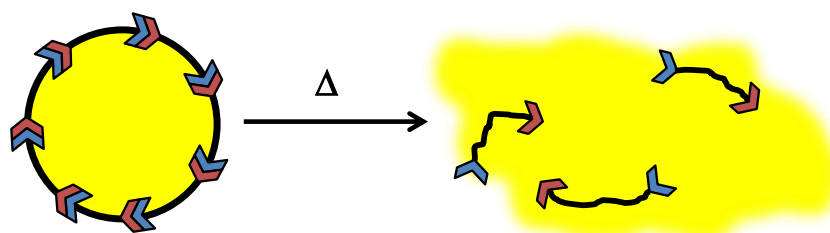


Figure 3.7. Schematic showing the dissociation of thermally-releasable microcapsules.

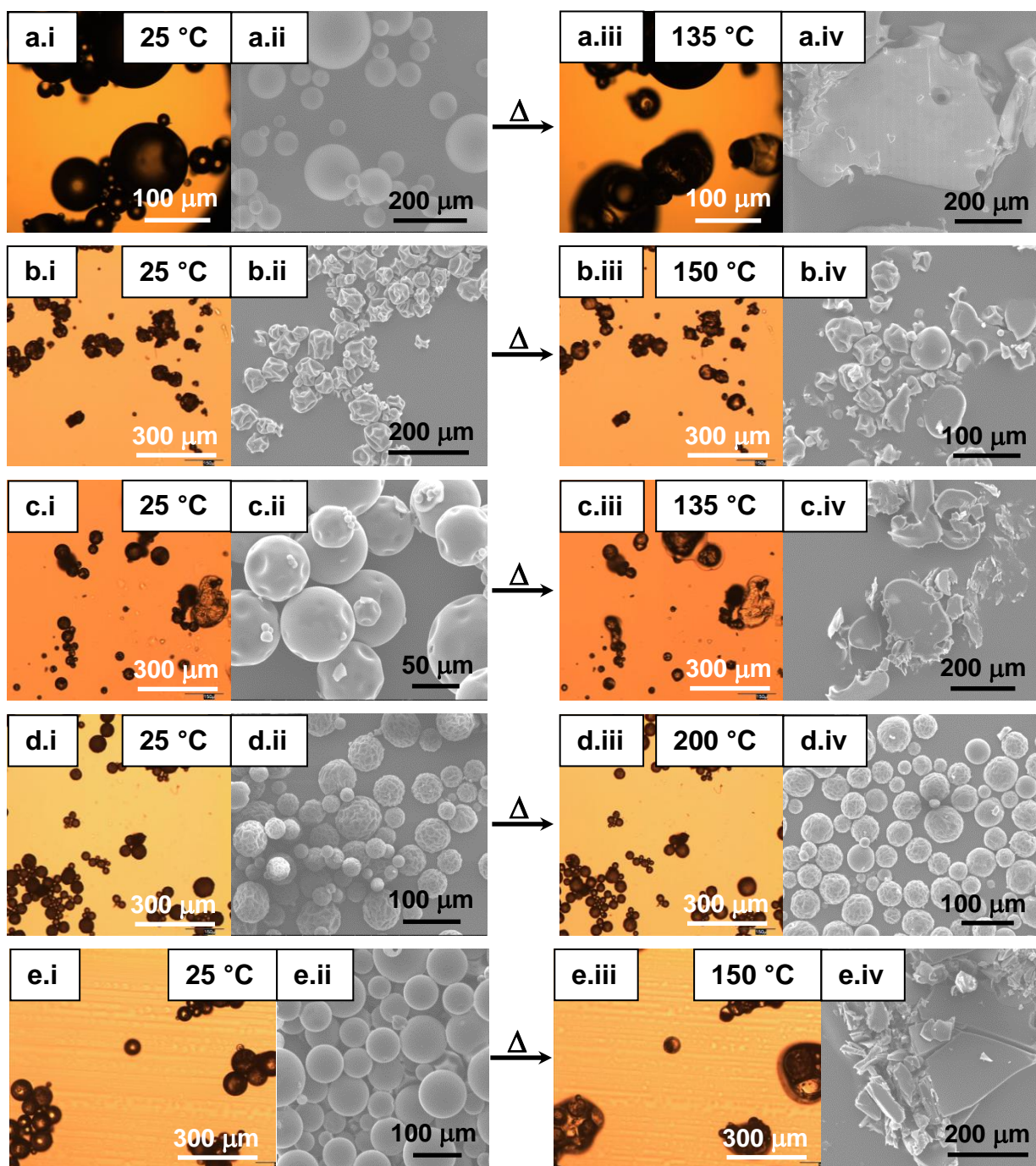


Figure 3.8. a.i) optical microscopic image of **3.1a** at 25 °C, a.ii) SEM image of **3.1a** before heating, a.iii) optical microscopic image of **3.1a** at 135 °C a.iv) SEM image of **3.1a** after heating to 200 °C, b.i) optical microscopic image of **3.1b** at 25 °C, b.ii) SEM image of **3.1b** before heating, b.iii) optical microscopic image of **3.1b** at 150 °C b.iv) SEM image of **3.1b** after heating to 200 °C, c.i) optical microscopic image of **3.1e** at 25 °C, c.ii) SEM image of **3.1e** before heating, c.iii) optical microscopic image of **3.1e** at 135 °C, c.iv) SEM image of **3.1e** after heating to 200 °C, d.i) optical microscopic image of **3.1f** at 25 °C, d.ii) SEM image of **3.1f** before heating, d.iii) optical microscopic image of **3.1f** at 200 °C d.iv) SEM image of **3.1f** after heating to 200 °C, e.i) optical microscopic image of **3.1g** at 25 °C, e.ii) SEM image of **3.1g** before heating, e.iii) optical microscopic image of **3.1g** at 150 °C e.iv) SEM image of **3.1g** after heating to 200.

Upon heating to 135 °C the microcapsules **3.1a** shell wall appeared to dissociate and the liquid core was released. Analysis of the microcapsules after heating to 200 °C using SEM revealed the absence of spherical-shaped microcapsules, suggesting that complete dissociation of the microcapsule shell wall was achieved. Optical microscopic images of **3.1b** suggested that only partial dissociation was achieved and SEM analysis revealed that indeed the majority of the microcapsules had remained intact, **3.1b** possessed a comparatively low core composition and this may suggest that the dissociation of the oxime-urethane linkages may be catalysed by the presence of the polar encapsulated solvent in the core. The observed dissociation of **3.1a** was replicated for **3.1e** and **3.1g** at 135 °C and 150 °C, respectively. VTIR studies described in **Chapter 2** suggested that microcapsules containing more sterically hindered oxime-urethane linkages in the shell wall would be expected to dissociate and release their core contents at a lower temperature. However, this was not observed and the high mechanical strength of **3.1g** may have prevented the release of the core at a lower temperature. As expected, no change to **3.1f** was observed upon exposure to heat.

3.2.7. Delayed Cure of HTPB Using Microencapsulated Crosslinkers

In addition to release studies, the potential of the generated microcapsules for the controlled delivery of IPDI in HTPB using an external stimulus of heat was investigated. Microcapsules **3.1g** were selected for this investigation because of their high mechanical strength and thus can withstand shear forces when mixed with HTPB. A formulation of HTPB (100 mg), DBTDL (0.24 mg) and **3.1g** (23 mg) were mixed together in a composition according to Rowanex 1100 1A formulation.

As a control experiment, 'control microcapsules' were synthesised using a shell wall precursor that did not possess thermally-labile linkages in the shell wall. This was achieved by first synthesising a shell wall precursor using 1,4-butanediol and an excess of TDI. Microcapsule synthesis followed an identical method employed in the synthesis of **3.1g**. The synthesis of this shell wall precursor and microcapsules is described in Section 3.4. A second formulation comprised of HTPB (100 mg), DBTDL (0.24 mg) and control microcapsules (18 mg) was generated. Both mixtures were placed between two films of cellulose acetate and heated to 150 °C for a period of 30 minutes followed by a further 24 hours at 60 °C. Tensile testing was performed before and after heating and revealed that upon exposure to heat an increase in the tensile

strength of both mixtures was observed, suggesting that IPDI had been released from both **3.1g** and control microcapsules leading to the cure of HTPB (Figure 3.9). The permeability of microencapsulated core through the shell wall has been reported²⁷ in literature investigations. The application of heat may have accelerated this diffusion process and resulted in the cure of HTPB observed in the control microcapsules. This characteristic could be exploited as a method of delivery of the microcapsule core.

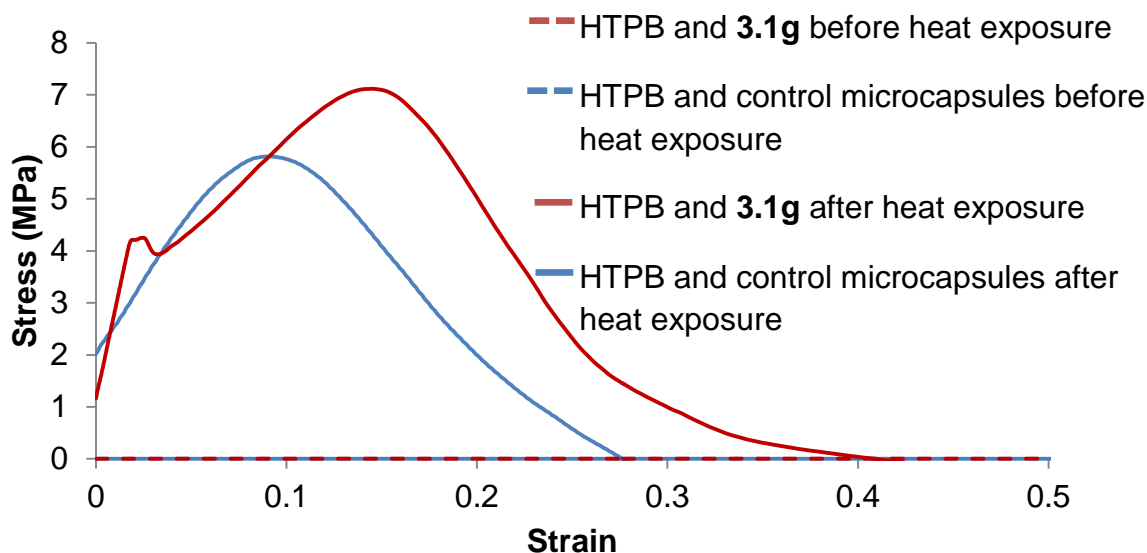


Figure 3.9. Stress-strain curves of - HTPB and **3.1g** before exposure to heat stimulus, HTPB and control microcapsules before exposure to heat stimulus, HTPB and **3.1g** after exposure to heat stimulus, HTPB and control microcapsules after exposure to heat stimulus.

It was also important to investigate the stability of microcapsules under the mixing conditions employed in the production of PBX. Both mixtures along with a third mixture comprised of IPDI, HTPB and DBTDL were placed between two films of cellulose acetate and heated at 60 °C for a period of 24 hours. Tensile testing after this time revealed no curing had occurred from either of the microcapsule mixtures suggesting IPDI had not been released from the microcapsules under these conditions (Figure 3.10).

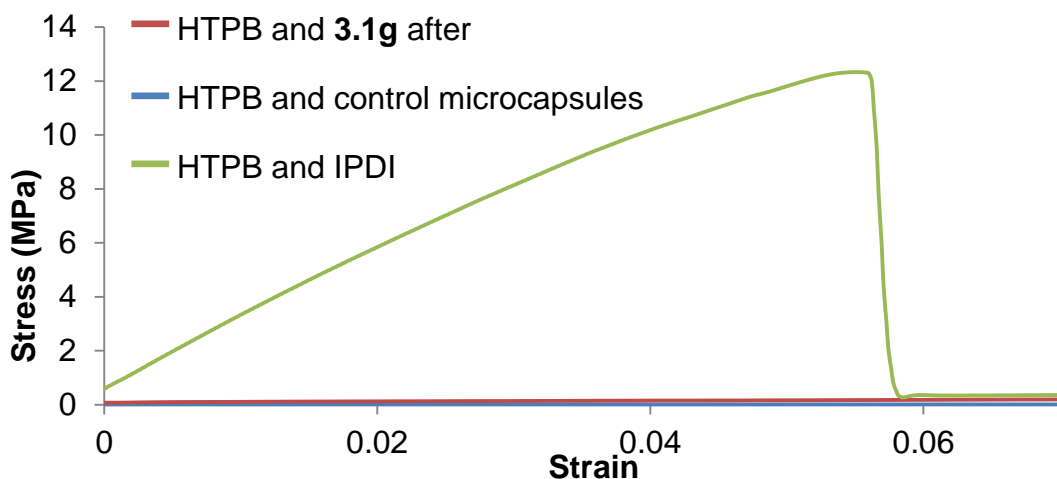


Figure 3.10. Stress-strain curves of HTPB and **3.1g**, HTPB and control microcapsules and HTPB and IPDI after 24 hours at 60 °C.

3.2.8. Control of the Microcapsule Properties

Microencapsulation using interfacial polymerisation has many reaction parameters associated with the synthetic process,²⁸ including - rate of agitation, type of agitation paddle employed, concentration of the core and its composition, shell wall precursor concentration, hydrophobic solvent used, chain extender concentration, surfactant concentration and type of surfactant, reaction temperature and reaction time. The following section describes how modification of these parameters allow control of the microcapsule properties - diameter and size distribution, shell wall thickness, amount of active crosslinker released²⁹ and the physical strength of microcapsules which are in turn dependent on diameter and shell wall thickness¹ in order to tailor microcapsules with specific physical properties (Figure 3.11).

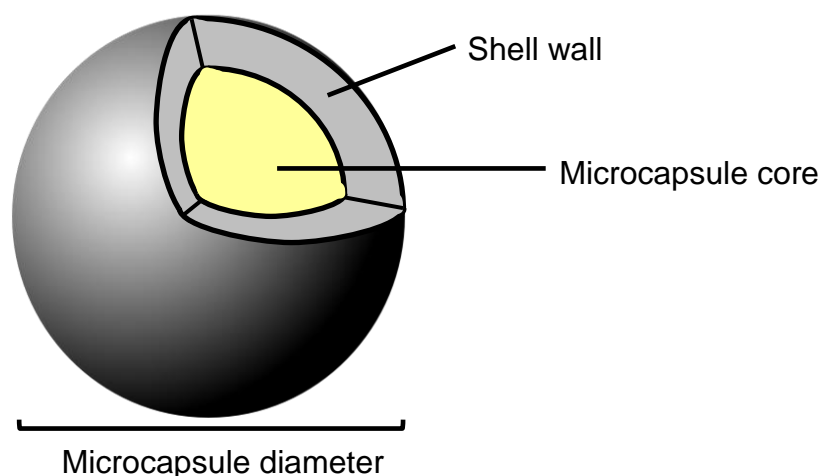
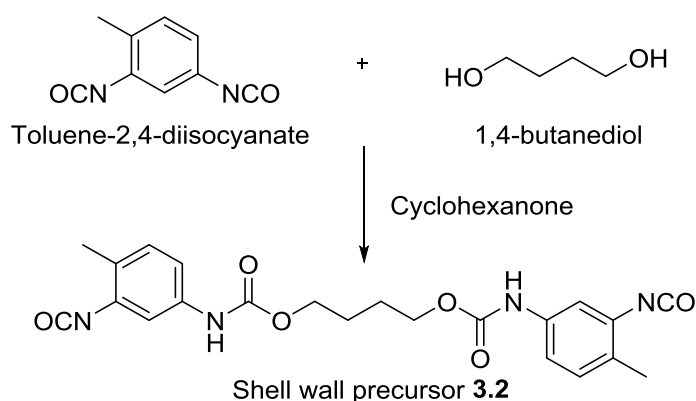


Figure 3.11. Design of a mononuclear microcapsule showing the microcapsule diameter, shell wall and microencapsulated core.

Previous studies undertaken¹⁷ at the University of Reading investigated the effect of the rate of agitation, shell wall precursor concentration and reaction time on the microcapsule properties. However, the conditions used in this investigation prevented the reproducibility of these results. Thus it was important to investigate the effect of these reaction parameters using a developed reproducible synthetic procedure.

Microcapsules in this section were synthesised using a shell wall precursor previously developed¹⁷ at University of Reading afforded by termination of 1,4-butanediol with toluene-2,4-diisocyanate **3.2** (TDI) (Scheme 3.2).



Scheme 3.2. Synthesis of a shell wall precursor **3.2** by reaction of 1,4-butanediol with toluene-2,4-diisocyanate.

3.2.8.1. The Effect of the Rate of Agitation

The interfacial polymerisation approach to the synthesis of microcapsules employs mechanical agitation in order to achieve a stable emulsion.³⁰ Increasing the speed of the applied agitation imparts a greater degree of shear force on the emulsion leading to the formation of smaller oil droplets. Literature studies have exploited^{18,31} this parameter in order to yield microcapsules with specific diameters. Microcapsules were synthesised at 500, 750, 1000, 1250, 1500, 1750 and 2000 rpm employing chlorobenzene as the hydrophobic solvent. Other experimental conditions include - 18 wt. % shell wall precursor concentration, 0.06 M chain extender concentration, 26 vol. % IPDI concentration, 11.0 wt. % surfactant concentration and a reaction time of 165 minutes at 70 °C.

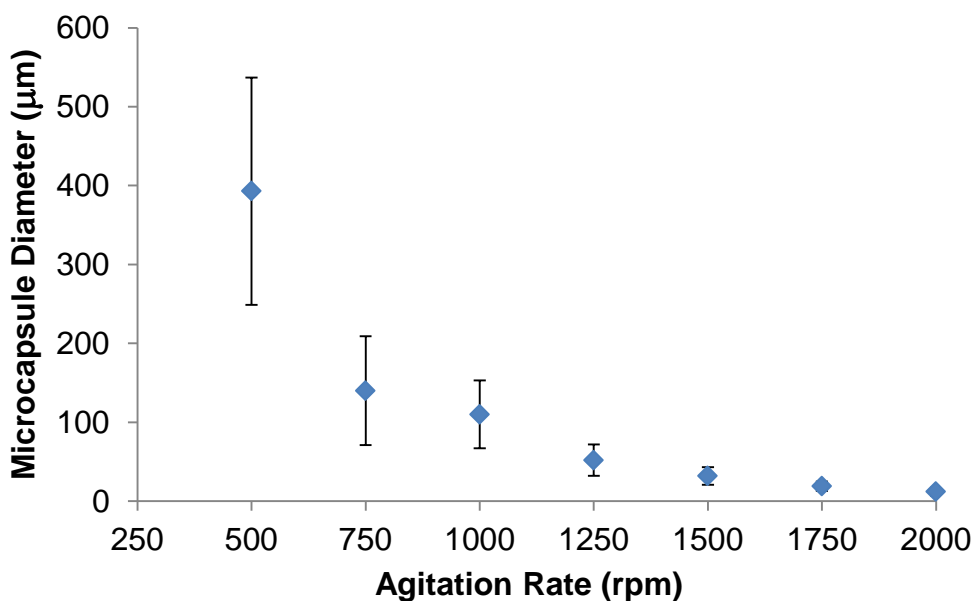


Figure 3.12. The effect of the rate of agitation on the average microcapsule diameter. Analysis using optical microscopy revealed a decrease in the average microcapsule diameter in an exponential fashion as the agitation rate was increased reaching an almost negligible change between 1750-2000 rpm. In addition, a decrease in the size distribution was observed in conjunction with the decrease in microcapsule diameter (Figure 3.12).

The minimum microcapsule diameter that could be obtained was $\sim 12 \mu\text{m}$ and this result is in agreement with literature studies.¹⁸ The generation of sub-micron sized microcapsules must employ the use of ultrasonic agitation.³² Analysis of the core composition of the microcapsules using ^1H NMR spectroscopy observed the amount of encapsulated IPDI per weight of microcapsules decreased in conjunction with the diameter (Table 3.6) and has also been observed in literature investigations.^{18,31,33}

Table 3.6. The amount of IPDI encapsulated is dependent on the average diameter of the generated microcapsules.

Agitation Rate (rpm)	Average Diameter (μm)	IPDI Composition (wt. %)
500	393	37.2
750	140	32.5
1000	110	29
1250	52	24.8
1500	32	24.5
1750	19	23.2
2000	12	22.8

Literature studies have observed¹⁸ a decrease in the shell wall thickness as the average microcapsule diameter decreased. The shell wall thicknesses of the generated microcapsules was investigated by preparing cross-sections using a microtome and measured using SEM and indeed a linear relationship between shell wall thickness and microcapsule diameter was observed (Figure 3.13).

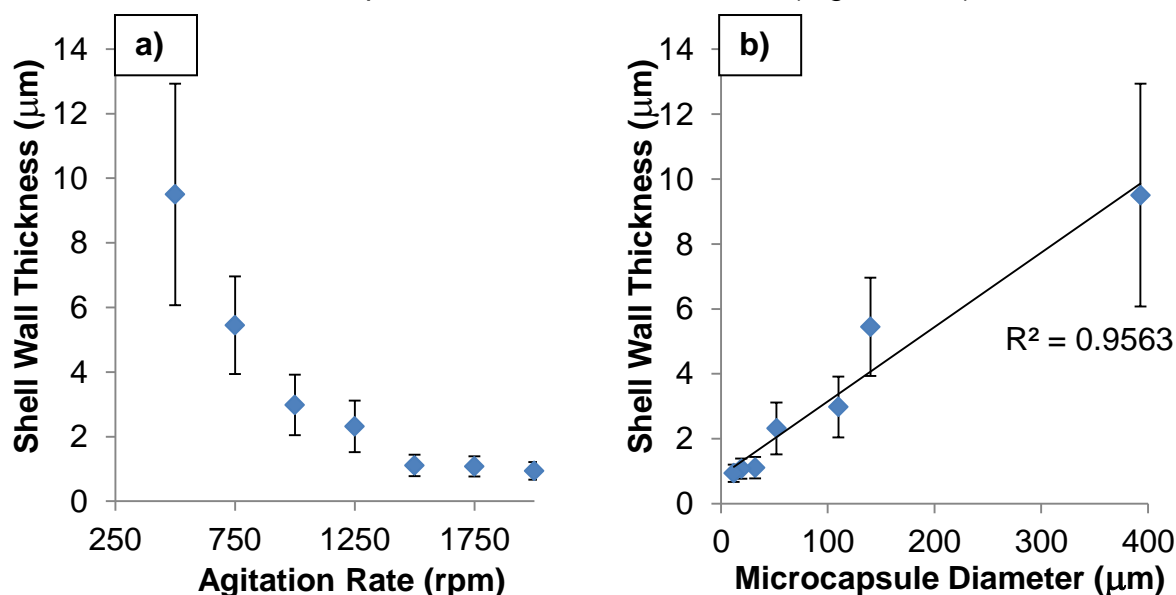


Figure 3.13. Relationship between shell wall thickness and **a)** agitation rate **b)** microcapsule diameter.

3.2.8.2. The Effect of the Surfactant Concentration

The role of the surfactant in microcapsule synthesis is to aid the formation of a stable emulsion, working by reducing the surface tension at the oil-water interface.^{34,35} Although only gum arabic has been used in this investigation, literature studies have reported a range of surfactants employed in the synthesis of microcapsules.³⁶ Studies have also reported³¹ increasing the surfactant concentration further reduces the surface tension at the interface, thus leading to the formation of smaller and more uniformly sized oil droplets. Microcapsules were synthesised using a range of different concentrations of gum arabic - 5, 10, 15, 20 and 25 wt. % in H₂O whilst employing chlorobenzene as the hydrophobic solvent and maintaining a constant agitation rate of 1000 rpm. Other experimental conditions include - 18 wt. % shell wall precursor concentration, 0.94 M chain extender concentration, 53 vol. % IPDI concentration, reaction time of 165 minutes at 70 °C. The generated microcapsules were measured using optical microscopy revealing, as expected, increasing the surfactant concentration generated smaller more uniform microcapsules (Figure 3.14). Although only a small amount of surfactant concentration is required to form a stable emulsion

< 1 wt. %, reducing the surfactant concentration below 5 wt. % did not lead to the formation of microcapsules. Thus the role of the surfactant may go beyond reducing the surface tension of the emulsion oil droplets - high concentrations of surfactant (> 5 wt. %) may form a hydrophobic layer around the oil-droplet thus preventing the undesired hydrolysis of the isocyanate end group whilst allowing the 1,4-butanediol chain extender to diffuse through this region and promoting the interfacial polymerisation reaction.

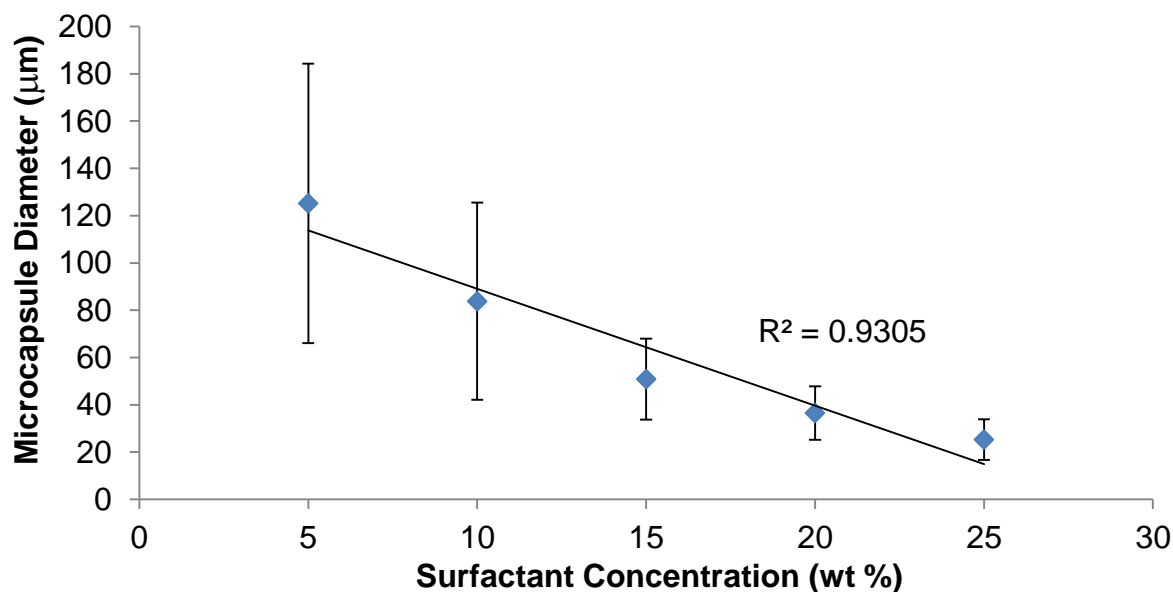


Figure 3.14. Graph showing the effect of surfactant concentration on the average diameter and size distribution of microcapsules.

3.2.8.3. The Effect of the Hydrophobic Solvent

Selection of the hydrophobic solvent used for the synthesis of microcapsules is important for several reasons. Organic solvents possess a unique surface tension³⁷ thus the microcapsule diameter is dependent on the solvent employed. Efficient dissolution of the shell wall precursor and a poor solubility of the consequent growing shell wall are desired in order to generate mononuclear microcapsules. In addition, release of microcapsules using a heat stimulus requires temperatures in excess of 100 °C - therefore the solvent must have low vapour pressure at the desired release temperature in order to prevent the formation of voids in the PBX material. A range of microcapsules were synthesised using several different solvents - chlorobenzene, 1,2-dichlorobenzene, 1,2,4-trichlorobenzene, phenyl acetate and ethyl phenylacetate. A rate of agitation of 1000 rpm was used and other reaction conditions include - 24 wt. % shell wall precursor concentration, 0.94 M chain extender concentration,

47 vol. % IPDI concentration, 15 wt. % surfactant concentration, reaction time of 165 minutes at 70 °C. All of the formulations using different solvents generated successfully mononuclear microcapsules and the average diameters and core compositions were measured using optical microscopy and ¹H NMR spectroscopy, respectively. A correlation between the surface tension of the hydrophobic solvent employed and the diameter of the generated microcapsules was expected, however optical microscopic analysis revealed that the microcapsule diameter was independent of the hydrophobic solvent. Table 3.7 lists the average diameter of the yielded microcapsules demonstrating the dependency of microcapsule diameter on the solvent used. In addition, as expected, the composition of the encapsulated core is dependent on the solvent employed, with more dense solvents contributing to a higher proportion by weight of the microencapsulate core.

Table 3.7. Average diameter and core composition of microcapsules synthesised using a range of hydrophobic solvents

Solvent	Surface Tension (dyn cm⁻¹)	Average Diameter (µm)	Composition of IPDI (wt. %)	Solvent composition (wt. %)
Chlorobenzene	33.59 ³⁷	51	44	21
Ethyl phenylacetate	24.92 ³⁷	38	48	24
Phenyl acetate	34.93 ³⁷	44	44	30
1,2-Dichlorobenzene	36.61 ³⁷	37	44	33
1,2,4-Trichlorobenzene	39.12 ³⁷	128	32	42

3.2.8.4. The Effect of the Concentration of the Shell Wall Precursor

The shell wall precursor forms the majority of the polyurethane material of the shell wall, thus it is expected that increasing the concentration of the shell wall precursor will lead to the formation of thicker shell walls. Microcapsules were synthesised using several concentrations of shell wall precursor - 13, 23, 35, 52 and 68 wt. % in chlorobenzene. Other reaction conditions employed include - A rate of agitation of 1000 rpm, 0.06 M chain extender concentration, 26 vol. % IPDI concentration, 11 wt. % surfactant concentration and a reaction time of 165 minutes at 70 °C. The shell wall thickness of the yielded microcapsules was measured using SEM following preparation of cross-sections using a microtome. As expected, as the concentration of the shell wall was increased thicker shell walls were formed (Figure 3.15). Although

only a small increase in the shell wall thickness was observed, this led to a significant increase in the microcapsules mechanical strength.

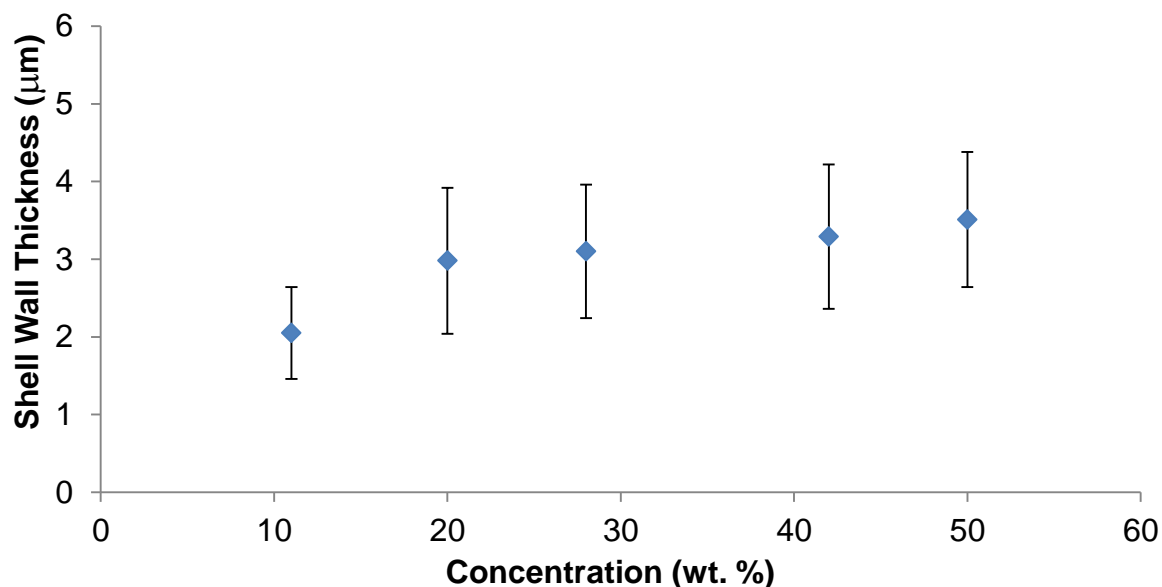


Figure 3.15. Graph showing the effect of the shell wall precursor concentration on the shell wall thickness of the generated microcapsules.

3.2.8.5. The Effect of the Reaction Time

Literature studies investigating^{38,16} the synthesis of polyurethane microcapsules reported that increasing the reaction time leads to the formation of microcapsules with thicker shell walls. It is thought that the formation of the initial shell wall occurs quickly and becomes progressively slower as the chain extender must diffuse through the increasingly thicker shell wall, therefore increasing the reaction time may allow the formation of a thicker shell. To investigate, microcapsules were synthesised at a range of reaction times - 45, 75, 105, 135 and 165 minutes employing chlorobenzene as the hydrophobic solvent. Other microencapsulation reaction conditions include - agitation rate of 1000 rpm, 18 wt. % shell wall concentration, 0.94 M chain extender concentration, 53 vol. % IPDI concentration, 15 wt. % surfactant concentration and a reaction temperature of 70 °C. Cross-sections of the microcapsules were prepared using a microtome and the shell wall thickness of the microcapsules measured using SEM. It was revealed that increasing the reaction time from 45-165 minutes only led to a small increase in the shell wall thickness (Figure 3.16). However, even this small change had a significant effect on the mechanical strength of the microcapsules. Further increasing the thickness of the microcapsule shell wall may be achieved by

combination of high concentration of shell wall precursor in conjunction with long reaction times.

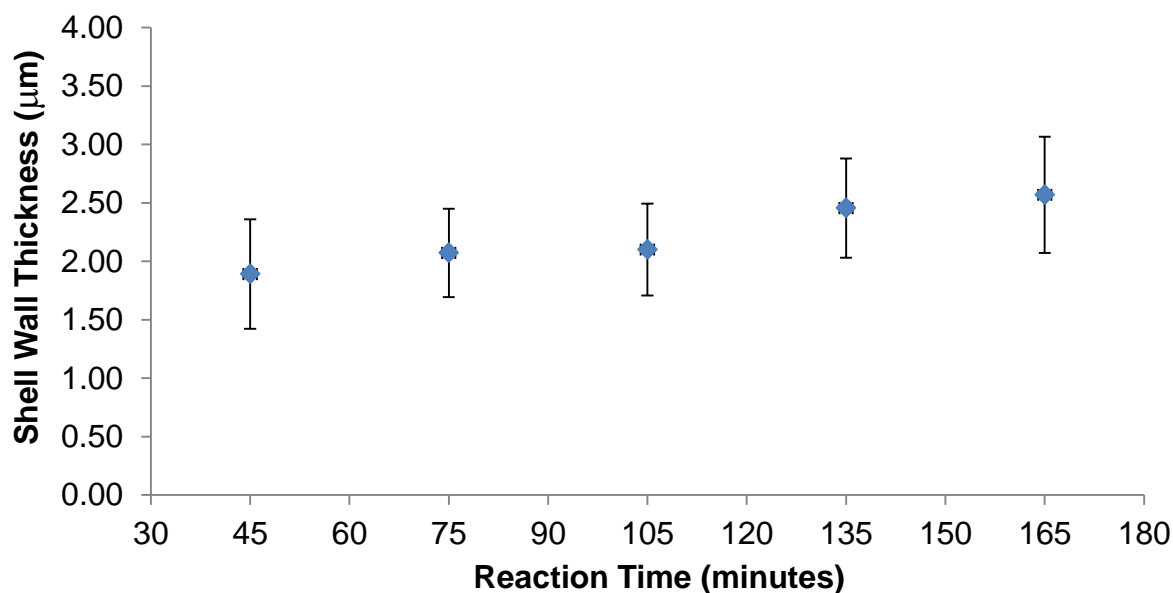


Figure 3.16. Graph showing that increasing the reaction time leads to the formation of microcapsules with thicker shell walls.

3.2.8.6. Maximising the IPDI Content of Microcapsules

The microcapsule core is comprised of IPDI and a solvent. Ideally, a maximum IPDI encapsulation is desired in order to achieve a high payload of the crosslinker. However, Yang *et al.* observed¹⁸ agglomeration when loading of IPDI microcapsules exceeded 70 wt. %. In order to investigate the maximum IPDI loading achievable, microcapsules were synthesised using a range of concentrations of IPDI - 0, 11, 26, 42, 53, 63, 79, 89 and 100 vol. % in chlorobenzene as the hydrophobic solvent. Other reaction conditions include - an agitation rate of 1000 rpm, 18 wt. % shell wall precursor concentration, 0.94 M chain extender concentration, 15 wt. % surfactant concentration and a reaction time of 165 minutes at 70 °C. The core composition of the microcapsules was assessed using ¹H NMR spectroscopy and this data is presented in Figure 3.17. As expected, increasing the concentration of IPDI used in the synthesis of microcapsules led to an increase in the IPDI composition of the generated microencapsulated core. The agglomeration reported¹⁸ by Yang *et al.* was not observed - however, as the composition of IPDI increased the structural integrity of the microcapsules became increasingly compromised reaching an extreme case where rupture occurred with minimal physical force. Therefore, a careful balance must be found between achieving a maximum payload of IPDI whilst avoiding significant

loss of the physical strength. Analysis of the yielded microcapsules with optical microscopy revealed that changing the core composition did not have an effect on the microcapsule diameter. However, when a concentration of 100 vol. % IPDI was used, larger microcapsules were generated and this is likely to have resulted from a change in the density of the hydrophobic phase.

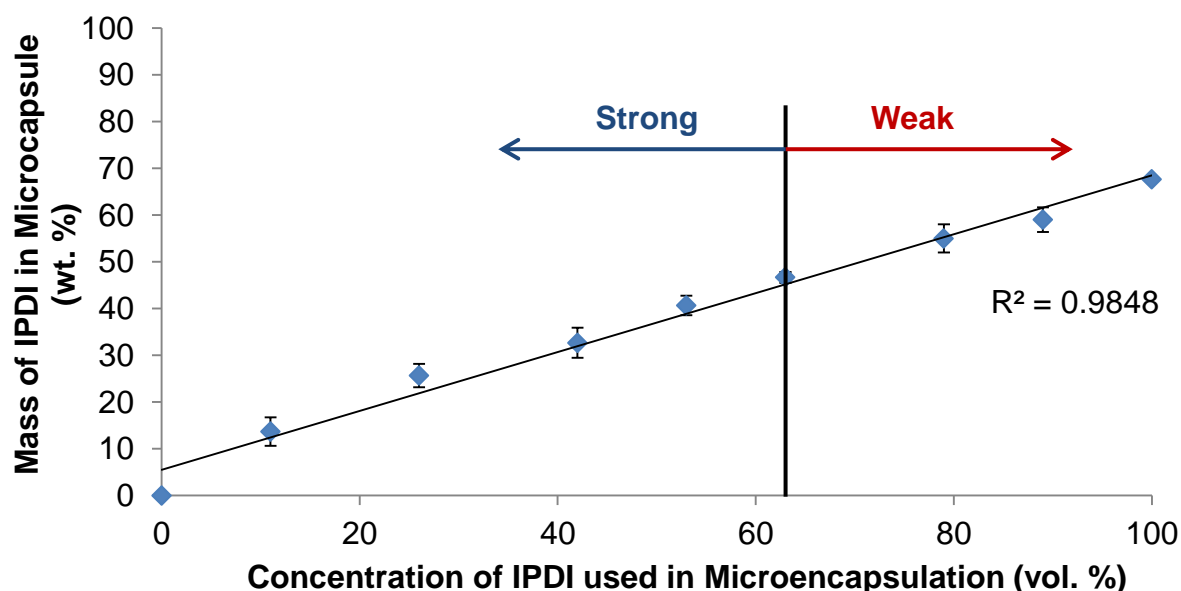


Figure 3.17. Graph showing the amount of IPDI encapsulated increases with the concentration of IPDI employed in microcapsule synthesis. Microcapsules were weaker when containing >50 wt. % IPDI.

3.2.8.7. The Effect of the Chain Extender Concentration

Long storage lifetimes of microcapsules containing IPDI are desired, thus the longevity of microcapsules was investigated by measuring the core composition after 4 weeks and observing the leaching of IPDI from the core. It was found that a loss of 14 wt. % of IPDI was observed after this period of time. Literature investigations have reported³⁹ that the porosity of microcapsules can be controlled by increasing the concentration of the chain extender. Microcapsules were synthesised using a range of concentrations of 1,4-butanediol - 0.06, 0.28, 0.65, 0.94 and 1.14 M. Other reaction conditions include - an agitation rate of 1000 rpm, 18 wt. % shell wall precursor concentration, 26 vol. % IPDI concentration in chlorobenzene, 11 wt. % surfactant concentration and a reaction time of 165 minutes at 70 °C. The surface morphology of all the afforded microcapsules was analysed using SEM revealing the formation of microcapsules that possessed smooth non-porous exterior shells. The leaching of IPDI from these microcapsules after a period of 4 weeks at a temperature of 20 °C was investigated by

measuring the core composition after this period of time using ^1H NMR spectroscopy. The loss of IPDI from microcapsules was significantly reduced upon increasing the concentration of 1,4-butanediol, this may be attributed to the formation of a denser polyurethane shell wall (Figure 3.18).

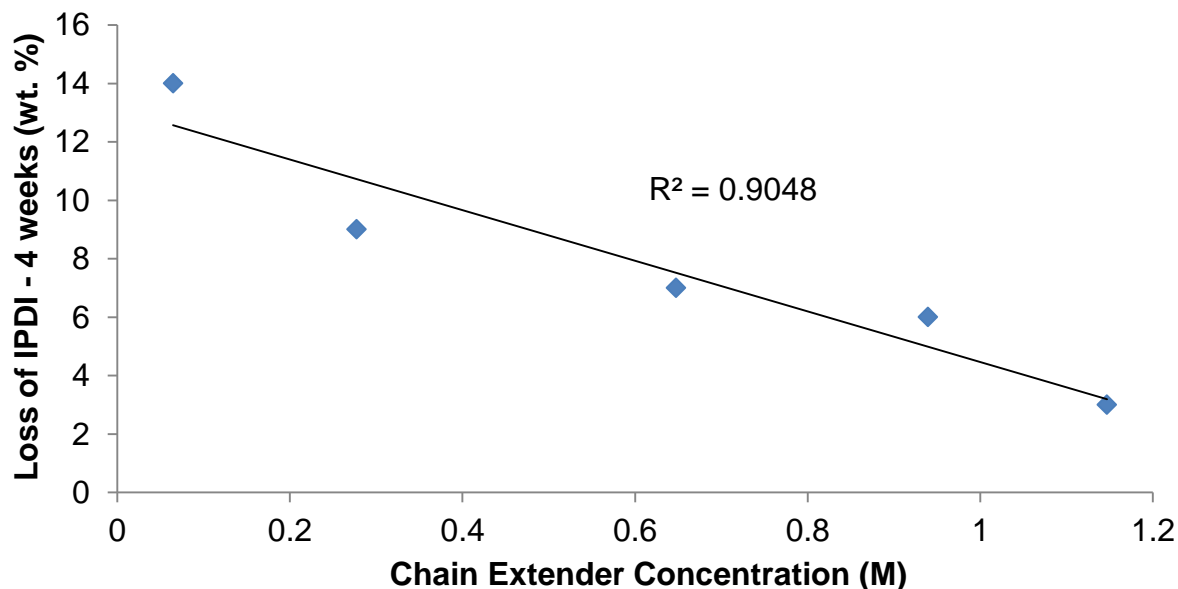


Figure 3.18. Graph showing the loss of IPDI from microcapsules after a period of 4 weeks from microcapsules synthesised using a range of chain extender concentrations.

3.2.9. Microencapsulation of a Dye

In order to aid in the study of the release of microcapsules core contents using the application of heat it was necessary to synthesise microcapsules containing a dye that can be easily quantified. Isocyanates react readily with functional groups such as alcohols, amines and carboxylic acids⁴⁰ typically present within the conjugated structure of many organic dyes, thus the apolar π -conjugated dye β -carotene was selected (Figure 3.19).

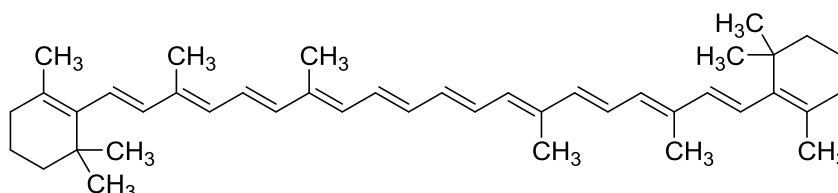


Figure 3.19. Structure of the apolar π -conjugated dye β -carotene.

Microcapsules containing IPDI, chlorobenzene and β -carotene were afforded utilising the developed interfacial polymerisation technique employing the shell wall precursor **3.7** at a rate of agitation of 1000 rpm in an aqueous gum arabic (15 wt. %) medium. The physical properties of the generated microcapsules were analysed and were all

within the expected range - average diameter of 37.2 μm within a range of 10.5-66.4 μm . The average microcapsule shell wall thickness was 1.74 μm and analysis of the encapsulated core revealed a composition of 42 wt. % IPDI and 27 wt. % chlorobenzene.

β -carotene absorbs UV light ($\lambda_{\text{max}} = 450 \text{ nm}$) and thus the encapsulated dye can be quantified using ultraviolet (UV) spectroscopy. A series of standard β -carotene concentrations were prepared in chloroform and the absorbance intensities measured. Plotting this data affords a linear plot of concentration vs. intensity, thus the concentration of an unknown solution from the microcapsule core can be determined (Figure 3.20).

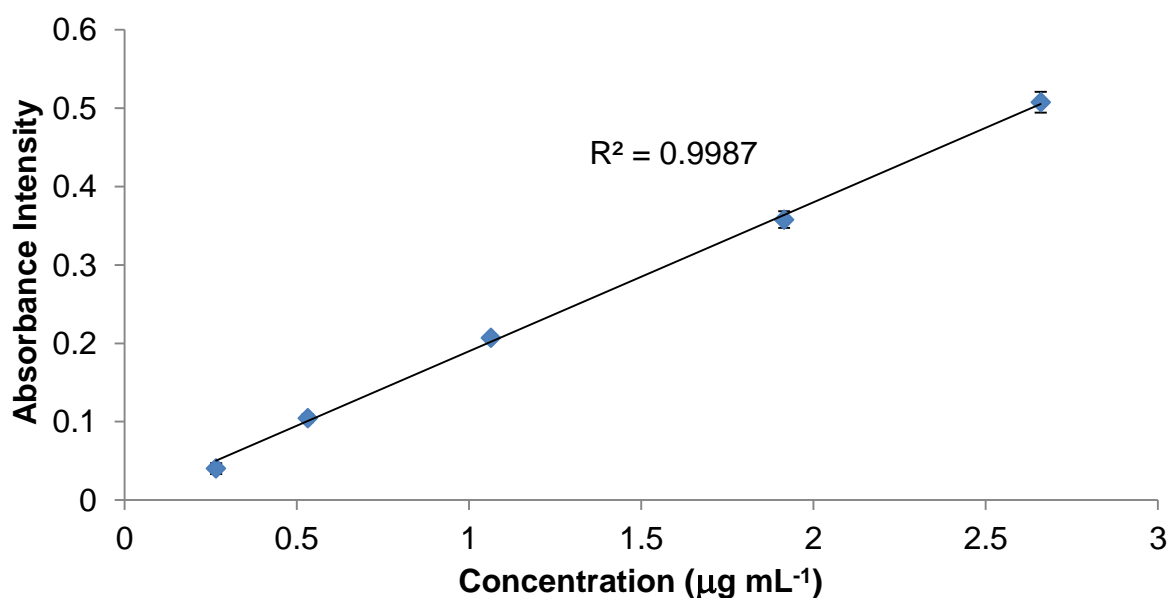


Figure 3.20. Linear plot of concentration vs. intensity of a known series of standard β -carotene concentrations.

Microcapsules containing β -carotene (112 mg) were crushed and the released core diluted in chloroform by a factor of 500 and a UV-spectrum of this solution was recorded (Figure 3.21). The measured absorbance intensity allows calculation of the amount of β -carotene released from the microcapsules: 14.1 mg g^{-1} of microcapsules. β -carotene filled microcapsules were afforded using 40 mg of the dye to yield 1.99 g of microcapsules, this equates to a maximum theoretical encapsulation of β -carotene of 21.0 mg g^{-1} of microcapsules and thus an encapsulation efficiency of the dye was calculated 67 %.

The permeability of the dye through the microcapsule shell was also studied by soaking a sample of microcapsules (112 mg) in chloroform (100 mL) for a period of 1 hour. The solution was diluted by a factor of 5 and the absorbance intensity measured, revealing a small portion of β -carotene (10 %) had leaked into the chloroform solution.

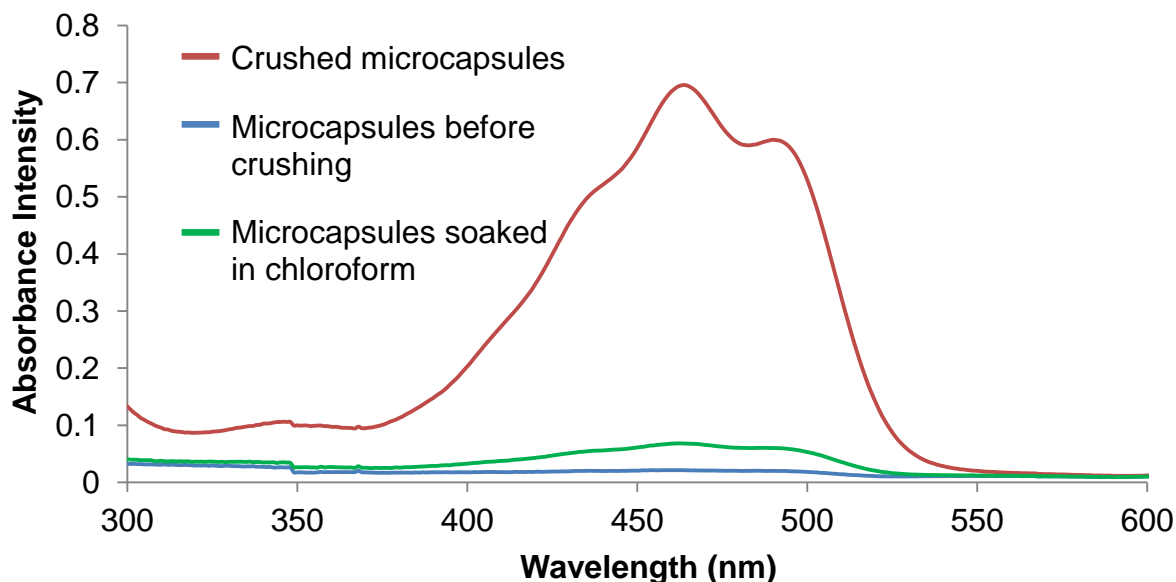


Figure 3.21. UV spectra of microcapsules before and after crushing and microcapsules soaked in chloroform for 1 hour.

3.3. Conclusion

IPDI has been contained successfully within polyurethane microcapsules that contain thermally-labile oxime-urethane bonds within the polymer of the microcapsule shell wall. Spectroscopic analysis of the encapsulated core has confirmed the presence of the active isocyanate crosslinker. The mechanical strength of the generated microcapsules is dependent on the nature of the shell wall precursor, in particular benzophenone oxime and IPDI based shell wall precursor led to the formation of structurally weak microcapsules. The successful release of the microencapsulated core was demonstrated using heat as the stimulus and the potential of these microcapsules to deliver IPDI in order to cure a non-energetic HTPB formulation that is analogous to Rowanex 1100 1A was investigated. The physical properties of microcapsules can be controlled by modification of the reaction parameters. Microcapsule diameter can be controlled by rate of agitation, surfactant concentration and selection of the hydrophobic solvent. Microcapsule shell wall thickness can also be controlled by increasing the concentration of the shell wall precursor and reaction

time. In addition, the maximum amount of IPDI that can be encapsulated has been investigated. The permeability of the microcapsule shell wall has been reduced by increasing the concentration of the diol chain extender. The encapsulation of a red dye, β -carotene has been achieved and the generated microcapsules have demonstrated how UV spectroscopy can be employed to quantify the microcapsule core. This will allow quantification of the release of the core contents of microcapsules that respond to a stimulus of heat in future investigations of this microcapsule technology.

3.4. Experimental

Chemicals. All chemicals and reagents were purchased from Sigma Aldrich with the exception of hydroxy-terminated polybutadiene (HTPB) (Mn 2800, \bar{D} 2.5) and dibutyltin dilaurate (DBTDL) which was provided by BAE Systems plc. Cyclohexanone was purified by vacuum distilling from CaH_2 (40 °C, 0.1 mmHg). All other chemicals were used as supplied without further purification.

Equipment. All experimental techniques employed in this chapter are identical to those described in **Chapter 2** with the exception of the following. Ultraviolet-visible spectroscopic analysis was carried out using a Cary 300 Bio UV-vis spectrophotometer. Optical microscopy was carried out using a Leica DM2500M optical microscope employing a Mettler Toledo FP82HT hot stage and images were recorded using an Infinity 1 digital camera. Samples analysed using electron microscopy were first coated with a layer of gold using an Edwards Sputter Coater S150B and then imaged using an FEI Quanta FEG 600 Environmental Scanning Electron Microscope operating under a high vacuum (0.45 torr). SEM images of microcapsule cross-sections were obtained by first embedding samples in Agar 100 epoxy resin and cured at 70 °C for 48 hours. Thin sections were prepared using a Reichert-Jung Ultracut microtome employing a glass knife and imaged using an FEI Quanta FEG 600 Environmental Scanning Electron Microscope operating in a thin aqueous atmosphere (0.68 torr).

Synthesis of Thermally-Releasable Microcapsules

The general procedure described below describes the synthesis of polyurethane microcapsules that contain a thermally-labile oxime-urethane bond in the shell wall of

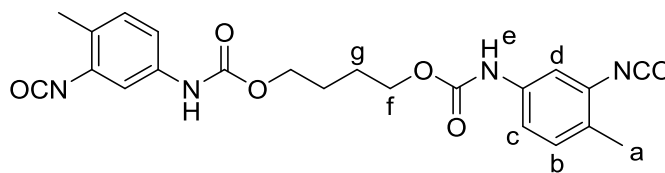
the microcapsule. A list of microcapsules synthesised using **3.1a-3.1h** is detailed in Table 3.8.

Gum arabic (9 g) was dispersed in H₂O (60 mL) in a 150 mL beaker with the aid of mechanical agitation at a rate of 1000 rpm. Shell wall precursor **2.5b** (0.104 g, 0.11 mmol) and IPDI (0.12 g, 0.54 mmol) were dissolved in ethyl phenylacetate (0.14 mL). This solution was added to the aqueous solution and the resultant emulsion heated to 70 °C at a rate of 10 °C/minute. When the temperature reached 50 °C, 1,4-butanediol (5.2 g, 56.6 mmol) was added and agitated at the same rate for an additional 30 seconds. Agitation was reduced to a rate of 150 rpm for 45 minutes at 70 °C followed by a further 2 hours at room temperature. After this period, agitation was ceased, H₂O (100 mL) was added and the generated microcapsules allowed to settle at the bottom of the beaker over a period of 1 hour at room temperature. The aqueous solution was decanted to leave polyurethane microcapsules **3.1b** that were collected by vacuum filtration, washed with H₂O and then air dried for a period of 48 hours (0.153 g). FTIR (ATR) ν (cm⁻¹): 3368 (N-H), 2256 (NCO), 1734 (C=O), 1540 (C-N), 1034 (C-O).

Table 3.8. list of conditions used for the synthesis of microcapsules **3.1a-3.1h**

Microcapsules	Shell Wall Precursor	IPDI (g)	Solvent	Yield (g)
3.1a	2.5a (0.900 g)	-	1,2-dichlorobenzene (1.6 mL)	0.714
3.1b	2.5b (0.104 g)	0.12	ethyl phenylacetate (0.14 mL)	0.153
3.1e	2.5e (0.126 g)	0.12	ethyl phenylacetate (0.14 mL)	0.180
3.1f	2.5f (0.110 g)	0.12	ethyl phenylacetate (0.14 mL)	0.112
3.1g	2.5g (0.100 g)	0.12	ethyl phenylacetate (0.14 mL)	0.213
3.1h	2.5h (0.875 g)	1.10	ethyl phenylacetate (0.90 mL)	-

Synthesis of Shell Wall Precursor **3.2**¹⁷



Toluene-2,4-diisocyanate (6.07 g, 35 mmol) was dissolved in cyclohexanone (19 mL). 1,4-Butanediol (9.15 g, 10 mmol) was added and the solution stirred for a period of 18 hours at 80 °C under argon. Cyclohexanone and excess toluene-2,4-diisocyanate were then removed by vacuum distillation (120 °C, 1 mmHg) over a period of 4 hours to leave a viscous dark yellow oil **3.2** (4.24 g, 97 %). ¹H NMR (400 MHz, CDCl₃) δ_H (ppm): 1.79 (4H, m, H_g), 2.30 (6H, s, H_a), 4.22 (4H, m, H_f), 7.01 (2H, app. d *J* = 9.0 Hz, H_b), 7.09 (2H, app. dd *J* = 8.0, 2.0 Hz, H_c), 7.23 (2H, app d *J* = 2.0 Hz, H_d); ¹³C NMR (100 MHz, CDCl₃) δ_C (ppm): 17.6, 26.4, 65.1, 115.5, 116.8, 127.5, 131.6, 133.3, 139.3, 154.5, 206.2; FTIR (ATR) ν (cm⁻¹): 3304 (N-H), 2955 (C-H), 2256 (NCO), 1701 (C=O), 1518 (C-N), 1062 (C-O); ESIMS of **3.2** derivative from its reaction with methylamine, calculated mass (C₂₄H₃₃O₆N₆)⁺ 501.2456 found 501.2452.

Microencapsulation of Isophorone Diisocyanate

The general procedure described below describes the synthesis of polyurethane microcapsules containing IPDI. A list of microcapsules synthesised using different reaction conditions is detailed in Table 3.9.

Gum arabic (9 g) was dispersed in H₂O (60 mL) in a 150 mL beaker with the aid of mechanical agitation at a rate of 1000 rpm. Shell wall precursor **3.2** (1.90 g, 4.3 mmol) and IPDI (5.5 g, 24.7 mmol) were dissolved in chlorobenzene (5.5 mL). This solution was added to the aqueous solution and the resultant emulsion heated to 70 °C at a rate of 10 °C/minute. When the temperature reached 50 °C, 1,4-butanediol (5.2 g, 56.6 mmol) was added and agitated at the same rate for an additional 30 seconds. Agitation was reduced to a rate of 150 rpm for 45 minutes at 70 °C followed by a further 2 hours at room temperature. After this period, agitation was ceased, H₂O (100 mL) was added and the generated microcapsules allowed to settle at the bottom of the beaker over a period of 1 hour at room temperature. The aqueous solution was decanted to leave polyurethane microcapsules that were collected by vacuum

filtration, washed with H₂O and then air dried for a period of 48 hours (9.80 g). FTIR (ATR) ν (cm⁻¹): 3312 (N-H), 2256 (NCO), 1701 (C=O), 1518 (C-N), 1062 (C-O).

Microencapsulation of β -carotene and Isophorone Diisocyanate

Gum arabic (9 g) was dispersed in H₂O (60 mL) in a 150 mL beaker with the aid of mechanical agitation at a rate of 1000 rpm. Shell wall precursor **3.2** (0.350 g, 0.8 mmol), IPDI (1.10 g, 4.9 mmol) and β -carotene (0.040 g, 0.07 mmol) were dissolved in chlorobenzene (0.9 mL). This solution was added to the aqueous solution and the resultant emulsion heated to 70 °C at a rate of 10 °C/minute. When the temperature reached 50 °C, 1,4-butanediol (5.2 g, 56.6 mmol) was added and agitated at the same rate for an additional 30 seconds. Agitation was reduced to a rate of 150 rpm for 45 minutes at 70 °C followed by a further 2 hours at room temperature. After this period, agitation was ceased, H₂O (100 mL) was added and the generated microcapsules allowed to settle at the bottom of the beaker over a period of 1 hour at room temperature. The aqueous solution was decanted to leave polyurethane microcapsules that were collected by vacuum filtration, washed with H₂O and then air dried for a period of 48 hours (1.99 g). FTIR (ATR) ν (cm⁻¹): 3302 (N-H), 2252 (NCO), 1704 (C=O), 1530 (C-N), 1067 (C-O).

Table 3.9. List of conditions used to synthesise microcapsules.

Agitation rate (rpm)	Shell wall precursor conc. (wt. %)	Chain extender concentration (mol dm ⁻³)	Solvent	IPDI concentration (vol. %)	Surfactant conc. (wt. %)	Reaction temperature (°C)	Reaction time (minutes)
500	18.0	0.06	Chlorobenzene	26	11.0	70	165
750	18.0	0.06	Chlorobenzene	26	11.0	70	165
1000	18.0	0.06	Chlorobenzene	26	11.0	70	165
1250	18.0	0.06	Chlorobenzene	26	11.0	70	165
1500	18.0	0.06	Chlorobenzene	26	11.0	70	165
1750	18.0	0.06	Chlorobenzene	26	11.0	70	165
2000	18.0	0.06	Chlorobenzene	26	11.0	70	165
1000	13.0	0.06	Chlorobenzene	26	11.0	70	165
1000	28.0	0.06	Chlorobenzene	26	11.0	70	165
1000	35.0	0.06	Chlorobenzene	26	11.0	70	165
1000	52.0	0.06	Chlorobenzene	26	11.0	70	165
1000	68.0	0.06	Chlorobenzene	26	11.0	70	165
1000	18.0	0.28	Chlorobenzene	26	11.0	70	165
1000	18.0	0.65	Chlorobenzene	26	11.0	70	165
1000	18.0	0.94	Chlorobenzene	26	11.0	70	165
1000	18.0	1.14	Chlorobenzene	26	11.0	70	165
1000	24.0	0.94	Dichlorobenzene	47	15.0	70	165
1000	24.0	0.94	Trichlorobenzene	47	15.0	70	165

Agitation rate (rpm)	Shell wall precursor conc. (wt. %)	Chain extender concentration (mol dm ⁻³)	Solvent	IPDI concentration (vol. %)	Surfactant conc. (wt. %)	Reaction temperature (°C)	Reaction time (minutes)
1000	24.0	0.94	Phenyl acetate	47	15.0	70	165
1000	24.0	0.94	Ethyl phenylacetate	47	15.0	70	165
1000	18.0	0.94	Chlorobenzene	0.0	15.0	70	165
1000	18.0	0.94	Chlorobenzene	11.0	15.0	70	165
1000	18.0	0.94	Chlorobenzene	26.0	15.0	70	165
1000	18.0	0.94	Chlorobenzene	42.0	15.0	70	165
1000	18.0	0.94	Chlorobenzene	53.0	15.0	70	165
1000	18.0	0.94	Chlorobenzene	63.0	15.0	70	165
1000	18.0	0.94	Chlorobenzene	79.0	15.0	70	165
1000	18.0	0.94	Chlorobenzene	89.0	15.0	70	165
1000	18.0	0.94	Chlorobenzene	100.0	15.0	70	165
1000	18.0	0.94	Chlorobenzene	53	5.0	70	165
1000	18.0	0.94	Chlorobenzene	53	10.0	70	165
1000	18.0	0.94	Chlorobenzene	53	20.0	70	165
1000	18.0	0.94	Chlorobenzene	53	25.0	70	165
1000	18.0	0.94	Chlorobenzene	53	15.0	70	45
1000	18.0	0.94	Chlorobenzene	53	15.0	70	75
1000	18.0	0.94	Chlorobenzene	53	15.0	70	105
1000	18.0	0.94	Chlorobenzene	53	15.0	70	135

3.5. References

- 1 T. Ohtsubo, S. Tsuda and K. Tsuji, *Polymer*, 1991, **32**, 2395-2399.
- 2 A. N. Zelikin, J. F. Quinn and F. Caruso, *Biomacromolecules*, 2006, **7**, 27-30.
- 3 N. Fomina, C. McFearin, M. Sermsakdi, O. Edigin and A. Almutairi, *J. Am. Chem. Soc.*, 2010, **132**, 9540-9542.
- 4 M. R. Böhmer, C. H. T. Chlon, B. I. Raju, C. T. Chin, T. Shevchenko and A. L. Klibanov, *J. Control. Release*, 2010, **148**, 18-24.
- 5 L. Chu, S. Park, T. Yamaguchi and S. Nakao, *Langmuir*, 2002, **18**, 1856-1864.
- 6 R. Arshady, *Polym. Eng. Sci.*, 1989, **29**, 1746-1758.
- 7 P. B. O'Donnell and J. W. McGinty, *Adv. Drug Deliver. Rev.*, 1997, **28**, 25-42.
- 8 T. M. Chang, *Science*, 1964, **146**, 524-525.
- 9 A. Gharsallaoui, G. Roudaut, O. Chambin, A. Voilley and R. Saurel, *Food Res. Int.*, 2007, **40**, 1107-1121.
- 10 A. P. R. Johnston, C. Cortez, A. S. Angelatos and F. Caruso, *Curr. Opin. Colloid In.*, 2006, **11**, 203-209.
- 11 N. Elvassore and A. Bertucco, *Ind. Eng. Chem. Res.*, 2001, **40**, 795-800.
- 12 Y. Senuma, C. Lowe, Y. Zweifel, J. G. Hilborn and I. Marison, *Biotechnol. Bioeng.*, 2000, **67**, 616-622.
- 13 G. T. Vladislavljević and R. A. Williams, *Adv. Colloid Interface Sci.*, 2005, **113**, 1-20.
- 14 M. V. Sefton and W. T. K. Stevenson, *Adv. Polym. Sci.*, 1993, **107**, 143-197.
- 15 P. Rambourg, J. Lévy and M. C. Lévy, *J. Pharm. Sci.*, 1982, **71**, 753-758.
- 16 K. Dietrich, H. Herma, R. Nastke, E. Bonatz and W. Teige, *Acta Polym.*, 1989, **40**, 243-251.
- 17 M. E. Budd, MSc Thesis, *Microencapsulation Approach for use in Delayed Quick Cure Munitions*, University of Reading, 2013.
- 18 J. L. Yang, M. R. Kessler, J. S. Moore, S. R. White and N. R. Sottos, *Macromolecules*, 2008, **41**, 9650-9655.
- 19 C. Perignon, G. Ongmayeb, R. Neufeld, Y. Frere and D. Poncelet, *J. Microencapsul.*, 2014, **32**, 1-15.
- 20 Y. Zhang and D. Rochefort, *J. Microencapsul.*, 2012, **29**, 636-649.
- 21 A. P. Esser-Khan, N. R. Sottos, S. R. White and J. S. Moore, *J. Am. Chem. Soc.*, 2010, **132**, 10266–10268.

- ²² I. Yamamoto, T. Furukawa, H. Nakajima and H. Gotoh, *J. Chem. Soc. Perkin Trans. 1*, 1976, 1597-1602.
- ²³ W. Chen, X. Liu and D. W. Lee, *J. Mater. Sci.*, 2012, **47**, 2040-2044.
- ²⁴ M. M. Caruso, B. J. Blaisik, H. Jin, S. R. Schelkopf, D. S. Stradley, N. R. Sottos, S. R. White and J. S. Moore, *ACS Appl. Mater. Interface.*, 2010, **2**, 1195-1199.
- ²⁵ L. Gonzalez, M. Kostrzewska, M. Baoguang, L. Li, J. H. Hansen, S. Hvilsted and A. L. Skov, *Macromol. Mater. Eng.*, 2014, **299**, 1259-1267.
- ²⁶ H. Yi, Y. Yang, X. Gu, J. Huang and C. Wang, *J. Mater. Chem. A*, 2015, **3**, 13749-13757.
- ²⁷ C. P. Chang, J. C. Chang, K. Ichikawa, T. Dobashi, *Colloid. Surface. B*, 2005, **44**, 187-190.
- ²⁸ R. Arshady, *J. Microencapsul.*, 1989, **6**, 13-28.
- ²⁹ S. K. Ghosh, *Functional Coatings by Polymer Microencapsulation*, Wiley, Chichester, 2006.
- ³⁰ P. Ni, M. Zhang and N. Yan, *J. Membrane. Sci.*, 1995, **105**, 51-55.
- ³¹ M. Huang and J. Yang, *J. Mater. Chem.*, 2011, **21**, 11123-11130.
- ³² U. Paiphansiri, J. Dausend, A. Musyanovych, V. Mailänder and K. Landfester, *Macromol. Biosci.*, 2009, **9**, 575-584.
- ³³ H. Guo, X. Zhao and J. Wang, *J. Colloid Interf. Sci.*, 2005, **284**, 646-651.
- ³⁴ R. Heinrich, H. Frensch and K. Albrecht, US Patent, *Pressure-resistant polyurethane-polyurea particles for the encapsulation of active ingredients and process for their manufacture*, 1980, 4 230 809.
- ³⁵ F. Saluan, E. Devaux, S. Bourbigot and P. Rumeau, *C. Eng. J.*, 2009, **155**, 457-465.
- ³⁶ S. Alexandridou, C. Kiparissides, F. Mange and A. Foissy, *J. Microencapsul.*, 2001, **18**, 767-781.
- ³⁷ J. J. Jasper, *J. Phys. Chem. Ref. Data*, 1972, **1**, 841-1009.
- ³⁸ L. Groenendaal, F. Jonas, D. Freitag, H. Pielartzik and J. R. Reynolds, *Adv. Mater.*, 2000, **7**, 3317-3319.
- ³⁹ E. Jabbari and M. Khakpour, *Biomaterials*, 2000, **21**, 2073-2079.
- ⁴⁰ S. Lee and D. Randall, *The Polyurethanes Book*, Wiley, Chichester, 2002.

Chapter 4

Exploiting Reversible Diels-Alder Adducts in the Design of Thermally-Releasable Microcapsules

Abstract

The crosslinking of polyurethane matrices used to bind explosives can be controlled by employing microcapsules that release the crosslinker from its core upon the application of a stimulus. Such stimuli include - pressure, ultrasound, chemical change, light and heat. The release of a substrate from microcapsules can be achieved by incorporating thermally-reversible bonds within the polymer of the shell wall. The Diels-Alder reaction involves the [4+2] cycloaddition of a conjugated diene and a substituted alkene and certain Diels-Alder adducts, such as maleimide-furans undergo the reverse reaction - the retro-Diels-Alder process - when exposed to elevated temperatures. This chapter describes the design and synthesis of polyurethane microcapsules that contain thermally-reversible Diels-Alder adducts within the polymer of the shell wall. The release of crosslinkers from such microcapsules using a heat stimulus is demonstrated showing the potential for such systems to be used in the controlled crosslinking of hydroxy-functionalised polymers used to bind explosives.

4.1. Introduction

The manufacture of plastic or polymer bonded explosives (PBX) involves the addition of an isocyanate crosslinker to a mixture of the explosive and a hydroxy-functionalised polymer. This process exhibits poor control of the crosslinking reaction and can lead to several detrimental processes that can lead to wasting of the hazardous material. Control of the crosslinking and more reliable production of PBX could be achieved by employing microcapsules that release the crosslinker from its core upon the application of a thermal stimulus.

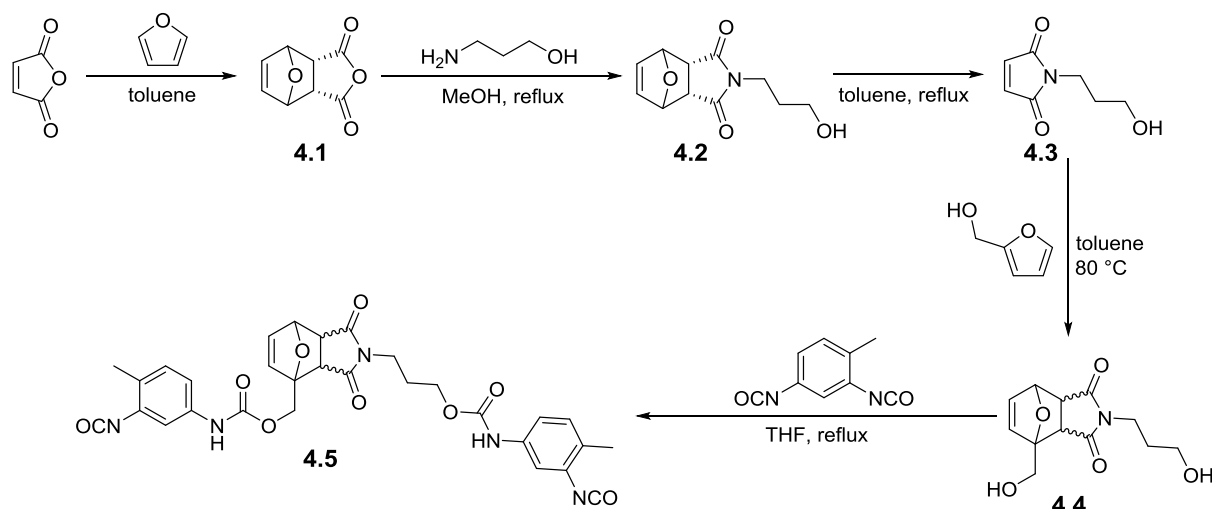
Chapter 2 and **3** describes the synthesis of polyurethane microcapsules that release their core contents upon exposure to a heat stimulus. This was achieved by incorporating thermally-labile oxime-urethane bonds within the polymeric shell of the microcapsule. However, it was important to investigate other thermally-reversible bonds that could also be used in the delivery of crosslinkers using microencapsulation technology.

Conjugated dienes and substituted alkenes can undergo a [4+2] cycloaddition to form a cyclic adduct.¹ This reaction is known as the Diels-Alder reaction and many adducts are able to undergo the reverse, retro-Diels-Alder reaction under certain conditions including elevated temperature.^{2,3}

One such adduct, maleimide-furan exhibits this reversible nature when exposed to heat (>80 °C).⁴ This character has been exploited for use in healable materials,⁵ degradable crosslinks⁶ and controlled release of substrates such as pharmaceuticals from polymeric delivery systems.^{7,8} In addition, Diels-Alder linkages have been incorporated⁹ into the shell wall of microcapsules prepared using a complex coacervation technique. However, to date polyurethane microcapsules have not been synthesised using an interfacial polymerisation technique that incorporates thermally-reversible Diels-Alder linkers within the microcapsule shell.

4.2. Results and Discussion

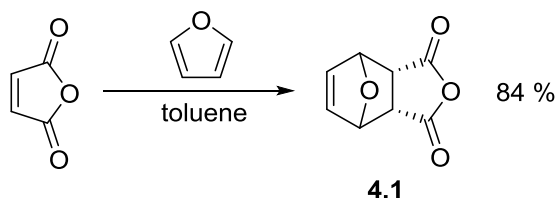
In order to synthesise such polyurethane microcapsules, first the preparation of an isocyanate-terminated shell wall precursor containing a Diels-Alder adduct was required. The synthetic approach initially involved the protection of maleic anhydride with furan to form a Diels-Alder adduct **4.1**. The reaction of this adduct with 3-amino-1-propanol to yield the alcohol **4.2** followed by deprotection afforded a hydroxy-functionalised maleimide **4.3**. A Diels-Alder reaction of **4.3** with furfuryl alcohol to yield the cycloadduct **4.4** followed by reaction with excess toluene-2,4-diisocyanate (TDI) led to the formation of an isocyanate-terminated shell wall precursor **4.5** capable of further chain extension to form polyurethane microcapsules (Scheme 4.1).



Scheme 4.1. Reaction scheme for the synthesis of a shell wall precursor **4.5** that incorporates a thermally-reversible Diels-Alder adduct.

4.2.1. Protection of Maleic Anhydride with Furan

The first step of the synthesis of the shell wall precursor **4.5** involved the protection of maleic anhydride with furan to form a Diels-Alder adduct **4.1**. This protection was necessary in order to prevent undesired Michael addition upon the required conversion of the anhydride to a maleimide (Scheme 4.2).



Scheme 4.2. Reaction of maleic anhydride and furan to form a Diels-Alder adduct **4.1**.

Maleic anhydride and excess furan were mixed in toluene for a period of 72 hours at room temperature. Removal of toluene and excess furan *in vacuo* afforded the desired product without the need for further purification. The protected maleic anhydride was analysed with a range of analytical techniques including ^{13}C NMR spectroscopy. The presence of resonances corresponding to the four different environments of carbon at 48.7, 82.2, 137.0 and 169.9 ppm were observed in the spectrum (Figure 4.1).

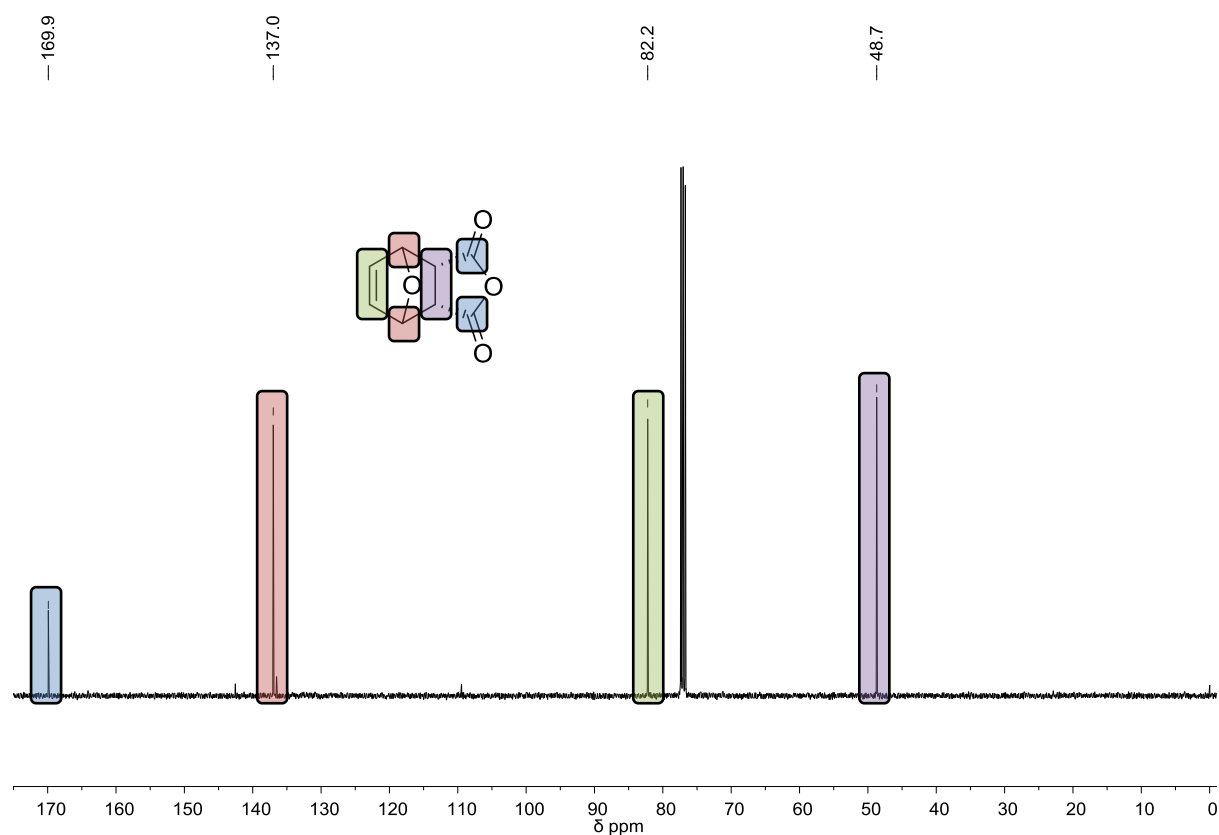
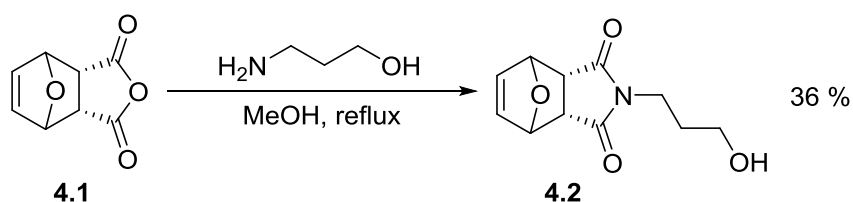


Figure 4.1. ^{13}C NMR spectrum of **4.1** highlighting key resonances at 48.7, 82.2, 137.0 and 169.9 ppm in CDCl_3 .

4.2.2. Conversion of Protected Maleic Anhydride to Maleimide

The second step of the synthesis involved the conversion of the protected maleic anhydride with 3-amino-1-propanol to the corresponding maleimide **4.2**. The superior nucleophilic nature of the amino-terminus of 3-amino-1-propanol allowed the generation of the desired maleimide whilst avoiding the formation of an ester (Scheme 4.3).



Scheme 4.3. Reaction of Diels-Alder adduct **4.1** with 3-amino-1-propanol to form the corresponding maleimide **4.2**.

The protected maleic anhydride was refluxed with 3-amino-1-propanol in MeOH to give the desired maleimide. Following purification using column chromatography, the product was analysed with FTIR spectroscopy. A broad absorbance corresponding to the newly formed hydroxy moiety was observed at 3516 cm^{-1} . Further notable absorptions corresponding to the carbonyl and C-N functionalities were also observed at 1692 and 1160 cm^{-1} , respectively (Figure 4.2).

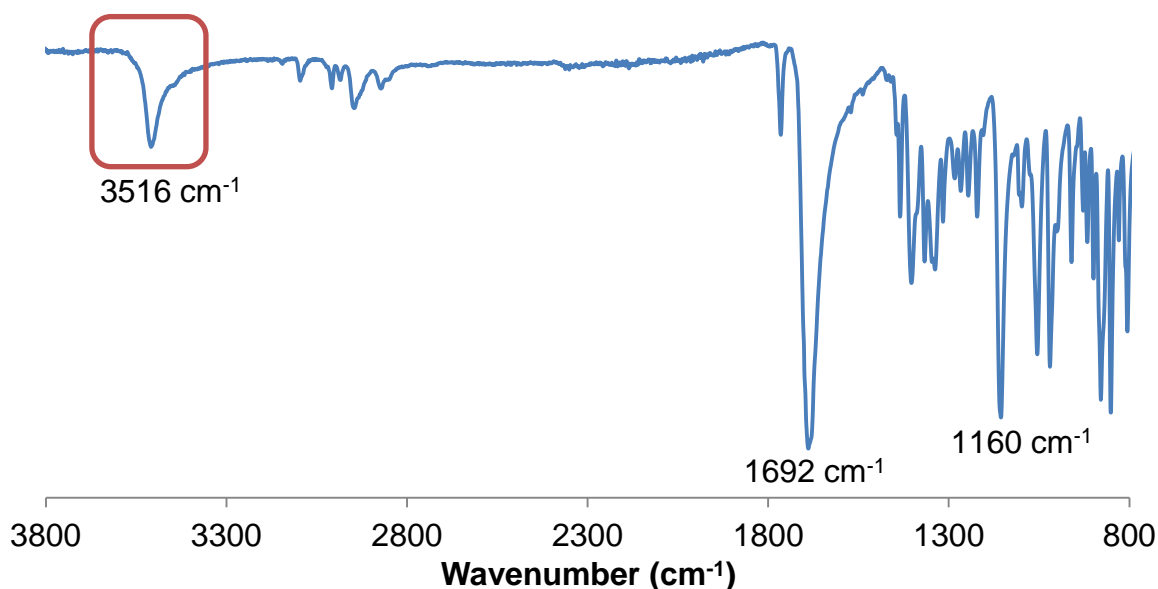
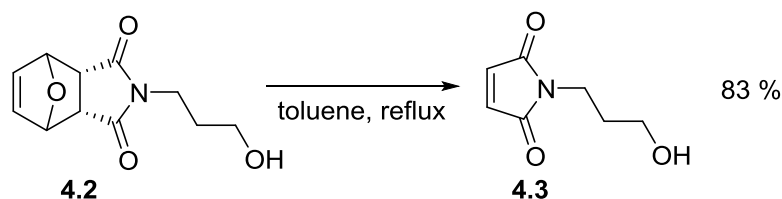


Figure 4.2. FTIR spectrum of maleimide **4.2** highlighting the key absorbance at 3516 cm^{-1} corresponding to the hydroxy moiety. Further notable resonances at 1692 and 1160 cm^{-1} corresponding to C=O and C-N moieties are also observed.

4.2.3. Deprotection to form Hydroxy-Functionalised Maleimide

The deprotection of **4.2** could be achieved easily by exploiting the thermally-reversible nature of Diels-Alder adducts. By maintaining a solution of **4.2** in toluene under reflux it was demonstrated that the retro-Diels-Alder reaction could be triggered to afford the desired maleimide **4.3**. The reaction temperature used exceeded the boiling point of furan, thus the protecting group was removed during the ensuing reaction and minimal workup was required to isolate **4.3** (Scheme 4.4).



Scheme 4.4. Deprotection of maleimide-furan **4.2** to form maleimide **4.3**.

Deprotection of **4.2** was achieved after exposure to toluene under reflux for 7 hours. The solvent was removed *in vacuo* to leave the desired maleimide **4.3** without the need for further purification. Resonances observed using ^1H NMR spectroscopy confirmed that the deprotection had been successful, notably the key resonance at 6.74 ppm corresponding to the formed alkene protons (Figure 4.3).

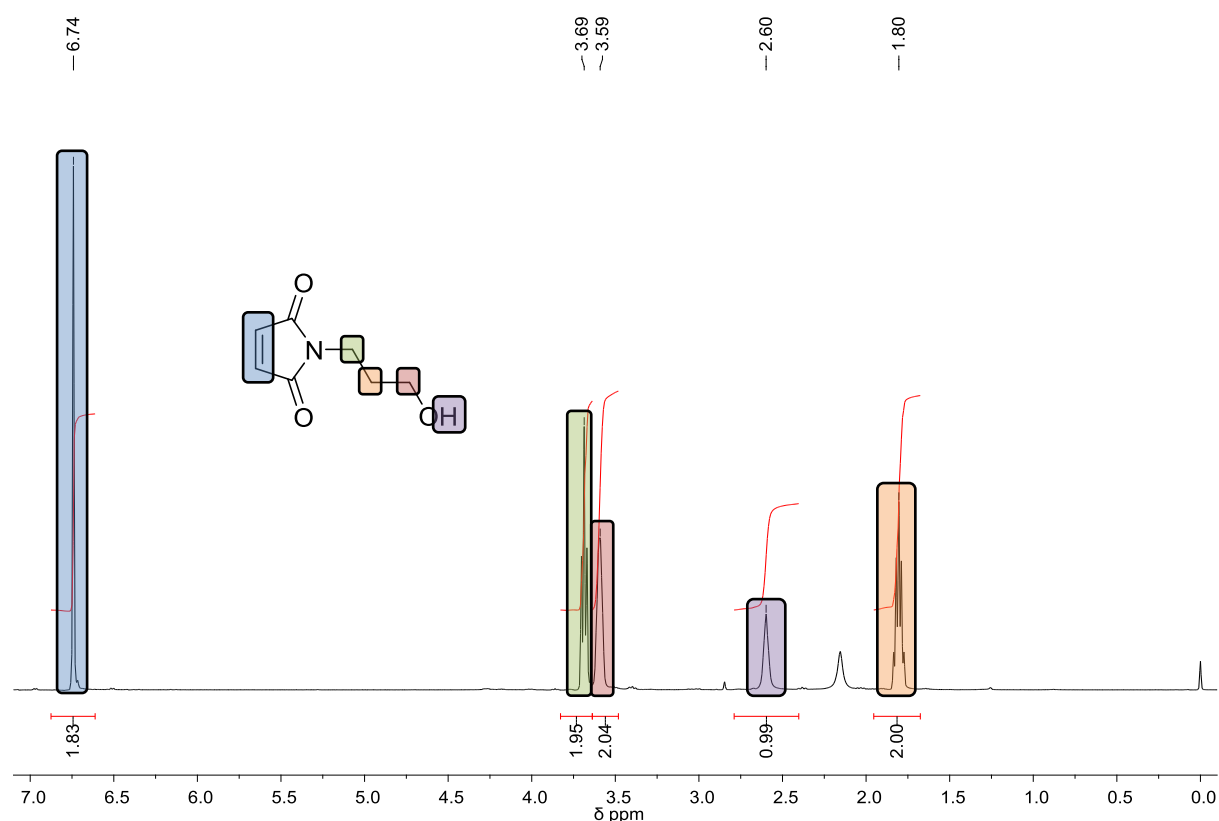
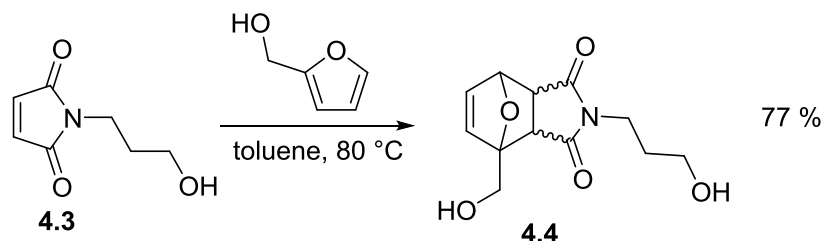


Figure 4.3. ^1H NMR spectrum of maleimide **4.3** highlighting the key resonances in CDCl_3 .

4.2.4. Diels-Alder Reaction of Maleimide and Furfuryl Alcohol

In order to synthesise an isocyanate-terminated shell wall precursor, first it was necessary to generate a Diels-Alder adduct that possesses two hydroxy moieties **4.4** capable of reaction with TDI. This was achieved by the Diels-Alder reaction of **4.3** with furfuryl alcohol (Scheme 4.5).



Scheme 4.5. Reaction of maleimide **4.3** with furfuryl alcohol to form Diels-Alder adduct **4.4**.

The dihydroxy-functionalised Diels-Alder adduct was analysed with a range of analytical techniques including mass spectrometry. Mass spectrometry utilising electrospray ionisation was employed and mass ions at 254.1025 and 276.0844 were observed, corresponding to the protonated $(C_{12}H_{15}O_5N+H)^+$ and sodiated $(C_{12}H_{15}O_5N+Na)^+$ forms of the molecular ions of **4.4**, respectively (Figure 4.4).

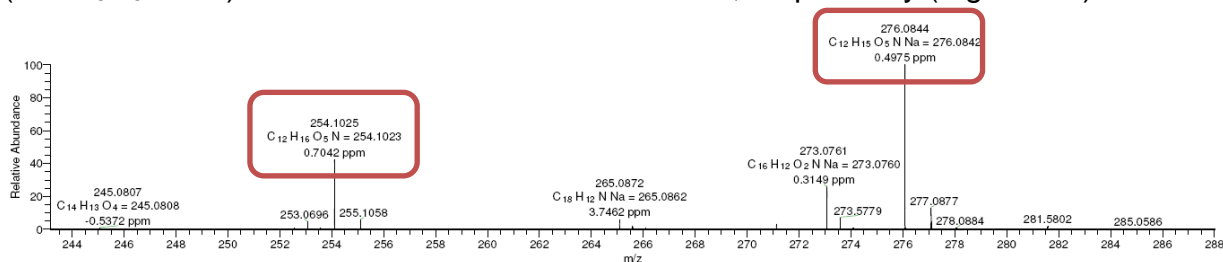
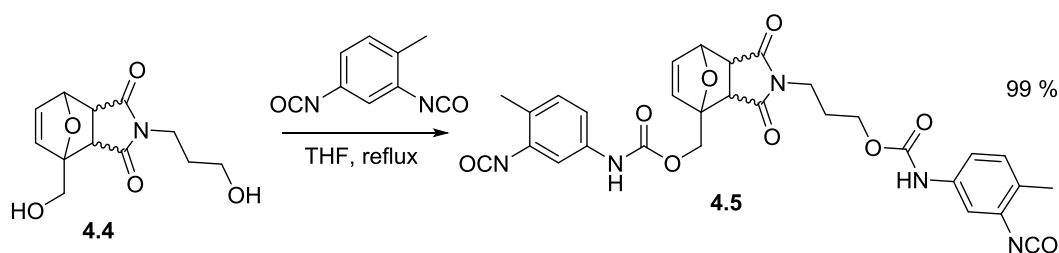


Figure 4.4. Mass spectrum highlighting mass ions at 254.1025 and 276.0844 corresponding to the protonated and sodiated forms of the molecular ions of **4.4**, respectively.

4.2.4. Synthesis of the Shell Wall Precursor

The shell wall precursor was generated by the reaction of Diels-Alder adduct **4.4** with an excess of TDI. Removal of the excess TDI by washing with cyclohexane at 80 °C left an isocyanate-terminated shell wall precursor **4.5** capable of further chain extension in order to form microcapsules (Scheme 4.6).



Scheme 4.6. Reaction of **4.4** with an excess of TDI to form shell wall precursor **4.5**.

Isocyanates possess a characteristic stretching vibration that appears as an absorption at $\sim 2250\text{ cm}^{-1}$ in an IR spectrum. Thus FTIR spectroscopy was employed to confirm the formation of the desired isocyanate-terminated shell wall precursor. Analysis indeed revealed the presence of a broad absorption at 2268 cm^{-1} corresponding to the isocyanate moiety (Figure 4.5).

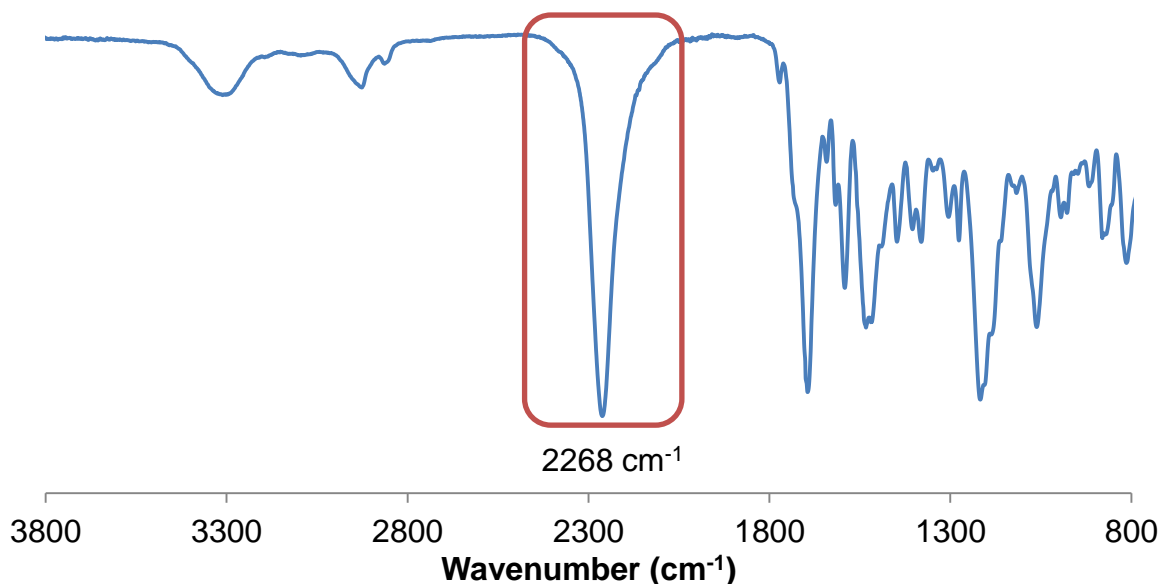


Figure 4.5. FTIR spectrum of **4.5** highlighting the absorbance at 2268 cm^{-1} corresponding to the isocyanate moiety.

It is possible that a polymerisation can occur in the reaction of **2.4** and TDI. The high molecular weight of the resulting oligomer can lead to poor solubility in the hydrophobic solvents employed in the synthesis of microcapsules. Thus it was important to determine the extent of chain extension. Mass spectrometry could not be performed on the isocyanate terminated shell wall precursor **4.5**, thus it was derivatised by reacting the isocyanate termini with MeOH to form the urethane analogue. Mass spectrometry of this derivative revealed a molecular ion with a mass of 688.2225 ($\text{C}_{32}\text{H}_{35}\text{O}_{11}\text{N}_5+\text{Na}$)⁺ confirming the desired shell wall precursor had been generated - mass of **4.5** = 601, mass of MeOH = 32, sodiated ion = 601 + 32 + 32 + 23 = 688.

In addition to mass spectrometry, the molecular weight of **4.5** was determined using end group analysis using titration. The shell wall precursor **4.5** was reacted with a known quantity of excess *n*-dibutylamine to form a urea. The resultant mixture was titrated with HCl (1M) using bromophenol blue as an indicator of the end point by a characteristic blue to yellow colour change. Employing Equation 4.1 allows the

determination of the quantity of isocyanate in the shell wall precursor and thus the molecular weight.

$$\text{NCO \%} = \left[\frac{(V_{\text{Blank}} - V_{\text{Sample}}) \times N \times 0.0420}{\text{Sample Mass}} \right] \times 100 \quad \text{Equation 4.1}$$

Where: V_{Blank} = blank titre, V_{Sample} = sample titre and N = normality of HCl.

Titration analysis revealed an isocyanate content of **4.5** of 12 %. Although comparison with the expected value, 14 %, suggests a small degree of polymerisation had occurred, in general the desired shell wall precursor had been afforded. In addition, the presence of excess TDI not removed during the workup procedure may have also prevented accurate measurement of the isocyanate content of **4.5**.

4.2.4. Dissociation of the Diels-Alder Adduct

^1H NMR spectroscopy was employed to investigate the potential of the maleimide-furan Diels-Alder adduct to dissociate upon exposure to heat. The dihydroxy-functionalised maleimide furan **4.4** was dissolved in deuterated DMSO (DMSO-d_6) and analysed using ^1H NMR spectroscopy before and after exposure to a temperature of $140\text{ }^\circ\text{C}$ for 15 minutes. Analysis revealed that after exposure to this temperature the Diels-Alder adduct had almost completely dissociated regenerating the maleimide and furan components (Figure 4.6).

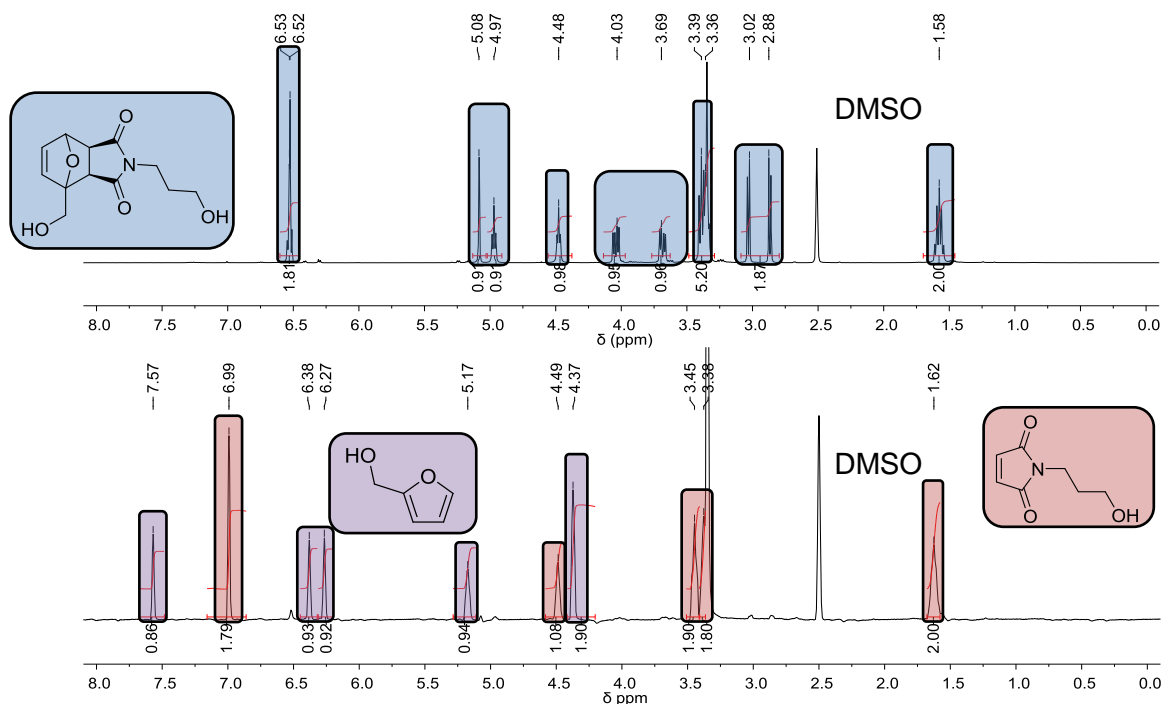


Figure 4.6. ^1H NMR spectra of maleimide-furan **4.4** before and after exposure to heat, regenerating the maleimide and furan components in DMSO-d_6 .

4.2.5. Synthesis of Microcapsules

The microencapsulation of isophorone diisocyanate (IPDI) crosslinkers in polyurethane microcapsules **4.6** using the shell wall precursor containing a thermally reversible Diels-Alder adduct **4.5** employed an interfacial polymerisation technique similar to that described in **Chapter 3**. The shell wall precursor **4.5** and IPDI were dissolved in a hydrophobic solvent, *o*-methoxyacetophenone and emulsified in a surfactant solution of gum arabic with the aid of mechanical agitation. Upon the addition of a water soluble chain extender, 1,4-butanediol, a reaction occurred at the oil-water interface to form a polyurethane shell that contained thermally-reversible Diels-Alder linkages. In addition to this polymerisation reaction, a host of other reactions are expected to occur. Water can react with the isocyanate to form a carbamic acid, decarboxylation of this leads to the formation of an amine which is in turn capable of reacting with further isocyanate to form a urea. In addition, crosslinking reactions between isocyanate and urea and urethane can form biuret and allophanate bonds (Figure 4.7). The generated microcapsules were isolated from the polymerisation medium by filtration, followed by washing with water and then allowed to air dry for 48 hours prior to analysis.

The properties of the microcapsules were assessed using a range of analytical techniques including - optical microscopy, scanning electron microscopy, FTIR spectroscopy and ¹H NMR spectroscopy.

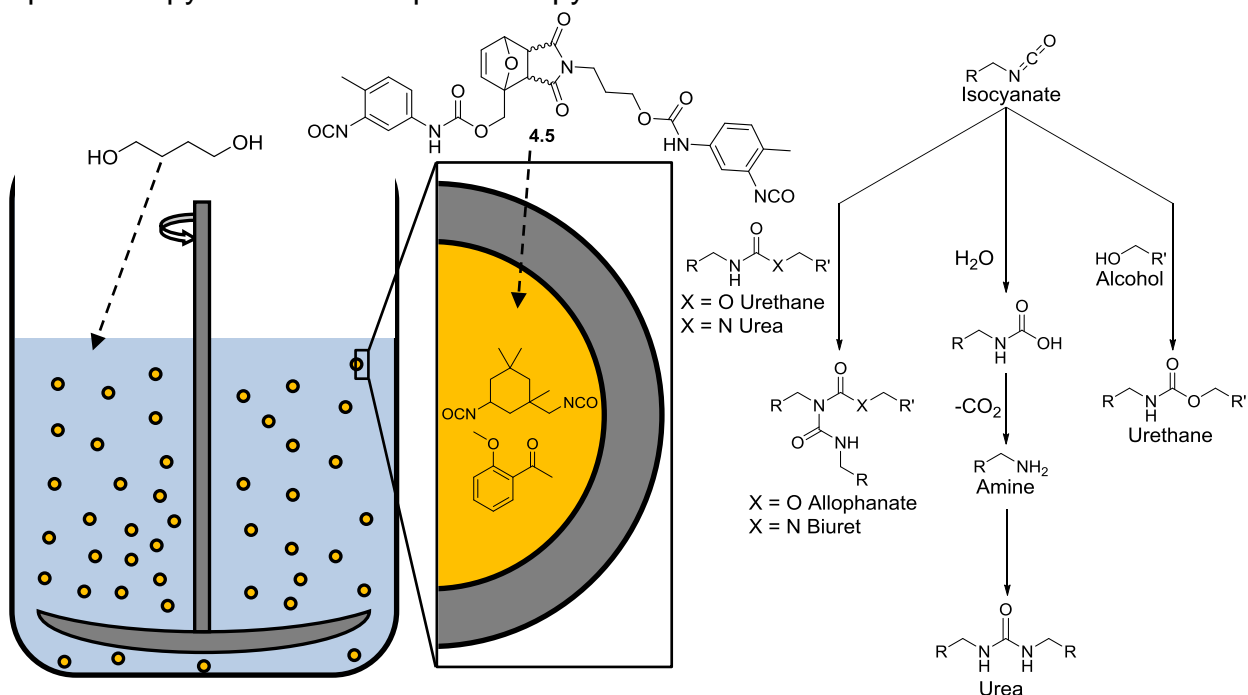


Figure 4.7. Interfacial polymerisation technique to synthesise the microcapsules incorporating a thermally-reversible Diels-Alder adduct in the shell walls and a core of IPDI.

4.2.6. Optical Microscopic Analysis of Microcapsules

The successful microencapsulation of a liquid core can be confirmed using optical microscopy. In addition, analysis using optical microscopy also allows measurement of the microcapsule diameter. The synthesis of microcapsules using a shell wall precursor that contains a thermally-reversible Diels-Alder adduct within the polymer of the shell wall was successful. Crushing the microcapsules between two microscope slides revealed the release of a liquid core. However, the microcapsules exhibited poor mechanical strength and were easily ruptured with minimal force. The high steric hindrance of the shell wall precursor may have prevented the formation of a strong polymer shell and this observation is supported by results described in **Chapter 3**. In addition, the non-linear structure of the shell wall precursor may have also contributed to the formation of a mechanically weak shell (Figure 4.8). The poor mechanical strength of the generated microcapsules demonstrates further optimisation of these initial studies is required.

Analysis of the microcapsule diameters revealed that the average diameter of the microcapsules was 76 μm within a range of 29-138 μm . This result is within the expected literature values for microcapsules synthesised at a rate of agitation of 1000 rpm.¹⁰

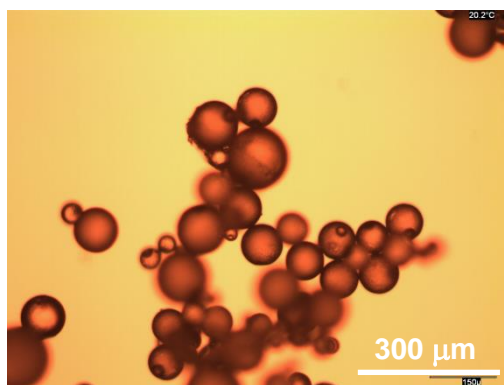


Figure 4.8. Optical microscopic image of microcapsules **4.6** synthesised using a shell wall precursor containing the thermally-reversible Diels-Alder adduct **4.5**.

4.2.7. Analysis of Microcapsules using Scanning Electron Microscopy

High resolution images of microcapsules can be obtained using scanning electron microscopy (SEM), thus providing detailed images of the internal and external microcapsule surface morphology. Microcapsules were analysed using an environmental scanning electron microscope operating in a thin aqueous atmosphere

(0.68 torr). Analysis revealed that spherical mononuclear microcapsules had been generated and they possessed a smooth external surface and a rough internal surface and this is in accordance with data in related literature studies.¹⁰ A sample of microcapsules was embedded in an epoxy resin and cross-sections prepared using an ultramicrotome employing a glass knife. The shell wall thickness of the microcapsules was measured in an environmental scanning electron microscope operating in a thin aqueous atmosphere (0.68 torr). An average shell wall thickness of 3.45 μm was observed, within the reported literature range of microcapsules prepared using an interfacial polymerisation technique (Figure 4.9).¹⁰

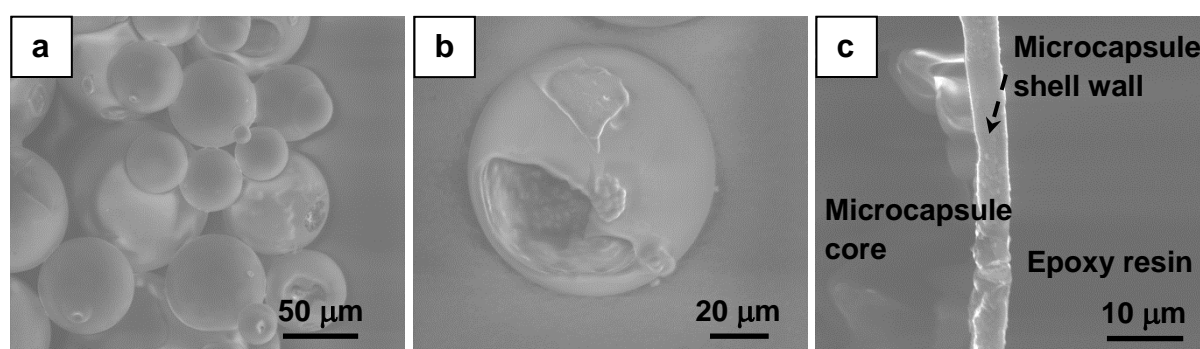


Figure 4.9. SEM images of a) microcapsules synthesised using a shell wall precursor containing a thermally-reversible Diels-Alder adduct b) internal surface morphology of a ruptured microcapsule c) cross-sectional image of a microcapsule highlighting the shell wall.

4.2.8. Analysis of Microencapsulated Core Using FTIR Spectroscopy

The delivery of active isocyanate crosslinkers is desired, thus it was important to confirm the successful encapsulation of the isocyanate functional group. Isocyanates possess a characteristic vibration that is observed as an absorbance $\sim 2250\text{ cm}^{-1}$ in an IR spectrum. Microcapsules were crushed and the released liquid core analysed using FTIR spectroscopy.¹¹

Indeed a broad absorption at 2255 cm^{-1} was observed corresponding to the isocyanate moiety of IPDI confirming the successful encapsulation of an isocyanate crosslinker in polyurethane microcapsules. Further absorbances were observed at 1706 and 1677 cm^{-1} corresponding to the urethane and maleimide carbonyl moieties, respectively (Figure 4.10).

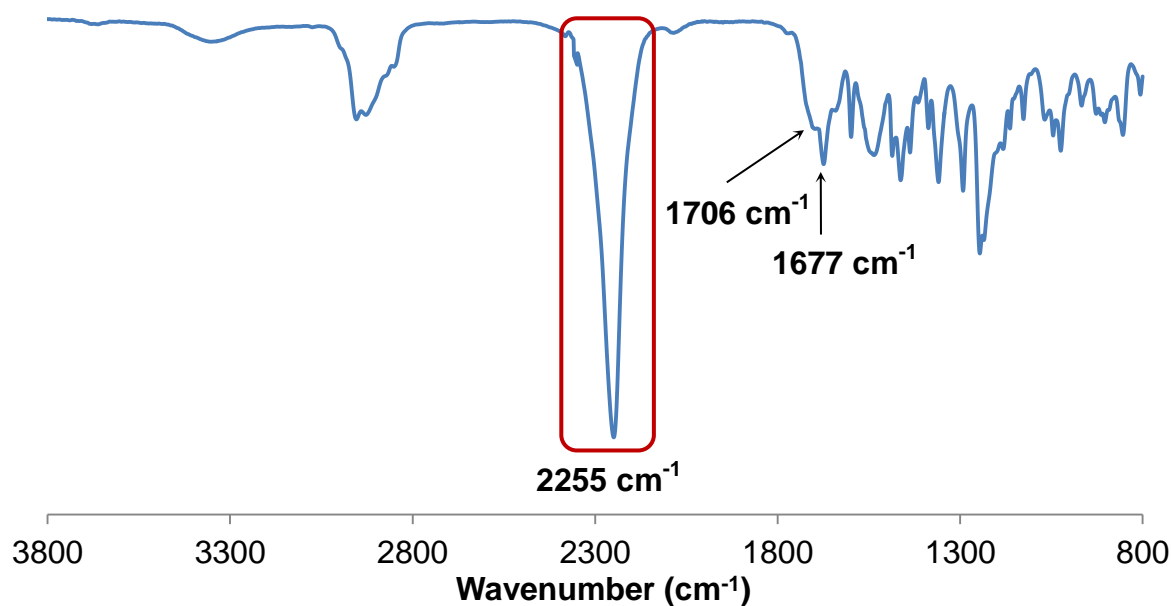


Figure 4.10. FTIR spectrum of microcapsule core, highlighting the absorption at 2255 cm⁻¹ corresponding to the isocyanate moiety of IPDI.

4.2.9. ¹H NMR Spectroscopic Analysis of the Microencapsulated Core

In addition to FTIR spectroscopy, the microcapsule core can also be analysed using ¹H NMR spectroscopy,¹² and allow the composition of the core to be determined. In addition, employing a known quantity of an internal standard can allow quantification of these components.

Microcapsules were crushed and the released core was washed with CDCl₃ and the washings analysed with ¹H NMR spectroscopy. The ¹H NMR spectrum was compared to spectra of IPDI and *o*-methoxyacetophenone and a clear overlap between the microcapsule core and the individual components was observed corroborating the observation *via* FTIR spectroscopic analysis of the successful microencapsulation of the active IPDI crosslinker (Figure 4.11).

Methyl 4-nitrobenzoate was employed as an internal standard since the resonances did not overlap with those of the microcapsule core components. Comparison of the integration of resonances of the internal standard at 8.23-8.29 with those of IPDI at 3.53-3.66 and *o*-methoxyacetophenone at 6.98 allowed the composition of the microcapsule core to be quantified. It was revealed the microcapsule core was composed of 40 wt. % IPDI and 10 wt. % of *o*-methoxyacetophenone. The quantity of IPDI encapsulated is within the expected values in accordance with results described in **Chapter 3**. In contrast only a small quantity of the solvent was encapsulated,

suggesting a large quantity was lost *via* evaporation during the microcapsule synthesis.

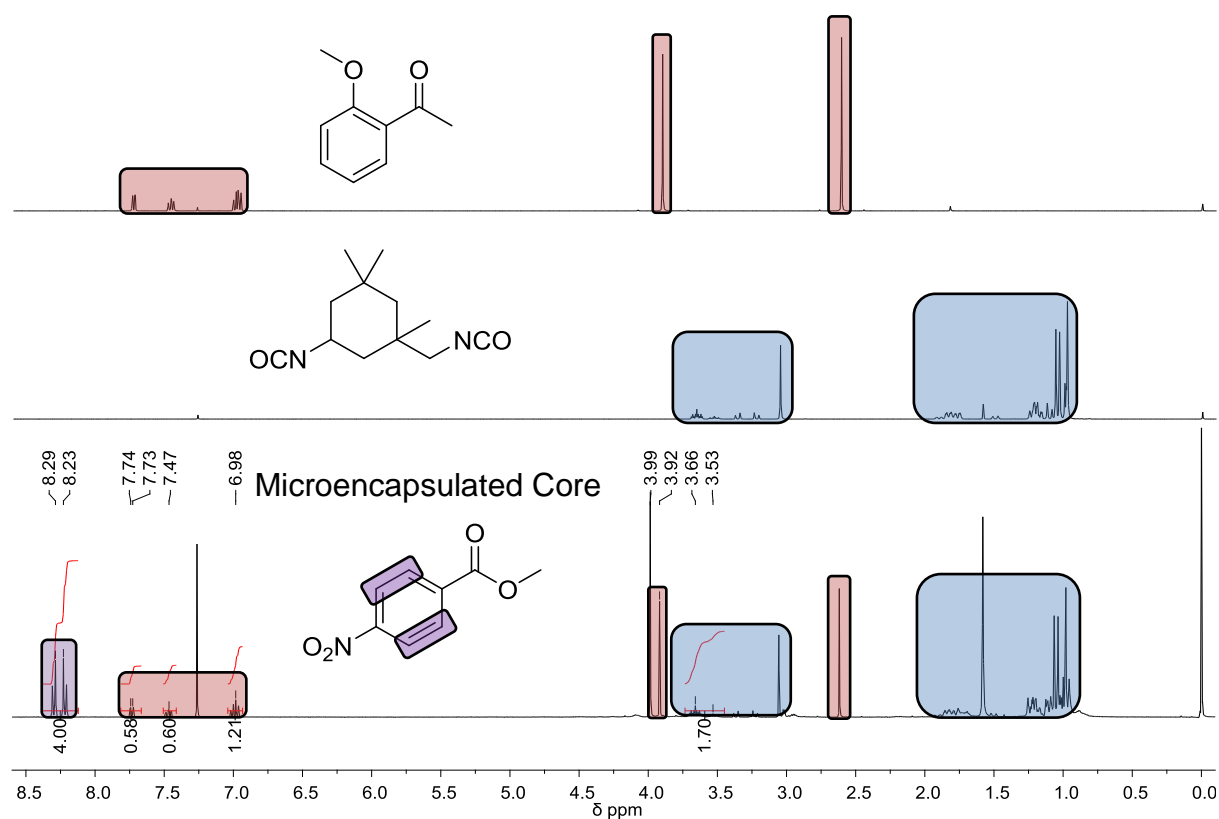


Figure 4.11. ^1H NMR spectra of *o*-methoxyacetophenone, IPDI and the released core of microcapsules including an internal standard in CDCl_3 .

4.2.10. Release of Microencapsulated Core Using a Heat Stimulus

A thermally-reversible maleimide-furan Diels-Alder adduct has been successfully incorporated into the polymer of the shell wall of microcapsules **4.6**. The capability of these microcapsules to release isocyanate crosslinkers upon exposure to a stimulus of heat was then investigated. Microcapsules were heated to 150 °C at a rate of 10 °C/minute using a hot stage mounted to an optical microscope and images recorded using a digital camera. In addition to optical microscopy, SEM images were obtained before and after heating.

Upon heating to 125 °C the shell wall of the microcapsules began to dissociate and shell wall breakdown occurred rapidly above this temperature reaching complete fracture of the shell wall and release of the core from the microcapsules by 140 °C. As expected, SEM analysis of the microcapsules after heating revealed the absence of spherical-shaped microcapsules suggesting complete dissociation of the microcapsules had been achieved (Figure 4.12). Microcapsules not containing a

thermally-reversible Diels-Alder adduct, designated as control microcapsules, were also heated to 140 °C. At this temperature the shells of the control microcapsules began to pucker, suggesting the core had leached from the microcapsules. However, dissociation of the shell wall was not observed.

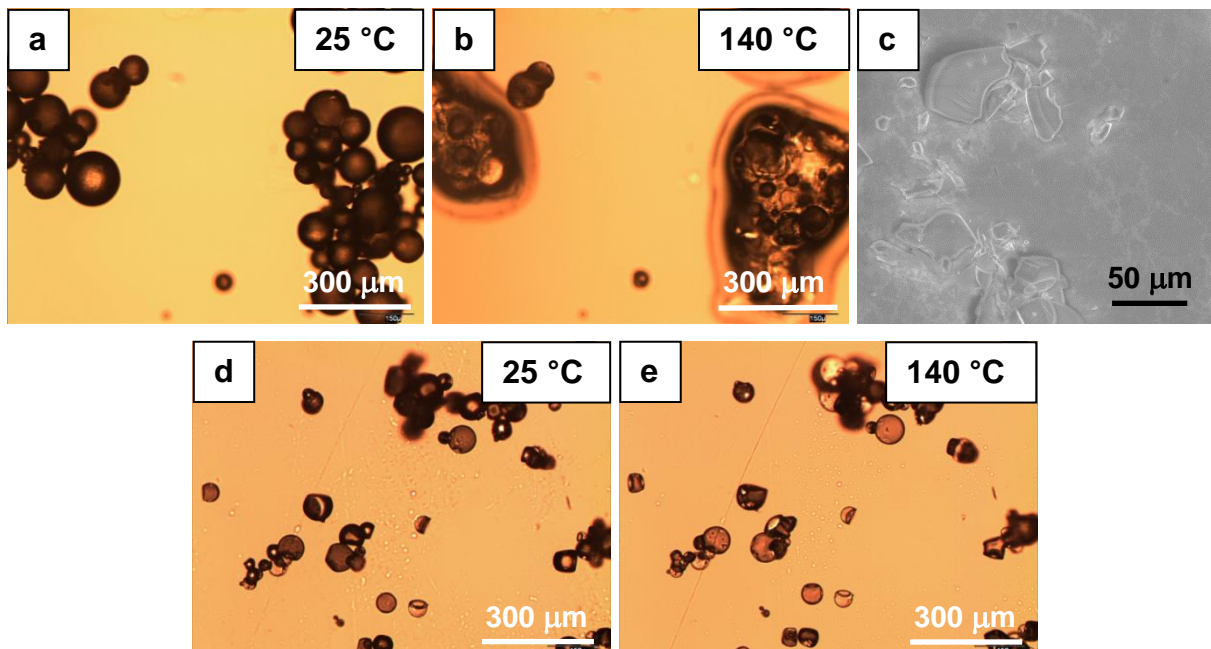


Figure 4.12. Optical microscopic images of microcapsules **a)** at 25 °C and **b)** 140 °C. **c)** SEM image of microcapsules after heating to 140 °C. Optical microscopic images of control microcapsules **d)** at 25 °C and **e)** 140 °C.

4.2.11. Increasing the Mechanical Strength of Microcapsules

Attempts were made to increase the mechanical strength of the microcapsules. This was achieved by using the same interfacial polymerisation technique described in **Section 4.25** with the exception of a mixture of the shell wall precursor containing the Diels-Alder adduct **4.5** and a shell wall precursor not containing the thermally-reversible adduct **3.2** (Figure 4.13) was employed. The synthesis of mechanically strong microcapsules required at least a ratio of 2:8 of **4.5:3.2**.

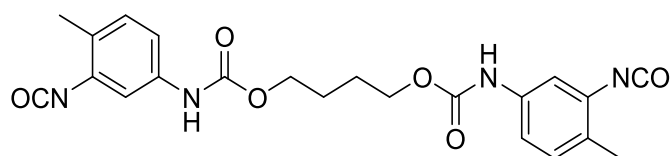


Figure 4.13. Structure of shell wall precursor not containing a thermally-reversible Diels-Alder adduct **3.2**.

The microcapsules were generated with an average diameter of 46 μm within a range of 12-98 μm and a shell wall thickness of 2.85 μm . Analysis of the microencapsulated core revealed a composition of 28 wt. % IPDI and 31 wt. % chlorobenzene.

The capability of these microcapsules to release their core contents upon exposure to a heat stimulus was also investigated. A sample of microcapsules was heated to 140 $^{\circ}\text{C}$ on a hot stage mounted to an optical microscope. The shell walls of the microcapsules began to dissociate at 140 $^{\circ}\text{C}$ and after a period of 1 hour the shells of adjacent microcapsules had fused together (Figure 4.14). As a result of the long term exposure to this temperature, a large portion of the microcapsule core had leached through the microcapsule shell wall.

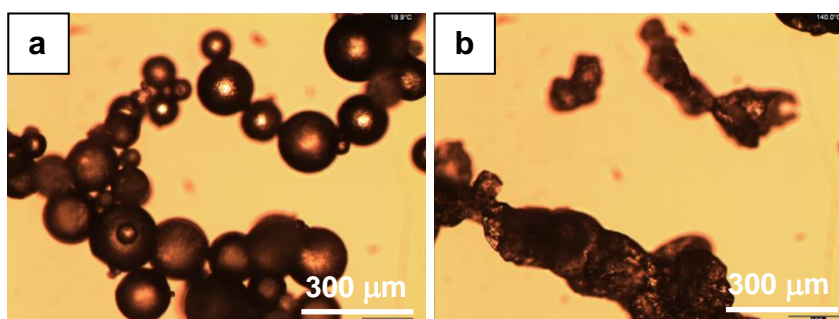


Figure 4.14. Optical microscopic images of microcapsules **a)** at 25 $^{\circ}\text{C}$ and **b)** 140 $^{\circ}\text{C}$.

Although the physical strength of these microcapsules was improved, their release capabilities were mitigated. Thus further studies will be required in order to generate strong microcapsules that can release their core contents effectively.

4.3. Conclusion

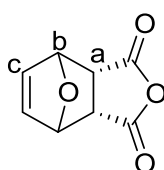
The successful synthesis of an isocyanate-terminated shell wall precursor that contains a thermally-reversible Diels-Alder adduct has been achieved. The synthetic route employed the initial protection of maleic anhydride with furan followed by conversion to a hydroxy-functionalised maleimide-furan. Deprotection afforded a maleimide that was reacted with furfuryl alcohol to generate a dihydroxy-functionalised maleimide-furan Diels-Alder adduct. The capability of this adduct to dissociate upon exposure to elevated temperature was demonstrated using ^1H NMR spectroscopy. The reaction of this adduct with an excess of TDI afforded the isocyanate-terminated shell wall precursor. The synthesis of microcapsules containing IPDI crosslinkers using this shell wall precursor was successful and the capability of the afforded microcapsules to release their core contents upon exposure to a heat stimulus was

demonstrated. The mechanical strength of the microcapsules was enhanced by using a synthesis that employed a mixture of a shell wall precursor containing the Diels-Alder adduct and a shell wall precursor not containing the thermally-reversible adduct. Although the mechanical strength of the microcapsules was increased the capability to release the core using a heat stimulus was significantly reduced.

4.4. Experimental

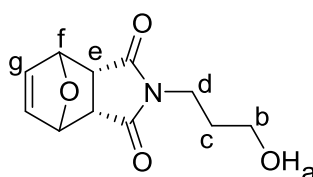
All chemical purification and experimental techniques employed in this chapter are identical to those described in **Chapter 2** and **3**.

Protection of Maleic Anhydride with Furan 4.1⁸



Maleic anhydride (3.07 g, 31.0 mmol) and furan (5.06g, 74.4 mmol) were dissolved in toluene (50 mL) and stirred at room temperature for a period of 72 hours. The solvent was removed *in vacuo* to leave a white solid **4.1** (4.35 g, 84 %) (m.p. 117-121 °C lit. 114-116 °C). ¹H NMR (400 MHz, CDCl₃) δ_H (ppm): 3.18 (2H, s, H_a), 5.47 (2H, s, H_b), 6.58, (2H, s, H_c); ¹³C NMR (100 MHz, CDCl₃) δ_C (ppm): 48.7, 82.2, 137.0, 169.9; FTIR (ATR) ν (cm⁻¹): 3060 (C-H), 2999 (C-H), 1785 (C=O), 1212 (C-O), 1086 (C-O).

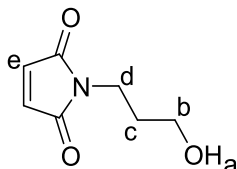
Conversion of Protected Maleic Anhydride to Maleimide 4.2¹³



The protected maleic anhydride **4.1** (1.53 g, 9.3 mmol) and 3-amino-1-propanol (0.830 g, 11.1 mmol) were dissolved in MeOH (50 mL) and maintained under reflux for a period of 18 hours. The solvent was removed *in vacuo* to leave a yellow coloured oil that was purified by column chromatography (R_f = 0.29, 2 % MeOH/CHCl₃) to afford a white solid **4.2** (0.694 g, 36 %) (m.p. 119-124 °C, lit. 118-120 °C). ¹H NMR (400 MHz, Acetone-*d*₆) δ_H (ppm): 1.70 (2H, quint. *J* = 6.5 Hz, H_c), 2.93 (2H, s, H_e), 3.51 (2H, t *J* = 5.0 Hz, H_d), 3.52 (2H, t *J* = 7.0 Hz, H_b), 4.84 (1H, s, H_a), 5.15 (2H, s, H_f), 6.59 (2H, s, H_g); ¹³C NMR (100 MHz, Acetone-*d*₆) δ_C (ppm): 31.6, 36.2, 48.3, 59.7, 81.8, 137.4,

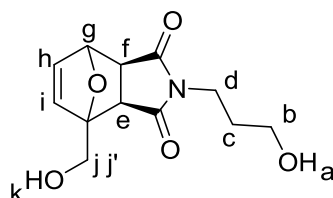
177.4; FTIR (ATR) ν (cm^{-1}): 3511 (O-H), 3099 (C-H), 2952 (C-H), 1691 (C=O), 1405 (C-N), 1158 (C-O); ESIMS calculated mass $(\text{C}_{11}\text{H}_{13}\text{O}_4\text{N}+\text{H})^+$ 224.0917 found 224.0918.

Deprotection to Form Hydroxy-Functionalised Maleimide 4.3



Protected maleimide **4.2** (0.650 g, 2.9 mmol) was dissolved in toluene (20 mL) and maintained under reflux for a period of 7 hours. The solvent was removed *in vacuo* to leave a pale pink coloured oil **4.3** (0.375 g, 83 %). ^1H NMR (400 MHz, CDCl_3) δ_{H} (ppm): 1.80 (2H, quint. $J = 6.0$ Hz, H_c), 2.60 (1H, s, H_a), 3.59 (2H, br. m, H_b), 3.69 (2H, t $J = 7.0$ Hz, H_d), 6.74 (2H, s, H_e); ^{13}C NMR (100 MHz, CDCl_3) δ_{C} (ppm): 31.7, 36.2, 58.0, 165.4, 170.5; FTIR (ATR) ν (cm^{-1}): 3478 (O-H), 3110 (C-H), 2954 (C-H), 1695 (C=O), 1409 (C-N), 1149 (C-O); ESIMS calculated mass $(\text{C}_7\text{H}_9\text{O}_3\text{N}+\text{H})^+$ 156.0655 found 156.0654.

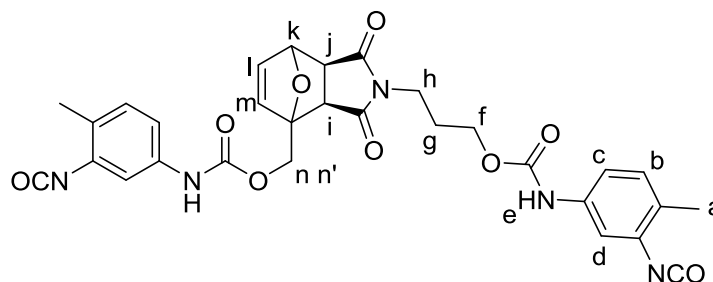
Synthesis of Dihydroxy-Functionalised Diels-Alder Adduct 4.4



Hydroxy-functionalised maleimide **4.3** (0.340 g, 2.19 mmol) and furfuryl alcohol (0.258 g, 2.6 mmol) were dissolved in toluene (40 mL) and maintained at 80 °C for a period of 72 hours. The solvent was removed *in vacuo* to leave a yellow coloured oil that was purified by column chromatography ($R_f = 0.15$, 5 % MeOH/ CHCl_3) to afford a colourless oil **4.4** obtained as a mixture of *exo* and *endo* isomers (7:3) that slowly transformed to the thermodynamically stable *exo* isomer over a period of several months (0.426 g, 77 %). ^1H NMR (400 MHz, $\text{DMSO}-d_6$) δ_{H} (ppm): 1.57 (2H, quint. $J = 7.0$ Hz, H_c), 2.88 (1H, d $J = 6.5$ Hz, H_f), 3.02 (1H, d $J = 6.5$ Hz, H_e), 3.36 (2H, t $J = 7.0$ Hz, H_b), 3.39 (2H, m, H_d), 3.69 (1H, dd $J = 6.0, 12.0$ Hz, H_j), 4.03 (1H, dd $J = 6.0, 12.0$ Hz, H_j'), 4.46 (1H, br. m, H_a), 4.97 (1H, br. m, H_k), 5.08 (1H, d, 1.0 Hz H_g), 6.52 (1H, d $J = 6.0$ Hz, H_i), 6.53 (1H, dd $J = 6.0, 1.0$ Hz, H_h); ^{13}C NMR (100 MHz,

DMSO- d_6) δ_C (ppm): 30.5, 35.4, 47.7, 49.9, 58.3, 59.0, 80.2, 91.6, 136.4, 138.1, 174.9, 176.4; FTIR (ATR) ν (cm^{-1}): 3460 (O-H), 3112 (C-H), 2960 (C-H), 1683 (C=O), 1404 (C-N), 1172 (C-O); ESIMS calculated mass $(\text{C}_{12}\text{H}_{15}\text{O}_5\text{N}+\text{H})^+$ 254.1023 found 254.1025.

Synthesis of Shell Wall Precursor 4.5



Dihydroxy-functionalised Diels-Alder adduct **4.4** (0.393 g, 1.6 mmol) and toluene-2,4-diisocyanate (TDI) (0.757 g, 4.4 mmol) were dissolved in tetrahydrofuran (15 mL) and maintained under reflux for a period of 18 hours under an atmosphere of argon. The solvent was removed *in vacuo* and excess TDI was removed by washing with cyclohexane (3 x 20 mL) at 80 °C to leave a yellow coloured solid **4.5** (0.926 g, 99%) (m.p. 125-129 °C). ^1H NMR (400 MHz, THF- d_8) δ_{H} (ppm): 1.23 (2H, m, H_g), 2.55-2.60 (6H, m, H_a), 2.93 (1H, m, H_i), 3.45 (2H, m, H_h), 3.73 (1H, m, H_j), 4.42 (2H, m, $\text{H}_{nn'}$), 4.64 (2H, m, H_f), 5.05 (1H, m, H_k), 5.84-6.03 (2H, m, H_{lm}), 6.40-7.24 (2H, m, H_e), 6.40-7.24 (6H, m, H_{bcd}); ^{13}C NMR (100 MHz, THF- d_8) δ_C (ppm): 16.6, 22.0, 25.6, 26.9, 50.1, 61.9, 67.1, 67.7, 81.0, 89.8, 114.7, 115.7, 124.8, 125.9, 130.3, 132.4, 139.0, 152.0, 175.4, 176.1; FTIR (ATR) ν (cm^{-1}): 3340 (N-H), 3124 (C-H), 2947 (C-H), 2265 (NCO), 1696 (C=O), 1537 (C-N), 1220 (C-O); ESIMS of **4.5** derivative from its reaction with MeOH, calculated mass $(\text{C}_{32}\text{H}_{35}\text{O}_{11}\text{N}_5+\text{Na})^+$ 688.2225 found 688.2225.

Synthesis of Microcapsules 4.6

Gum arabic (9 g) was dispersed in H_2O (60 mL) in a 150 mL beaker with the aid of mechanical agitation at a rate of 1000 rpm. Shell wall precursor **4.5** (0.100 g, 0.17 mmol) and IPDI (0.09 g, 0.40 mmol) were dissolved in *o*-methoxyacetophenone (0.14 mL). This solution was added to the aqueous solution and the resultant emulsion heated to 70 °C at a rate of 10 °C/minute. When the temperature reached 50 °C, 1,4-butanediol (5.2 g, 56.6 mmol) was added and agitated at the same rate for an additional 30 seconds. Agitation was reduced to a rate of 150 rpm for 45 minutes at

70 °C followed by a further 2 hours at room temperature. After this period, agitation was ceased, H₂O (100 mL) was added and the generated microcapsules allowed to settle at the bottom of the beaker over a period of 1 hour at room temperature. The aqueous solution was decanted to leave polyurethane microcapsules **4.6** that were collected by vacuum filtration, washed with H₂O and then air dried for a period of 48 hours (0.149 g).

Synthesis of Mechanically Robust Microcapsules

Gum arabic (9 g) was dispersed in H₂O (60 mL) in a 150 mL beaker with the aid of mechanical agitation at a rate of 1000 rpm. Shell wall precursor **4.5** (0.075 g, 0.12 mmol), **3.2** (3.15 g, 0.72 mmol) and IPDI (0.550 g, 2.5 mmol) were dissolved in chlorobenzene (0.9 mL). This solution was added to the aqueous solution and the resultant emulsion heated to 70 °C at a rate of 10 °C/minute. When the temperature reached 50 °C, 1,4-butanediol (5.2 g, 56.6 mmol) was added and agitated at the same rate for an additional 30 seconds. Agitation was reduced to a rate of 150 rpm for 45 minutes at 70 °C followed by a further 2 hours at room temperature. After this period, agitation was ceased, H₂O (100 mL) was added and the generated microcapsules allowed to settle at the bottom of the beaker over a period of 1 hour at room temperature. The aqueous solution was decanted to leave polyurethane microcapsules that were collected by vacuum filtration, washed with H₂O and then air dried for a period of 48 hours (1.50 g).

4.5. References

- ¹ O. Diels, K. Alder, *Justus Liebigs Ann. Chem.*, 1928, **460**, 98-122.
- ² J. C. C. Atherton and S. Jones, *Tetrahedron*, 2003, **59**, 9039-9057.
- ³ B. Gacal, H. Durmaz, M. A. Tasdelen, G. Hizal, U. Tunca, Y. Yagci and A. L. Demirel, *Macromolecules*, 2006, **39**, 5330-5336.
- ⁴ V. Froidevaux, M. Borne, E. Laborbe, R. Auvergne, A. Gandini and B. Boutevin, *RSC Adv.*, 2015, **5**, 37742-37754.
- ⁵ X. Chen, M. A. Dam, K. Ono, A. Mal, H. Shen, S. R. Nutt, K. Sheran and F. Wudl, *Science*, 2002, **295**, 1698-1702.
- ⁶ J.R. McElhanon, E.M. Russick, D.R. Wheeler, D.A. Loy and J.H. Aubert, *J. Appl. Polym. Sci.*, 2002, **85**, 1496-1502.
- ⁷ M. Shi and M. S. Shoichet, *J. Biomat. Sci.-Polym. E.*, 2008, **19**, 1143-1157.

- ⁸ W. H. Heath, F. Palmieri, J. R. Adams, B. K. Long, J. Chute, T. W. Holcombe, S. Zieren, M. J. Truitt, J. L. White and C. G. Wilson, *Macromolecules*, 2008, **41** 719-726.
- ⁹ K. Eggers, D. Szopinski and G. A. Luinstra, *Macromol. Symp.*, 2014, **346**, 32-35.
- ¹⁰ J. L. Yang, M. R. Kessler, J. S. Moore, S. R. White and N. R. Sottos, *Macromolecules*, 2008, **41**, 9650-9655.
- ¹¹ M. Huang and J. Yang, *J. Mater. Chem.*, 2011, **21**, 11123-11130.
- ¹² L. T. T. Nguyen, X. K. D. Hillewaere, R. F. A. Teixeira, O. van den Berg and F. E. Du Prez, *Polym. Chem.*, 2015, **6**, 1159-1170.
- ¹³ B. J. Neubert and B. B. Snider, *Org. Lett.*, 2003, **5**, 765-768.

Chapter 5

Delayed Quick-Cure of Hydroxy-Terminated Polybutadiene using Thermally-Reversible Blocked Isocyanates

The following chapter has, in part, been published by the author as a patent application in collaboration with BAE Systems plc. - *M. E. Budd, W. C. Hayes, R. Stephens, Great British/European Patent Application, PBX Composition, 2015, GB1511869.8/ EP15275169.9.*

Abstract

The manufacture of plastic/polymer bonded explosives (PBX) involves binding the energetic material within a polymer matrix. Typically, the matrix is formed by the crosslinking reaction of a hydroxy-functionalised aliphatic polymer with a diisocyanate. The current manufacturing procedure employed can lead to several detrimental processes that render the product unusable and thus it must be destroyed - a process that is both costly and hazardous. The following chapter demonstrates how reactive isocyanate functionality can be generated when desired by triggering the dissociation of thermally-labile oxime-urethanes using a thermal stimulus. In addition, control of the dissociation temperature can be achieved by modification of the steric and electronic properties around the thermally-labile bond. Finally, the potential of these oxime-urethanes to cure hydroxy-functionalised aliphatic polymers has been demonstrated.

5.1. Introduction

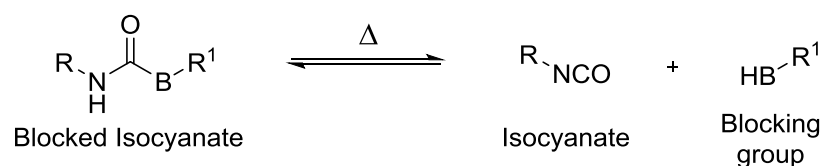
Modern explosives typically consist of the energetic material bound within a rubbery polyurethane matrix formed from the polymerisation reaction of an isocyanate crosslinker with a hydroxy-functionalised polymer in the presence of a catalyst. Such composite materials are known as plastic or polymer bonded explosives (PBX). The current manufacturing process of one such explosive formulation, Rowanex 1100 1A (Table 5.1), involves the addition of isophorone diisocyanate (IPDI) to a mixture of the explosive, hydroxy-terminated polybutadiene (HTPB) and the catalyst dibutyltin dilaurate (DBTDL), upon this addition an immediate crosslinking reaction occurs. As a result, the missiles or shells - designated herein as stores - must be filled with the rapidly curing mixture almost immediately. This can prevent the uniform delivery of the crosslinker and thus lead to the formation of an inhomogeneously crosslinked polymer matrix. In addition, consecutively filled stores often have varying degrees of

crosslinking consistency and can lead to the formation of voids. Upon firing, the explosive stores are subjected to an increased force of 13,000 G, sufficient to cause undesired detonation of the explosive thus posing a potentially fatal hazard to the gun operators. These detrimental properties mean that the defective explosive material must be disposed of in a safe manner, an expensive and dangerous process.

Table 5.1. Rowanex 1100 1A explosive formulation.

Constituent	Composition (wt %)
RDX	> 80
HTPB R45HT	< 20
Plasticiser	
Antioxidant	
Surfactant	
IPDI	
DBTDL	
Antifoaming Agent	

Polyurethanes are employed extensively in the adhesives and coatings industry. The high reactivity of isocyanates renders formulations containing free isocyanate unstable, polymerising readily under mild conditions.¹ Blocking agents that react with the isocyanate moiety have thus been developed,² preventing undesired polymerisation. The blocking reaction is thermally-reversible, generating free isocyanate when desired by the application of heat (Scheme 5.1).



Scheme 5.1 The reversible reaction of blocked isocyanates, regenerating isocyanate and blocking group.

An extensive range of blocking agents have been developed³ for polyurethane coatings and adhesives including - aromatic heterocycles,⁴ sterically hindered secondary amines,⁵ phenols,⁶ amides⁷ and oximes.⁸ It is hoped that such systems can be used to control the curing process of polyurethane rubber composites used to bind high explosives such as RDX.

5.2. Results and Discussion

Explosive formulations that utilise blocked isocyanates must meet certain processing requirements - the blocked isocyanates must be soluble or uniformly dispersed within the HTPB binder, the released blocking groups must not be volatile at the curing temperature in order to avoid the formation of voids, the blocked isocyanate must be stable at the process mixing temperatures (55 - 70 °C) and curing temperature must not approach the ignition temperature of RDX (~220 °C), ideally it should be < 100 °C. Thus, it was important to investigate several different types of blocking groups - amines, amides, oximes, aromatic heterocycles and phenols - as potential candidates for the curing of hydroxy-functionalised polymers (Figure 5.1).

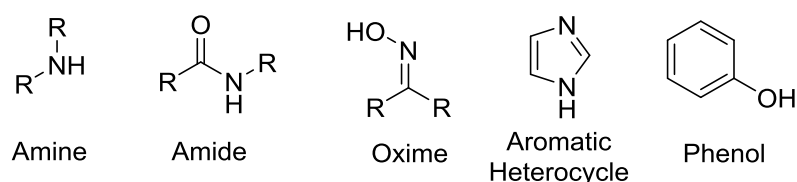
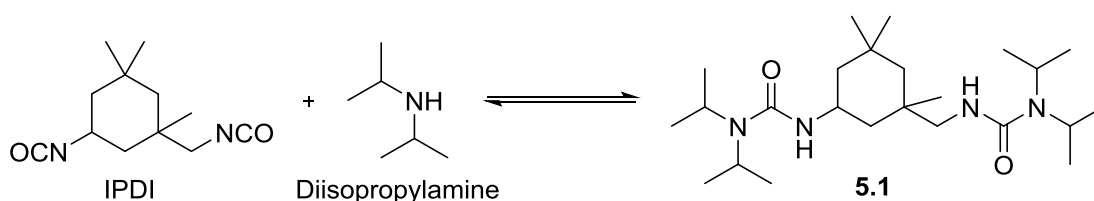


Figure 5.1. Structures of blocking groups - amines, amides, oximes, aromatic heterocycles and phenols.

5.2.1. Amine Blocking Groups

The urea bond is stabilised by conjugation of the lone pair of the nitrogen and the π -electrons of the carbonyl. However, literature investigations have revealed⁹ the presence of steric groups prevent this conjugation and thus reduce the stability of ureas sufficiently to bring about its dissociation under mild conditions. Further to this, the temperature at which dissociation occurs can be controlled by modification of the degree of steric hindrance.¹⁰ Literature studies, have reported¹¹ that such amine-blocked diisocyanates can be used to cure HTPB at elevated temperatures.



Scheme 5.2. Reaction of IPDI and diisopropylamine to form a urea 5.1.

IPDI was reacted with an excess of diisopropylamine for a period of 1 hour (Scheme 5.2). Purification by washing with HCl (1M), afforded a white solid 5.1 which was analysed using FTIR spectroscopy. The absence of an absorption corresponding

to the isocyanate moiety and the presence of a urea carbonyl at 1620 cm^{-1} was observed (Figure 5.2).

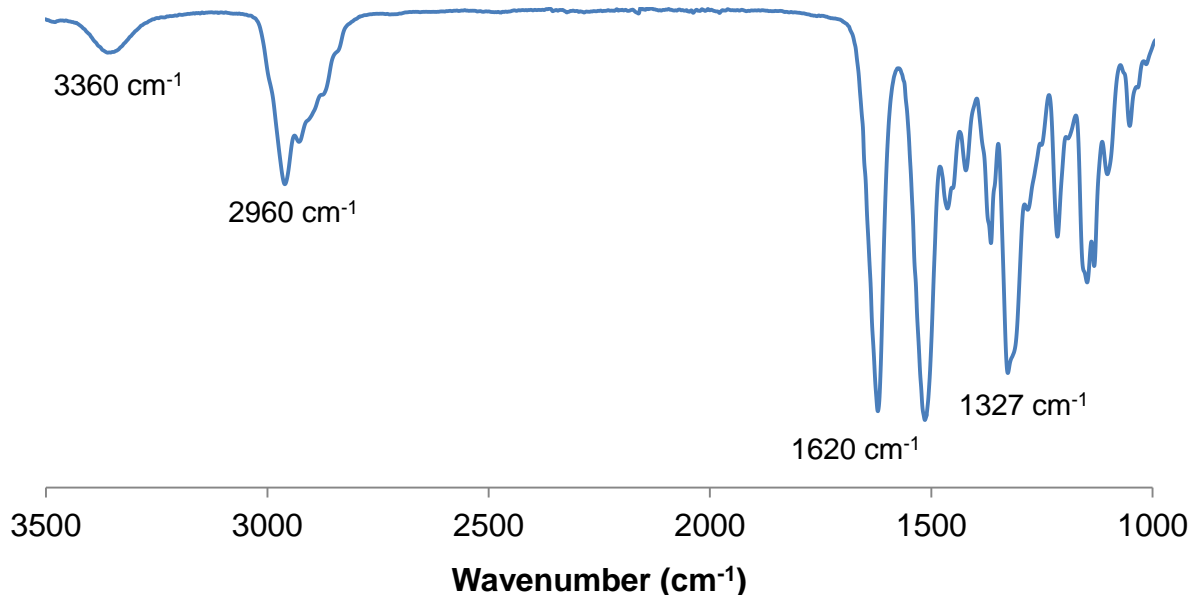
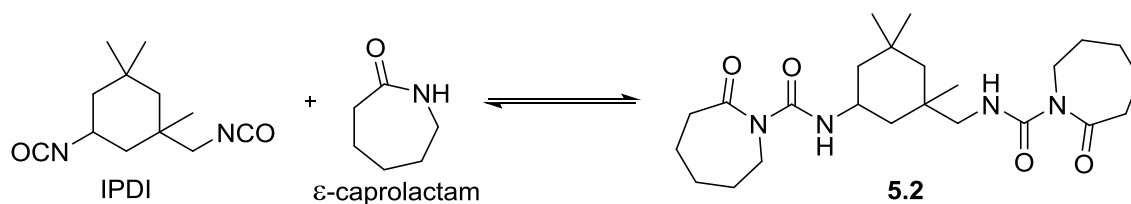


Figure 5.2. FTIR spectrum of urea **5.1**, highlighting the absorption at 1620 cm^{-1} corresponding to the urea carbonyl moiety.

5.2.2. Amide Blocking Groups

The lone pair of the nitrogen of amides typically exhibits poor reactivity resulting from its delocalisation into the carbonyl bonding system. However, the lone pair has demonstrated to possess sufficient reactivity with certain electrophilic carbons including isocyanates.⁷ A short study investigated¹² the synthesis and dissociation of isocyanates blocked with amides. It was found dissociation of such compounds to regenerate isocyanate could be achieved within the temperature range $100 - 157\text{ }^{\circ}\text{C}$. Further studies have demonstrated^{13, 14} how amide-blocked isocyanates can be employed to cure hydroxy-functionalised polymers at high temperatures.

IPDI was reacted with an excess of ϵ -caprolactam in order to yield an amide-blocked diisocyanate **5.2** able to regenerate the reactive isocyanate moiety when exposed to heat (Scheme 5.3).



Scheme 5.3. Reaction of IPDI and ϵ -caprolactam to afford amide-blocked IPDI **5.2**

The amide-blocked diisocyanate **5.2** was characterised using a range of analytical techniques including ^{13}C NMR spectroscopy. Resonances at 154.0 and 155.2 ppm were observed corresponding to the newly formed urea carbonyl functionality. Furthermore, resonances at 179.3 and 179.6 corresponding to the amide carbonyl verify the synthesis of an amide-blocked diisocyanate (Figure 5.3). In addition, FTIR spectroscopic analysis revealed absorbances at 1694 and 1651 cm^{-1} confirming the presence of amide and urea carbonyl functionalities, respectively.

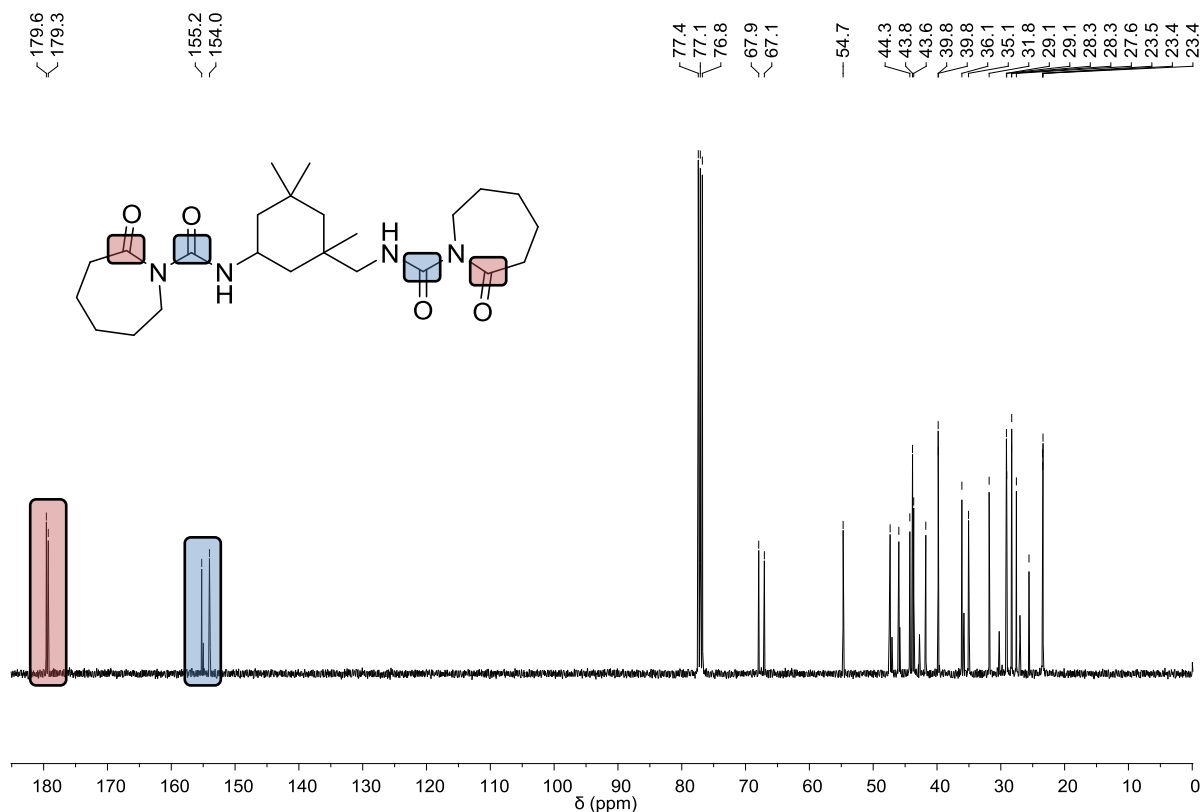
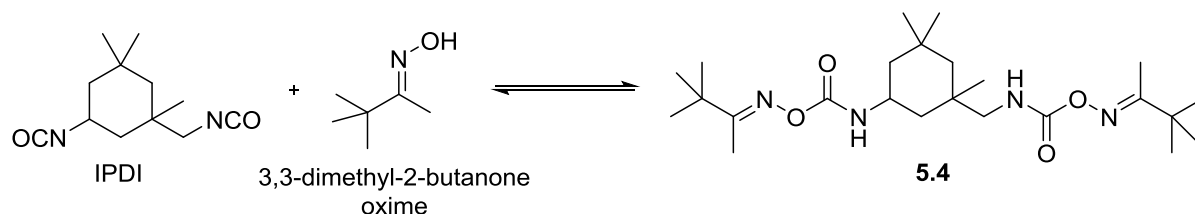


Figure 5.3. ^{13}C NMR spectrum of ϵ -caprolactam-blocked IPDI highlighting resonances corresponding to the urea and amide carbonyl moieties.

5.2.3. Oxime Blocking Groups

Oximes react readily with isocyanates to form oxime-urethanes. The thermally-reversible nature of this bond has led to its extensive employment as a blocking agent in the adhesives industry.^{15,16} Studies have revealed¹⁷ that increasing the steric hindrance around the oxime increases the rate at which dissociation occurs. **Chapter 2** describes the synthesis of thermally-labile oxime-urethanes and demonstrates how they can be used to generate isocyanates upon the application of a thermal stimulus.

IPDI blocked with an oxime, often referred to as an oxime-urethane was synthesised in a similar approach described in **Chapter 2** and first involved the generation of 3,3-dimethyl-2-butanone oxime **5.3**. The reaction involved heating of 3,3-dimethyl-2-butanone with hydroxylamine hydrochloride in the presence of triethylamine. Subsequent reaction of the afforded oxime with isophorone diisocyanate in a 2:1 ratio afforded the oxime-urethane **5.4** without the need for further purification (Scheme 5.4).



Scheme 5.4. Thermally reversible reaction of IPDI and 3,3-dimethyl-2-butanone oxime to yield oxime-urethane **5.4**.

The oxime-urethane was analysed using a range of analytical techniques including ¹H NMR spectroscopy. The chemical shift values of the methyl and ^tbutyl protons were subject to a downfield shift from 1.07 and 1.81 ppm on the oxime to 1.19 and 2.99 respectively on the oxime-urethane, verifying the reaction of the oxime and isocyanate. Further resonances that reinforce the observed reaction at 6.13 and 6.57 ppm correspond to the urethane nitrogen protons (Figure 5.4).

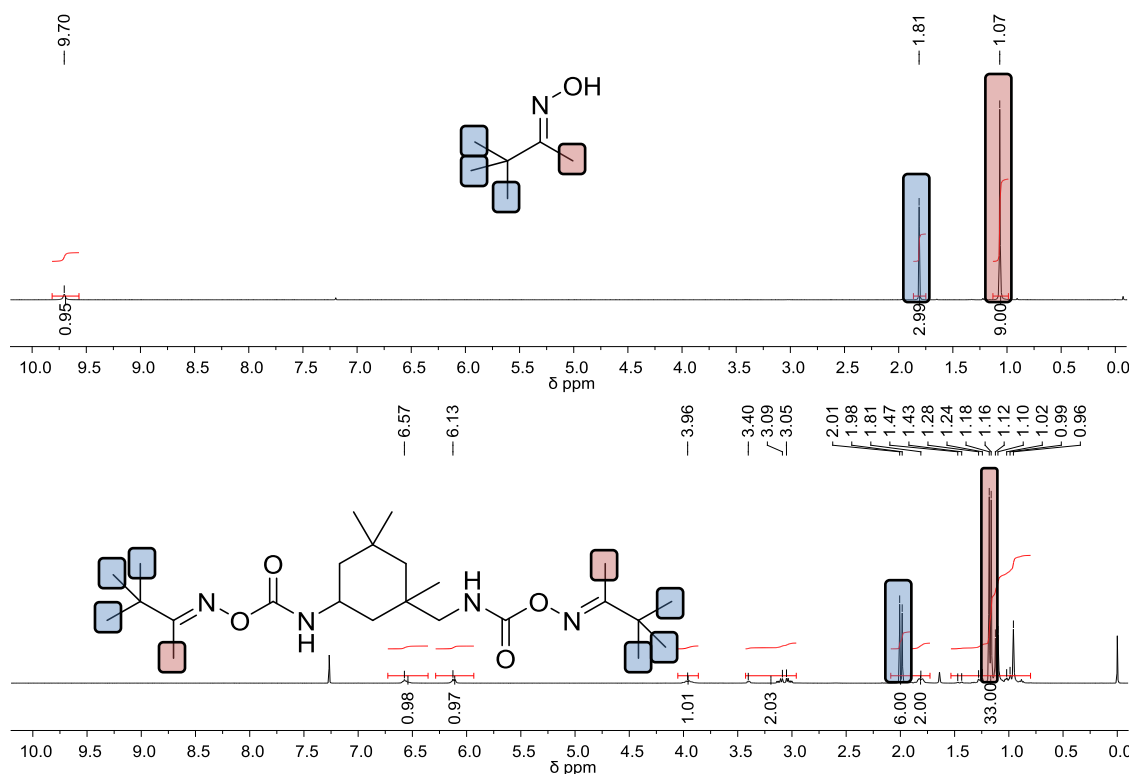
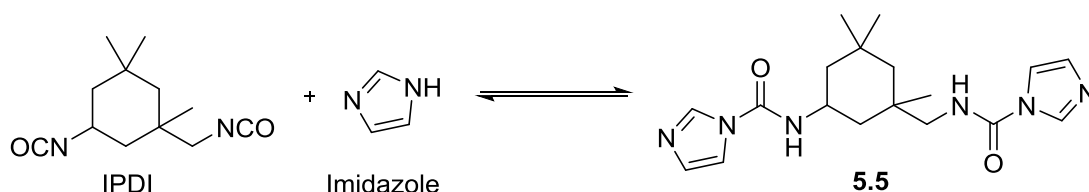


Figure 5.4. ¹H NMR spectra of 3,3-dimethyl-2-butanone oxime **5.3** and oxime-urethane **5.4**.

5.2.4. Aromatic Heterocycle Blocking Groups

Aromatic heterocyclic compounds including pyrazoles, imidazoles and triazoles that possess a nucleophilic heteroatom have been demonstrated to exhibit reversible reactions with isocyanates.^{18,19,20} Heterocycle-blocked isocyanates have indeed been used to cure hydroxy and amine-functionalised pre-polymers that are employed in adhesives and coatings.²¹

Imidazole-blocked IPDI **5.5** was afforded by the reaction of imidazole and IPDI in a 2:1 ratio to give white crystals that did not require further purification (Scheme 5.5).



Scheme 5.5. Reaction of IPDI and imidazole to yield imidazole-blocked IPDI **5.5**.

The blocked isocyanate **5.5** thus produced was analysed using a variety of techniques including mass spectrometry. Mass spectrometry utilising electrospray ionisation was employed and a mass of 359.2190 was observed corresponding to the proton ionised imidazole-blocked IPDI with a molecular ion formula of $C_{18}H_{27}O_2N_6^+$. A further mass ion at 381.2010 was also observed corresponding to the Na^+ ionised imidazole-blocked IPDI with a molecular ion formula of $C_{18}H_{26}O_2N_6Na^+$ (Figure 5.5).

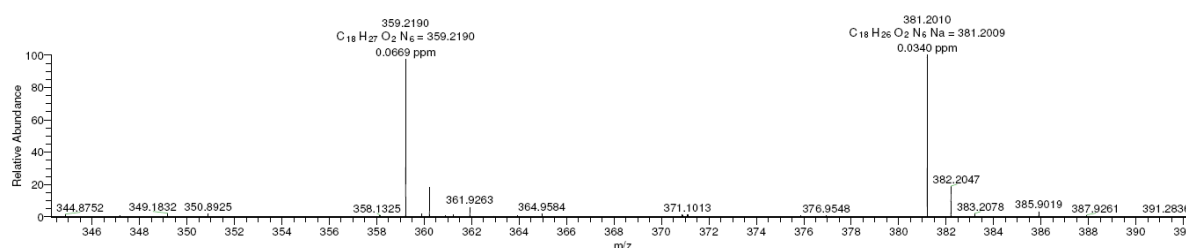
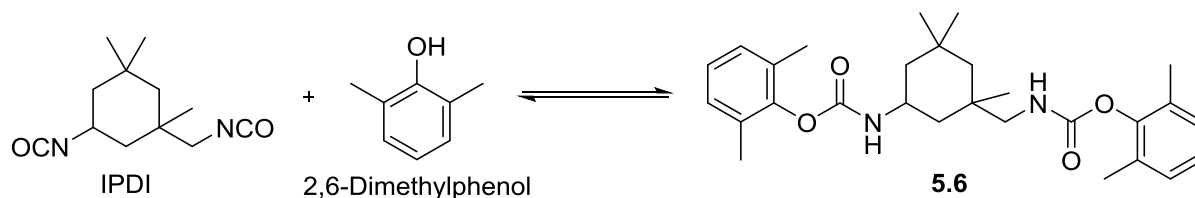


Figure 5.5. Mass spectrum of imidazole-blocked IPDI **5.5** highlighting the ions observed with masses of $C_{18}H_{27}O_2N_6^+$ and $C_{18}H_{26}O_2N_6Na^+$ at 359.2190 and 381.2010, respectively.

5.2.5. Phenol Blocking Groups

The reversible nature of urethanes synthesised from phenol compounds has been well documented.²² The temperature at which phenol-blocked isocyanates dissociate can be controlled to some extent by conjugating the aromatic ring with electron donating groups. Polyisocyanates blocked with salicylate esters and other phenolic groups have been demonstrated to cure hydroxy-functionalised polymers used to bind high explosives.^{23,24,25}

A phenol-blocked isocyanate **5.6** was obtained by reaction of 2,6-dimethylphenol and IPDI in the presence of a catalytic quantity of DBTDL. The removal of the catalyst was achieved by washing with hexane to leave the pure compound obtained as a white powder (Scheme 5.6).



Scheme 5.6. Reaction of IPDI and 2,6-dimethylphenol to afford a thermally-labile urethane.

The phenol-blocked IPDI **5.6** was characterised with a range of analytical techniques including FTIR spectroscopy. Characteristic absorptions at 3314 and 1706 cm^{-1} typical of vibrations corresponding to urethane N-H and C=O functionalities (Figure 5.6) were observed.

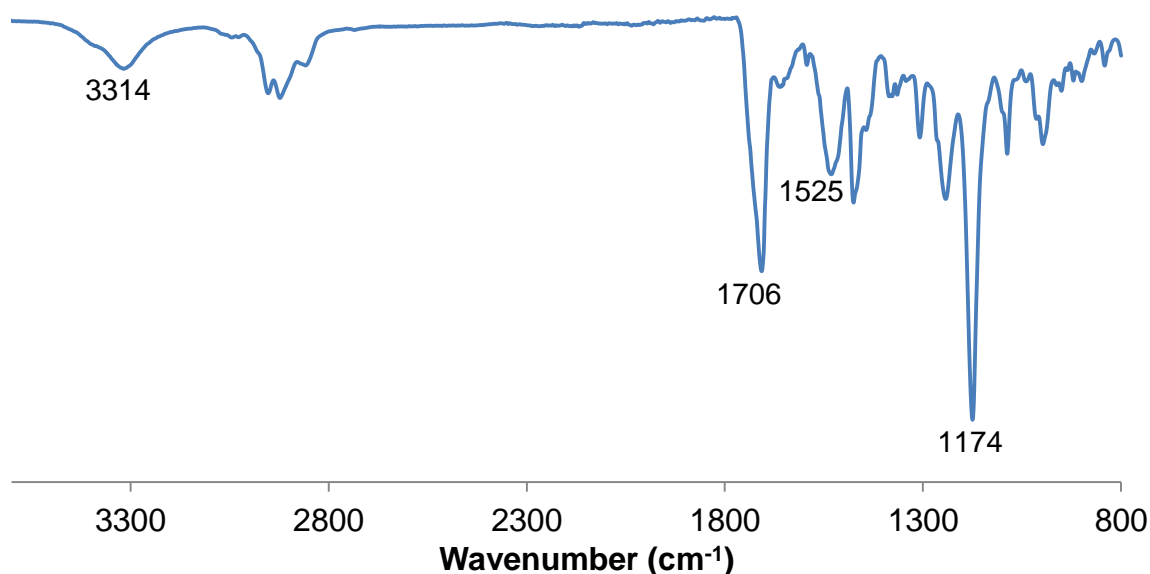


Figure 5.6. FTIR spectrum of phenol-blocked IPDI **5.6** highlighting the key absorption at 1706 cm^{-1} corresponding to the urethane carbonyl moiety.

5.2.6. Dissociation of Blocked-IPDI

It was important to measure the dissociation temperature of the generated blocked isocyanates **5.1-6** in order to ascertain the conditions that will be required in order to achieve the cure of HTPB. **Chapter 2** describes how variable temperature infra-red spectroscopy (VTIR) can be employed to observe the dissociation of thermally-labile oxime-urethanes.

The blocked isocyanates **5.1-6** were dissolved in dried tetraethylene glycol dimethyl ether in a ratio of 1:0.25 wt. %. This solution was injected into a variable temperature cell and an IR spectrum recorded at 10 °C increments. In accordance with literature studies, the dissociation temperature was recorded as the onset at which an absorption characteristic of the isocyanate stretching vibration $\sim 2250 \text{ cm}^{-1}$ was observed (Table 5.2).

Table 5.2. Dissociation temperatures of blocked-isocyanates **5.1-6** measured using VTIR spectroscopy

	Blocking group	Dissociation Temperature (°C)
5.1	diisopropylamine	90-110
5.2	ϵ -caprolactam	120-130
5.4	3,3-dimethyl-2-butanone oxime	110-120
5.5	imidazole	65-70
5.6	2,6-dimethylphenol	150-160

Ideally, the dissociation temperature should be $< 100 \text{ }^\circ\text{C}$ but not below $70 \text{ }^\circ\text{C}$ - the current mixing conditions for Rowanex 1100 1A. Imidazole-blocked IPDI **5.5** began to dissociate at $70 \text{ }^\circ\text{C}$, well within the desired temperature range. Diisopropylamine-blocked IPDI **5.1** exhibited dissociation at $100 \text{ }^\circ\text{C}$ and it is expected that increasing the steric hindrance around the bond will lead to a reduction in the dissociation temperature and can be easily achieved by blocking with more sterically hindered amines.¹¹ 3,3-Dimethyl-2-butanone oxime-blocked IPDI **5.4** began to dissociate at $120 \text{ }^\circ\text{C}$, although this is above the desired temperature, literature studies¹⁷ and results obtained in **Chapter 2** suggest the dissociation temperature of oxime-urethanes can also be reduced by increasing the steric hindrance around the oxime. ϵ -Caprolactam-blocked IPDI **5.2** dissociated at $130 \text{ }^\circ\text{C}$, above the desired temperature. The dissociation of these blocked isocyanates cannot be controlled easily by modification of the blocking group structure. Literature studies report²² the dissociation of 2,6-dimethylphenol-blocked isocyanates occurred at $125 \text{ }^\circ\text{C}$, however, the dissociation of **5.6** was not observed until $150 \text{ }^\circ\text{C}$, significantly above the desired temperature range.

5.2.7. Cure of HTPB using Blocked-IPDI

The potential of these blocked-isocyanates to cure hydroxy-functionalised polymers at elevated temperatures was investigated. The blocked isocyanates **5.1-6** (8.01 mmol) were dispersed in a mixture of HTPB (18.22 g) and DBTDL (0.044 g) in accordance with the Rowanex 1100 1A formulation using an overhead stirrer at 70 °C. In order to achieve uniform curing of HTPB, complete dispersion of the blocked isocyanates within HTPB was desired and indeed **5.1 5.2** and **5.4** exhibited excellent solubility at 70 °C. In contrast, imidazole-blocked IPDI **5.5** and 2,6-dimethylphenol-blocked IPDI **5.6** exhibited poor solubility in HTPB and thus efficient dispersion was not achieved.

The mixtures were heated for a period of 72 hours at 120 °C in an evacuated atmosphere. Curing of HTPB was achieved using diisopropylamine-blocked IPDI **5.1** - however, as a result of the evolution of volatile diisopropylamine, bubbles were formed within the polyurethane rubber. The high dissociation temperature of ϵ -caprolactam-blocked IPDI **5.2** (130 °C) prevented the cure of HTPB. The cure of HTPB was successfully achieved using oxime-urethane **5.4**. The poor solubility of **5.5** in HTPB prevented the formation of a homogeneously crosslinked polyurethane, thus the formation of a uniformly crosslinked matrix was not achieved. The high temperatures required for the dissociation of 2,6-dimethylphenol-blocked IPDI **5.6** and its poor solubility in HTPB prevented the formation of a polyurethane matrix (Table 5.3).

Table 5.3. Solubility and curing capability of blocked isocyanates **5.1-6** in HTPB

	Blocking group	Soluble in HTPB (70 °C)	Cure of HTPB (120 °C)
5.1	diisopropylamine	yes	yes
5.2	ϵ -caprolactam	yes	no
5.4	3,3-dimethyl-2-butanone oxime	yes	yes
5.5	imidazole	no	no
5.6	2,6-dimethylphenol	no	no

These results identify that oxime-urethanes possess the ideal properties required for their potential employment in explosive formulations - soluble in HTPB, low volatility of

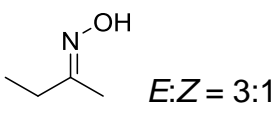
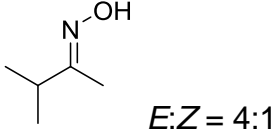
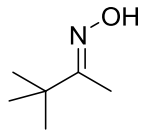
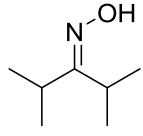
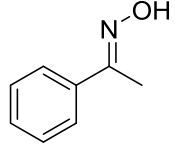
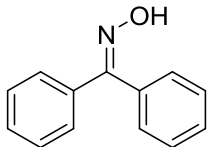
released oxime and relatively low dissociation temperature that could be decreased by modification of the steric and electronic properties of the oxime.

5.2.8. Effect of Steric Hindrance on the Dissociation of Oxime-Urethanes

Literature investigations have reported¹⁷ that the dissociation of oxime-urethanes is accelerated by increasing the steric hindrance of the oxime. In addition, results reported in **Chapter 2** describe how the increased steric hindrance of a benzophenone oxime analogue led to a reduction in the dissociation temperature. IPDI was reacted with a range of oximes in order to generate a library of IPDI-based oxime-urethanes that possess varying degrees of steric hindrance. All oximes with the exception of benzophenone oxime were afforded by the reaction of the corresponding ketones with hydroxylamine hydrochloride and triethylamine. The high steric hindrance of benzophenone prevented efficient reaction using triethylamine, thus the smaller base NaOH was employed. 2-Butanone oxime and 3-methyl-2-butanone oxime were obtained as a mixture of *E* and *Z* isomers, all other oximes were afforded isomerically pure. The dissociation temperature of the oxime-urethanes **5.12-16** was measured using VTIR spectroscopy and the results are listed in Table 5.4.

The least sterically encumbered oxime-urethane **5.12** dissociated at 135 °C. It was expected the dissociation of **5.13** would occur at the next highest temperature followed by **5.4**. However, the dissociation of **5.13** was observed 20 °C below that of **5.4**. This result suggests that sterically encumbered *Z*-oximes have a greater effect on the dissociation temperature than the corresponding *E*-isomer. Furthermore, the dissociation of **5.14** was observed at the same temperature as **5.13**. This steric effect was also observed in aromatic oximes, benzophenone-based oxime-urethane **5.16** dissociating at a lower temperature than the acetophenone analogue **5.15**.

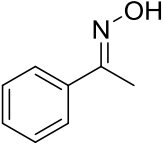
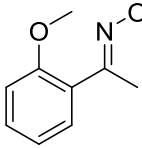
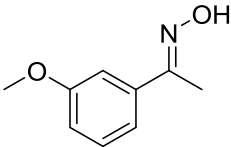
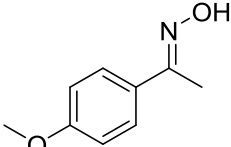
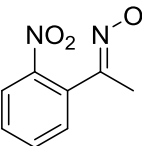
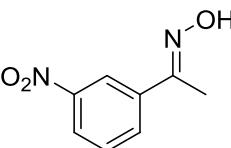
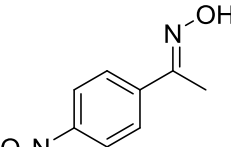
Table 5.4. Dissociation temperatures of IPDI blocked with a range of oximes possessing varying degrees of steric hindrance.

	Blocking Group	Dissociation Temperature (°C)
5.12	 <chem>CC(=NO)C</chem> $E:Z = 3:1$	135-140
5.13	 <chem>CC(C)C(=NO)C</chem> $E:Z = 4:1$	100-110
5.4	 <chem>CC(C)(C)C(=NO)C</chem>	110-120
5.14	 <chem>CC(C)C(C)C(=NO)C</chem>	90-100
5.15	 <chem>CC(=NO)c1ccccc1</chem>	120-130
5.16	 <chem>CC(=NO)c1ccccc1</chem>	95-100

5.2.9. Electronic Effects on the Dissociation of Oxime-Urethanes

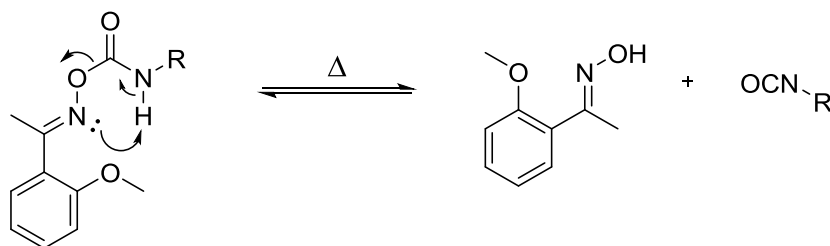
Alongside the effects of steric hindrance on the dissociation temperature of oxime-urethanes, the electronic effects were also investigated. A range of oxime-urethanes using acetophenone oxime analogues were generated that contain electron-withdrawing and electron donating moieties at the *ortho*, *meta*, and *para*-positions. The dissociation temperatures of the generated oxime-urethanes **5.23-28** were measured using VTIR spectroscopy (Table 5.5).

Table 5.5. Dissociation temperatures of IPDI blocked with a range of acetophenone oxime analogues that possess electron withdrawing or electron donating groups at the *ortho*, *meta* or *para* positions.

	Blocking Group	Dissociation Temperature (°C)
5.15		120-130
5.23	 <i>E:Z</i> = 9:1	90-100
5.24		100-110
5.25		120-130
5.26	 <i>E:Z</i> = 1:2	125-130
5.27		130-135
5.28		120-125

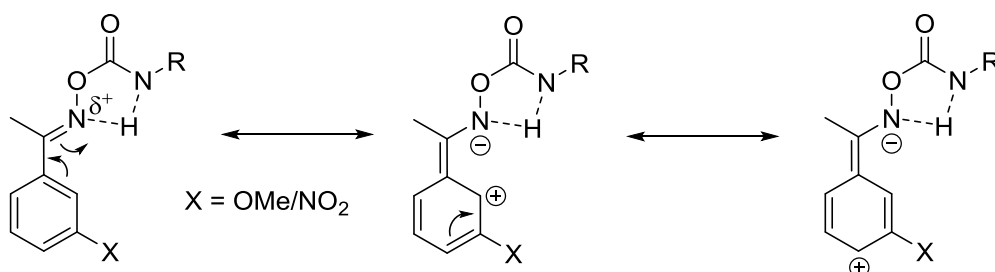
The dissociation temperature appeared to be significantly reduced by the presence of an electron donating group at the *ortho*-position **5.23**. The dissociation mechanism of oxime-urethanes proposed⁸ by Levine *et al.* occurs via a five-membered transition state, the close proximity of the polar methoxy moiety may have assisted the

dissociation (Scheme 5.7). However, the presence of an *ortho* nitro-substituent did not reduce the dissociation temperature.



Scheme 5.7. Dissociation mechanism of an oxime-urethane, showing the close proximity of the methoxy moiety.

The dissociation temperature was also decreased by the presence of an electron donating group at the *meta*-position and in turn increased by an electron withdrawing moiety - this trend is in agreement with literature studies.²⁶ The formation of the five-membered transition state proposed by Levine *et al.* may be stabilised by conjugation of the electrons within the aromatic system and thus forming an electron deficient centre at the *ortho*-position (Scheme 5.8). The electron withdrawing nitro moiety located *meta* on the aromatic ring further increases this electron deficiency and thus destabilises the system. In contrast, electron donating groups stabilise this transition state by providing electron density at the electron deficient centre.



Scheme 5.8. Conjugation of the dissociation transition state into the aromatic system.

The presence of *para*-substituents did not have any effect on the dissociation temperature, both **5.28** and **5.25** dissociating at 120 °C. Conjugation of these moieties did not contribute any stabilising or destabilising effect and were not in close proximity to the oxime-urethane bond to assist the dissociation.

5.2.10. Curing Studies of HTPB Using Oxime-Urethanes

The potential of the generated oxime-urethanes **5.12-28** to cure HTPB was investigated. Each oxime-urethane (8.01 mmol) was mixed with HTPB (18.22 g) and DBTDL (0.044 g) in ratios according to the Rowanex 1100 1A formulation using an overhead stirrer at 70 °C. All aliphatic oxime-urethanes exhibited excellent solubility in

HTPB at 70 °C, thus complete dispersion was achieved. In contrast, all of the aromatic oxime-urethanes exhibited poor solubility at 70 °C and uniform dispersion of **5.15,16** and **23** could only be achieved at high temperatures (> 100 °C) with vigorous mixing. Uniform dispersion of all of the other aromatic oxime-urethanes was not achieved.

The mixtures were heated to 120 °C for a period of 72 hours in an evacuated atmosphere. Cured HTPB was produced successfully using sterically encumbered aliphatic oxime-urethanes **5.13** and **5.14**. The generation of a polyurethane matrix was achieved using **5.15, 16** and **23**, however, the poor solubility of these oxime-urethanes led to separation from the polymer and the formation of crystallised regions was observed. The poor solubility of aromatic oximes **5.24-28** prevented the formation of a polyurethane matrix and only curing small regions of HTPB.

Table 5.6. Solubility and curing capability of oxime-urethanes **5.12-28** in HTPB.

	Blocking group	Soluble in HTPB (70 °C)	Cure of HTPB (120 °C)
5.12	2-Butanone oxime	yes	no
5.13	3-Methyl-2-butanone oxime	yes	yes
5.4	3,3-Dimethyl-2-butanone oxime	yes	yes
5.14	2,4-Dimethyl-3-pentanone oxime	yes	yes
5.15	Acetophenone oxime	no	yes
5.16	Benzophenone oxime	no	yes
5.23	<i>o</i> -Methoxyacetophenone oxime	no	yes
5.24	<i>m</i> -Methoxyacetophenone oxime	no	no
5.25	<i>p</i> -Methoxyacetophenone oxime	no	no
5.26	<i>o</i> -Nitroacetophenone oxime	no	no
5.27	<i>m</i> -Nitroacetophenone oxime	no	no
5.28	<i>p</i> -Nitroacetophenone oxime	no	no

5.2.11. Monitoring the Curing of HTPB

A variety of techniques can be employed to monitor the reaction of curing polyurethanes.²⁷ These include ¹H NMR spectroscopy,²⁸ IR spectroscopy,²⁹ differential scanning analysis (DSC),³⁰ swelling behaviour³¹ and tensile testing.²⁷

As a result of the high molecular weight and restricted mobility of the polymer chains in curing HTPB, traditional methods for observing chemical reaction using ¹H NMR spectroscopy is restricted. In addition, the elastomeric nature of the cured material prevented the preparation of a fine powder required for solid state NMR techniques.

In an IR spectrum, isocyanates exhibit a stretching vibration that appears as an absorption at 2250 cm⁻¹, thus observing the appearance of this characteristic absorption upon dissociation of the blocked isocyanate followed by its disappearance as the crosslinking reaction reaches completion could be an effective method for monitoring the curing reaction.²⁹ However, no absorption corresponding to the isocyanate was observed during curing, suggesting the reaction occurred immediately upon the dissociation of the blocked isocyanates.

As the curing reaction ensues, the crosslinking density in turn also increases, this may be observed by an increase in the glass transition temperature T_g as the mobility of the polymer chains decreases.³⁰ However, the glass transition of the fully cured polyurethane was below the detectable limits of DSC or indeed the high crosslinking density prevented the observation of a defined transition.

Tensile testing offers a route to monitor the curing reaction, as the curing reaction ensues and the crosslinking density increases, the elastic modulus ($=\Delta\text{stress}/\Delta\text{strain}$) is expected to increase.⁴ Tensile testing of the curing mixture of HTPB and **5.4** was measured at 24, 48 and 72 hours at 120 °C. In addition, tensile testing was performed on a control polyurethane generated from IPDI, HTPB and DBTDL cured for 72 hours at 60 °C in accordance with current processing conditions used for manufacture of Rowanex 1100 1A. An increase in the elastic modulus was observed after 48 hours and a small increase was observed after 72 hours, suggesting the majority of the curing had occurred within 48 hours at 120 °C. The elastic modulus of cured control polyurethane was significantly higher than the **5.4** mixture. A plasticising effect of the released oxime may account for this change in elastic modulus (Figure 5.7).

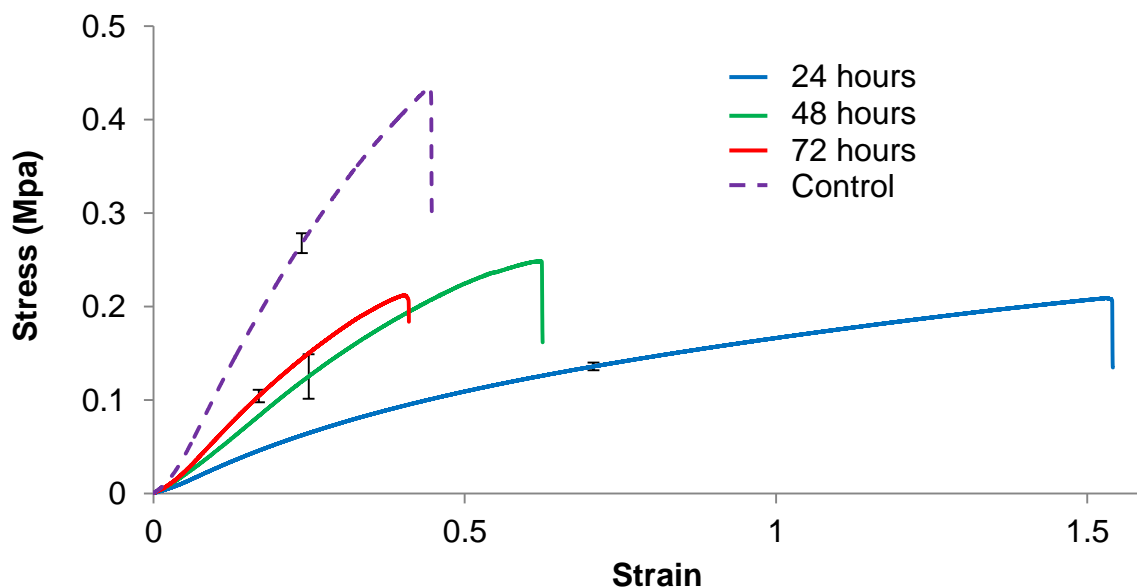


Figure 5.7. Stress-strain curves of curing HTPB using **5.4** at 24, 48 and 72 hours at 120 °C and control polyurethane.

A further technique that can be employed for monitoring the curing reaction is to measure the swelling behaviour of the polyurethane. Crosslinked polymers readily absorb organic solvents and as the crosslinking density of the polyurethane increases the permeation of solvent into the polymer in turn decreases.³⁰ Segments (~ 50 mg) of the polyurethane cured using **5.4** after 24, 48 and 72 hours were immersed in toluene (5 mL) and weighed after a period of 15 minutes. The swelling behaviour of the control polyurethane was also measured. Employing Equation 5.1 allows the calculation of parameter Q_{15} - moles of toluene absorbed by 1g of polymer after 15 minutes.

$$Q_{15} = \frac{M_s/M_{r_s}}{M_p} \times 1000 \quad \text{Equation 5.1}$$

Where M_s = mass of solvent absorbed (mg), M_{r_s} = molecular weight of solvent and M_p = initial mass of polymer (mg).

As the curing time increases the amount of toluene absorbed by the polymer decreases, suggesting the crosslinking density increases. A large decrease is observed after 48 hours and only a small change is observed after this time, implying that the majority of the curing has occurred within 48 hours supporting tensile testing results. In addition, there is only a small difference between the swelling behaviour of the polyurethane cured using **5.4** and the control polyurethane, further implying that almost complete crosslinking can be achieved using blocked isocyanates after 72 hours at 120°C (Figure 5.8). The swelling behaviour test revealed excellent

reproducibility with only a small range of error (< 0.6%) demonstrating how this simple reproducible test can be effectively employed to monitor the curing reaction.

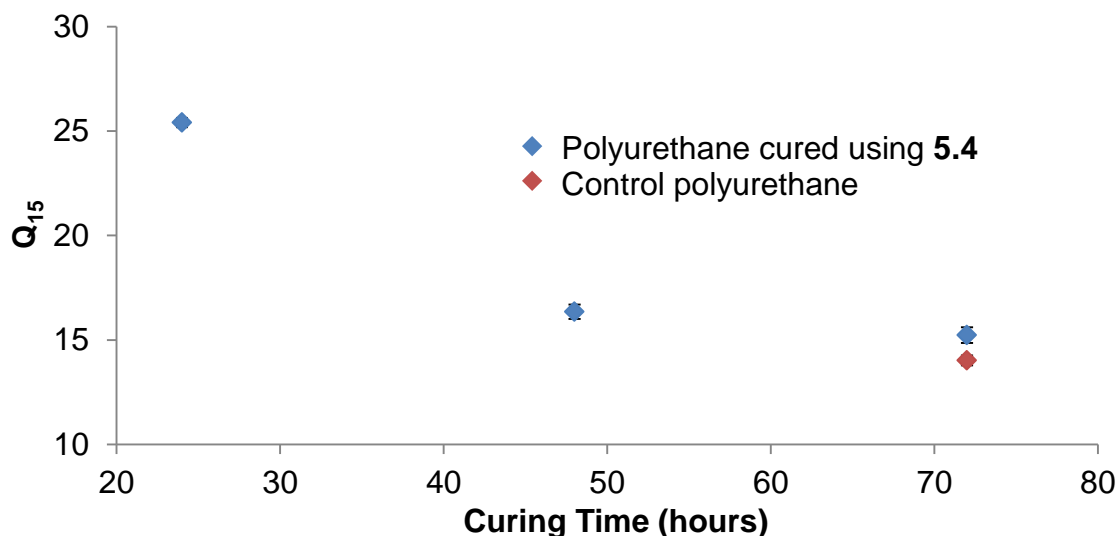


Figure 5.8. Swelling behaviour of polyurethane cured using **5.4** at 24, 48 and 72 hours at 120 °C and control polyurethane.

5.2.12. Synthesis of Blocked Isocyanate Prepolymer

Although most of the oxime-urethanes exhibited good solubility in HTPB at 70 °C, some oxime-urethanes, particularly **5.16** could not be easily dispersed, requiring temperatures up to 100 °C. This poor solubility caused a small quantity of the oxime-urethane to separate from the polymer and can be observed as dark crystallised regions in the cured polyurethane (Figure 5.9). The formation of a uniformly crosslinked polyurethane is desired, thus it was necessary to explore an alternative route to employ blocked isocyanates.



Figure 5.9. Image of a cured polyurethane using **5.4** observing dark crystallised regions in the cured polyurethane.

Benzophenone oxime and IPDI were reacted in a ratio of 1:2, this ensured a mixture of IPDI, mono-blocked IPDI and di-blocked IPDI was generated. To this mixture, HTPB

and DBTDL were added in order to afford an oligomeric mixture that contains benzophenone oxime-blocked HTPB based prepolymer **5.29** (Figure 5.10).

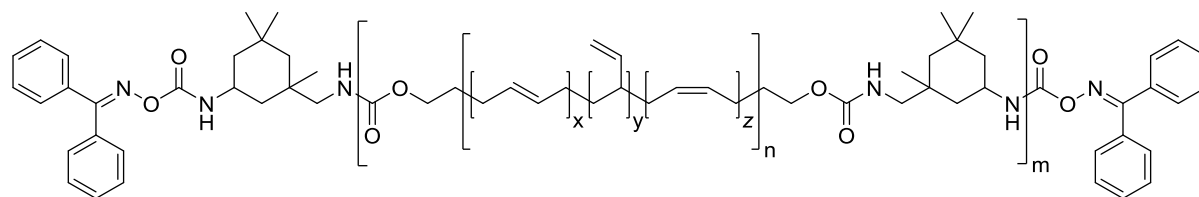


Figure 5.10. Structure of benzophenone oxime-blocked HTPB based prepolymer **5.29**.

The oligomeric mixture **5.29** was cured at 120 °C for a period of 72 hours and a uniformly crosslinked polyurethane was generated successfully. Swelling tests revealed that complete crosslinking was achieved after 72 hours (Figure 5.11).

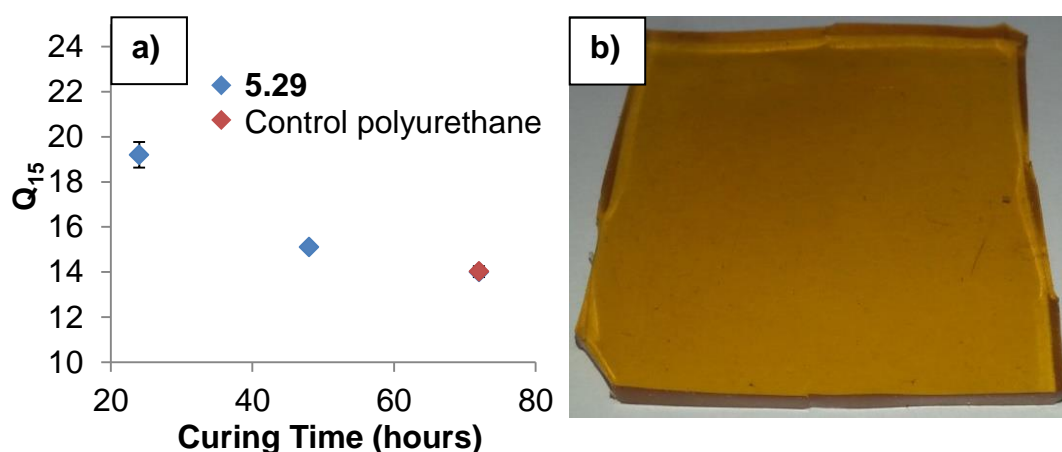


Figure 5.11. a) Swelling behaviour of polyurethane cured using **5.29** at 120 °C for 24, 48, 72 hours and control polyurethane at 72 hours. **b)** Image of cured **5.29** after 72 hours at 120 °C.

5.3. Conclusion

The synthesis of isocyanate crosslinkers blocked with amines, amides, oximes, aromatic heterocycles and phenols that can be cleaved using an application of heat has been achieved and this thermal reversibility has been confirmed using VTIR spectroscopy. The potential of these blocked isocyanates to cure hydroxy-functionalised polymers was investigated and oxime-urethanes were revealed to possess the ideal solubility and curing properties required for potential employment in explosive formulations. Increasing the steric hindrance on the oxime significantly reduced the dissociation temperature of the thermally-labile bond. In addition, the dissociation temperature can be reduced by the close proximity of electron donating groups to the oxime-urethane. The effect of electron donating and electron withdrawing *meta*-substituents was also investigated, electron donating methoxy

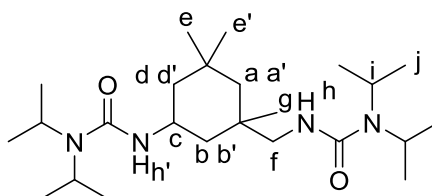
moieties reducing the dissociation temperature and electron withdrawing nitro functionality increasing the dissociation temperature. Methods to monitor the curing of polyurethane rubbers were investigated - tensile testing and swelling behaviour tests proved efficient methods of analysis. The poor solubility of certain aromatic oximeurethanes led to the formation of an inhomogeneously crosslinked rubber. The formation of blocked HTPB-based prepolymer was demonstrated to eliminate this problem and allowed the successful formation of a uniform polyurethane matrix.

5.4. Experimental

All chemical purification and experimental techniques employed in this chapter are identical to those described in **Chapter 2** and **3** with the exception of the following.

Gel permeation chromatography (GPC) was carried out using an Agilent Technologies 1260 Infinity Series Chromatograph employing an Agilent Technologies PLgel 5 μ m MIXED-D column (300 x 7.5 mm) eluting tetrahydrofuran (THF) at 40 °C calibrated with polystyrene standards. Tensile stress tests were carried out using a Stable Microsystems TA.XT Plus Texture Analyser.

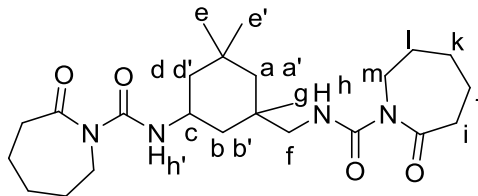
Synthesis of diisopropylamine-blocked IPDI **5.1**



Diisopropylamine (5.06 g, 50.0 mmol) and isophorone diisocyanate (IPDI) (5.30 g, 24.0 mmol) were dissolved in dichloromethane (100 mL) and stirred at room temperature for a period of 1 hour in an atmosphere of argon. The excess amine was removed by washing with HCl (1M) (3 x 50 mL) followed by NaHCO₃ (2 x 20 mL). The solution was dried over MgSO₄, filtered and solvent removed *in vacuo* to leave a white solid **5.1** (9.95 g, 99 %) (m.p. 72-75 °C). ¹H NMR (400 MHz, CDCl₃) δ _H (ppm): 0.87 (3H, m, H_e), 0.90 (1H, m, H_a), 0.93 (3H, s, H_g), 1.08 (1H, m, H_d), 1.09 (1H, m, H_b), 1.10 (3H, m, H_{e'}), 1.22 (1H, m, H_{a'}), 1.23 (24H, m, H_j), 1.74 (1H, m, H_{d'}), 1.80 (1H, m, H_{b'}), 3.05 (2H, m, H_f), 3.87 (4H, m, H_i), 4.03 (1H, m, H_c), 4.30 (1H, m, H_{h'}), 4.67 (1H, m, H_h); ¹³C NMR (100 MHz, CDCl₃) δ _C (ppm): 21.5, 23.4, 27.7, 32.1, 35.3, 36.4, 42.9, 43.7, 44.8, 47.3, 48.1, 54.7, 156.6, 157.5; FTIR (ATR) ν (cm⁻¹): 3361 (N-H), 2960 (C-H),

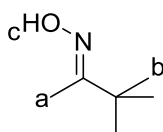
1620 (C=O), 1514 (N-H), 1327 (C-N); ESIMS calculated mass (C₂₄H₄₈O₂N₄+H)⁺ 425.3850 found 425.3841.

Synthesis of ϵ -caprolactam-blocked IPDI 5.2



IPDI (4.96 g, 22.3 mmol) and ϵ -caprolactam (7.57 g, 66.9 mmol) were dissolved in THF (100 mL) and maintained under reflux for a period of 18 hours in an atmosphere of argon. The solution was poured into water (500 mL) and decanted to leave a viscous colourless oil that was dissolved in THF (50 mL), dried over MgSO₄, filtered and the solvent removed *in vacuo* to yield a white solid **5.2** (9.79 g, 98 %) (m.p. 58-60 °C). ¹H NMR (400 MHz, CDCl₃) δ_{H} (ppm): 0.93 (3H, s, H_e), 1.00 (2H, m, H_{bd}), 1.03 (3H, s, H_g), 1.08 (3H, s, H_{e'}), 1.08 (1H, m, H_a), 1.26 (1H, m, H_{a'}), 1.72 (2H, m, H_k), 1.76 (2H, m, H_j), 1.78 (2H, m, H_i), 1.78 (2H, m, H_{b'd'}), 2.71 (2H, m, H_i), 3.07 (2H, m, H_f), 3.98 (2H, m, H_m), 4.04 (1H, m, H_c), 9.13 (1H, m, H_{h'}), 9.44 (1H, m, H_h); ¹³C NMR (100 MHz, CDCl₃) δ_{C} (ppm): 23.4, 23.4, 27.6, 28.3, 29.1, 31.8, 35.1 36.1, 39.8, 41.8, 43.8, 44.3, 46.0, 47.4, 54.7, 154.0, 155.2, 179.3; FTIR (ATR) ν (cm⁻¹): 3260 (N-H), 1694 (C=O amide), 1651 (C=O urea), 1163 (C-N); ESIMS calculated mass (C₂₄H₄₀O₄N₄+Na)⁺ 471.2942 found 471.2935.

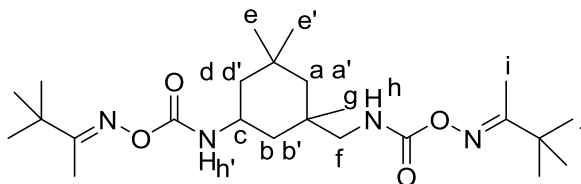
Synthesis of 3,3-dimethyl-2-butanone oxime 5.3³²



Hydroxylamine hydrochloride (10.15 g, 146.0 mmol), triethylamine (14.77 g, 146.0 mmol) and 3,3-dimethyl-2-butanone (13.28 g, 133.0 mmol) were dissolved in EtOH (100 mL) and maintained under reflux for a period of 4 hours. The solvent was removed *in vacuo* and the product extracted with Et₂O to afford a white solid **5.3** (12.73 g, 83 %) (m.p. 73-76 °C, lit. 75-76°C). ¹H NMR (400 MHz, CDCl₃) δ_{H} (ppm): 1.07 (9H, s, H_b), 1.81 (3H, s, H_a), 9.70 (1H, br., H_c); ¹³C NMR (100 MHz, CDCl₃) δ_{C}

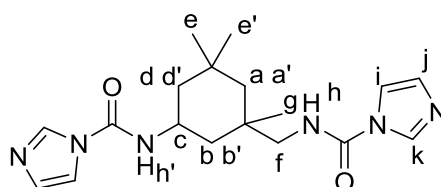
(ppm): 10.1, 27.5, 37.2, 164.2; FTIR (ATR) ν (cm^{-1}): 3236 (O-H), 1661 (C=N), 929 (N-O); ESIMS calculated mass $(\text{C}_6\text{H}_{13}\text{ON}+\text{H})^+$ 116.1070 found 116.1067.

Synthesis of 3,3-dimethyl-2-butanone oxime-blocked IPDI **5.4**



3,3-Dimethyl-2-butanone oxime **5.3** (12.73 g, 110.5 mmol) and IPDI (12.28 g, 55.3 mmol) were dissolved in THF (150 mL) and maintained under reflux for a period of 18 hours in an atmosphere of argon. The solvent was removed *in vacuo* to leave a white solid **5.4** (24.90 g, 99 %) (m.p. 57-61 °C). ^1H NMR (400 MHz, CDCl_3) δ_{H} (ppm): 0.96 (6H, s, H_{eg}), 0.99 (2H, m, H_{bd}), 1.10 (1H, m, H_{a}), 1.13 (3H, s, $\text{H}_{\text{e'}}$), 1.18 (18H, m, H_{j}) 1.25 (1H, m, $\text{H}_{\text{a'}}$), 1.83 (2H, m, $\text{H}_{\text{b'd'}}$), 2.00 (6H, m, H_{i}), 3.07 (2H, m, H_{f}), 3.96 (1H, m, H_{c}), 6.13 (1H, m, $\text{H}_{\text{h'}}$), 6.58 (1H, m, H_{h}); ^{13}C NMR (100 MHz, CDCl_3) δ_{C} (ppm): 12.1, 23.4, 27.3, 30.0, 31.9, 35.1, 36.4, 37.9, 42.8, 44.6, 46.9, 47.2, 54.7, 155.1, 156.3, 169.0; FTIR (ATR) ν (cm^{-1}): 3408 (N-H), 1726 (C=O), 1638 (C=N), 1495 (C-N), 997 (C-O), 904 (N-O); ESIMS calculated mass $(\text{C}_{24}\text{H}_{44}\text{O}_4\text{N}_4+\text{H})^+$ 453.3435 found 453.3435.

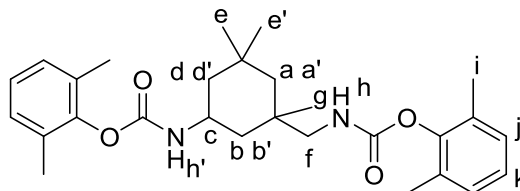
Synthesis of imidazole-blocked IPDI **5.5**



Imidazole (3.80 g, 55.8 mmol) and IPDI (6.2 g, 27.9 mmol) were dissolved in tetrahydrofuran (THF) (100 mL) and stirred for a period of 2 hours at room temperature in an atmosphere of argon. The solvent was removed *in vacuo* to leave a white solid **5.5** (9.8 g, 98 %) (m.p. 85-89 °C). ^1H NMR (400 MHz, CDCl_3) δ_{H} (ppm): 0.97 (3H, s, H_{e}), 1.13 (3H, s, H_{g}), 1.19 (3H, s, $\text{H}_{\text{e'}}$), 1.19 (2H, m, H_{bd}), 1.25 (1H, m, H_{a}), 1.32 (1H, m, $\text{H}_{\text{a'}}$), 1.80 (2H, m, $\text{H}_{\text{b'd'}}$), 3.20 (2H, m, H_{f}), 4.18 (1H, m, H_{c}), 7.01 (2H, m, H_{j}), 7.60 (1H, m, H_{h}) 7.65 (2H, m, H_{i}), 7.86 (1H, m, H_{h}), 8.22 (2H, m, H_{k}); ^{13}C NMR (100 MHz, CDCl_3) δ_{C} (ppm): 23.8, 28.0, 29.7, 35.5, 37.9, 41.7, 45.7, 46.0, 47.7, 54.8, 117.1,

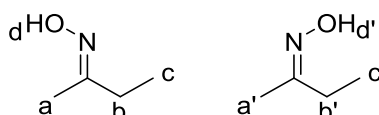
130.6, 136.7, 149.2, 150.6; FTIR (ATR) ν (cm^{-1}): 3223 (N-H), 1698 (C=O), 1282 (C-N); ESIMS calculated mass ($\text{C}_{18}\text{H}_{26}\text{O}_2\text{N}_6+\text{H}$)⁺ 359.2190 found 359.2190.

Synthesis of 2,6-dimethylphenol-blocked IPDI **5.6**



2,6-Dimethylphenol (5.0 g, 40.9 mmol), IPDI (4.55 g, 20.46 mmol) and dibutyltin dilaurate (DBTDL) (0.387 g, 0.6 mmol) were dissolved in THF (100 ml) and maintained under reflux for a period of 24 hours under an atmosphere of argon. The product was precipitated in hexane (300 mL), filtered, washed with a further portion of hexane (200 mL) and dried under high vacuum to leave a white solid **5.6** (8.95, 94 %) (m.p. 80-84 °C). ¹H NMR (400 MHz, CDCl₃) δ_{H} (ppm): 0.96 (3H, s, H_e), 1.01 (2H, m, H_{bd}), 1.09 (3H, s, H_g), 1.12 (3H, s, H_{e'}), 1.12 (1H, m, H_a), 1.25 (1H, m, H_{a'}), 1.83 (2H, m, H_{b'd'}), 2.20 (12H, m, H_i), 3.03 (2H, m, H_f), 3.90 (1H, m, H_c), 6.74 (1H, m, H_{h'}), 6.95 (1H, m, H_h), 7.04 (6H, m, H_{jk}); ¹³C NMR (100 MHz, CDCl₃) δ_{C} (ppm): 15.9, 23.2, 27.6, 31.9, 35.1, 36.6, 41.7, 45.0, 46.2, 47.1, 55.1, 120.1, 125.6, 128.5, 130.9, 153.3, 154.5; FTIR (ATR) ν (cm^{-1}): 3314 (N-H), 1706 (C=O), 1241 (C-N), 1174 (C-O); ESIMS calculated mass ($\text{C}_{28}\text{H}_{38}\text{O}_4\text{N}_2+\text{Na}$)⁺ 489.2724 found 489.2711.

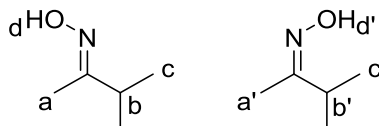
Synthesis of 2-butanone oxime **5.7**³²



2-Butanone (14.4 g, 200 mmol), hydroxylamine hydrochloride (15.3 g, 220 mmol) and triethylamine (22.26 g, 220 mmol) were dissolved in MeOH (200 mL) and maintained under reflux for a period of 4 hours. The solvent was removed *in vacuo* and the product extracted with Et₂O to give a colourless oil **5.7** (16.8 g, 96 %) (*E*:*Z*, 3:1). (*E*)-2-butanone oxime: ¹H NMR (400 MHz, CDCl₃) δ_{H} (ppm): 1.01 (3H, t J = 7.5 Hz, H_c), 1.81 (3H, s, H_a), 2.15 (2H, q J = 7.5 Hz, H_b), 9.79 (1H, br., H_d); ¹³C NMR (100 MHz, CDCl₃) δ_{C} (ppm): 10.7, 13.2, 29.1, 159.4; (*Z*)-2-butanone oxime: ¹H NMR (400 MHz, CDCl₃) δ_{H} (ppm): 1.00 (3H, t J = 8.0 Hz, H_{a'}), 1.80 (3H, s, H_{c'}), 2.33 (2H, q J = 8.0 Hz, H_{b'}), 9.79 (1H, br., H_{d'}); ¹³C NMR (100 MHz, CDCl₃) δ_{C} (ppm): 9.8, 19.1, 21.8, 159.9; FTIR (ATR)

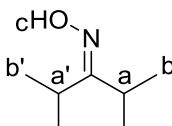
ν (cm^{-1}): 3232 (O-H), 1664 (C=N), 929 (N-O); ESIMS calculated mass ($\text{C}_4\text{H}_9\text{ON}+\text{H}$)⁺ 88.0757 found 88.0753.

Synthesis of 3-methyl-2-butanone oxime **5.8**³²



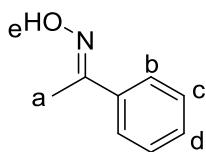
Hydroxylamine hydrochloride (9.00 g, 129.0 mmol), triethylamine (13.1 g, 129.0 mmol) and 3-methyl-2-butanone (10.16 g, 118 mmol) were dissolved in EtOH (50 mL) and maintained under reflux for a period of 4 hours. The solvent was removed *in vacuo* and the product extracted with Et₂O to yield a colourless oil **5.8** (11.63 g, 97 %) (*E:Z*, 4:1). (*E*)-3-methyl-2-butanone oxime: ¹H NMR (400 MHz, CDCl₃) δ_{H} (ppm): 1.10 (6H, d $J = 7.0$ Hz, H_c), 1.86 (3H, s, H_a), 2.51 (1H, hept. $J = 7.0$ Hz, H_b) 9.79 (1H, br., H_d); ¹³C NMR (100 MHz, CDCl₃) δ_{C} (ppm): 11.1, 19.6, 34.4, 162.4; (*Z*)-3-methyl-2-butanone oxime: ¹H NMR (400 MHz, CDCl₃) δ_{H} (ppm): 1.05 (6H, d $J = 7.0$ Hz, H_{c'}), 1.79 (3H, s, H_{a'}), 3.48 (1H, hept. $J = 7.0$ Hz, H_{b'}), 9.79 (1H, br., H_{d'}); ¹³C NMR (100 MHz, CDCl₃) δ_{C} (ppm): 15.3, 18.8, 25.7, 162.9; FTIR (ATR) ν (cm^{-1}): 3252 (O-H), 1657 (C=N), 937 (N-O); ESIMS calculated mass ($\text{C}_5\text{H}_{11}\text{ON}+\text{H}$)⁺ 102.0913 found 102.0909.

Synthesis of 2,4-dimethyl-3-pentanone oxime **5.9**³²



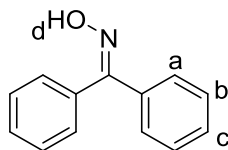
Hydroxylamine hydrochloride (3.20 g, 46.0 mmol), triethylamine (4.65 g, 46.0 mmol) and 2,4-dimethyl-3-pentanone (4.80 g, 42.0 mmol) were dissolved in EtOH (50 mL) and maintained under reflux for a period of 4 hours. The solvent was removed *in vacuo* and the product extracted with Et₂O to yield a white solid **5.9** (4.50 g, 83 %) (m.p. 33-34 °C, lit. 33-34 °C). ¹H NMR (400 MHz, CDCl₃) δ_{H} (ppm): 1.06 (6H, d $J = 7.0$ Hz, H_b), 1.10 (6H, d $J = 7.5$ Hz, H_{b'}), 2.49 (1H, hept. $J = 7.0$ Hz, H_a), 3.14 (1H, hept. $J = 7.5$ Hz, H_{a'}), 9.75 (1H, br., H_c); ¹³C NMR (100 MHz, CDCl₃) δ_{C} (ppm): 18.8, 21.3, 27.5, 30.7, 168.5; FTIR (ATR) ν (cm^{-1}): 3266 (O-H), 1651 (C=N), 941 (N-O); ESIMS calculated mass ($\text{C}_7\text{H}_{15}\text{ON}+\text{H}$)⁺ 130.1226 found 130.1223.

Synthesis of acetophenone oxime **5.10**³²



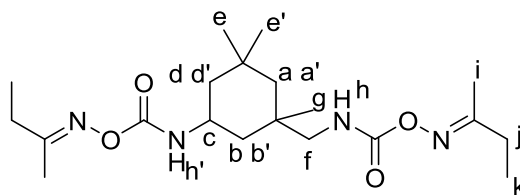
Hydroxylamine hydrochloride (3.89 g, 56.0 mmol), triethylamine (5.66 g, 56.0 mmol) and acetophenone (6.13 g, 51.0 mmol) were dissolved in EtOH (100 mL) and maintained under reflux for a period of 18 hours. The solvent was removed *in vacuo* and the product extracted with Et₂O to yield a white solid **5.10** (5.75 g, 94 %) (m.p. 54-55 °C, lit. 55-60 °C). ¹H NMR (400 MHz, CDCl₃) δ_H (ppm): 2.31 (3H, s, H_a), 7.39 (3H, m, H_{bd}), 7.63 (2H, m, H_c), 9.43 (1H, br., H_e); ¹³C NMR (100 MHz, CDCl₃) δ_C (ppm): 12.4, 126.1, 128.6, 129.3, 136.5, 156.0; FTIR (ATR) ν (cm⁻¹): 3235 (O-H), 1599 (C=N), 923 (N-O); ESIMS calculated mass (C₈H₉ON+H)⁺ 136.0757 found 136.0754.

Synthesis of benzophenone oxime **5.11**³³



Benzophenone (5.00 g, 27.4 mmol), hydroxylamine hydrochloride (3.82 g, 54.8 mmol) and sodium hydroxide (2.02 g, 54.8 mmol) were dissolved in MeOH (40 ml) for 18 hours. The solution was precipitated into H₂O, filtered and dried under high vacuum to give a white solid **5.11** (5.38 g, 99 %) (m.p. 136-140 °C, lit. 139-141 °C). ¹H NMR (400 MHz, CDCl₃) δ_H (ppm): 7.30-7.47 (10H, m, H_{abc}), 9.08 (1H, br., H_d); ¹³C NMR (100 MHz, CDCl₃) δ_C (ppm): 127.9, 128.2, 128.3, 121.9, 129.2, 129.5, 132.7, 136.2, 158.0; FTIR (ATR) ν (cm⁻¹): 3222 (O-H), 3056 (C-H), 1444 (C=N), 918 (N-O); ESIMS calculated mass (C₁₃H₁₁ON+H)⁺ 198.0913 found 198.0910.

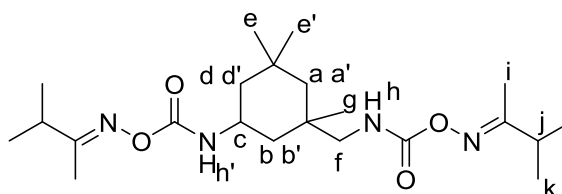
Synthesis of 2-butanone oxime-blocked IPDI **5.12**



Isophorone diisocyanate (11.21 g, 50.0 mmol) and 2-butanone oxime **5.7** (8.79 g, 100.0 mmol) were dissolved in THF (100 mL) and maintained under reflux for a period

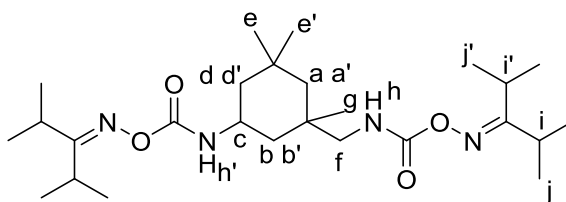
of 18 hours. The solvent was removed *in vacuo* to give a white solid **5.12** (19.38 g, 98 %), (m.p. 65-69 °C). ^1H NMR (400 MHz, CDCl_3) δ_{H} (ppm): 0.96 (6H, s, H_{eg}), 1.01 (2H, m, H_{db}), 1.10 (1H, m, H_{a}), 1.12 (3H, s, $\text{H}_{\text{e}'}$), 1.17 (6H, m, H_{k}), 1.27 (1H, m, $\text{H}_{\text{a}'}$), 1.82 (2H, m, $\text{H}_{\text{b'd}'}$), 1.96-2.01 (6H, m, H_{i}), 2.30-2.49 (4H, m, H_{j}), 3.06 (2H, m, H_{f}), 3.96 (1H, m, H_{c}), 6.12 (1H, m, $\text{H}_{\text{h}'}$), 6.47 (1H, m, H_{h}); ^{13}C NMR (100 MHz, CDCl_3) δ_{C} (ppm): 10.4, 15.2, 19.4, 23.7, 27.7, 29.2, 35.1, 41.6, 44.7, 46.2, 47.2, 54.7, 154.9, 156.2, 164.4; FTIR (ATR) ν (cm^{-1}): 3404 (N-H), 2952 (C-H), 1714 (C=O), 1651 (C=N), 1504 (C-N), 1001 (C-O), 905 (N-O); ESIMS calculated mass ($\text{C}_{20}\text{H}_{36}\text{O}_4\text{N}_4+\text{Na}$) $^+$ 419.2629 found 419.2627.

Synthesis of 3-methyl-2-butanone oxime-blocked IPDI **5.13**



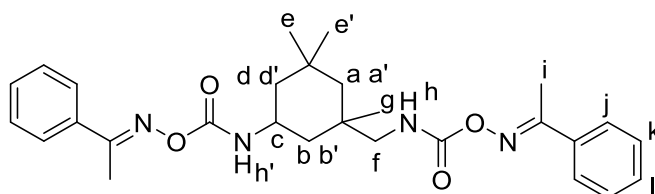
Isophorone diisocyanate (12.78 g, 57.5 mmol) and 3-methyl-2-butanone oxime **5.8** (11.63 g, 115.0 mmol) were dissolved in THF (60 ml) and maintained under reflux for 18 hours in an atmosphere of argon. The solvent was removed *in vacuo* to leave a white solid **5.13** (15.0 g, 63 %) (m.p. 45-49 °C). ^1H NMR (400 MHz, CDCl_3) δ_{H} (ppm): 0.96 (6H, s, H_{eg}), 1.01 (2H, m, H_{bd}), 1.05 (3H, s, $\text{H}_{\text{e}'}$), 1.05 (1H, m, H_{a}), 1.12 (12H, m, H_{k}), 1.27 (1H, m, $\text{H}_{\text{a}'}$), 1.79 (2H, m, $\text{H}_{\text{b'd}'}$), 1.98-2.00 (6H, m, H_{i}), 2.30-2.49 (2H, m, H_{j}), 3.06 (2H, m, H_{f}), 3.95 (1H, m, H_{c}), 6.12 (1H, m, $\text{H}_{\text{h}'}$), 6.47 (1H, m, H_{h}); ^{13}C NMR (100 MHz, CDCl_3) δ_{C} (ppm): 10.4, 15.1, 19.4, 23.7, 27.7, 29.2, 31.8, 35.1, 36.5, 41.6, 44.7, 46.2, 47.2, 54.7, 154.9, 156.2, 164.3; FTIR (ATR) ν (cm^{-1}): 3411 (N-H), 2962 (C-H), 1723 (C=O), 1644 (C=N), 1498 (C-N), 999 (C-O), 911 (N-O); ESIMS calculated mass ($\text{C}_{22}\text{H}_{40}\text{O}_4\text{N}_4+\text{H}$) $^+$ 425.3122 found 425.3124.

Synthesis of 2,4-dimethylpentanone oxime-blocked IPDI **5.14**



Isophorone diisocyanate (4.00 g, 18.0 mmol) and 2,4-dimethyl-3-pentanone oxime **5.9** (4.65 g, 36.0 mmol) were dissolved in THF (100 ml) and maintained under reflux for 18 hours. The solvent was removed *in vacuo* to leave a white solid **5.14** (8.50 g, 98 %) (m.p. 56-62 °C). ^1H NMR (400 MHz, CDCl_3) δ_{H} (ppm): 0.96 (6H, s, H_{eg}), 0.96 (3H, s, $\text{H}_{\text{e}'}$), 1.01 (1H, m, H_{d}), 1.04 (1H, m, H_{b}), 1.10 (1H, m, H_{a}), 1.15 (12H, m, H_{j}), 1.17 (12H, m, $\text{H}_{\text{j}'}$), 1.28 (1H, m, $\text{H}_{\text{a}'}$), 1.84 (2H, m, $\text{H}_{\text{b'd'}}$), 2.64 (2H, m, H_{i}), 3.06 (2H, m, H_{f}), 3.23 (2H, m, $\text{H}_{\text{f}'}$), 3.96 (1H, m, H_{c}), 6.12 (1H, m, $\text{H}_{\text{h'}}$), 6.54 (1H, m, H_{h}); ^{13}C NMR (100 MHz, CDCl_3) δ_{C} (ppm): 19.0, 21.0, 21.2, 29.2, 29.2, 31.4, 35.1, 36.4, 41.7, 44.6, 46.2, 47.3, 54.7, 155.0, 156.3, 173.8; FTIR (ATR) ν (cm^{-1}): 3408 (N-H), 1728 (C=O), 1635 (C=N), 1496 (C-N), 991 (C-O), 898 (N-O); ESIMS calculated mass ($\text{C}_{26}\text{H}_{48}\text{O}_4\text{N}_4+\text{H}$) $^+$ 481.3748 found 481.3745.

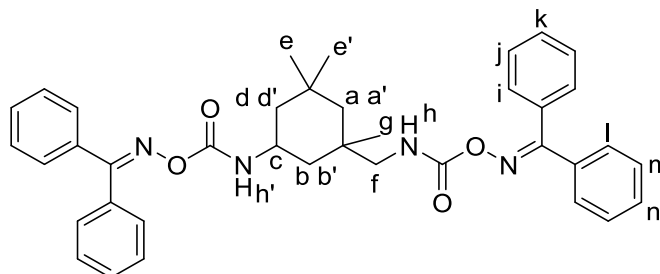
Synthesis of acetophenone oxime-blocked IPDI **5.15**



Isophorone diisocyanate (4.73 g, 21.3 mmol) and acetophenone oxime **5.10** (5.75 g, 42.5 mmol) were dissolved in THF (100 ml) and maintained under reflux for 18 hours. The solvent was removed *in vacuo* to leave a white solid **5.15** (10.43 g, 99 %), (m.p. 72-74 °C). ^1H NMR (400 MHz, CDCl_3) δ_{H} (ppm): 0.97 (6H, s, H_{eg}), 1.05 (2H, m, H_{bd}), 1.12 (3H, s, $\text{H}_{\text{e}'}$), 1.17 (1H, m, H_{a}), 1.27 (1H, m, $\text{H}_{\text{a}'}$), 1.85 (2H, m, $\text{H}_{\text{b'd'}}$), 2.43 (6H, s, H_{i}), 3.14 (2H, m, H_{f}), 4.02 (1H, m, H_{c}), 6.25 (1H, m, $\text{H}_{\text{h'}}$), 6.60 (1H, m, H_{h}), 7.45 (4H, m, H_{k}), 7.45 (2H, m, H_{l}), 7.66 (4H, m, H_{k}); ^{13}C NMR (100 MHz, CDCl_3) δ_{C} (ppm): 14.6, 23.3, 27.7, 32.0, 35.1, 36.6, 41.7, 44.9, 46.2, 47.2, 54.9, 126.8, 128.8, 130.5, 134.9, 154.6, 156.0, 160.1; FTIR (ATR) ν (cm^{-1}): 3319 (N-H), 1722 (C=O), 1622 (C=N), 1495

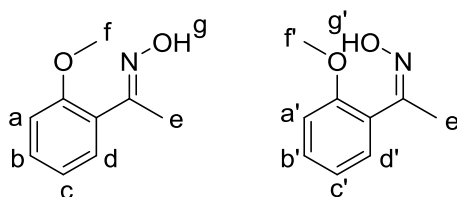
(C-N), 989 (C-O), 912 (N-O); ESIMS calculated mass (C₂₈H₃₆O₄N₄+Na)⁺ 515.2629 found 515.2622

Synthesis of benzophenone oxime-blocked IPDI **5.16**



Isophorone diisocyanate (3.01 g, 13.5 mmol) and benzophenone oxime **5.11** (5.34 g, 27.1 mmol) were dissolved in THF (40 ml) and refluxed for 18 hours under an atmosphere of argon. The solvent was removed to give a white solid **5.16** (8.14 g, 97 %), (m.p. 93-96 °C). ¹H NMR (400 MHz, CDCl₃) δ_H (ppm): 0.98 (6H, s, H_{eg}), 0.99 (3H, s, H_{e'}), 1.06 (2H, m, H_{bd}), 1.16 (1H, m, H_a), 1.28 (1H, m, H_{a'}), 1.86 (2H, m, H_{b'd'}), 3.10 (2H, m, H_f), 4.01 (1H, m, H_c), 6.14 (1H, m, H_{h'}), 6.53 (1H, m, H_h), 7.38 (8H, m, H_{il}), 7.45 (4H, m, H_{nk}), 7.50 (8H, m, H_{jm}); ¹³C NMR (100 MHz, CDCl₃) δ_C (ppm): 29.8, 32.0, 35.1, 35.1, 36.5, 41.7, 45.7, 46.2, 47.2, 54.9, 128.3, 128.9, 129.9, 129.4, 130.8, 132.0, 135.1, 154.4, 155.8, 161.4; FTIR (ATR) ν (cm⁻¹): 3408 (N-H), 1728 (C=O), 1638 (C=N), 1493 (C-N), 959 (C-O), 910 (N-O); ESIMS calculated mass (C₃₈H₄₀O₄N₄+Na)⁺ 639.2942 found 639.2936.

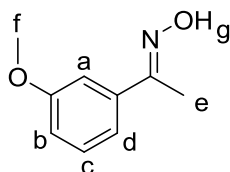
Synthesis of *o*-methoxyacetophenone oxime **5.17**³⁴



Hydroxylamine hydrochloride (5.53 g, 79.6 mmol), *o*-methoxyacetophenone (10.87 g, 72.4 mmol) and triethylamine (8.05 g, 79.6 mmol) were dissolved in EtOH (100 mL) and maintained under reflux for a period of 18 hours. The solvent was removed *in vacuo* and the product extracted with EtOAc. The organic phase was washed with H₂O (3 x 50 mL), dried over MgSO₄ and then filtered. The solvent was removed *in vacuo* to leave a white solid **5.17** (11.80 g, 99 %) (m.p. 83-86 °C, lit. 96-97 °C) (*E:Z*, 9:1). (*E*)-*o*-methoxyacetophenone oxime: ¹H NMR (400 MHz, CDCl₃) δ_H (ppm): 2.24 (3H, s, H_e),

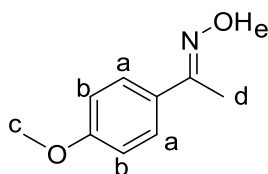
3.83 (3H, s, H_f), 6.92 (1H, d *J* = 8.0 Hz, H_a), 6.96 (1H, td *J* = 7.5, 1.0 Hz, H_c), 7.30 (1H, m, H_b), 7.32 (1H, m, H_d), 9.43 (1H, br., H_g); ¹³C NMR (100 MHz, CDCl₃) δ_C (ppm): 15.2, 55.4, 111.1, 120.6, 126.8, 129.4, 130.2, 156.8, 157.4; (*Z*)-*o*-methoxyacetophenone oxime: ¹H NMR (400 MHz, CDCl₃) δ_H (ppm): 2.18 (3H, s, H_{e'}), 3.82 (3H, s, H_f), 6.96 (1H, d *J* = 8.0 Hz, H_{a'}), 6.99 (1H, td *J* = 7.5, 1.0 Hz, H_{c'}), 7.30 (1H, m, H_{b'}), 7.35 (1H, m, H_{d'}), 8.52 (1H, br., H_g); ¹³C NMR (100 MHz, CDCl₃) δ_C (ppm): 21.4, 55.6, 111.2, 120.5, 124.2, 128.4, 129.9, 156.8, 157.4; FTIR (ATR) ν (cm⁻¹): 3210 (O-H), 2962 (C-H), 1460 (C=N), 1023 (C-O), 915 (N-O); ESIMS calculated mass (C₉H₁₁O₂N+H)⁺ 166.0863 found 166.0860.

Synthesis of *m*-methoxyacetophenone oxime **5.18**³⁴



Hydroxylamine hydrochloride (5.53 g, 79.6 mmol), *m*-methoxyacetophenone (10.87 g, 72.4 mmol) and triethylamine (8.05 g, 79.6 mmol) were dissolved in EtOH (100 mL) and maintained under reflux for a period of 18 hours. The solvent was removed *in vacuo* and the product extracted with EtOAc. The organic phase was washed with H₂O (3 x 50 mL), dried over MgSO₄ and then filtered. The solvent was removed *in vacuo* to leave a white solid **5.18** (11.59 g, 99 %) (m.p. 44-45 °C, lit. 44-45 °C). ¹H NMR (400 MHz, CDCl₃) δ_H (ppm): 2.29 (3H, s, H_e), 3.82 (3H, s, H_f), 6.92 (1H, ddd *J* = 8.0, 3.0, 1.0 Hz H_c), 7.20 (2H, m, H_{ab}), 7.29 (1H, d *J* = 8.0 Hz, H_d), 9.76 (1H, br., H_g); ¹³C NMR (100 MHz, CDCl₃) δ_C (ppm): 12.5, 55.3, 111.14, 115.1, 118.7, 129.6, 137.9, 156.0, 159.7; FTIR (ATR) ν (cm⁻¹): 3234 (O-H), 2938 (C-H), 1578 (C=N), 1038 (C-O), 939 (N-O); ESIMS calculated mass (C₉H₁₁O₂N+H)⁺ 166.0863 found 166.0859.

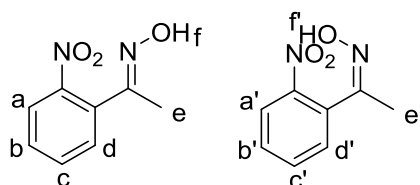
Synthesis of *p*-methoxyacetophenone oxime **5.19**³⁴



Hydroxylamine hydrochloride (5.53 g, 79.6 mmol), *p*-methoxyacetophenone (10.87 g, 72.4 mmol) and triethylamine (8.05 g, 79.6 mmol) were dissolved in EtOH (100 mL)

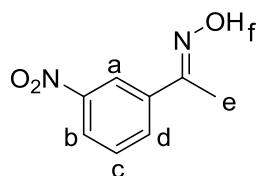
and maintained under reflux for a period of 18 hours. The solvent was removed *in vacuo* and the product extracted with EtOAc. The organic phase was washed with H₂O (3 x 50 mL), dried over MgSO₄ and then filtered. The solvent was removed *in vacuo* to leave a white solid **5.19** (11.48 g, 96 %) (m.p. 82-84 °C, lit. 85-86 °C). ¹H NMR (400 MHz, CDCl₃) δ_H (ppm): 2.28 (3H, s, H_d), 3.82 (3H, s, H_c), 6.90 (2H, d *J* = 9.0 Hz, H_b), 7.57 (2H, d *J* = 9.0 Hz, H_a), 9.61 (1H, br., H_e); ¹³C NMR (100 MHz, CDCl₃) δ_C (ppm): 12.3, 55.3, 113.9, 127.4, 129.0, 155.5, 160.5; FTIR (ATR) ν (cm⁻¹): 3212 (O-H), 2936 (C-H), 1514 (C=N), 1023 (C-O), 920 (N-O); ESIMS calculated mass (C₉H₁₁O₂N+H)⁺ 166.0863 found 166.0859.

Synthesis of *o*-nitroacetophenone oxime **5.20**³⁴



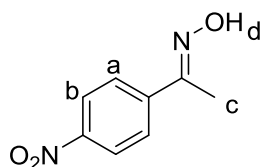
Hydroxylamine hydrochloride (5.27 g, 75.9 mmol), *o*-nitroacetophenone (11.34 g, 69.0 mmol) and triethylamine (7.68 g, 75.9 mmol) were dissolved in EtOH (100 mL) and maintained under reflux for a period of 18 hours. The solvent was removed *in vacuo* and the product extracted with EtOAc. The organic phase was washed with H₂O (3 x 50 mL), dried over MgSO₄ and then filtered. The solvent was removed *in vacuo* to leave a white solid **5.20** (11.60 g, 93 %) (m.p. 83-86 °C, lit. 118-119 °C) (*E:Z*, 1:2). (*E*)-*o*-nitroacetophenone oxime: ¹H NMR (400 MHz, Acetone-d₆) δ_H (ppm): 2.21 (3H, s, H_e), 7.65 (1H, dd *J* = 8.0, 1.5 Hz, H_d), 7.63 (1H, td *J* = 8.0, 1.5 Hz, H_b), 7.76 (1H, td *J* = 8.0, 1.5 Hz, H_c), 7.95 (1H, dd *J* = 8.0, 1.5 Hz, H_a), 10.55 (1H, s, H_f); ¹³C NMR (100 MHz, Acetone-d₆) δ_C (ppm): 14.8, 125.0, 130.3, 131.2, 133.7, 132.2, 133.9, 153.5; (*Z*)-*o*-nitroacetophenone oxime: ¹H NMR (400 MHz, Acetone-d₆) δ_H (ppm): 2.26 (3H, s, H_{e'}), 7.47 (1H, dd *J* = 8.0, 1.5 Hz, H_{d'}), 7.61 (1H, td *J* = 8.0, 1.0 Hz, H_{b'}), 7.82 (1H, td *J* = 8.0, 1.5 Hz, H_{c'}), 8.08 (1H, dd *J* = 8.0, 1.5 Hz, H_{a'}), 9.87 (1H, s, H_{f'}); ¹³C NMR (100 MHz, Acetone-d₆) δ_C (ppm): 21.0, 124.6, 129.5, 130.2, 132.2, 133.9, 134.6, 153.5; FTIR (ATR) ν (cm⁻¹): 3194(O-H), 2873 (C-H), 1521 (C=N), 1348 (N-O), 930 (N-O); ESIMS calculated mass (C₈H₈O₃N₂+H)⁺ 181.0608 found 181.0605.

Synthesis of *m*-nitroacetophenone oxime **5.21**³⁴



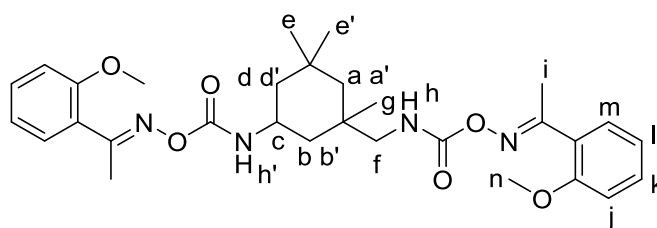
Hydroxylamine hydrochloride (5.27 g, 75.9 mmol), *m*-nitroacetophenone (11.34 g, 69 mmol) and triethylamine (7.68 g, 75.9 mmol) were dissolved in EtOH (100 mL) and maintained under reflux for a period of 18 hours. The solvent was removed *in vacuo* and the product extracted with EtOAc. The organic phase was washed with H₂O (3 x 50 mL), dried over MgSO₄ and then filtered. The solvent was removed *in vacuo* to leave a white solid **5.21** (11.55 g, 93 %) (m.p. 131-134 °C, lit. 131-132 °C). ¹H NMR (400 MHz, Acetone-d₆) δ_H (ppm): 2.23 (3H, s, H_e), 7.70 (1H, t *J* = 8.0 Hz, H_c), 8.13 (1H, dd *J* = 8.0, 2.0 Hz, H_b), 8.23 (1H, dd *J* = 8.0, 2.0 Hz, H_d), 8.54 (1H, t *J* = 2.0 Hz, H_a), 10.76 (1H, s, H_f); ¹³C NMR (100 MHz, Acetone-d₆) δ_C (ppm): 11.4, 121.0, 123.9, 130.6, 132.6, 139.8, 149.4, 152.9; FTIR (ATR) ν (cm⁻¹): 3222 (O-H), 3081 (C-H), 1521 (C=N), 1351 (N-O), 947 (N-O); ESIMS calculated mass (C₈H₈O₃N₂+H)⁺ 181.0608 found 181.0605.

Synthesis of *p*-nitroacetophenone oxime **5.22**³⁴



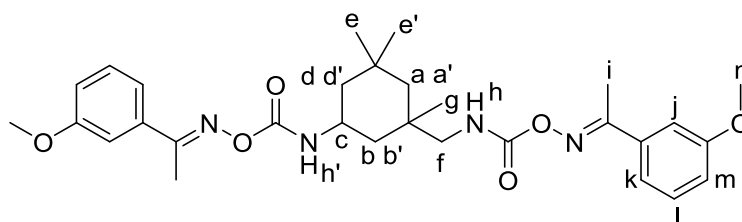
Hydroxylamine hydrochloride (5.27 g, 75.9 mmol), *p*-nitroacetophenone (11.34 g, 69 mmol) and triethylamine (7.68 g, 75.9 mmol) were dissolved in EtOH (100 mL) and maintained under reflux for a period of 18 hours. The solvent was removed *in vacuo* and the product extracted with EtOAc. The organic phase was washed with H₂O (3 x 50 mL), dried over MgSO₄ and then filtered. The solvent was removed *in vacuo* to leave a white solid **5.22** (12.04 g, 97 %) (m.p. 171-175 °C, lit. 174-175 °C). ¹H NMR (400 MHz, Acetone-d₆) δ_H (ppm): 2.31 (3H, s, H_c), 7.98 (2H, d *J* = 8.0 Hz, H_a), 8.25 (2H, d *J* = 8.0 Hz, H_b), 10.90 (1H, s, H_d); ¹³C NMR (100 MHz, Acetone-d₆) δ_C (ppm): 11.4, 124.3, 127.5, 144.3, 148.8, 153.3; FTIR (ATR) ν (cm⁻¹): 3216 (O-H), 3078 (C-H), 1510 (C=N), 1336 (N-O), 927 (N-O); ESIMS calculated mass (C₈H₈O₃N₂+H)⁺ 181.0608 found 181.0605.

Synthesis of *o*-methoxyacetophenone oxime-blocked IPDI **5.23**



Isophorone diisocyanate (7.62 g, 34.3 mmol) and *o*-methoxyacetophenone oxime **5.17** (11.32 g, 68.5 mmol) were dissolved in THF (100 mL) and maintained under reflux for 18 hours under an atmosphere of argon. The solvent was removed to leave a white solid **5.23** (18.94 g, 100 %) (m.p. 58-62 °C). ^1H NMR (400 MHz, CDCl_3) δ_{H} (ppm): 0.93 (3H, s, H_{e}), 1.00 (2H, m, H_{bd}), 1.09 (1H, m, H_{a}), 1.09 (3H, s, H_{g}), 1.11 (3H, s, $\text{H}_{\text{e}'}$), 1.23 (1H, m, $\text{H}_{\text{a}'}$), 1.80 (2H, m, $\text{H}_{\text{b'd}'}$), 2.37 (6H, s, H_{i}), 3.05 (2H, m, H_{f}), 3.86 (6H, s, H_{n}), 3.98 (1H, m, H_{c}), 6.21 (1H, m, $\text{H}_{\text{h}'}$), 6.55 (1H, m, H_{h}), 6.96 (2H, td $J = 7.0, 2.0$ Hz, H_{j}), 7.00 (2H, td $J = 7.0, 2.0$ Hz, H_{l}), 7.31 (2H, td $J = 7.0, 2.0$ Hz, H_{k}), 7.43 (2H, td $J = 7.0, 2.0$ Hz, H_{m}); ^{13}C NMR (100 MHz, CDCl_3) δ_{C} (ppm): 17.2, 23.3, 27.4, 31.9, 35.0, 36.6, 41.8, 44.3, 46.2, 47.2, 54.8, 55.4, 111.1, 120.5, 125.3, 129.6, 131.2, 154.8, 156.1, 157.6, 161.9; FTIR (ATR) ν (cm^{-1}): 3411 (N-H), 2952 (C-H), 1724 (C=O), 1600 (C=N), 1491 (C-N), 1021 (C-O), 996 (C-O), 904 (N-O); ESIMS calculated mass ($\text{C}_{30}\text{H}_{40}\text{O}_6\text{N}_4+\text{Na}$) $^+$ 575.2840 found 575.2843.

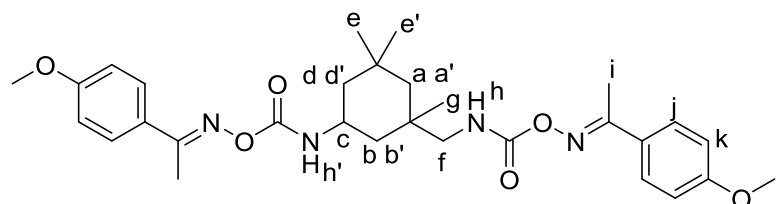
Synthesis of *m*-methoxyacetophenone oxime-blocked IPDI **5.24**



Isophorone diisocyanate (7.61 g, 34.2 mmol) and *m*-methoxyacetophenone oxime **5.18** (11.31 g, 68.5 mmol) were dissolved in THF (100 mL) and maintained under reflux for 18 hours under an atmosphere of argon. The solvent was removed to leave a white solid **5.24** (18.05 g, 95 %) (m.p. 59-63 °C). ^1H NMR (400 MHz, CDCl_3) δ_{H} (ppm): 0.96 (3H, s, H_{e}), 1.05 (1H, m, H_{b}), 1.05 (1H, m, H_{d}), 1.11 (3H, s, H_{g}), 1.14 (1H, m, H_{a}), 1.15 (3H, s, $\text{H}_{\text{e}'}$), 1.29 (1H, m, $\text{H}_{\text{a}'}$), 1.83 (1H, m, $\text{H}_{\text{b}'}$), 1.85 (1H, m, $\text{H}_{\text{d}'}$), 2.41 (6H, s, H_{i}), 3.11 (2H, m, H_{f}), 3.85 (6H, s, H_{n}), 4.00 (1H, m, H_{c}), 6.21 (1H, m, $\text{H}_{\text{h}'}$), 6.60 (1H, m, H_{h}), 7.00 (2H, dd $J = 8.0, 2.0$ Hz, H_{l}), 7.19 (2H, m, H_{j}), 7.24 (2H, m, H_{k}), 7.35 (2H, m, H_{m});

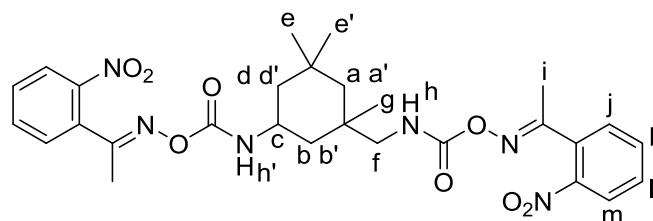
^{13}C NMR (100 MHz, CDCl_3) δ_{C} (ppm): 14.6, 23.1, 27.3, 31.9, 35.1, 36.6, 41.8, 44.7, 46.2, 47.3, 55.0, 55.2, 112.3, 115.9, 119.0, 129.7, 136.6, 154.6, 155.9, 159.7, 160.1; FTIR (ATR) ν (cm^{-1}): 3409 (N-H), 2951 (C-H), 1725 (C=O), 1599 (C=N), 1495 (C-N), 1041 (C-O), 993 (C-O), 923 (N-O); ESIMS calculated mass ($\text{C}_{30}\text{H}_{40}\text{O}_6\text{N}_4+\text{Na}$) $^+$ 575.2840 found 575.2843.

Synthesis of *p*-methoxyacetophenone oxime-blocked IPDI **5.25**



Isophorone diisocyanate (7.54 g, 33.9 mmol) and *p*-methoxyacetophenone oxime **5.19** (11.20 g, 67.8 mmol) were dissolved in THF (100 mL) and maintained under reflux for 18 hours under an atmosphere of argon. The solvent was removed to leave a white solid **5.25** (18.29 g, 97 %) (m.p. 59-64 °C). ^1H NMR (400 MHz, CDCl_3) δ_{H} (ppm): 0.97 (3H, s, H_{e}), 1.05 (1H, m, H_{b}), 1.08 (1H, m, H_{d}), 1.13 (3H, s, H_{g}), 1.16 (3H, s, $\text{H}_{\text{e}'}$), 1.16 (1H, m, H_{a}), 1.30 (1H, m, $\text{H}_{\text{a}'}$), 1.84 (1H, m, H_{b}), 1.86 (1H, m, $\text{H}_{\text{d}'}$), 2.39 (6H, s, H_{i}), 3.12 (2H, m, H_{f}), 3.85 (6H, s, H_{l}), 4.01 (1H, m, H_{c}), 6.24 (1H, m, $\text{H}_{\text{h}'}$), 6.62 (1H, m, H_{h}), 6.94 (4H, d $J = 8.0$ Hz, H_{k}), 7.64 (4H, d $J = 8.0$ Hz, H_{j}); ^{13}C NMR (100 MHz, CDCl_3) δ_{C} (ppm): 14.4, 23.2, 27.6, 31.9, 35.1, 36.6, 41.7, 44.8, 46.3, 47.2, 54.8, 55.2, 114.0, 127.0, 128.3, 154.8, 156.1, 159.6, 161.5; FTIR (ATR) ν (cm^{-1}): 3406 (N-H), 2953 (C-H), 1722 (C=O), 1605 (C=N), 1496 (C-N), 1028 (C-O), 996 (C-O), 912 (N-O); ESIMS calculated mass ($\text{C}_{30}\text{H}_{40}\text{O}_6\text{N}_4+\text{Na}$) $^+$ 575.2840 found 575.2832.

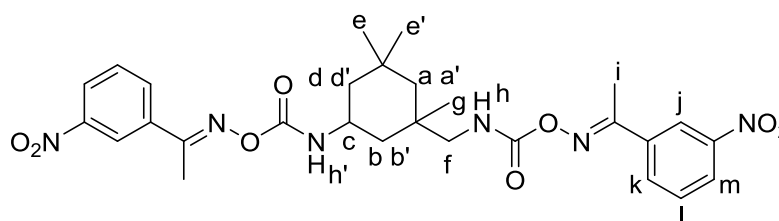
Synthesis of *o*-nitroacetophenone oxime blocked-IPDI **5.26**



Isophorone diisocyanate (7.13 g, 32.1 mmol) and *o*-nitroacetophenone oxime **5.20** (11.55 g, 64.1 mmol) were dissolved in THF (100 mL) and maintained under reflux for 18 hours under an atmosphere of argon. The solvent was removed to leave a pale yellow coloured solid **5.26** (18.65 g, 100 %) (m.p. 78-80 °C). ^1H NMR (400 MHz,

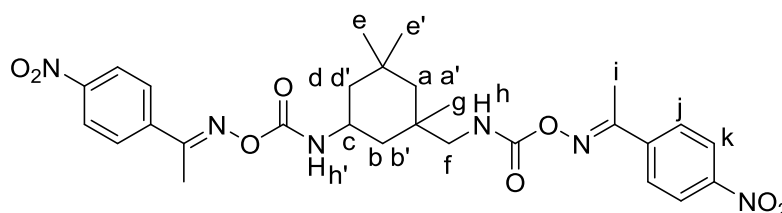
CDCl₃ δ_H (ppm): 0.94 (3H, s, H_e), 1.00 (2H, m, H_{bd}), 1.06 (1H, m, H_a), 1.08 (3H, s, H_g), 1.09 (3H, s, H_{e'}), 1.22 (1H, m, H_{a'}), 1.75 (1H, m, H_{d'}), 1.79 (1H, m, H_{b'}), 2.38 (6H, s, H_i), 3.03 (2H, m, H_f), 3.92 (1H, m, H_c), 5.95 (1H, m, H_{h'}), 6.20 (1H, m, H_h), 7.47-7.74 (6H, m, H_{ijlm}), 8.01-8.22 (2H, m, H_k); ¹³C NMR (100 MHz, CDCl₃) δ_C (ppm): 17.4, 21.6, 23.1, 27.4, 31.9, 34.8, 36.5, 41.3, 45.0, 46.2, 46.9, 54.8, 124.7, 128.1, 130.1, 130.6, 131.3, 131.7, 133.6, 133.7, 134.4, 145.6, 147.7, 154.0, 155.3, 160.0; FTIR (ATR) ν (cm⁻¹): 3411 (N-H), 2954 (C-H), 1731 (C=O), 1612 (C=N), 1525 (N-O), 1499 (C-N), 1028 (C-O), 993 (C-O), 913 (N-O); ESIMS calculated mass (C₂₈H₃₄O₈N₆+Na)⁺ 605.2330 found 605.2328.

Synthesis of *m*-nitroacetophenone oxime blocked-IPDI **5.27**



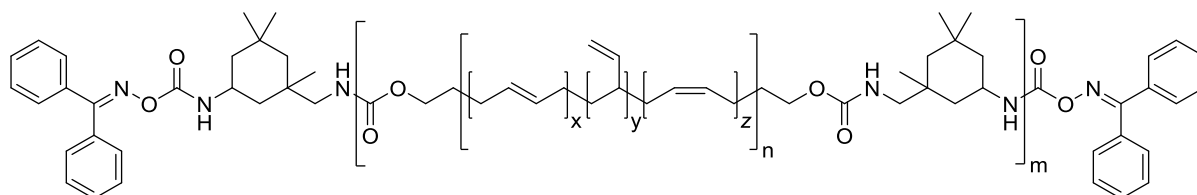
Isophorone diisocyanate (7.05 g, 31.7 mmol) and *m*-nitroacetophenone oxime **5.21** (11.43 g, 63.4 mmol) were dissolved in THF (100 mL) and maintained under reflux for 18 hours under an atmosphere of argon. The solvent was removed to leave a pale yellow coloured solid **5.27** (18.65 g, 100 %) (m.p. 78-80 °C). ¹H NMR (400 MHz, CDCl₃) δ_H (ppm): 1.00 (3H, s, H_e), 1.10 (2H, m, H_{bd}), 1.13 (3H, s, H_g), 1.15 (1H, m, H_a), 1.17 (3H, s, H_{e'}), 1.30 (1H, m, H_{a'}), 1.85 (1H, m, H_{b'}), 1.89 (1H, m, H_{d'}), 2.50 (6H, s, H_i), 3.14 (2H, m, H_f), 4.03 (1H, m, H_c), 6.07 (1H, m, H_{h'}), 6.45 (1H, m, H_h), 7.65 (2H, br. m, H_l), 8.03 (2H, br. m, H_m), 8.32 (2H, td *J* = 2.0, 1.0 Hz, H_j), 8.54 (2H, br. m, H_k); ¹³C NMR (100 MHz, CDCl₃) δ_C (ppm): 14.5, 23.11, 27.7, 32.0, 34.7, 36.8, 41.5, 45.1, 46.0, 47.2, 54.8, 121.7, 124.9, 129.9, 132.5, 136.6, 148.4, 154.0, 155.3, 158.2; FTIR (ATR) ν (cm⁻¹): 3408 (N-H), 2953 (C-H), 1727 (C=O), 1623 (C=N), 1528 (N-O), 1498 (C-N), 994 (C-O), 929 (N-O); ESIMS calculated mass (C₂₈H₃₄O₈N₆+Na)⁺ 605.2330 found 605.2329.

Synthesis of *p*-nitroacetophenone oxime blocked-IPDI **5.28**



Isophorone diisocyanate (7.33 g, 32.0 mmol) and *p*-nitroacetophenone oxime **5.22** (11.88 g, 65.9 mmol) were dissolved in THF (100 mL) and maintained under reflux for 18 hours under an atmosphere of argon. The solvent was removed to leave a pale yellow coloured solid **5.28** (19.21 g, 99 %) (m.p. 81-85 °C). ^1H NMR (400 MHz, CDCl_3) δ_{H} (ppm): 0.99 (3H, s, H_e), 1.08 (1H, m, H_d), 1.09 (1H, m, H_b), 1.12 (3H, s, H_g), 1.14 (1H, m, H_a), 1.15 (3H, s, $\text{H}_{e'}$), 1.29 (1H, m, $\text{H}_{a'}$), 1.83 (1H, m, $\text{H}_{d'}$), 1.90 (1H, m, $\text{H}_{b'}$), 2.49 (6H, s, H_i), 3.13 (2H, m, H_f), 4.01 (1H, m, H_c), 6.04 (1H, m, H_h), 6.40 (1H, m, H_h), 7.86 (4H, d $J = 9.0$ Hz, H_j), 8.29 (4H, d $J = 9.0$ Hz, H_k); ^{13}C NMR (100 MHz, CDCl_3) δ_{C} (ppm): 14.4, 22.8, 27.6, 32.0, 35.0, 36.7, 41.6, 45.1, 45.8, 47.3, 54.8, 123.9, 127.8, 140.8, 148.9, 153.9, 155.3, 158.7; FTIR (ATR) ν (cm^{-1}): 3405 (N-H), 2953 (C-H), 1727 (C=O), 1594 (C=N), 1516 (N-O), 1497 (C-N), 993 (C-O), 921 (N-O); ESIMS calculated mass ($\text{C}_{28}\text{H}_{34}\text{O}_8\text{N}_6+\text{Na}$) $^+$ 605.2330 found 605.2329.

Synthesis of benzophenone-blocked HTPB prepolymer **5.29**



IPDI (17.8 g, 8.0 mmol) and benzophenone oxime (0.808 g, 4.1 mmol) were dissolved in THF (100 mL) and maintained under reflux for a period of 18 hours under an atmosphere of argon. The solution was added to a mixture of hydroxy-terminated polybutadiene (HTPB) (18.22 g) and DBTDL (0.044 g, 0.07 mmol) and maintained under reflux for a further period of 18 hours. The solvent was removed *in vacuo* to give a pale yellow coloured viscous oil **5.29** (21.03 g, 100 %). FTIR (ATR) ν (cm^{-1}): 3007 (C-H), 2915 (C-H), 2844 (C-H), 1714 (C=O), 1639 (C=N), 1511 (C-N), 1216 (C-N), 965 (C-O), 911 (N-O), 754 (C=C); GPC (THF, BHT 250 ppm): $M_n = 12718$ Da, $M_w = 76566$ Da, $D = 6.02$.

5.5. References

- 1 A. Blencowe, A. Clarke, M. G. B. Drew, W. Hayes, A. Slark, P. Woodward, *React. Funct. Polym.*, 2006, **66**, 1284-1295.
- 2 Z. W. Wicks, *Prog. Org. Coat.*, 1981, **9**, 3-28.
- 3 D. A. Wicks and Z. W. Wicks, *Prog. Org. Coat.*, 1999, **36**, 148-172.
- 4 F. W. C. Lee and K. S. B. Dublin, US Patent, *Single package epoxy resin system*, 4 533 715, 1985.
- 5 M. Hutchby, C. E. Houlden, J. G. Ford, S. N. G. Tyler, M. R. Gagne, G. C. Lloyd-Jones, K. I. Booker-Milburn, *Angew. Chem. Int. Ed.*, 2009, **48**, 8721-8724.
- 6 H. Kothandaraman and A. S. Nasar, *Polymer*, 1993, **34**, 610-615.
- 7 P. F. Wiley, *J. Am. Chem. Soc.*, 1949, **71**, 1310-1311.
- 8 A. W. Levine and J. Fech, *J. Org. Chem.*, 1972, **37**, 1500-1503.
- 9 M. Hutchby, C. E. Houlden, J. G. Ford, S. N. G. Tyler, M. R. Gagne, G. C. Lloyd-Jones and K. I. Booker-Milburn, *Angew. Chem. Int. Ed.*, 2009, **48**, 8721-8724.
- 10 J. C. Stowell and S. J. Padegimas, *J. Org. Chem.*, 1974, **39**, 2448-2449.
- 11 G. Sankar and A. S. Nasar, *J. Polym. Sci. Pol. Chem.* 2007, **45**, 1557-1570.
- 12 I. Muramatsu, Y. Tanimoto, M. Kase and N. Okoshi, *Prog. Org. Coat.*, 1993, **22**, 279-286.
- 13 S. Subramani, I. W. Cheong and J. H. Kim, *Prog. Org. Coat.*, 2004, **51**, 329-338.
- 14 S. Subramani, Y. J. Park, Y. S. Lee and J. H. Kim, *Prog. Org. Coat.*, 2003, **48**, 71-79.
- 15 S. Lee and D. Randall, *The Polyurethanes Book*, Wiley, Chichester, 2002.
- 16 H. T. Truc-Chi and C. L. Shioh, US Patent, *Storage stable, low temperature, solventless curable urethane composition*, 1988, 4 722 969.
- 17 J. S. Witzeman, *Prog. Org. Coat.*, 1996, **27**, 269-276.
- 18 Beitchman and P. J. Zaluzka, US Patent, *Isocyanate blocked imidazoles and imidazolines for epoxy powder coating*, 1982, 4 335 228.
- 19 F. W. C. Lee and K. S. B. Dublin, US Patent, *Single package epoxy resin system*, 1985, 4 533 715,
- 20 A. Mühlebach, *J. Polym. Sci. Pol. Chem.*, 1994, **32**, 753-765.
- 21 A. Wenning and F. Schmitt, Canadian Patent, *Pulverulent compounds, a process for their preparation and use*, 1998, 2 210 043.

- ²² A. S. Nasar, V. Shrinivas, T. Shanmugam and A. Raghavan, *J. Polym. Sci. Pol. Chem.*, 2004, **42**, 4047-4055.
- ²³ J. Allabashi, US Patent, *Process for producing crosslinked propellants*, 1974, 3 798 090.
- ²⁴ W. H. Graham, I. G. Shepard, US Patent, *Hydroxy-terminated polybutadiene based polyurethane bound propellant grains*, 1978, 4 098 626.
- ²⁵ A. Lefumeux, US Patent, *Continuous process for the solventless manufacture of composite pyrotechnic products*, 1997, 5 596 232.
- ²⁶ H. Kothandaraman and R, Thangavel, *J. Polym. Sci. Pol. Chem.*, 1993, **31**, 2653-2657.
- ²⁷ N. Ducruet, L. Delmotte, G. Schrodj, F. Stankiewicz, N. Desgardin, M. Vallat and B. Haidar, *J. Appl. Polym. Sci.* 2013, **128**, 436-443.
- ²⁸ K. Hailu, G. Guthausen, W. Becker, A. König, A. Bendfeld and E. Geissler, *Polymer Testing*, 2010, **29**, 513-519.
- ²⁹ F. Burel, A. Feldman and C. Bunal, *Polymer*, 2005, **46** 15-25.
- ³⁰ S. Desai, I. M. Thakore, B. D. Sarawade and S. Devi, *Eur. Poly. J.*, 2000, **36**, 711-725.
- ³¹ S. Desai, I. M. Thakore and S. Devi, *Polym. Int.*, 1998, **47**, 172-178.
- ³² H. Diekmann and W. Lüttke, *Angew. Chem.*, 1968, **80**, 395-396.
- ³³ H. Kothandaraman and R, Thangavel, *J. Polym. Sci. Pol. Chem.*, 1993, **31**, 2653-2657.
- ³⁴ B. J. Gregory, R. B. Moodie and K. Schofield, *J. Chem. Soc. B*, 1970, 338-346.

Chapter 6

Conclusions

The limitations and complications associated with the current procedure used for the manufacture of plastic or polymer bonded explosives (PBX) have been recognised. Two approaches to eliminate these issues using thermally-reversible bonds have been identified. The first approach encompasses the encapsulation of the reactive crosslinker in polyurethane microcapsules that are able to release their core contents upon the application of heat. The second approach utilises thermally-reversible blocked-isocyanates to regenerate the active isocyanate moiety when desired using an application of heat.

Initial studies involved the synthesis of isocyanate-terminated shell wall precursors capable of further chain extension in order to afford polyurethane microcapsules using an interfacial polymerisation technique. The synthesis involved the protection of a hydroxy-functionalised aromatic ketone in the form of a silyl ether followed by conversion of the ketone to an oxime using hydroxylamine hydrochloride. This approach then allowed reaction with a diisocyanate to form the thermally-labile oxime-urethane. Subsequent deprotection to afford the hydroxyl moiety followed by reaction with excess toluene-2,4-diisocyanate (TDI) yielded the shell wall precursor. It was important to investigate the effect of steric hindrance around the thermally-labile bond on the dissociation temperature. Thus a library of shell wall precursors possessing varying degrees of steric hindrance was generated by employing two oximes - benzophenone oxime and an acetophenone oxime analogue and four diisocyanates - HDI, XDI, IPDI and TMXDI. Methods to observe the dissociation of the oxime-urethanes were investigated. Variable temperature infrared spectroscopy proved to be an effective analytical tool for measuring the dissociation, revealing increasing steric hindrance around the oxime-urethane decreases the temperature at which dissociation occurs. This dissociation did not generate any volatile products and thus thermogravimetric analysis was demonstrated to be unsuitable analytical tool for observing the desired bond dissociation. In addition, differential scanning calorimetry was also demonstrated to be an ineffective tool for observing the dissociation of oxime-urethanes.

The generated shell wall precursors were employed in an interfacial polymerisation technique to successfully yield polyurethane microcapsules. Spectroscopic analysis of the released microcapsule core revealed the successful encapsulation of active isophorone diisocyanate (IPDI). Increasing the steric hindrance of the shell wall precursors led to the formation of structurally weaker microcapsules. The release of these microcapsules using the application of heat was confirmed and was used to successfully cure hydroxy-terminated polybutadiene (HTPB) demonstrating the potential for such microencapsulated systems for large scale deployment in the manufacture of PBX. Control of the physical properties of microcapsules was achieved by manipulation of the reaction parameters of the microcapsule synthesis. Microcapsule diameter can be controlled by agitation rate, surfactant concentration and selection of the hydrophobic solvent. The shell wall thickness is dependent on concentration of the shell wall precursor and reaction time. In addition, the maximum loading of IPDI in the microencapsulated core was investigated. The permeability of the microcapsule core can be controlled by increasing the concentration of the chain extender. Furthermore, the successful encapsulation of a dye, β -carotene, demonstrated how UV spectroscopy could be employed to observe and quantify the release of microencapsulated core.

The thermally-reversible nature of the maleimide-furan Diels-Alder adduct was exploited in order to generate microcapsules that released IPDI from the core upon exposure to heat. This study initially involved the synthesis of an isocyanate-terminated shell wall precursor that contained the Diels-Alder adduct. This was achieved by protection of maleic anhydride with furan followed by conversion to the maleimide to form a hydroxy-functionalised Diels-Alder adduct. Deprotection followed by reaction with furfuryl alcohol generated a dihydroxy-functionalised Diels-Alder adduct that was reacted with an excess of TDI to afford the desired shell wall precursor. The synthesis of microcapsules containing IPDI was achieved using an interfacial polymerisation technique that employed this shell wall precursor to form the microcapsule shell wall. The release of the microcapsule core using a heat stimulus was demonstrated. The mechanical strength of the microcapsules was improved by using a synthesis that employed a mixture of a shell wall precursor containing the Diels-Alder adduct and a shell wall precursor not containing the thermally-reversible

bond. Although mechanical strength was improved, the capability of the microcapsules to release the core was reduced.

The final part of this thesis investigated the potential of thermally-reversible blocked isocyanates to cure HTPB using an application of heat. Studies involved the synthesis of IPDI blocked with a range of groups - amines, amides, oximes, aromatic heterocycles and phenols. Crosslinking studies of HTPB using these generated blocked isocyanates revealed oxime blocking groups referred to as oxime-urethanes demonstrated ideal solubility and curing properties for potential employment in the manufacture of PBX. Attempts to reduce the dissociation of oxime-urethanes were successfully achieved by increasing the steric hindrance of the oxime. In addition, the presence of electron donating groups at the *ortho* and *meta* position of aromatic oximes led to a reduction of the dissociation temperature. Methods to measure the curing of HTPB were investigated - tensile testing and observing the swelling behaviour of the curing material were identified as reliable methods of analysis. The poor solubility of aromatic oxime-urethanes in HTPB was remedied by generation of an oxime-blocked HTPB-based prepolymer. The cure of HTPB using such blocked-isocyanates revealed promising results, however, further development is still required before such systems can be deployed in explosive formulations.

Chapter 7

Future Perspectives

Chapter 4 has described how the presence of an electron donating methoxy moiety at the *meta*-position of acetophenone oximes has significantly reduced the dissociation temperature of oxime-urethanes, thus it is expected that increasing this electron density will further reduce the dissociation temperature. This could be achieved by generating analogues of acetophenone oxime that possesses electron donating substituents at both the available *meta*-positions. Further electron density could be imparted into the system by employing more strongly donating substituents - tertiary amines in particular exhibit strong electron donating nature. The effect of electron donating substituents could be fully exploited by the synthesis of 3,3',5,5'-substituted benzophenone oxime analogues (Figure 7.1).

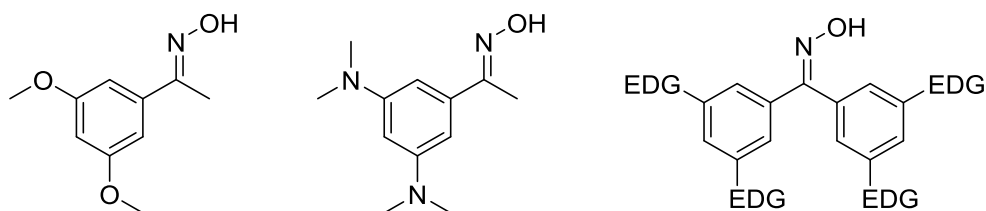


Figure 7.1. The structures of analogues of acetophenone oxime and benzophenone oxime possessing methoxy and dimethylamine electron donating groups (EDG).

Another approach that can be employed to reduce the dissociation temperature of oxime-urethanes is to position polar functional groups in close proximity to the labile bond. Acetophenone oxime functionalised with an *ortho*-methoxy moiety has reduced the dissociation temperature of oxime-urethanes - therefore the presence of an additional methoxy group is expected to enhance this effect and could be further enhanced by the addition of an acetyl moiety (Figure 7.2).

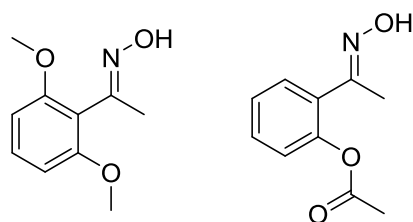


Figure 7.2. The structures of analogues of acetophenone oxime that possess polar methoxy and acetyl groups in close proximity to the oxime functional group.

In addition, the dissociation temperature of oxime-urethanes is dependent on the steric hindrance around the thermally-labile bond and this effect has been demonstrated in

Chapter 2 and **4**. Reduction of the dissociation temperature could be achieved by employing sterically hindered aliphatic oximes such as - 2,2,4-trimethyl-3-pentanone oxime and 2,2,4,4-tetramethyl-3-pentanone oxime. A combination of the steric and electronic effects could also significantly lead to a reduction in the dissociation temperature of oxime-urethanes (Figure 7.3).

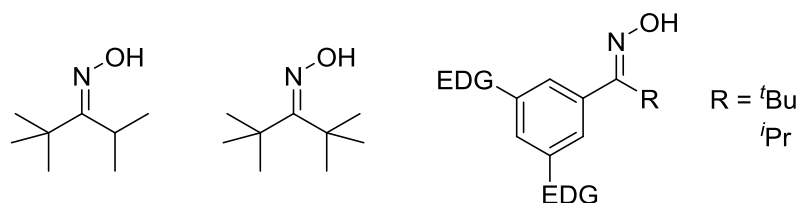


Figure 7.3. Structures of sterically encumbered aliphatic oximes and an analogue of sterically encumbered acetophenone oxime that possesses electron donating groups at the *meta*-positions.

The future investigative work outlined in this chapter can be used in the development of microcapsules that release their core contents with an application of heat. Shell wall precursors can be designed in order to exploit the steric and electronic effects that reduce the dissociation temperature of the oxime-urethane bond.

Although microencapsulation technology has demonstrated the potential for employment in PBX formulations, further development is required. Firstly the scale of the microcapsule synthesis will need to be increased in order to meet scale requirements of explosive formulations. Release of the microcapsule core using a range of temperatures and exposure times will need to be performed. Microcapsules will be required to possess sufficient mechanical strength in order to survive the mixing process of the explosive formulation thus a method to measure the mechanical strength of microcapsules will be required. This has been the subject of many literature studies and methods include - crushing between two plates,¹ shear breakage in a turbine reactor^{2,3} and compression using micromanipulation.^{4,5} Of these methods measuring the shear breakage in a turbine reactor may be suitable, since it most closely represents the forces microcapsules will experience in the mixing process employed in the manufacture of PBX. Alongside this, controlling the mechanical strength of the microcapsules will be important. Studies have shown¹ that the mechanical strength is dependent on the microcapsule diameter and the thickness of the shell wall. Although control of these properties has been described in **Chapter 3**,

further studies may be required in order to tailor microcapsules that possess a desired mechanical strength for employment in PBX formulations.

Microcapsules that utilise Diels-Alder adducts within the shell wall also require development. The mechanical strength of these microcapsules may be improved by the addition of a short polymer chain to the Diels-Alder adduct and thus facilitate in formation of a stronger polymer shell (Figure 7.4).

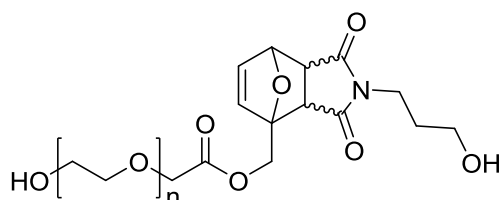


Figure 7.4. Modified Diels-Alder adduct with a short PEG chain.

The potential to synthesise microcapsules that contain alternative Diels-Alder adducts within the shell wall also need to be investigated. Tricyanoacrylate-fulvene adducts have demonstrated⁶ excellent reversibility at 25-50 °C. In addition, Diels-Alder adducts have been developed⁷ that are formed by reaction of a thio-thiocarbonyl RAFT agent with cyclopentadiene (Figure 7.5).

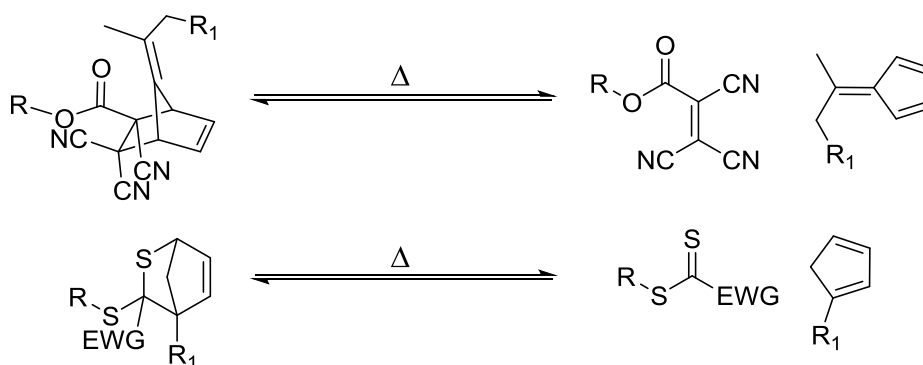


Figure 7.5. Reversible reactions of Diels-Alder adducts formed from tricyanoacrylate with fulvene and thio-thiocarbonyl RAFT agent with cyclopentadiene.

It may be necessary to investigate other thermally-labile bonds that can be incorporated into the shell wall of microcapsules. Results described in **Chapter 4** demonstrate the potential of other thermally-labile linkers that could be incorporated into the shell wall of microcapsules. Amines and aromatic heterocycles in particular show promising dissociation character.

In addition to release of microcapsule core using an application of direct heat, the release using ultrasound could also be explored. Ultrasound cavitation brings about

localised regions of short lived high temperature environments⁸ that could be sufficient to bring about the dissociation of thermally-labile bonds.

The development of thermally-labile bonds described in this thesis have been designed specifically for the purpose of controlling the crosslinking of polyurethane matrices. The release of the core from microcapsules using heat is not restricted to isocyanate crosslinkers and potential for the release of other chemicals is recognised. In recent years there has been demand for recyclable and degradable materials⁹ and the thermally-labile bonds developed herein could be employed as degradable crosslinks in thermoset plastics. The reversible nature of the oxime-urethane bonds described in this thesis also needs to be investigated as such thermally-reversible systems are used in healable materials.¹⁰

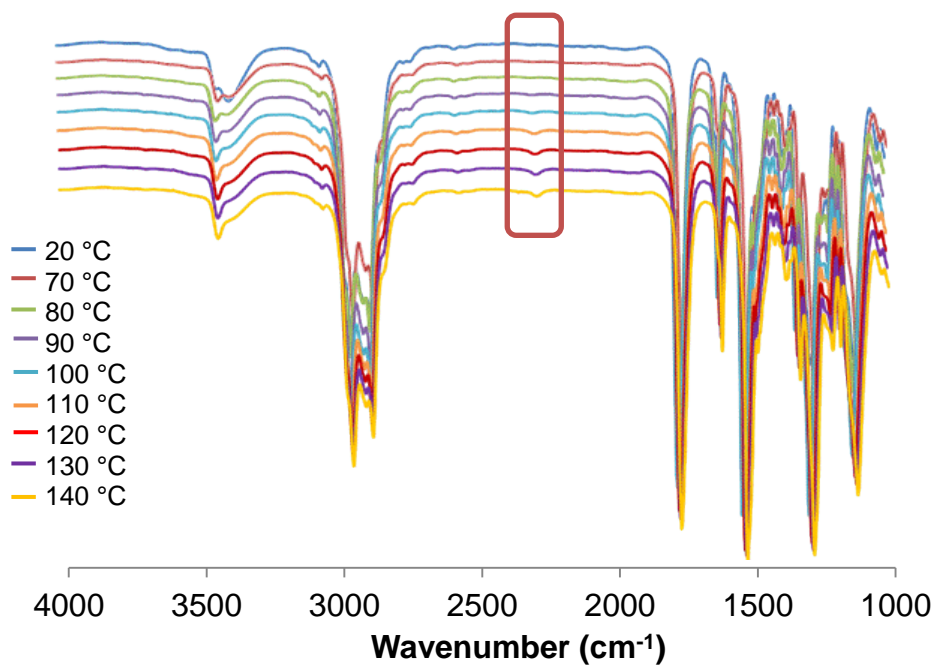
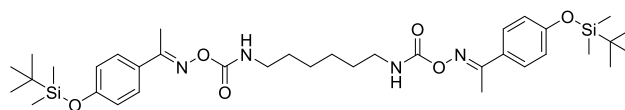
References

- ¹ T. Ohtsubo, S. Tsuda, and K. Tsuji, *Polymer*, 1991, **32**, 2395-2399.
- ² A. Ortmanis, R. J. Neufeld and T. M. S. Chang, *Enzyme Microb. Tech.*, 1984, **6**, 135-139.
- ³ D. Poncelet, and R. J. Neufeld, *Biotechnol. Bioeng.*, 1989, **33**, 98-103.
- ⁴ Z. Zhang, R. Saunders and C. R. Thomas, *J. Microencapsul.*, 1999, **16**, 117-124.
- ⁵ G. Sun and Z. Zhang, *J. Microencapsul.*, 2001, **18**, 593-602.
- ⁶ P. J. Boul, P. Reutenauer and J. M. Lehn, *Org. Lett.*, 2005, **7**, 15-18.
- ⁷ A. J. Inglis, S. Sinnwell, M.H. Stenzel and C. Barner-Kowollik, *Angew. Chem. Int. Ed.*, 2009, **48**, 2411-2414.
- ⁸ M. W. A. Kuijpers, P. D. Iedema, M. F. Kemmere and J. T. F. Keurentjes, *Polymer*, 2004, **45**, 6461-6467.
- ⁹ H. Nishida, *Polym. J.*, 2011, **43**, 435-447.
- ¹⁰ H. Ying, Y. Zhang and J. Cheng, *Nat. Commun.*, 2014, **5**, 3218-3226.

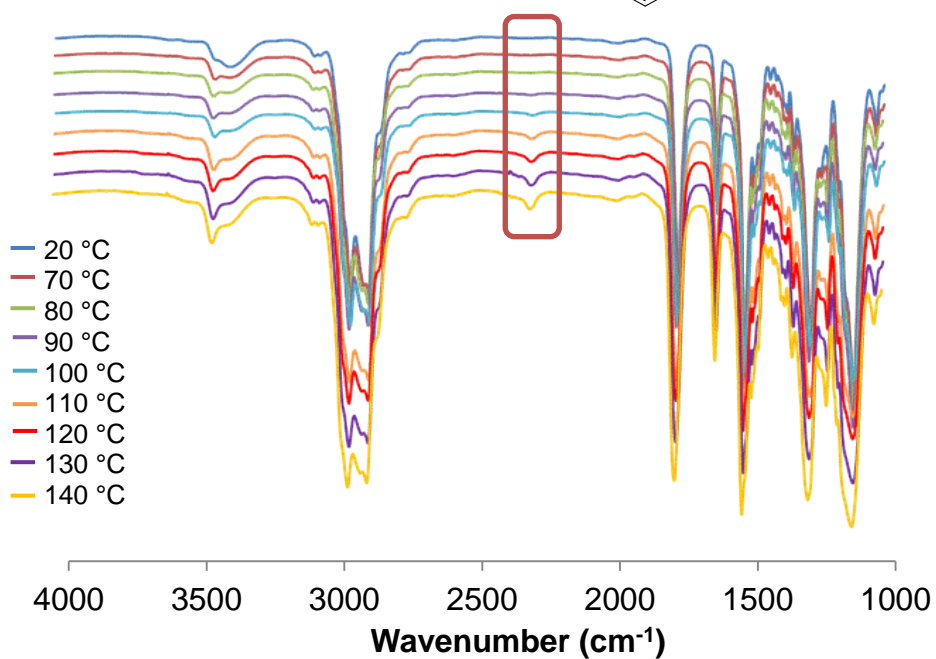
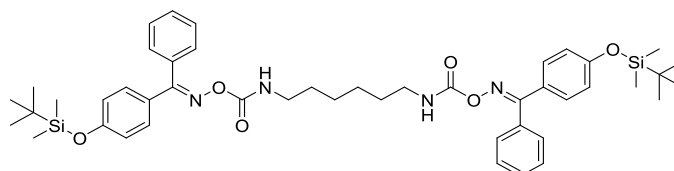
Chapter 8

Appendix

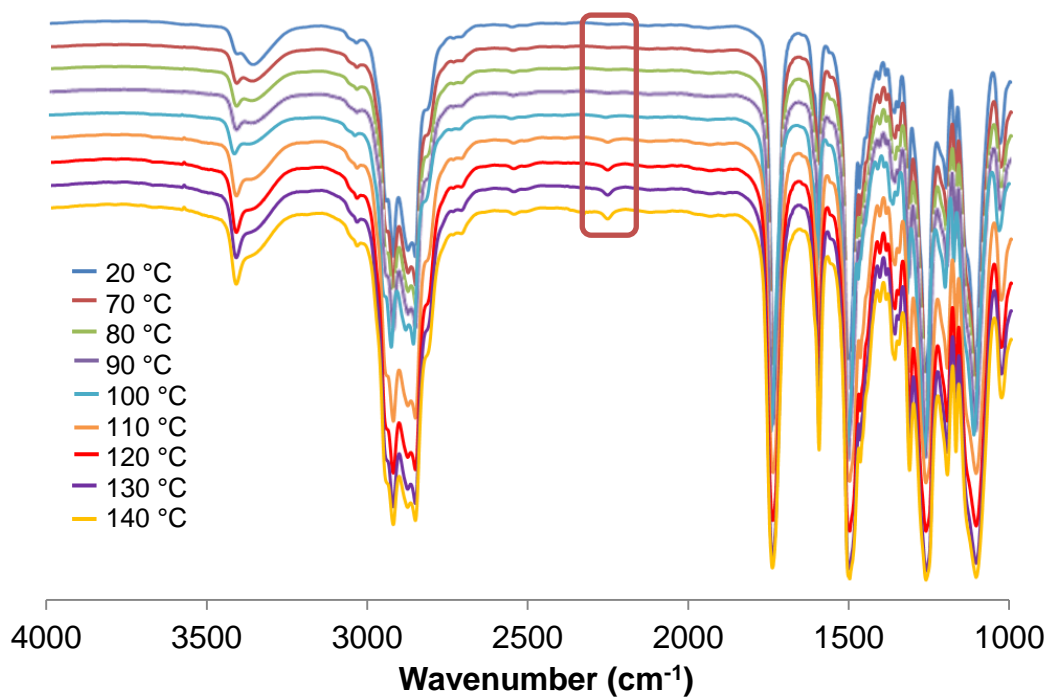
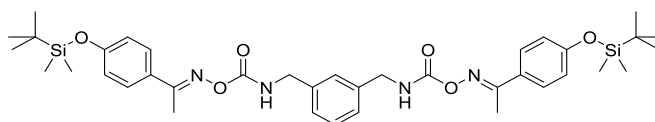
VTIR spectra of 2.3a



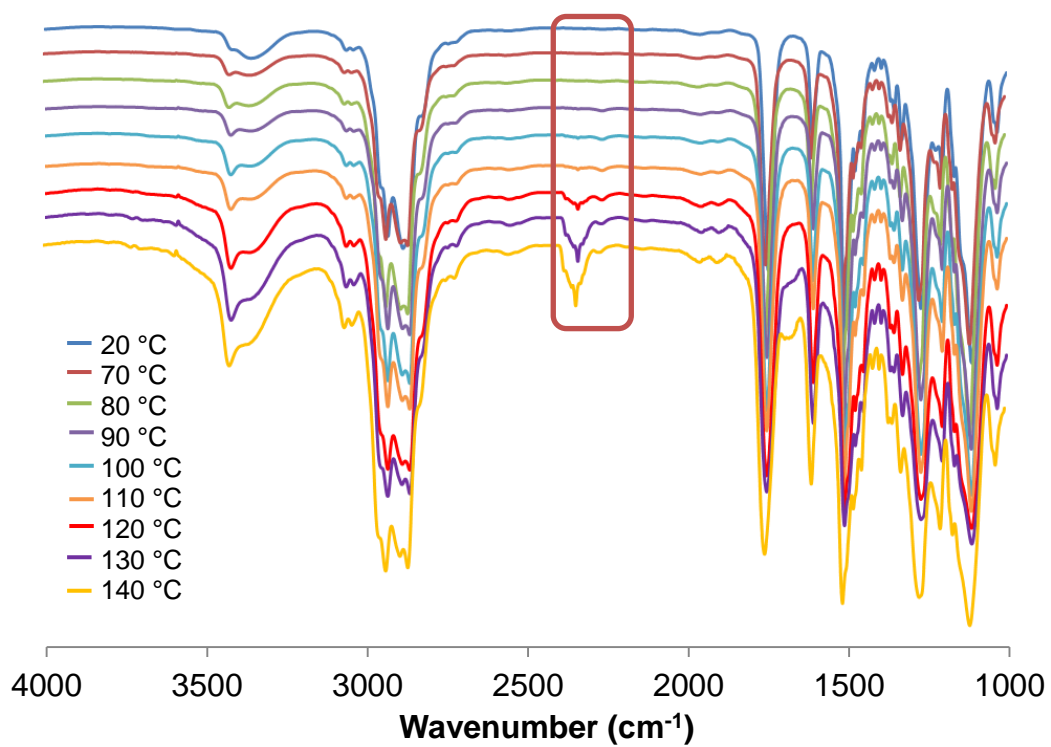
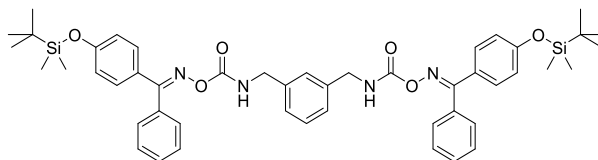
VTIR spectra of 2.3b



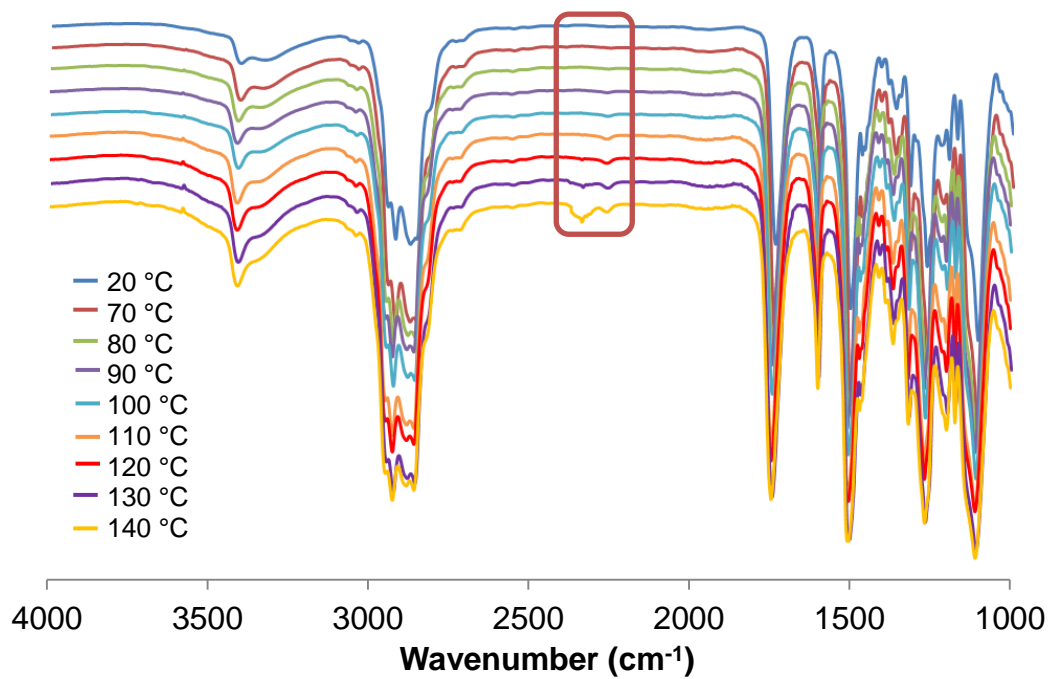
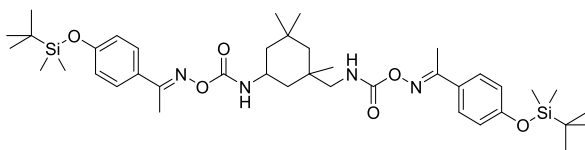
VTIR spectra of 2.3c



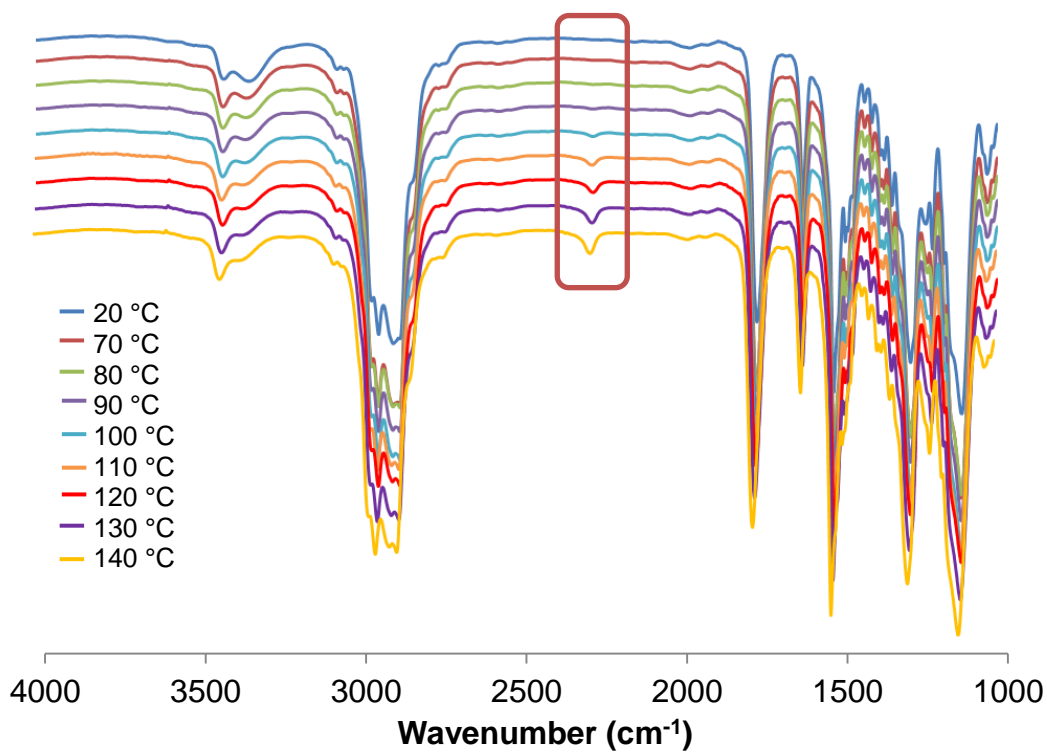
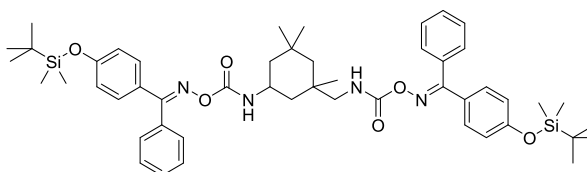
VTIR spectra of 2.3d



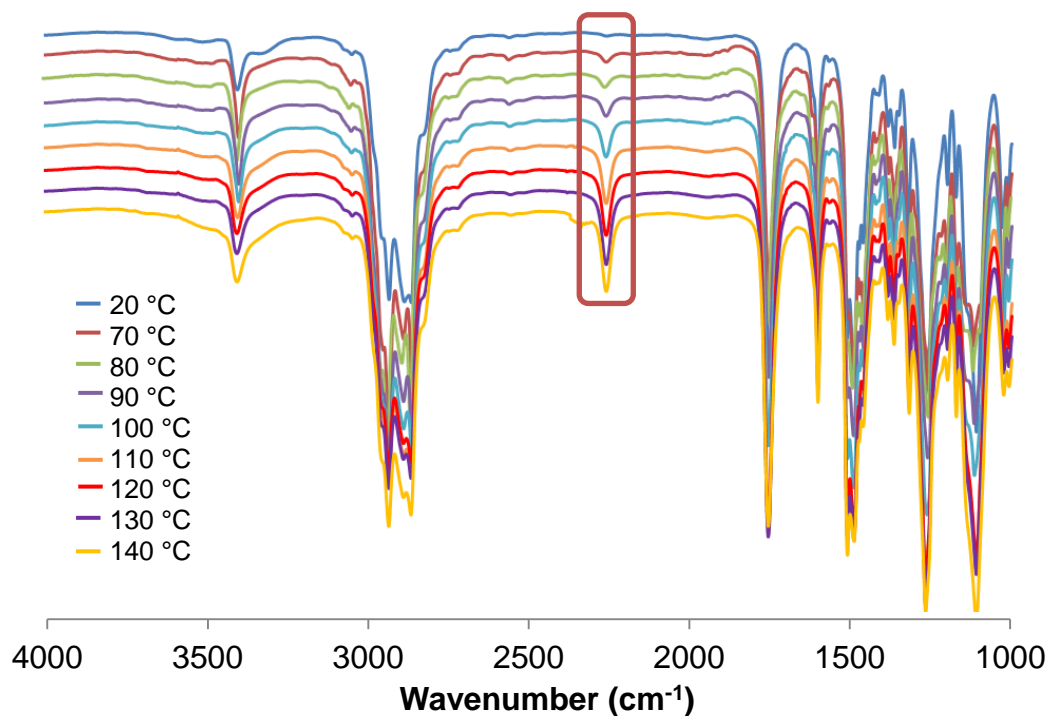
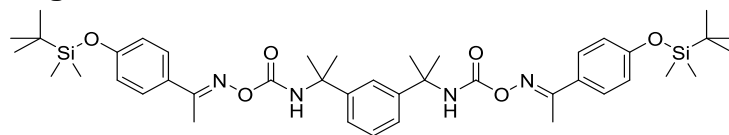
VTIR spectra of 2.3e



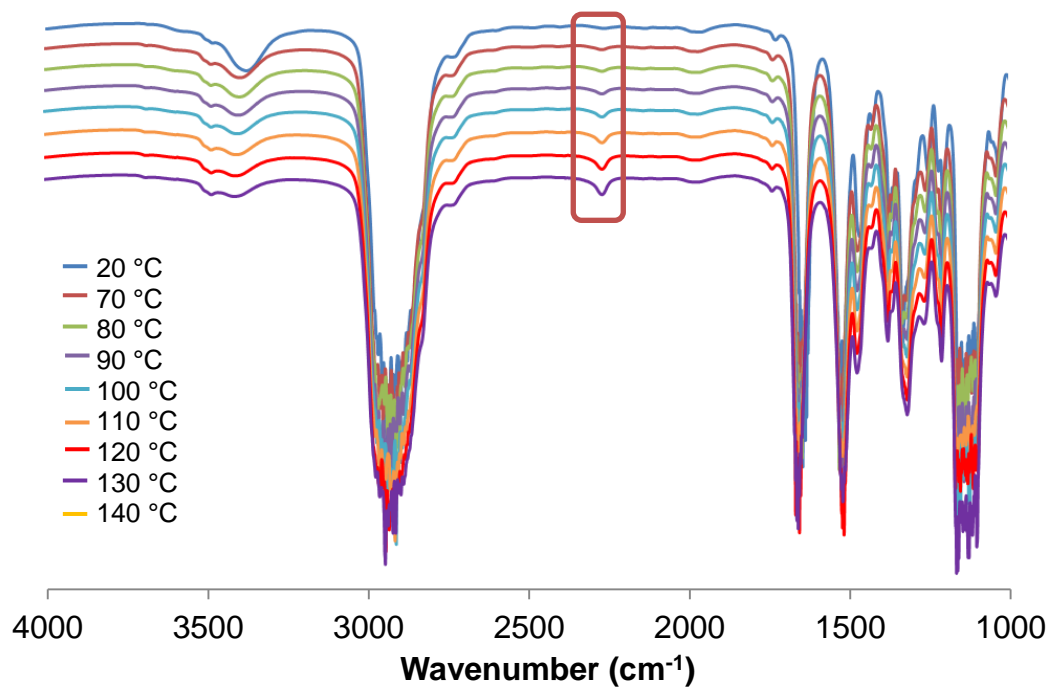
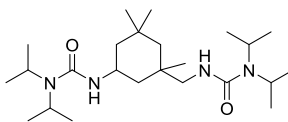
VTIR spectra of 2.3f



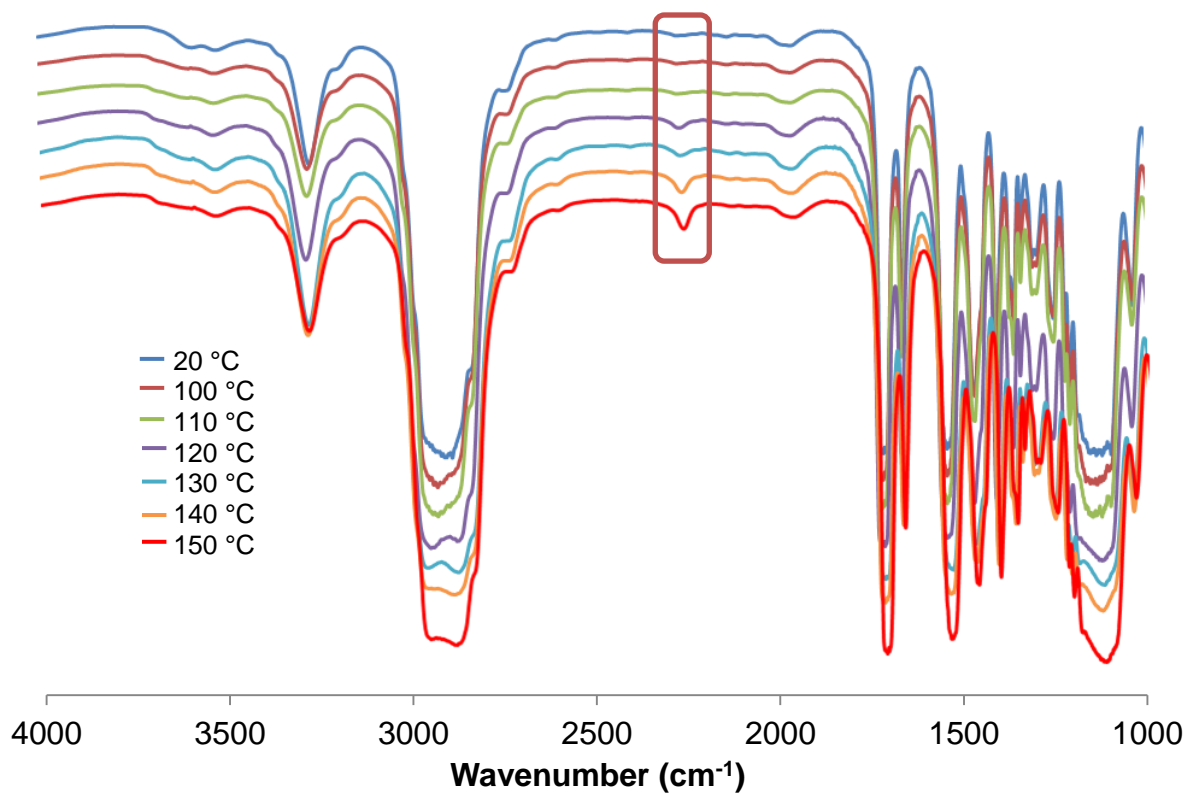
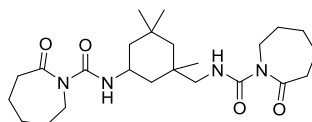
VTIR spectra of 2.3g



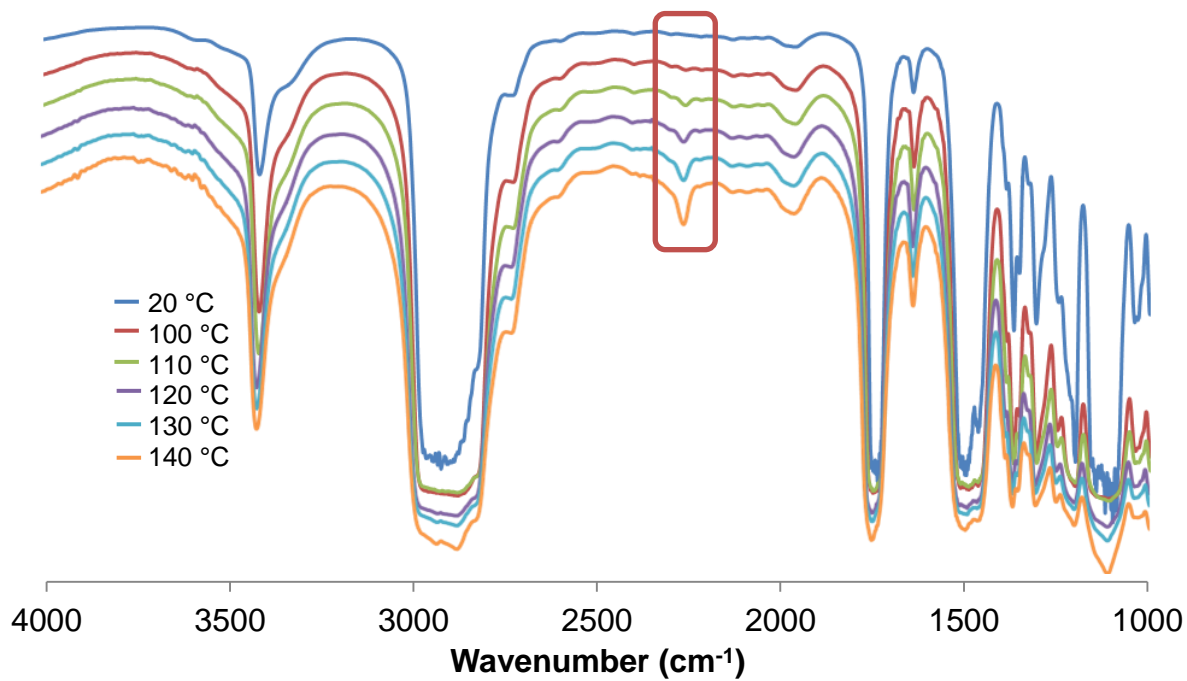
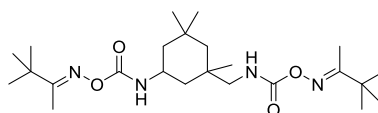
VTIR spectra of 5.1



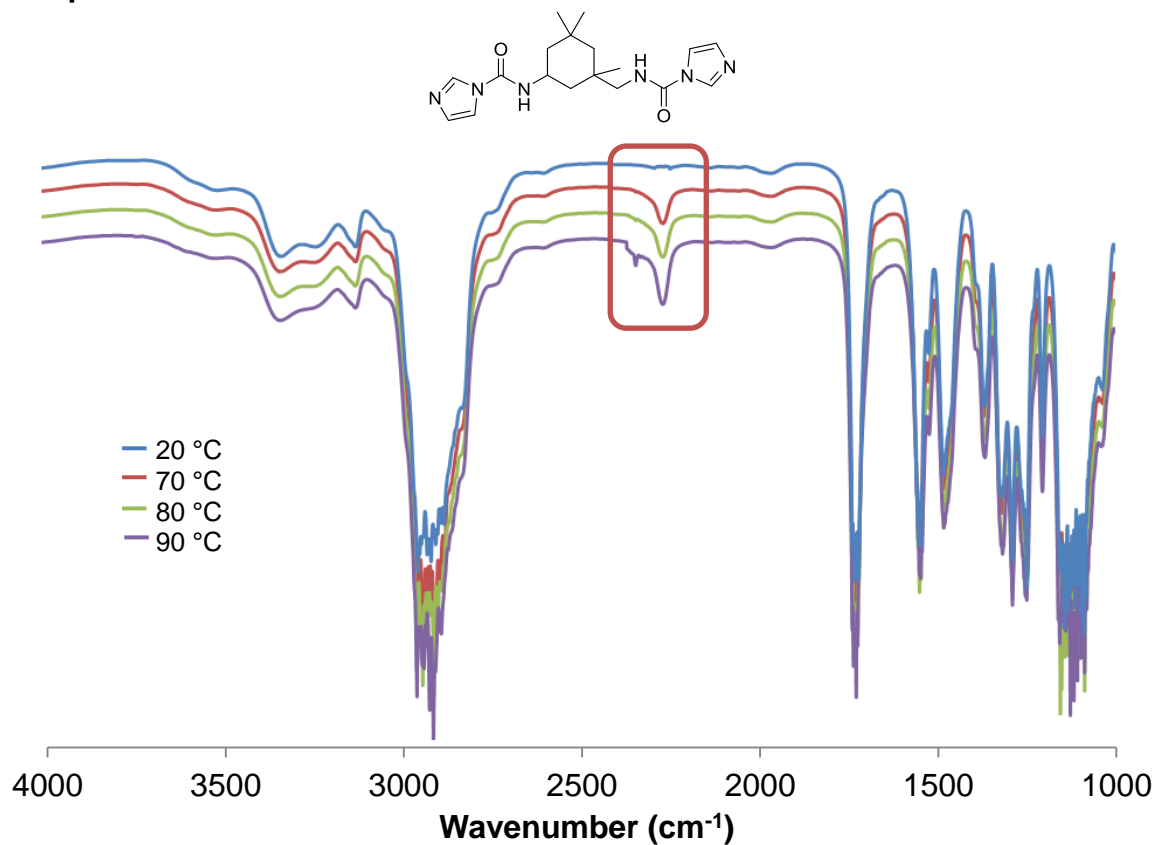
VTIR spectra of 5.2



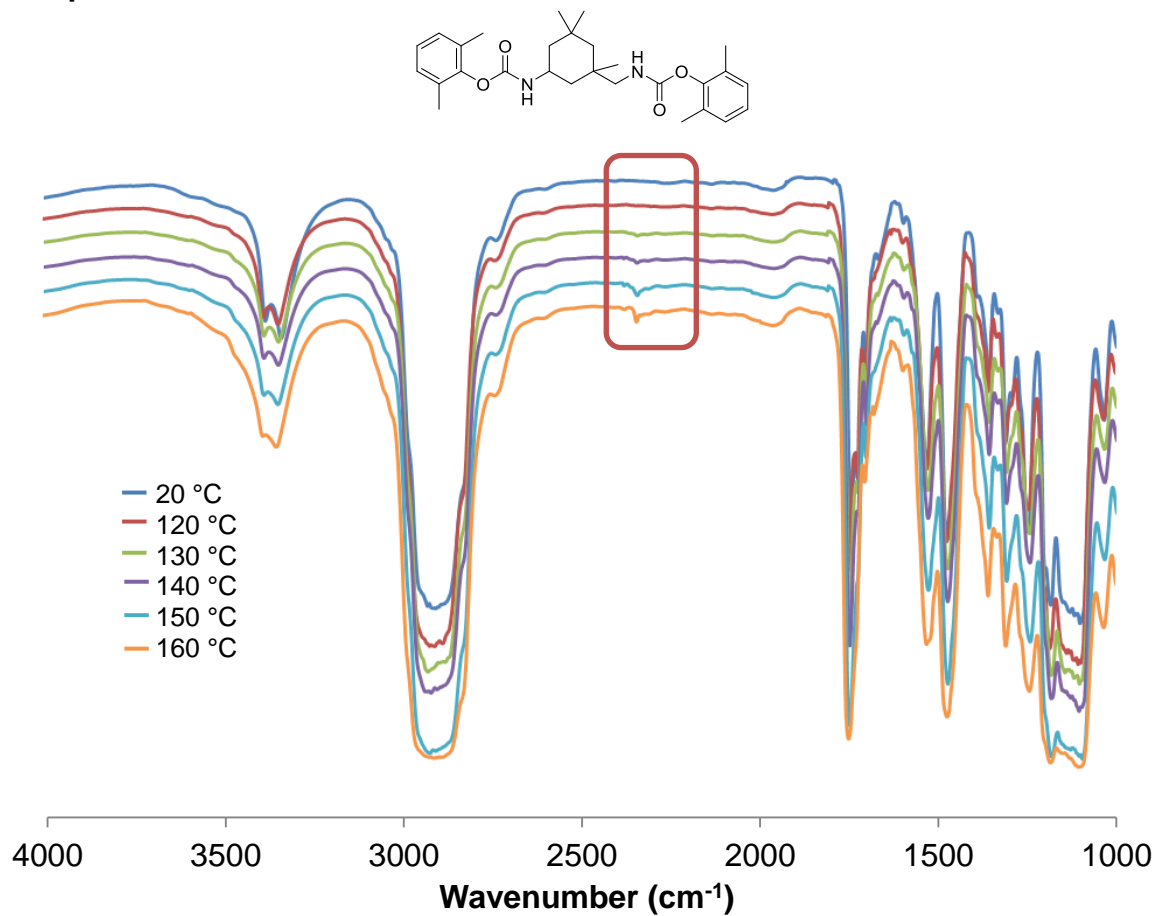
VTIR spectra of 5.4



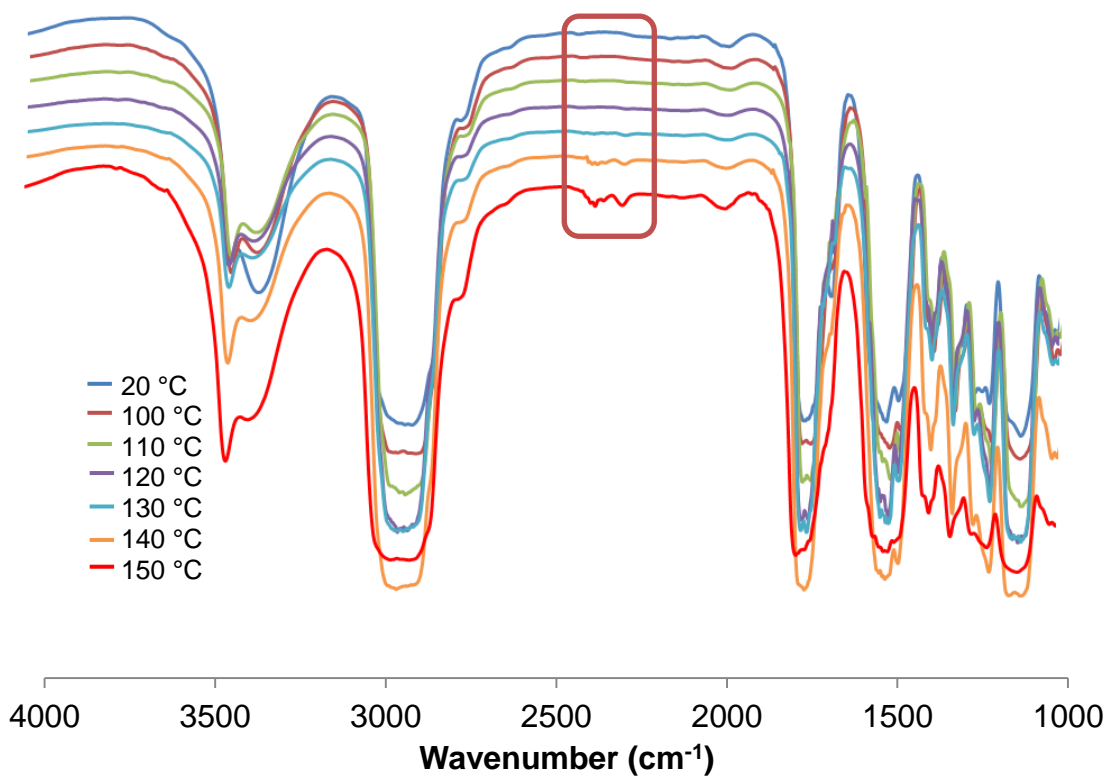
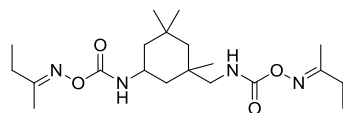
VTIR spectra of 5.5



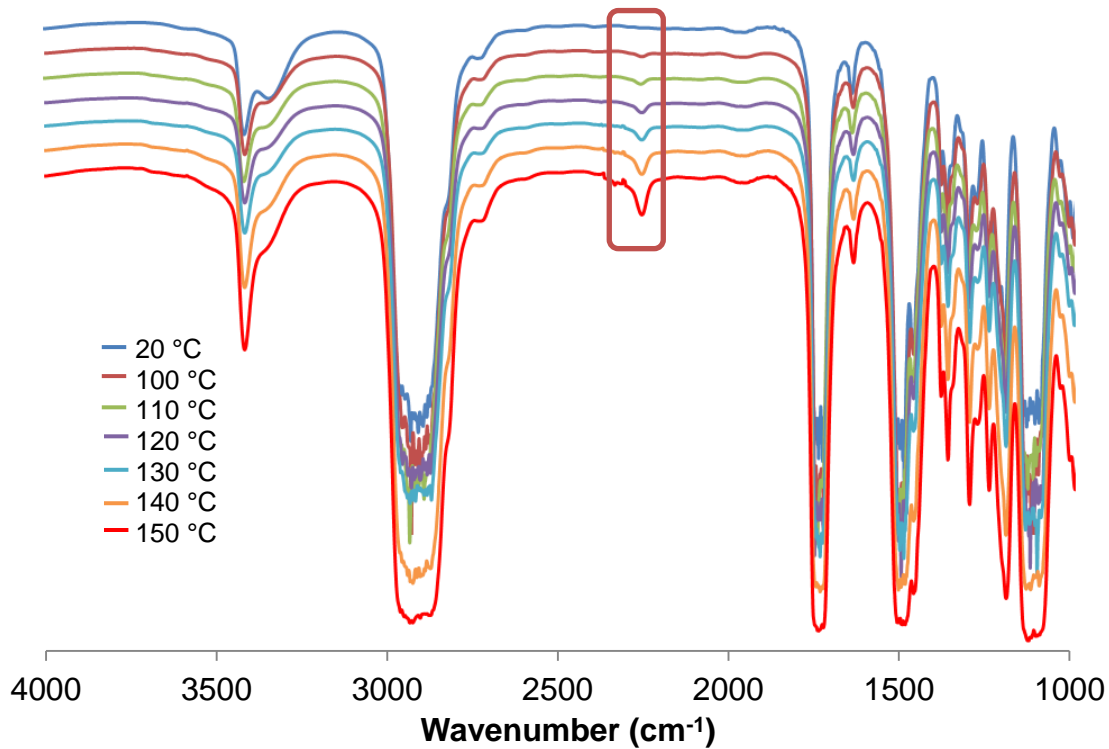
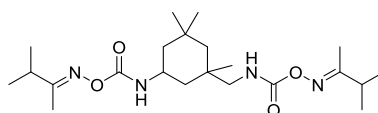
VTIR spectra of 5.6



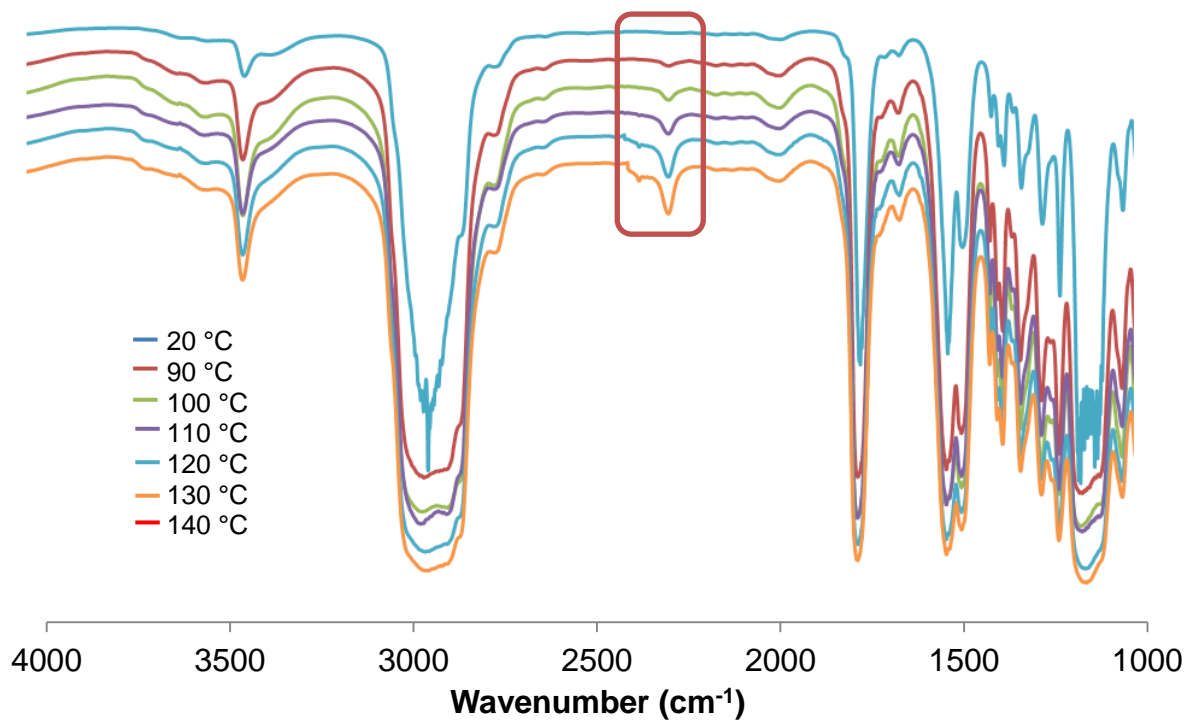
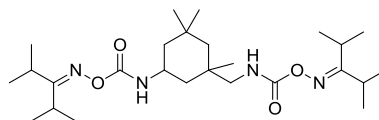
VTIR spectra of 5.12



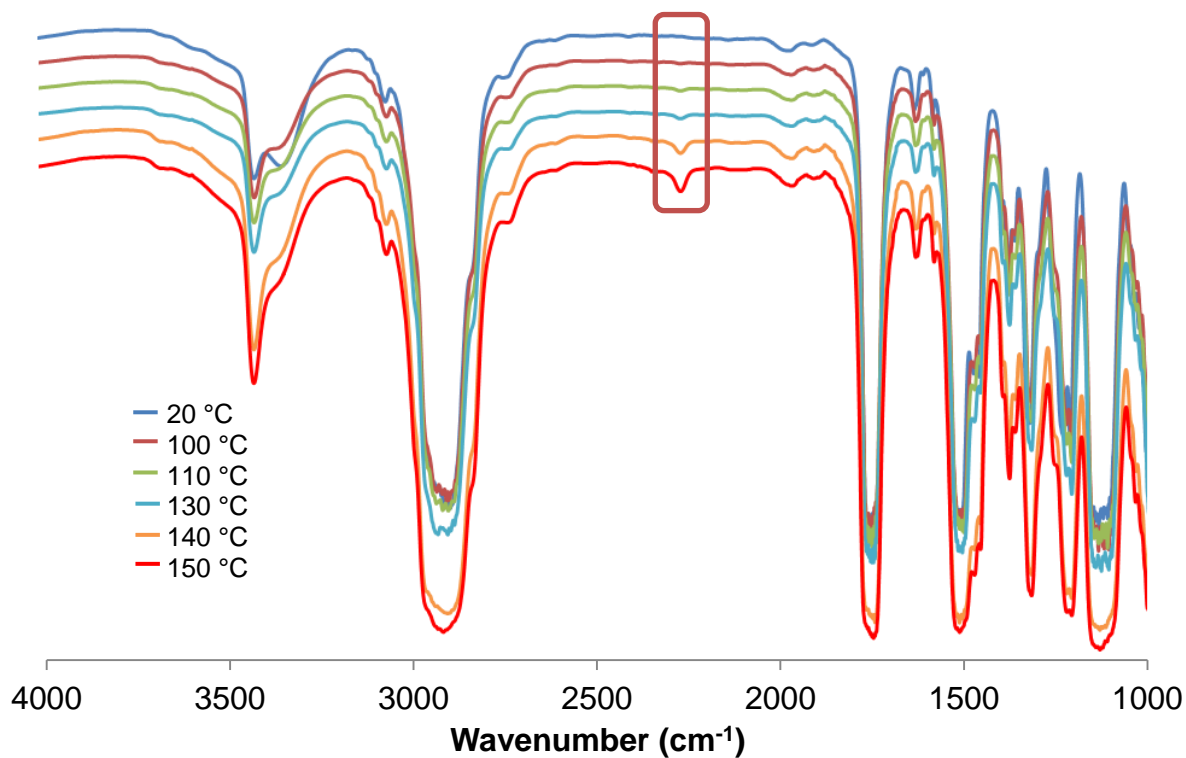
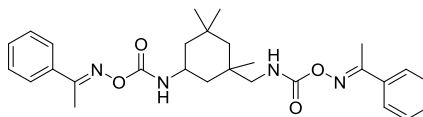
VTIR spectra of 5.13



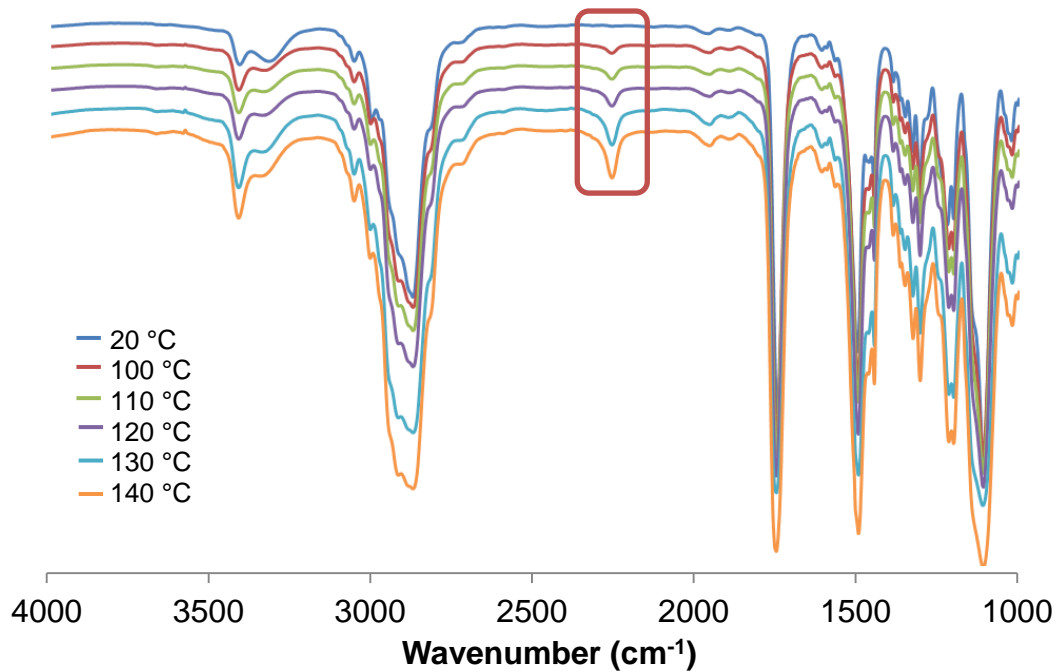
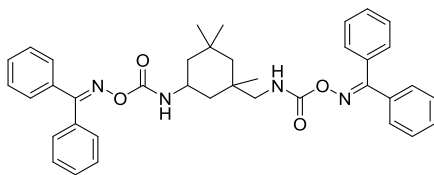
VTIR spectra of 5.14



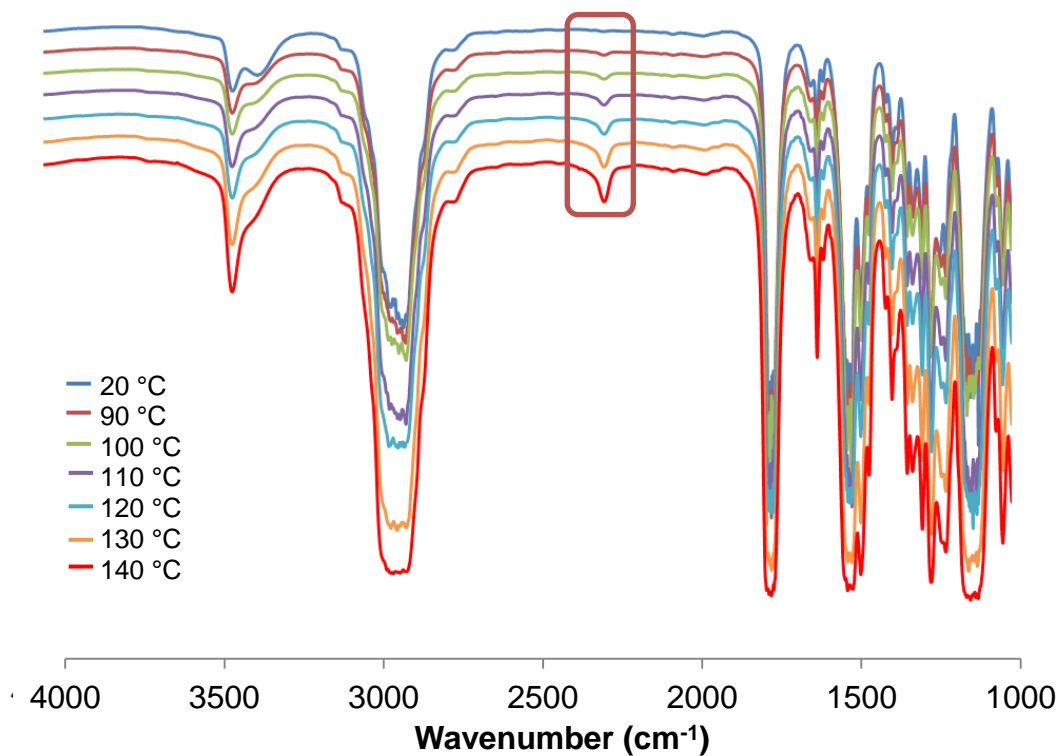
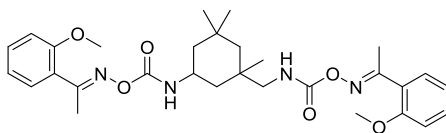
VTIR spectra of 5.15



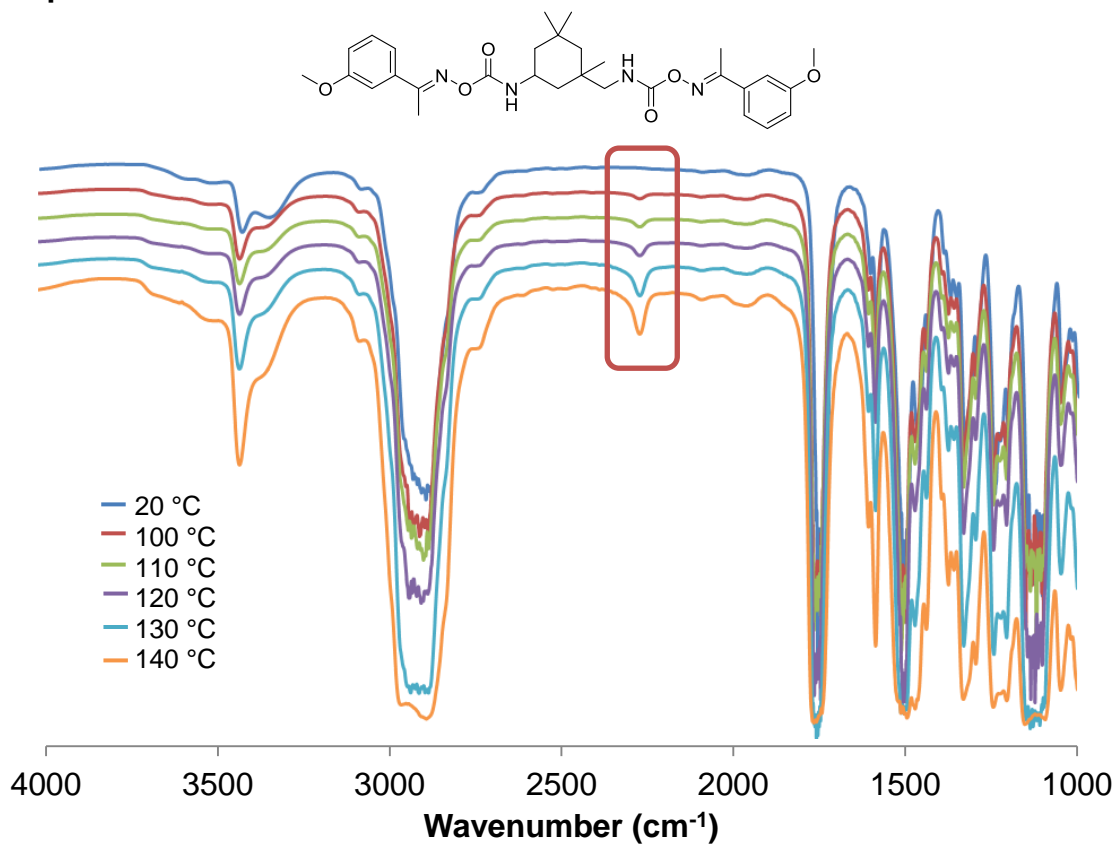
VTIR spectra of 5.16



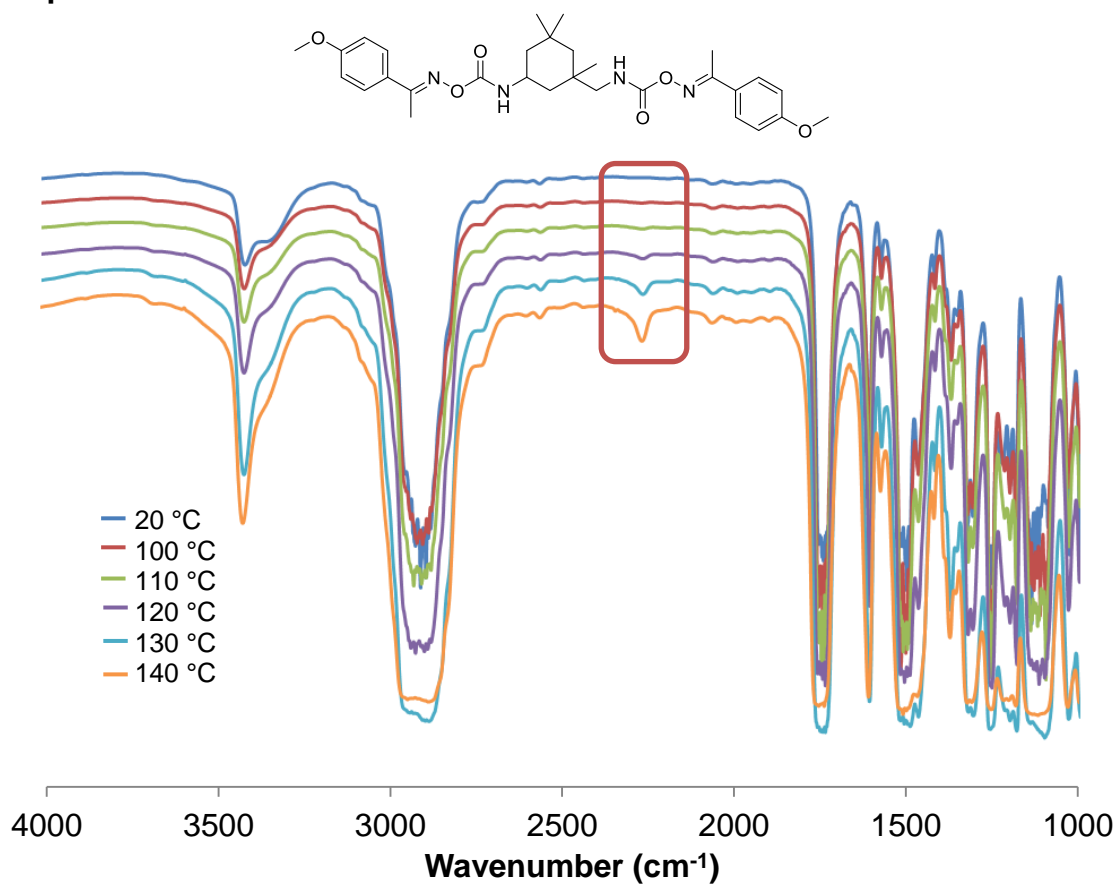
VTIR spectra of 5.23



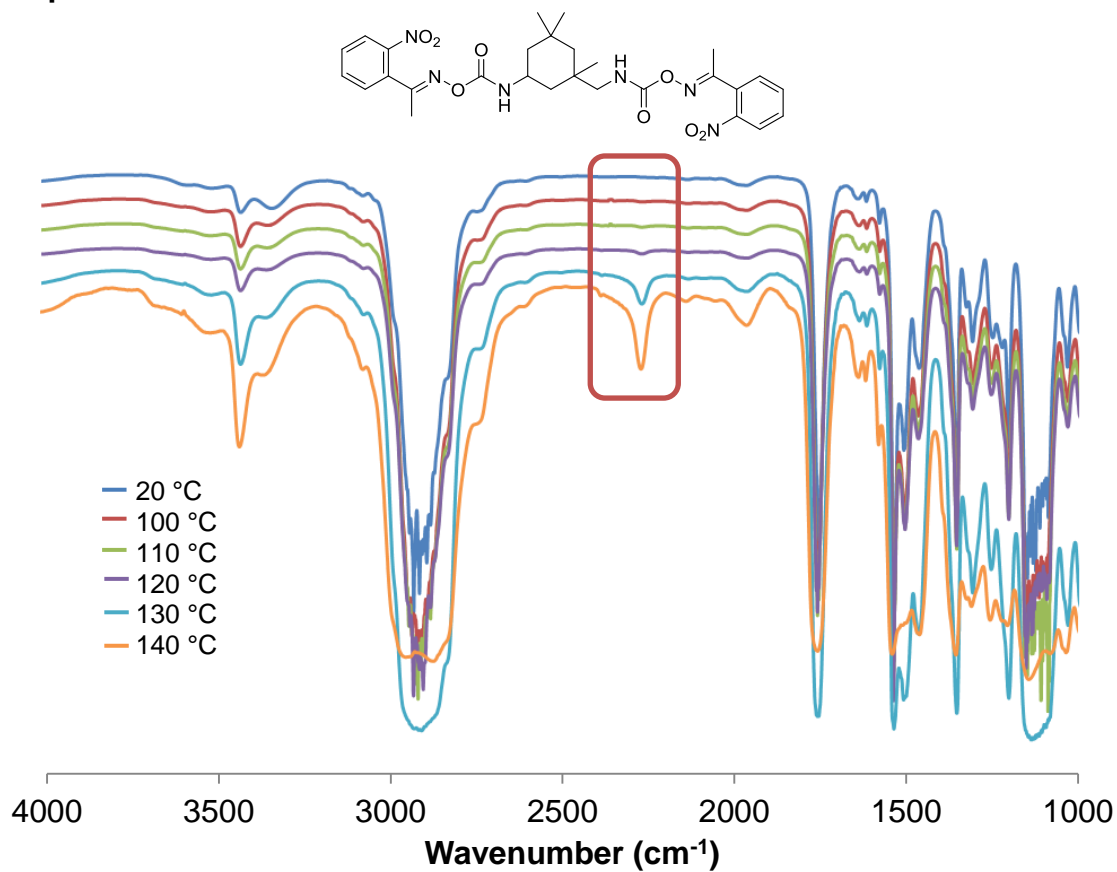
VTIR spectra of 5.24



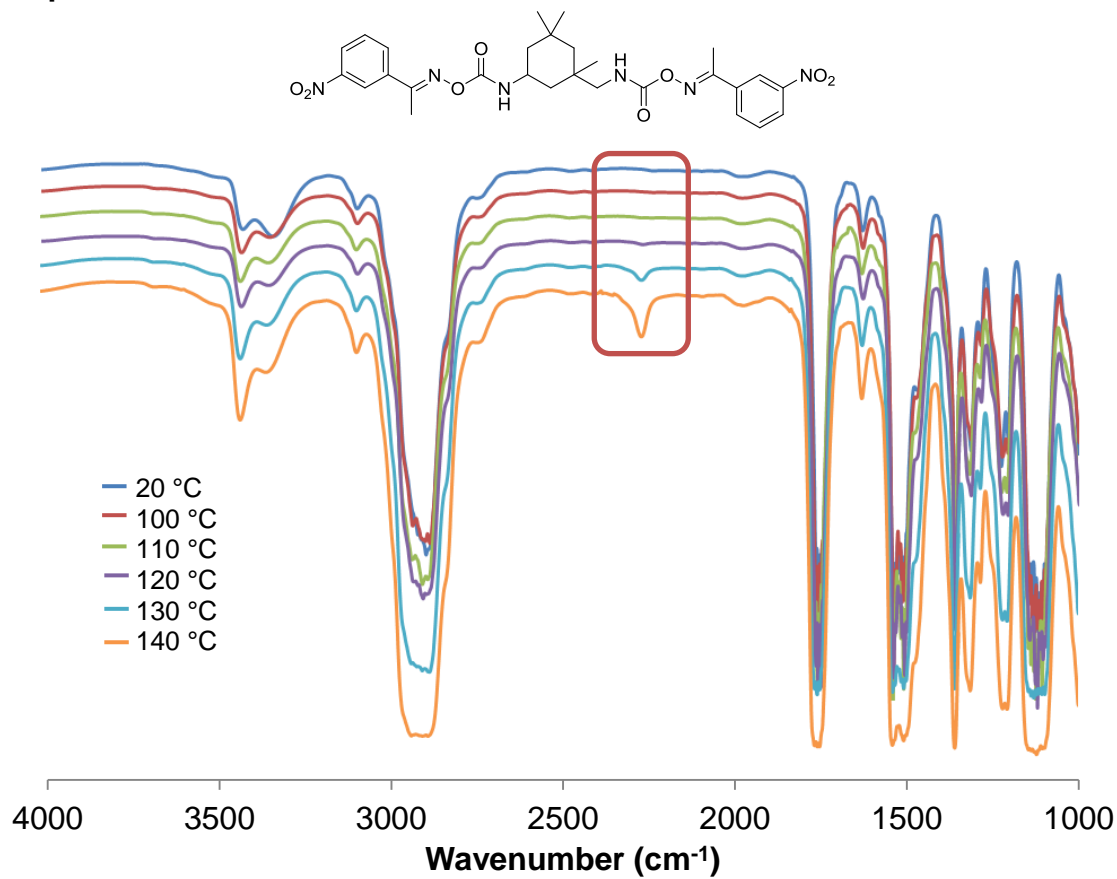
VTIR spectra of 5.25



VTIR spectra of 5.26



VTIR spectra of 5.27



VTIR spectra of 5.28

